

Quantitative flood risk analysis of road infrastructure affected by river flooding.

A Case Study considering Climate Change effect.

by
Ignacio Aranguren Rojas

*to obtain the degree of Master of Science
at the Delft University of Technology,
to be defended publicly on January 30th, 2019.*

Student number: 4626028

Project duration: April 9th, 2018 – December 12th, 2018

Thesis committee: Prof. Dr. Ir. S. N. Jonkman

Dr. J.D. Bricker

Dr. Katerina Varveri

Dr. Adrián Morales (Company Supervisor)

Dr. Jessica Castillo (Company Supervisor)

An electronic version of this MSc thesis is available at
<https://repository.tudelft.nl/>

DISCLAIMER

This MSc thesis is based on a consultancy work performed for iPresas company as part of the final graduation process to obtain the Master of Science in Civil Engineering at the Delft University of Technology, as was previously agreed by all parties involved. The author has worked independently, with the necessary supervision of company and university committee members, and the methods and results hereby presented belong to his own merit.

The main author contribution to the thesis work can be found in the Introduction (Chapter 1), the Literature review (Chapter 2), Proposed Integral Methodology for Road Flood Risk Assessment (Chapter 3) and Conclusions and Suggestions (Chapter 13), which consist of a theoretical background and methods elaborated explicitly for this graduation work and that could be used as a departure point for further improvements and research on the topic.

The Case study (Chapters 4 to 12) used to illustrate the proposed methodology is part of a professional project of iPresas company and, even if was modified explicitly for this graduation project and the assumptions and results do not represent in any case a rigorous representation of the real case, the Case Study may contain sensitive professional information for the company and client interest and it was decided to classify a substantial part of the document.

The contributions of the professional work (where the author had a primary involvement) to the graduation project consisted of: Review of site available information, Road failure Mode Identification and Classification, Definition of risk scenarios and Flood Load analysis and Design and Management Recommendations. However, several contributions were particularized for the Graduation project case: For instance, only a small study area of the whole professional project was considered for the analysis, including other Road Failure Modes and methods for System Response analysis and Consequence Analysis regarding Bridge response that were not considered in the real case. Also, the Final Quantitative risk model and Final Quantitative risk results presented are contributions elaborated explicitly for this graduation project. Despite some unavoidable similarities, the final risk model and results are different from the ones found in the real case project. In addition, the final MSc conclusions regarding the usefulness and further improvements on the proposed methodology were elaborated specifically for this thesis and they consist of a theoretical approach based on a state-of-the-art review performed individually and in parallel to the professional case study.

PREFACE

This master thesis represents the conclusion of a two-year learning cycle in the field of Hydraulic Engineering at the Delft University of Technology, with special focus on Hydraulic Structures and Flood risk analysis. This graduation work was performed in cooperation with iPresas company in the city of Valencia (Spain), and therefore my sincere gratefulness with everyone involved.

First of all, I would like to express my very great appreciation to my committee members, Dr. S.N. (Bas) Jonkman, Dr. J.D. Bricker and Dr. Katerina Varveri, for their invaluable feedback and guidance during the planning and development of this graduation work, my company supervisors Jessica Castillo for the careful reviews and shared knowledge; and Adrián Morales, to whom I am most grateful for his patience and mentorship throughout this project of unexpected challenges and for always being there when needed. I would like to express my honest gratitude to all of them not only for the opportunity of conducting this graduation project, but also for giving me the chance to be part of the iPresas team and to start growing as a professional engineer.

I would equally like to acknowledge my mentors and professors at Delft University of Technology, at the École Polytechnique Fédérale de Lausanne and at the Universidad Politécnica de Madrid, an echo of every lesson learned during my education was present within this project. I would also like to dedicate a few words to thank Professor Ignacio Escuder, to whom I am grateful for his precious insights and orientation and his enlightening perspective on flood risk analysis.

To my university colleagues, with whom I shared invaluable memories, experiences and ideas. Alberto, Berta, Guille, Adrián, Álvaro, Nacho, Enrique and Hani, thanks for being outstanding human beings and for brighten my days even in the saddest winters. A special mention to my friend Pablo. Your intelligence, tenacity and dedication have encouraged me to be a better engineer. Your courage, loyalty and deep care for the others has inspired me to be a better person.

Furthermore, thanks also to my deepest friends Virginia and Sebas, for their constant confidence on my projects and decisions. And, of course, to Clau, your unexpected appearance has filled my days with the brightest light and happiness. Thank you for encouraging me to go beyond my limits and to be the best version of myself.

Lastly, I would like to thank my parents, Maria José and Ignacio and my sisters, Maria and Lulu, for being my family and support throughout this graduation period. To my mother, because nobody knows me better and for her precious life lessons; to my father, for being a vital example of honesty and hard work; to my sister Maria, for her example of bravery and dedication to make a fairer and human world, and Lulu, for her sweetest energy and extraordinary ability to face challenges with the most positive attitude.

A small but important life-cycle is closed within this graduation work. It is a rewarding and stimulating feeling to look backwards and to observe one's personal evolution in a relatively short period of time and to understand that there will always be new concepts to be learned and that I feel prepared and confident for the new challenges to come.

“When you work you are a flute through whose heart the whispering of the hours turns to music.”

Kahlil Gibran

Ignacio Aranguren

Valencia, December 2018

EXECUTIVE SUMMARY

This document describes the graduation work: "*Quantitative flood risk analysis of road infrastructure affected by river flooding: A case study considering Climate Change in Country Z*" conducted as part of the Hydraulic Engineering MSc at Technical University of Delft.

The main objective of this report is to adopt existing methodologies for flood-risk assessment in other civil infrastructure (such as dams or urban flooding) and to apply them in road type infrastructure in order to quantitatively assess flood vulnerability and risk in project locations where historical closure data is not available and the complex global network-approach usually implemented cannot be used for road risk management issues.

By looking from a designer/ manager perspective, the aim is to deal directly with the specific road-segment under hydrological threat, shifting the interest to a more detailed comprehension of: the hazards likelihood of occurrence, the system (road pavement and bridges) response, the potential failure modes involved, and the expected consequences derived from a failure. Doing so, the proposed methodology has proven to be useful to support decision making and prioritization of risk reduction actions during and after the completion of the road design works.

The methodology that has been adopted in the course of this graduation work is based in the SUFRI methodology fundamentals [1], where a collaborative failure mode analysis represents the basis to derive a quantitative risk model. Due to the special nature of transportation infrastructure, when applying this methodology for road flood risk analysis it was found that special attention is required to evaluate the system response during a flood event and the derived consequences. In this context, direct damage associated to infrastructure reconstruction costs and indirect damage due to economic and traffic disruption during road closure and repair time need to be included in the analysis.

Three critical road failure modes during a river flood are studied in detail in this graduation work: Road pavement deterioration due to general river flooding, Bridge deck-pier connection failure due to hydrodynamic forces; and Bridge collapse due to scour and destabilization. To do so, flood damage-depth curves for different road conditions (paved and unpaved) are obtained from the literature; Ultimate Limit State functions for deck-pier connection under hydrodynamic forces are evaluated using the main hydrodynamic coefficients as stochastic parameters; and the methodology proposed by FHWA is used for scour assessment and evaluation near bridge piers foundations.

To prove the usefulness of implementing the innovative road flood risk analysis proposed in this MSc thesis, the methodology has been applied to a case study of an existing road (X), which is intended to be re-designed, in Region Z (Country Z), a vulnerable area toward natural hazards, which lies along the strip of hurricanes in the Caribbean, where roads tend to cross flood-prone areas, leaving the inhabitants exposed to high levels of vulnerability.

During this case study, an identification of potential failure modes that directly affect the transportation infrastructure between the population centers of B and A has been carried out, including failure modes related to: the failure of road pavement; the failure of the drainage system; the failure of bridges; the failure of slopes and embankments; and the failure of the risk management system in the study area.

This process has led to recommendations for the design of new works projected in the road, and to recommendations targeted to perform more detailed studies to support the new road design. At the same time, the results of the failure mode identification session have been applied as an input to develop a quantitative risk model to calculate and analyze the flood risk on the road, specifically in the road sections identified as critical, where the available information was sufficient to determine the feasibility of its occurrence.

After the proposed analysis, it was possible to obtain Frequency-Damage (FD) curves for different scenarios, analyzing the impact of climate change, the effect of the pavement rehabilitation along the entire road, the effect

of the projected variation on traffic volume, the effect of possible improvements in watershed management and the effect of management improvements in the road maintenance and response after a natural disaster.

The failure mode identification and risks results highlight an increasing risk in the infrastructure for the future due to the combined effect of projected rehabilitation works (that increases the vulnerability and exposure due to an economic revaluation of the road) and the effect of climate change (that increases the probability of occurrence of severe storms and flood events), a fact that multiplies the need to complement any structural measure of rehabilitation with a maintenance and monitoring plan, a better management of the watersheds and a more optimal response to a potential catastrophe, especially by reducing the reconstruction times and indirect damage caused by road closure and incremental circulation costs on a deteriorated pavement, in order to avoid an extensive increase of flood risk in the study area.

In addition, the results from the review of available information, failure mode identification, complementary hydrologic and hydraulic studies and risk calculation suggest that the current design works should be especially cautious regarding the possible risk of bridge collapse (due to hydrodynamic induced-failure and scour induced-failure) during future floods on climate change scenario.

The methodology to assess pavement response to flooding allowed to conclude that indirect damage during road closure and road rehabilitation time are critical damage-metrics in the analysis and their incorporation can suggest important and efficient measures for road flood risk reduction (such as improved and optimized maintenance plan) that would not have been considered if only direct consequences were considered.

Also, when applying the proposed methodology to analyze risk variation due to road design improvements it was found that an increase in economic risk is normally expected because of both climate change and an economic revaluation of the new infrastructure. The latter should be understood as a cost for the benefits derived from its improvement, and that are not included in a flood risk analysis, such as a greater utility of the infrastructure, economic development of the connected populations or less time to travel the road once rehabilitated.

Results of successfully applying the methodology to a case study in a road in Country Z, highlighted the usefulness of promoting this culture of integral risk analysis in the least developed countries, which are normally the most vulnerable countries in the world against natural hazards and will be endangered in the future due to climate change effects.

The above connects with the major finding of this MSc thesis, which is that an implementation of existing quantitative flood risk assessment methodologies for other civil engineering fields (such as dam safety or flood risk management in urban areas) to a critical road stretch to support decision-making within the project-design stage is feasible and useful. Not only this type of integral flood risk assessment could allow overcoming the complexities that are commonly found when applying traditional global-network road risk/vulnerability assessment methodologies but also turns to be a potential alternative for projects where lack of data and poor developed infrastructure network is a deniable reality.

Finally, the innovative approach described in this MSc thesis, from collaborative work to failure mode identification/classification and to risk quantification, could be further applied to other roads and types of natural risks (landslides, earthquakes.) to support other improvement and/or risk reduction, if further research on this topic is carried out.

TABLE OF CONTENT

1. INTRODUCTION.....	20
1.1. Problem Statement.....	20
1.2. MSc thesis Objectives	20
1.3. MSc thesis Structure.....	22
2. LITERATURE REVIEW.....	23
2.1. Basic Concepts in Natural Disasters Risk Assessment.....	23
2.2. Flood Risk Assessment Methodologies	24
2.2.1. Concepts on Flood Risk Management	24
2.2.2. Flood Risk Analysis: Methodologies applied in civil infrastructure	26
2.3. Road infrastructure response to river flooding: A probabilistic approach.....	31
2.3.1. Pavement response in case of flooding	31
2.3.2. Bridges response in case of flooding.....	33
2.4. Road vulnerability	39
2.4.1. Transportation Network Reliability.....	39
2.4.2. Measuring Vulnerability	42
2.5. Literature review conclusions.....	46
3. INTENDED APPROACH.....	48
3.1. The Failure Mode Identification Process.....	49
3.1.1. Failure Mode Identification	49
3.1.2. Failure Mode Classification.....	50
3.2. Definition of Climate Change Scenarios.....	51
3.2.1. Mathematical models used for Climate Change prediction.....	52
3.2.2. Methodology proposed	53
3.3. Quantitative Risk Calculation.....	55
3.3.1. The risk analysis process.....	55
3.3.2. Load analysis.....	58
3.3.3. System response analysis.....	63
3.3.4. Consequence Estimation.....	71
4. REVIEW OF AVAILABLE INFORMATION.....	75
5. TECHNICAL VISIT.....	76
5.1. Introduction	76
6. FAILURE MODE IDENTIFICATION	77
6.1. Failure Mode Classification	78

7.	DEFINITION OF CLIMATE CHANGE SCENARIOS	82
7.1.	Recommendations to include the effect of the CC: Design storms	83
7.2.	Recommendations to include the effect of the CC: Land – use cover	84
8.	LOAD ANALYSIS: HYDROLOGICAL & HYDRAULIC MODELING	85
8.1.	Watersheds and land use	85
8.2.	Historical rain data and design storms	85
8.3.	Hydrological model results	86
8.4.	Hydraulic model results.....	88
8.5.	Hydrologic and hydraulic characterization update with CC effect	90
8.5.1.	Conclusions	95
9.	QUANTITATIVE RISK CALCULATION.....	96
9.1.	Risk model architecture.....	97
9.2.	Risk scenarios	98
9.3.	Input data for the road risk model.....	99
10.	RISK RESULTS: FLOOD RISK MAPS AND FD CURVES	101
10.1.	Global Risk calculation results: F-D curves.....	102
10.2.	Analysis of Climate Change and improvement measures on road risk: Comparison between scenarios.	104
11.	RECOMMENDATIONS FOR THE DESIGN AND MANAGEMENT OF THE X.....	106
11.1.	Recommendations for the design of the X road.....	106
11.2.	Recommendations for the risk management of the X road	108
12.	CASE STUDY CONCLUSIONS	109
13.	MSc THESIS CONCLUSIONS AND RECCOMENDATIONS.....	112
13.1.	Main conclusions	112
13.2.	Further improvements and recommendations	113
14.	REFERENCES	116

TABLE INDEX

Table 2-1: Semi-quantitative risk matrix to address pavement performance after a flood. Source: [26]	32
Table 2-2: K_1 values. “Live-Bed” contraction scour.	38
Table 2-3: K_1 Correction factor.....	39
Table 2-4: K_2 Correction factor.....	39
Table 2-5: K_3 Correction factor.....	39
Table 2-6: Cost of time value for Jessore region (Bangladesh). Source: (Department for International Development, 2002).....	45
Table 2-7: Cost of time value for New Zealand. Source: (NZ Transport Agency, 2016)	45
Table 3-1: CN values depending on hydraulic condition of soil (A, B, C, D) and land-use type according to the classification by IGBP	61
Table 3-2: Definition of typical geometrical parameters for a bridge.....	65
Table 3-3: Variables that influence the main resisting and soliciting forces on submerged bridge deck.	66
Table 3-4: Minimum and maximums values estimates for hydrodynamic coefficients as a function of proximity ratio, inundation ratio and Froude number. Source: [41], [42], [45].....	67
Table 6-1: Failure Mode Classification. X road (Country Z).....	78
Table 8-1: Daily rainfall data of historical records for several stations close to the X road.	85
Table 8-2: Maximum daily rainfall for different return periods. Several meteorological stations within the project area.	85
Table 8-3: Parameters required to perform a hydrological modeling for each of the sub-basins.	87
Table 8-4: Values of maximum daily rainfall (mm in 24 h) expected for each weather station, range return periods and two climate-trend scenarios (current and RCP8.5).....	90
Table 8-5: Summary of hydraulic modelling results	95
Table 9-1: Input data for the road risk model: loads.	99
Table 9-2: Input data for the road risk model: system response.....	99
Table 9-3: Input data for the road risk model: potential consequences	100
Table 10-1: Economic risk (\$/year) calculation results (Direct, Indirect and Total risk). Five scenarios.....	102
Table 14-1: Damage quantification for X ROAD road after hurricanes I and H (2008). Source: [40]	166
Table 14-2: Unitary prices for road construction materials. Source [40]	166
Table 14-3: Considerations for direct economic consequences calculation.	167
Table 14-4: Updated cost of time after GDP comparison between countries with available data. Ratios between Country Z and countries of study (New Zealand and Bangladesh).....	167
Table 14-5: Road closure time vs flood event frequency. Estimates based on hurricanes duration in the study area.	168
Table 14-6: Daily traffic volume for X ROAD road as a function of road condition.....	168

Table 14-7: Reparation road time (in weeks) as a function of management practices.	168
Table 14-8: Cost of vehicles exploitation (\$/ km) depending on the pavement condition and vehicle type for Country Z.....	169
Table 14-9: IRI values estimated for X ROAD road after flood as a function of flood return period, climate scenario and road type.	170
Table 14-10: Inputs for the risk model. Section node.....	173
Table 14-11: Input for flood analysis road.	174
Table 14-12: Pavement Failure Node.....	174
Table 14-13: Estimated values for the variables used in bridge scour evaluation.....	175
Table 14-14: Calculation of contraction scour. Current climate scenario.	175
Table 14-15: Calculation of contraction scour. Future climate scenario.....	175
Table 14-16: Bridge piers localized scour. Current climate scenario. Rounded pier ($a=1$ m / $L=7$ m), angle of flow attack $=15^\circ$, plane riverbed.....	176
Table 14-17: Bridge piers localized scour. Future climate scenario. Rounded pier ($a=1$ m / $L=7$ m), angle of flow attack $=15^\circ$, plane riverbed.....	176
Table 14-18: Total scour. Current and future climate scenarios. Rounded pier ($a=1$ m / $L=7$ m), angle of flow attack $=15^\circ$, plane riverbed.	176
Table 14-19: Estimation of foundation's geometric dimension.	177
Table 14-20: Relation between scour and likelihood of bridge failure for destabilization. Foundation depth equal to 3 m (simple spread footing foundation)	177
Table 14-21: Failure probability by bridge destabilization due to scour for both climatic scenarios and seven flood return periods. BS6 bridge	177
Table 14-22: Ranges for hydrodynamic coefficients values. Current climate scenario.	178
Table 14-23: Ranges for hydrodynamic coefficients values. Trend-based scenario.	178
Table 14-24: Bridge geometry (typical 3-concrete girder deck).	179
Table 14-25: Failure probability of the deck-pier connection for both climate scenarios and seven flood return periods. Bridge BS6.....	183
Table 14-26: Considerations for direct economic consequences calculation.....	184
Table 14-27: Inputs for the direct consequence node.	185
Table 14-28: Indirect economic damage (in \$) during the road closure. Calculation scenarios and flood return periods.....	185
Table 14-29: Weekly indirect economic damage (in \$) during the road rehabilitation. Calculation scenarios and flood return periods.	186
Table 14-30: Total indirect economic damage (in \$) during the road rehabilitation. Calculation scenarios and flood return periods.	186
Table 14-31: Annual risk results for current scenario.	188
Table 14-32: Annual risk results for future climate scenario.	189
Table 14-33: Annual risk results for current climate design scenario.	191

Table 14-34: Annual risk results for future climate design scenario.	192
Table 14-35: Annual risk results for optimal future climate design scenario.....	194

FIGURES INDEX

Figure 2-1: General approach for flood risk management. Source: [12].....	25
Figure 2-2: FD graphical representation of quantitative risk in terms of economic values. Source: [1].....	25
Figure 2-3: Graphical representation of tolerability regions. Source: HSE [18].....	26
Figure 2-4: Integrated Dam Safety Management and Links to Risk Models and Dam Safety File. Source: SPANCOLD [22]	27
Figure 2-5: Generic dam risk model architecture.	28
Figure 2-6: Generic Structure of Processes for Risk Analysis. Source: SPANCOLD 2012.	28
Figure 2-7: Overall scheme proposed by the SUFRI methodology to assess flood risk.....	29
Figure 2-8: SUFRI methodology to assess economic losses.....	30
Figure 2-9: Acting forces on a submerged bridge-deck. Source: [39]	34
Figure 2-10: Concept wheel for road risk assessment. Source: [2].	41
Figure 2-11: Methodology to evaluate economic consequences after flooding and calculate depth-damage curves. [69].....	42
Figure 2-12: Damage-depth function for both, paved and unpaved roads. Source: [69].	43
Figure 2-13: Indicative IRI values according to the road type, and firm condition. Source: [73].....	45
Figure 3-1: Proposed methodology for road risk analysis, adopting SUFRI methodology fundamentals.	48
Figure 3-2: Generic diagram for a Failure Mode.....	49
Figure 3-3: Failure Mode Identification process.	50
Figure 3-4: Screening of the evolution in atmospheric radiation and emission of CO ₂ for the four RCPs scenarios and Horizon 2000-2100.....	52
Figure 3-5: Methodology for obtaining rainfall IDF values for a climate change scenario.	53
Figure 3-6: Example of regression adjustment (simulation CanESM2 vs observed data).	54
Figure 3-7: Example of frequency of extreme values analysis (Several probability distributions).	54
Figure 3-8: The road flood risk analysis process.	56
Figure 3-9: Relationship between influence diagram and event trees. Source: [76]	57
Figure 3-10: GIS-based methodological procedure for hydrological-hydraulic characterization.....	59
Figure 3-11: SCS type III hyetograph. P / Pmax in 24h vs storm duration.	60
Figure 3-12: Calculation mesh and boundary conditions example. HEC-RAS 2D model. Case study: Watershed BS1	63
Figure 3-13: Typical geometrical parameters for a 3-girder bridge with concrete deck. Source: [39]	64
Figure 3-14: Relation between the road pavement condition (IRI) and vehicle operational costs for the case study.	73
Figure 4-1: Proposed methodology for road risk analysis. Phase 1: Review of available information and complementary studies.....	75
Figure 5-1: Methodology for the analysis of natural hazards on the X highway. Phase II: Technical visit.	76

Figure 6-1: Methodology for the analysis of natural hazards on the X highway. Phase III: Failure Mode Identification 77

Figure 6-2: Generic structure for a failure mode 77

Figure 6-3: Failure Mode A1. Description and “less likely” and “more likely” occurrence factors. 79

Figure 6-4: Failure Mode C2. Description and “less likely” and “more likely” occurrence factors. 80

Figure 6-5: Failure Mode C3. Description and “less likely” and “more likely” occurrence factors. 81

Figure 7-1: Methodology for the analysis of natural hazards in the X. Definition of future climate change scenarios 82

Figure 7-2: Increase (in %) with respect to the historical data for maximum daily rainfall (mm in 24 h) expected for three climate-trend scenarios (RCP2.6, RCP4.5 and RCP8.5), 7 return periods. 83

Figure 7-3: Values of the CN for each sub-basin and climate trend-based scenario. 84

Figure 8-1: SCS type III design storm for case study. S1 basin, 100 return period and current climate conditions. 86

Figure 8-2: Flood hydrograph (Design storm 24h). Basin S6. 87

Figure 8-3: Summary of the results for the peak flow rate (in m³/s). 6 basins and seven return (2 to 500 years) periods..... 88

Figure 8-4: Summary results of hydraulic modelling. Current climate scenario. Maximum flow depth on top of the road axis at each road-river intersection. 89

Figure 8-5: Summary results of hydraulic modelling. Current climate scenario. Flooded road length on top of the road axis at each road-river intersection. 89

Figure 8-6: Summary of hydraulic modelling. Current climate scenario. Inundation ratio for culvert (BS1) and Bridge (BS6). 90

Figure 8-7: Summary results for peak flow rate (in m³/s). 6 basins and seven return periods. RCP8.5 scenario. 91

Figure 8-8: Increase (%) Future climate scenario vs current climate scenario. 6 sub-basins and seven return periods..... 91

Figure 8-9: Summary of hydraulic modelling results. Max depth on road at each river – road intersection analyzed. Future Climate trend-based scenario. 92

Figure 8-10: Summary of hydraulic modelling results. Flooded length on road at each river – road intersection analyzed. Future Climate trend-based scenario. 92

Figure 8-11: Summary of hydraulic modelling results. Inundation ratio on road at each river – road intersection analyzed. Future Climate trend-based scenario. 93

Figure 8-12: Increase (in %) for max depth on road at each river-road intersection analyzed. Future Climate trend-based scenario vs current scenario. 93

Figure 8-13: Increase (in %) for flooded length on road at each river-road intersection analyzed. Future Climate trend-based scenario vs current scenario. 94

Figure 8-14: Increase (in %) for inundation ratio on bridge deck at each river-road intersection analyzed. Future Climate trend-based scenario vs current scenario..... 94

Figure 9-1: Methodology proposed to perform a quantitative analysis of the natural hazards that threaten the X highway of Country Z. In Orange, the stages related to the calculation of risk.	96
Figure 9-2: General risk model architecture	97
Figure 9-3: Risk model architecture for the X road.	98
Figure 10-1: Methodology for the analysis of natural risks in the X. Representation in FD curves.	101
Figure 10-2: FD curve for the different risk calculations. Direct damage.	102
Figure 10-3: FD curve for the different risk calculations. Indirect damage.....	103
Figure 10-4: FD curve for the different risk calculations. Total damage.	103
Figure 11-1: Methodology for the analysis of natural hazards in the X road. Recommendations for the design and management.	106
Figure 14-1: Failure Mode A1. Description and “less likely” and “more likely” occurrence factors.	123
Figure 14-2: Failure Mode A2. Description and “less likely” and “more likely” occurrence factors.	124
Figure 14-3: Failure Mode A3. Description and “less likely” and “more likely” occurrence factors.	125
Figure 14-4: Failure Mode A4. Description and “less likely” and “more likely” occurrence factors.	126
Figure 14-5: Failure Mode A5. Description and “less likely” and “more likely” occurrence factors.	127
Figure 14-6: Failure Mode B1. Description and “less likely” and “more likely” occurrence factors.	128
Figure 14-7: Failure Mode B2. Description and “less likely” and “more likely” occurrence factors.	129
Figure 14-8: Failure Mode B3. Description and “less likely” and “more likely” occurrence factors.	130
Figure 14-9: Failure Mode B4. Description and “less likely” and “more likely” occurrence factors.	131
Figure 14-10: Failure Mode C1. Description and “less likely” and “more likely” occurrence factors.	132
Figure 14-11: Failure Mode C2. Description and “less likely” and “more likely” occurrence factors.	133
Figure 14-12: Failure Mode C3. Description and “less likely” and “more likely” occurrence factors.	134
Figure 14-13: Failure Mode D1. Description and “less likely” and “more likely” occurrence factors.	135
Figure 14-14: Failure Mode D2. Description and “less likely” and “more likely” occurrence factors.....	136
Figure 14-15: Failure Mode D3. Description and “less likely” and “more likely” occurrence factors.	137
Figure 14-16: Failure Mode D4. Description and “less likely” and “more likely” occurrence factors.	138
Figure 14-17: Failure Mode D5. Description and “less likely” and “more likely” occurrence factors.....	139
Figure 14-18: Failure Mode E1. Description and “less likely” and “more likely” occurrence factors.	140
Figure 14-19: Failure Mode E2. Description and “less likely” and “more likely” occurrence factors.	141
Figure 14-20: Failure Mode E3. Description and “less likely” and “more likely” occurrence factors.	142
Figure 14-21: Data adjustment (CanESM2 model simulation vs Historical observed data) A station.	146
Figure 14-22: Data adjustment (CanESM2 model simulation vs Historical observed data) B station.	147
Figure 14-23: Frequency extreme value analysis for annual maximum daily rainfall. Current climate scenario. Station A.....	148

Figure 14-24: Frequency extreme value analysis for annual maximum daily rainfall. Future climate scenario RCP2.6. Station B. 148

Figure 14-25: Frequency extreme value analysis for annual maximum daily rainfall. Future climate scenario RCP4.5. A Station. 149

Figure 14-26: Frequency extreme value analysis for annual maximum daily rainfall. Future climate scenario RCP8.5. A Station. 149

Figure 14-27: Frequency extreme value analysis for annual maximum daily rainfall. Current climate scenario. B Station. 150

Figure 14-28: Frequency extreme value analysis for annual maximum daily rainfall. Future climate scenario RCP2.6. B Station. 150

Figure 14-29: Frequency extreme value analysis for annual maximum daily rainfall. Future climate scenario RCP4.5. B Station. 151

Figure 14-30: Frequency extreme value analysis for annual maximum daily rainfall. Future climate scenario RCP8.5. B Station. 151

Figure 14-31: Current climate. Flood hydrograph from 24 h Design storm SCS type III. BS1 Watershed. 153

Figure 14-32: Future climate. Flood hydrograph from 24 h Design storm SCS type III). BS1 Watershed. 153

Figure 14-33: Flood peak flow (current scenario vs future climate scenario). X-BS1 intersection. 154

Figure 14-34: Current climate. Flood hydrograph from 24 h Design storm SCS type III). BS2 Watershed. 154

Figure 14-35: Future climate. Flood hydrograph from 24 h Design storm SCS type III). BS2 Watershed. 155

Figure 14-36: Flood peak flow (current scenario vs future climate scenario). X-BS2 intersection. 155

Figure 14-37: Current climate. Flood hydrograph from 24 h Design storm SCS type III. BS3 Watershed. 156

Figure 14-38: Future climate. Flood hydrograph from 24 h Design storm SCS type III. BS3 Watershed. 156

Figure 14-39: Future climate & Watershed reforestation. Flood hydrograph from 24 h Design storm SCS type III). BS3 Watershed. 157

Figure 14-40: Flood peak flow (current scenario vs future climate scenario). X-BS3 intersection. 157

Figure 14-41: Flood peak flow (future climate scenario vs optimal future climate scenario). X-BS3 intersection. 158

Figure 14-42: Current climate. Flood hydrograph from 24 h Design storm SCS type III. BS4 Watershed. 158

Figure 14-43: Future climate. Flood hydrograph from 24 h Design storm SCS type III). BS4 Watershed. 159

Figure 14-44: Future climate & Watershed reforestation. Flood hydrograph from 24 h Design storm SCS type III). BS4 Watershed. 159

Figure 14-45: Flood peak flow (current scenario vs future climate scenario). X-BS4 intersection. 160

Figure 14-46: Flood peak flow (future climate scenario vs optimal future climate scenario). X-BS4 intersection. 160

Figure 14-47: Current climate. Flood hydrograph from 24 h Design storm SCS type III. BS5 Watershed. 161

Figure 14-48: Future climate. Flood hydrograph from 24 h Design storm SCS type III). BS5 Watershed. 161

Figure 14-49: Flood peak flow (current scenario vs future climate scenario). X-BS5 intersection. 162

Figure 14-50: Current climate. Flood hydrograph from 24 h Design storm SCS type III. BS6 Watershed. 162

Figure 14-51: Future climate. Flood hydrograph from 24 h Design storm SCS type III). BS6 Watershed.....	163
Figure 14-52: Flood peak flow (current scenario vs future climate scenario). X-BS6 intersection.....	163
Figure 14-53: Average cost per trip and vehicle on the X ROAD (length 25km) depending on road pavement deterioration.....	169
Figure 14-54: IRI values estimated for X ROAD road after flood as a function of flood return period and road type	170
Figure 14-55: Relation between the range of return periods considered in the analysis with the annual exceedance probability.....	172
Figure 14-56: Geometric dimensions of a simple spread footing foundation.....	177
Figure 14-57: Vertical ULS stability (Zvert, d). Seven return periods. Current climate scenario. Sensitivity analysis based on hydrodynamic coefficients.	180
Figure 14-58: Horizontal ULS stability (Zvert, d). Seven return periods. Current climate scenario. Sensitivity analysis based on hydrodynamic coefficients.	180
Figure 14-59: Rotation ULS stability (Zvert, d). Seven return periods. Current climate scenario. Sensitivity analysis based on hydrodynamic coefficients.	181
Figure 14-60: Vertical ULS stability (Zvert, d). Seven return periods. Climate trend scenario. Sensitivity analysis based on hydrodynamic coefficients.....	181
Figure 14-61: Horizontal ULS stability (Zvert, d). Seven return periods. Climate trend scenario. Sensitivity analysis based on hydrodynamic coefficients.	182
Figure 14-62: Rotation ULS stability (Zvert, d). Seven return periods. Climate trend scenario. Sensitivity analysis based on hydrodynamic coefficients.....	182
Figure 14-63: Water depth – Damage curves. Paved and unpaved roads. Source: [69]	183
Figure 14-64: FD curve for current scenario.	188
Figure 14-65: FD curve for future climate trend scenario.	190
Figure 14-66: FD curve for current climate design scenario.	191
Figure 14-67: FD curve for future climate design scenario.	193
Figure 14-68: FD curve for optimal future climate design scenario.	195

ACRONYMS

ANCOLD	Comité Nacional Australiano de Grandes Presas
CN	Curve Number
DEM	Digital Elevation Model
FHWA	Federal Highway Administration (USA)
FM	Failure Mode
GCMs	Global Circulation Models
HSE	Health Safety Executive (UK)
ICOLD	International Commission on Large Dams
IGBP	<i>International Geosphere-Biosphere Program</i>
IPCC	Intergovernmental Panel on Climate Change
MODIS	<i>Moderate Resolution Imaging Spectroradiometer</i>
MTPTC	Ministry of Transport and Public Communication (Country Z)
NRCS	<i>National Ressources Conservations Service (EE UU)</i>
PK	Kilometric Point
RCMs	Regional Circulation Models
SIG/GIS	Geographical Information System
SPANCOLD	Spanish Committee of Large Dams
USACE	United States Army Corps of Engineers
UNDP	United Nations Program for Development
USBR	United States Bureau of Reclamation
VOC / VEC	Vehicle operational/exploitation costs

PART I. PROBLEM STATEMENT AND LITERATURE REVIEW

1. INTRODUCTION

1.1. Problem Statement

Roads are deeply connected to day-to-day life and incidents within their network can have high repercussion on the whole society [2]. Recent catastrophic events and climate change projections have led to an increasing awareness of the transportation infrastructure's vulnerability, specifically, with regard to natural hazards [3]. Induced damage by hurricanes and river flooding can produce large financial repair-costs and also impact local economies through indirect damage caused by transportation disruption [4]. As stated in [5], the transportation system is the most important lifeline in the event of natural disasters since the restoration of other systems such as water supply or electrical power heavily depends on the ability to transport people and equipment to damaged sites. This is especially important in the case of developing countries where there is a great dependency on their transportation network to provide accessibility and a safe environment for communication of people and goods [6].

Probabilistic risk analysis aims to determine the distribution function of the losses/damages that the infrastructure could experience by the occurrence of natural hazards, integrating rationally the existing uncertainties in the different parts of the process [7]. According to various authors [8] [9] a complete probabilistic risk analysis should take into account risk as a combination of hazard susceptibility and potential to be harmed (vulnerability and exposure). In this context, road vulnerability has risen as a growing field of study for researchers, with focus on reliability assessments of transportation infrastructure [4]. However, despite the fundamental importance of road networks as being one of the critical lifelines for the society, only a few examples [10] have aimed at providing an integral framework for road risk assessment, from potential hazards identification to consequence estimation and risk quantification, which could give transportation-infrastructure operators and designers advice and support regarding the definition of risk-management strategies to achieve to optimal solutions from a risk-informed point of view.

Looking at what has been done in recent years regarding other critical civil infrastructures such as dams or dykes, where risk-informed methods are a common practice, the aim of this MSc thesis is to review and adapt an existing methodology for flood risk analysis proposed by [1] which has been already applied in other civil engineering fields, to prove its utility during the decision-making process of a road-stretch design project. The development of this risk-informed framework will be applied to a Case Study of a road affected by recurrent river flooding in North-Artibonite (Country Z) to illustrate the whole risk analysis process.

1.2. MSc thesis Objectives

Based on an integral risk analysis of the natural hazards (mainly river flooding) that affect the X (Region Z, Country Z), this graduation project aims to adapt an existing methodology that has been already applied in other fields such as dam risk assessment or urban flood risk assessment, to road risk assessment, in order to support decision-making during the design process, optimize investments and minimize damage due to natural hazards that, in some cases, are prone to be more intense due to climate change.

In other words, relying on a probabilistic risk analysis of a specific stretch of the road by means of integrating river flooding, failure of singular infrastructure such as road pavement, culverts and bridges and the impact of climate change, the adaptability of already existing risk-informed methods to support the design process of a road will be examined. The major concern of this Msc thesis addresses the quantification of natural hazard's risk in road type infrastructure, from a thorough hazard identification process (qualitative phase), to system response analysis, consequence estimation and final risk quantification (quantitative phase) that could be applied to provide recommendations for selecting alternatives for a road design project.

During an integral probabilistic risk assessment, there are several objectives to be fulfilled to provide the decision-makers with a robust and reliable information. The following objectives and research questions are pointed out:

- The first objective within this MSc thesis will be to review existing methodologies in the field of Road Vulnerability and Natural Disasters Risk assessments with main focus on Flood Risk analysis, in order to identify potential frameworks that could be adapted for the specific case of a road-type infrastructure risk assessment.
- The second objective of this MSc thesis is to qualitatively identify the different failure modes that could impact the transportation infrastructure, and that are related with natural hazards, by means of a technical inspection and organization of a Failure Mode Identification session with project managers and designers. Once they are identified, the following question arises: Is it possible to quantify the risk of every potential hazard? A classification of failure modes adapted to an infrastructure threatened by natural hazards should be provided.
- Once the potential failure modes affecting the road and the risk methodology are established, the following objective is focused on the hazard susceptibility assessment. How to calculate the likelihood (i.e. probability of occurrence) of river flooding and the considered failure modes? Which hydraulic parameters are important for the quantitative risk calculation?
- Once the loads on the infrastructure are defined, the system response should be assessed. In other words, how likely is the system to fail given a specific set of infrastructure configuration and flow conditions? Which parameters can be used to assess the damage to road pavement? What would be the pavement damage in case of flooding? How can we calculate the failure probability of a bridge for a given flow depth and velocity?
- An important aspect in the design of future infrastructure, and specifically in countries underlying within a tropical region, is to assess the impact of climate change in future conditions, taking into consideration the associated uncertainty. What are the climate change projections in the region of study? How to adapt IDF curves for future emission scenarios?
- The main aspect that differentiates the risk assessment process of a road from other civil infrastructure like dams or dykes (apart from the nature of the potential failure modes) are the consequences derived from a failure. How to assess the direct damage of a flood to a road pavement? What are the reconstruction costs in case of bridge or culvert failure? How to assess the indirect costs derived from the closure and pavement deterioration after a natural disaster? Those questions will be answered during this graduation project.
- Finally, hazard susceptibility (probability of occurrence) and infrastructure vulnerability (consequence calculations) should be integrated by means of a quantitative risk model, considering different climate scenarios and road design alternatives. Differently from other civil infrastructure, for which failure modes are concentrated in a single location, this MSc thesis will cope with the fact that, in a road stretch, failures could happen in separate locations and the risk model architecture should be adapted consequently.

All the aforementioned objectives will provide a guideline to reach the following main research goal:

Implementation of an existing quantitative risk assessment methodology for other civil engineering fields (such as dam safety or flood risk management in urban areas) to a critical road stretch to support decision-making within the project-design stage.

1.3. MSc thesis Structure

The Msc thesis is comprised of five chapters and contains a full description of the author's graduation project.

The document is structured to guide the reader through the different aspects of the above question. First, *Literature Review*, where an introduction to the background concepts in Natural Disaster Risk Analysis, Flood Risk assessment methodologies, Pavement and Bridge response to flooding and Road Vulnerability is presented. Then, *Intended Approach*, where an overview of the proposed risk-informed methodology for road risk assessment is provided. Within the *Case Study Chapter*, a critical review of the discussed problematic and the current state of the X road system (Country Z) will be performed. In this chapter, the results from applying the risk-informed methodology will be presented, concluding with management and design recommendations to support decision-making in the road-segment design. Finally, the *Conclusions* to the graduation work will be presented.

2. LITERATURE REVIEW

The following chapter comprises a state-of-art review regarding the main fields that will be treated along this graduation project.

First, the basic concepts in Natural Disasters Risk Analysis and Management are presented, with focus on what has been done in the field of Flood Risk assessment, as river flooding is the most critical natural hazard in the case study region. Then, different methodologies for the risk-assessment of civil infrastructure are shown. The risk term is employed in different fields of research and its conceptualization can change depending on the field of study. In this project, risk term is treated as a combination of hazard's likelihood, system response and infrastructure vulnerability. These last two terms - system response and vulnerability/consequence estimation - are the key aspect that differentiates the risk-assessment of a road from what has been done in the risk-assessment of other civil infrastructure such as dams or urban flooding. Thus, a literature review regarding how to assess the response of transportation infrastructure to flooding and how to calculate road vulnerability is also presented in this chapter. Finally, after the thorough review of the above concepts, the author will try to find a gap in the literature regarding road risk-assessment that will try to be fulfilled along the rest of this Msc thesis work.

2.1. Basic Concepts in Natural Disasters Risk Assessment

The development of natural processes that constitute a hazard to the population and the exposed infrastructure in a determined region is linked with the economic losses and loss of life and it is always a function of the local intensity generated by the hazardous event, the degree of exposure and vulnerability of the elements exposed [7].

The terminology found in the technical literature concerning the natural risk assessment is not unique. The term risk itself is widely used in different fields and thus, diverse definitions can be found depending on the field of research. In the following, an introduction to the basic concepts in Risk Analysis and Management is presented.

Several attempts in the literature have put an effort to give a definition for risk [9] [8]. As stated in [11] it is important to remark a difference between hazard and risk. The hazard term is defined as a *physical event, phenomenon or human activity with the potential to result in harm*. The definition for risk adopted in the context of this Msc thesis is now presented.

The definition of the risk term should incorporate various sub-elements [9]: The nature and probability of the hazard, the degree of exposure to the hazard, the susceptibility to the hazard and the value of potential consequences. Thus, risk is expressed as a function of the previous components. Other authors describe risk as the combination of three concepts: what can happen, how likely is to happen and which are its consequences [8].

In the simplest terms, risk can be expressed as a combination of susceptibility (hazard) and a value which includes the system characteristics describing its potential to be harmed (vulnerability and exposure). This last term - vulnerability - is described as a sub-function of risk [11] and expresses the combination of the susceptibility to the hazard and value of the potential consequence. The definition of risk can be given as in Eq. (2.1).

$$Risk = Hazard * Exposure * Vulnerability \quad (2.1)$$

If one considers that the consequences term, quantified (e.g. monetary value) or described (e.g. high, medium, low), normally captures both exposure and vulnerability, the Eq. (2.1) can also be expressed as shown in Eq. (2.2).

$$Risk = Probability * Consequences \quad (2.2)$$

A more general definition of risk is the following “*Risk is a set of scenarios (s_i) each of which has a probability (p_i) and a consequence (d_i)*” [8]. From this last interpretation of risk one can quantify and depict the total risk expressing the value of the damage $E(d)$ for a set of discrete scenarios as follows in Eq. (2.3).

$$E(d) = \sum p_i * d_i \quad (2.3)$$

However, this expected value neither gives an insight in the magnitude of probability and consequences nor an understanding in the contribution of individual scenarios [12]. This is why the risk curves, such as the FD-Curve, that shows the probability of exceedance of a certain magnitude of consequences are broadly used (See Figure 2-2).

2.2. Flood Risk Assessment Methodologies

2.2.1. Concepts on Flood Risk Management

Floods are a global cause for natural disasters causing significant economic costs to people around the world [1]. Only during 2000-2006, water related disasters killed more than 290,000 people and inflicting more than 422 \$ billion damage [13]. A rise in the frequency of this disasters is expected due to climate variability, natural and social pressures and socioeconomic shifts [14] [15].

In this context, the flood risk management concept is defined as *the continuous and holistic societal analysis, assessment and mitigation of flood risk* [9], and is a critical task and of high public interest [14] and should be based on the identification, characterization and analysis of all risk components, including hazard, exposure and vulnerability [16].

In addition to the risk assessment of a given system, flood risk management should also consider the element risk reduction and control by means of structural and non-structural measures. Thus, the risk management turns into a continuing cycle of assessing, implementing and maintaining measures to achieve acceptable residual risk and aiming at a sustainable development. A general approach for flood risk management [12] is presented in Figure 2-1.

Moreover, flood risk is defined as *the combination of the probability of a flood event and of the potential adverse consequences* for human health, the environment, cultural heritage and economic activity associated with a flood event [17]. In the flood risk management context, a widely used definition is: *Flood risk is the probability of a flood event multiplied by the consequences* [12].

As shown in Figure 2-1, the following stages conform the base of flood risk management: a) definition of the system and setting the scope and objectives of the analysis; b) qualitative analysis of undesired events; c) quantitative analysis of the flood risk; and d) risk evaluation.

While the *qualitative analysis* comprises the identification and description of hazards, failure modes and scenarios, the *quantitative analysis* determines the probabilities and consequences of the previously defined events. This entails the quantification of risk in a number or a graph as a function of probabilities and consequences in terms of economic, individual and societal risk. An example of graphical representation of quantitative risk in terms of economic values is displayed in Figure 2-2.

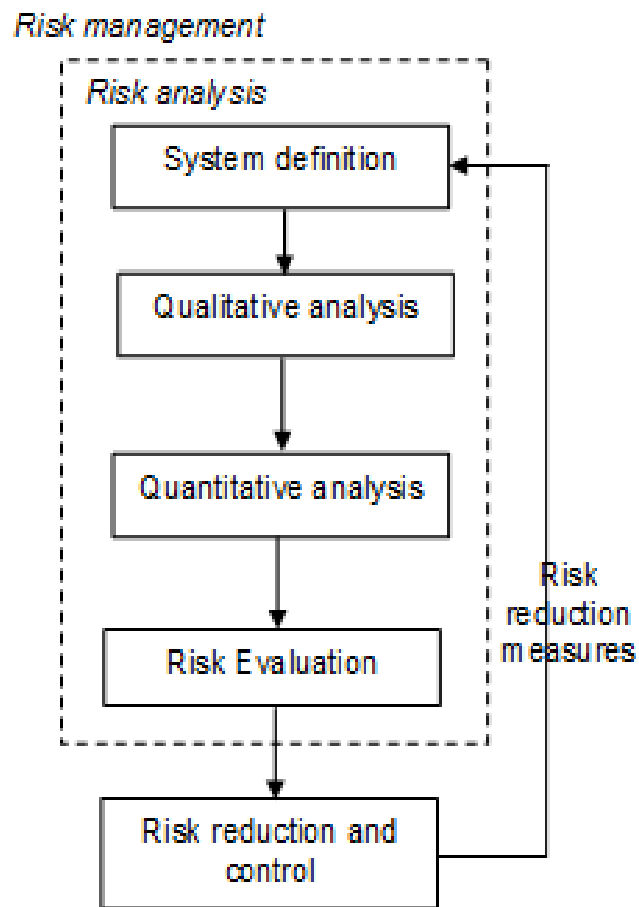


Figure 2-1: General approach for flood risk management. Source: [12]

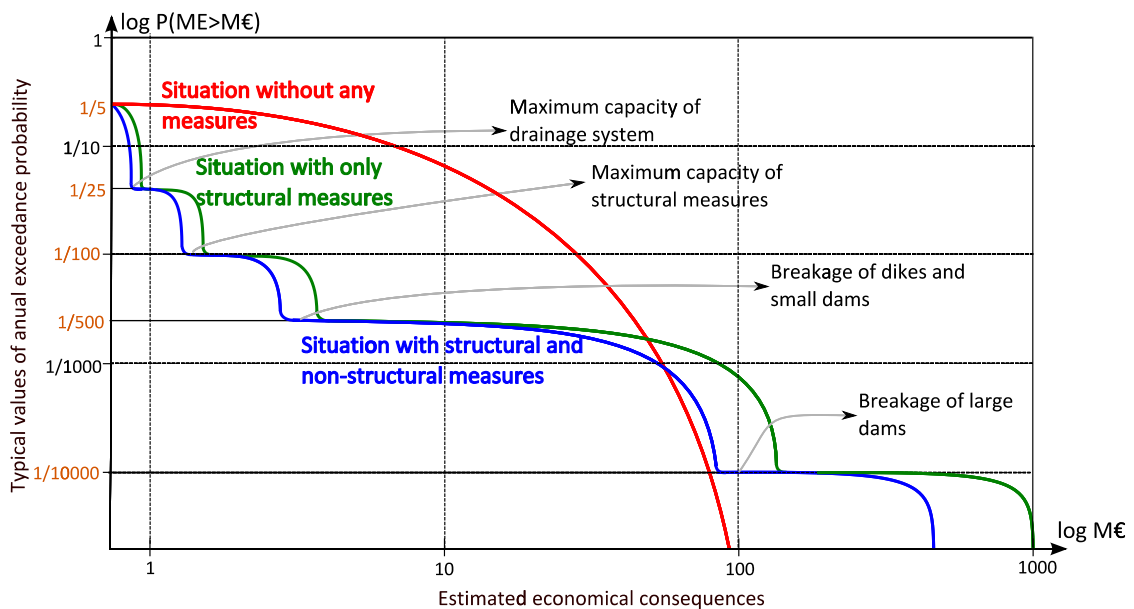


Figure 2-2: FD graphical representation of quantitative risk in terms of economic values. Source: [1]

Finally, the *Risk evaluation* involves understanding and interpreting risks and compared them with existing tolerability recommendations, to inform decisions and actions for flood risk management. It is the point where the judgments and values are introduced in the decision-making process (implicit or explicitly) when including the importance of the estimated risks.

Following the recommendations of the HSE [18] three tolerability ranges could be defined. The first region is the non-acceptance region, where the existent risk can only be justified by extraordinary circumstances. The second region is the tolerable region, where risk is under the tolerable limit. In this region, risk should be analyzed as it is only socially accepted if it accomplishes the ALARP principle (As Low AS Reasonably Practicable). Thus, risk is only tolerable if its reduction is not practicable or if the reduction costs are high. Finally, within the acceptance region, the risk could be considered low or adequately managed. These regions are shown in Figure 2-3.

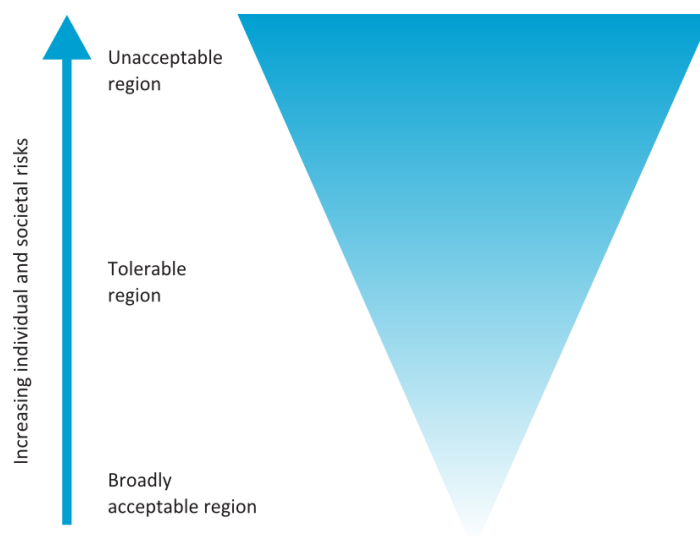


Figure 2-3: Graphical representation of tolerability regions. Source: HSE [18].

An example of tolerability criteria regarding social risk that have been applied to different flood risk cases is given by [12]. These standards are limits over the FN figures and are based on the local population's acceptance level, which are less restrictive if the population is aware of its risky situation and voluntarily decide to stay, and more restrictive if the risk is assumed involuntarily.

2.2.2. Flood Risk Analysis: Methodologies applied in civil infrastructure

Floods being a major cause for significant damage worldwide have increased the need for the application of risk analysis techniques to analyze and assess flood risk from natural hazards and response of civil engineering infrastructure to a flood event [16].

In this context, several authors and projects have addressed the issue of dam and flood risk analysis: The SUFRI project [1] proposed a methodology for analyzing flood risk in urban areas and the study of the effect of non-structural measures; In the Netherlands, a number of recent publications provide information and examples with a focus on flood risk analysis for dike ring areas [19], [20]; the United States Army Corps of Engineers (USACE) have initiated in the 1990's their own processes for risk-informed dam safety management [21]; In Spain, a Technical Guide on Dam Safety [22] was published, entitled *Risk analysis applied to dam safety management* which is a recent milestone in the field of dam safety management.

In the following, some of the above methodologies are presented to give a starting point and describe the basis to implement a Flood Risk Methodology that could be used for the flood risk assessment of road type infrastructure.

Dam Risk Analysis

Flood defenses and dams provide significant benefits to society, such as hydroelectric production, flood protection, water supply, irrigation and recreation. Such a great value for society is faced with a likelihood of a failure that can trigger flooding and damage to downstream areas. For that reason, dam risk assessment has turned into an excellent technique to evaluate different failure scenarios [16].

In 2012, the publication *Risk analysis applied to management of dam safety* by the Spanish National Committee on Large Dams (SPANCOLD) [22] is a recent milestone in the field of dam safety management. This document describes the general process for the application of Risk Analysis in dams with the objective of supporting decision making and the prioritization of risk reduction measures.

In this context, dam safety management is linked to the different components of risk: loads, system response, and consequences. Every process involved in dam safety management is integrated in a logic system (or risk model) capable to aggregate all information inherent to the system to help dam owners and operators in decision making as shown in Figure 2-4.

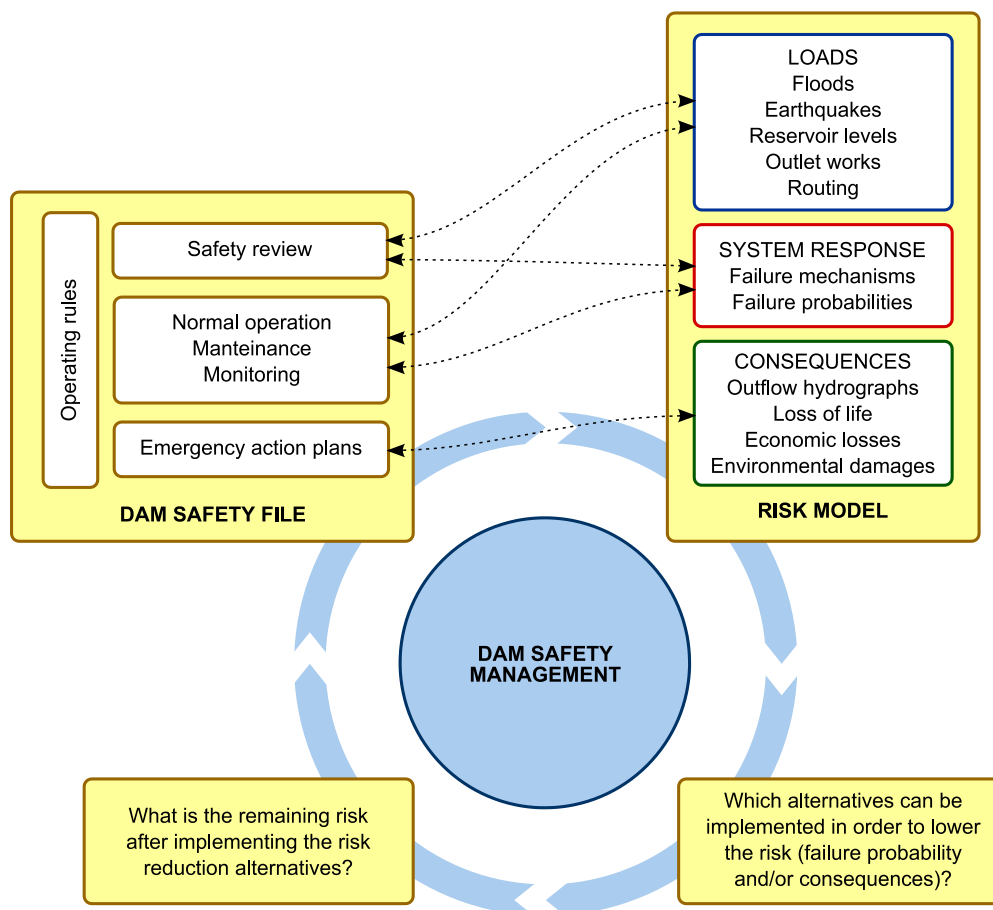


Figure 2-4: Integrated Dam Safety Management and Links to Risk Models and Dam Safety File. Source: SPANCOLD [22] .

SPANCOLD [22] proposed a methodology to analyze risk in dam infrastructure. The different steps of the recommended Risk Analysis process are shown in Figure 2-6. .

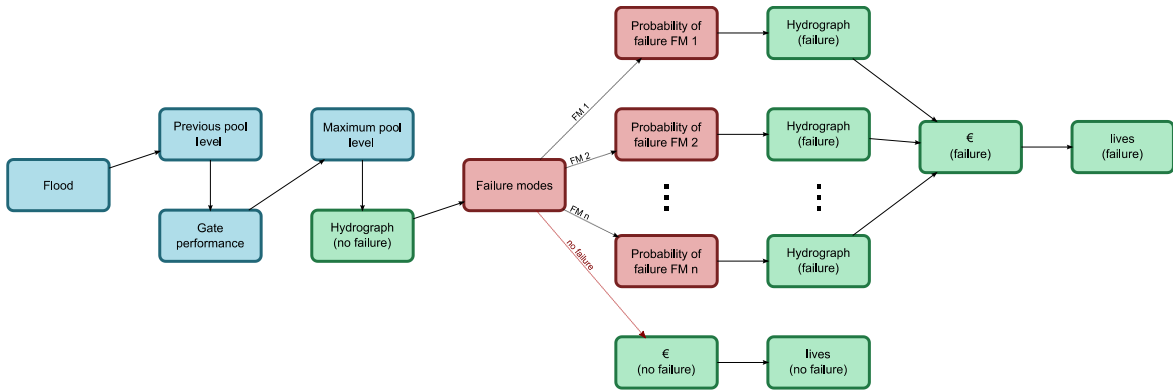


Figure 2-5: Generic dam risk model architecture.

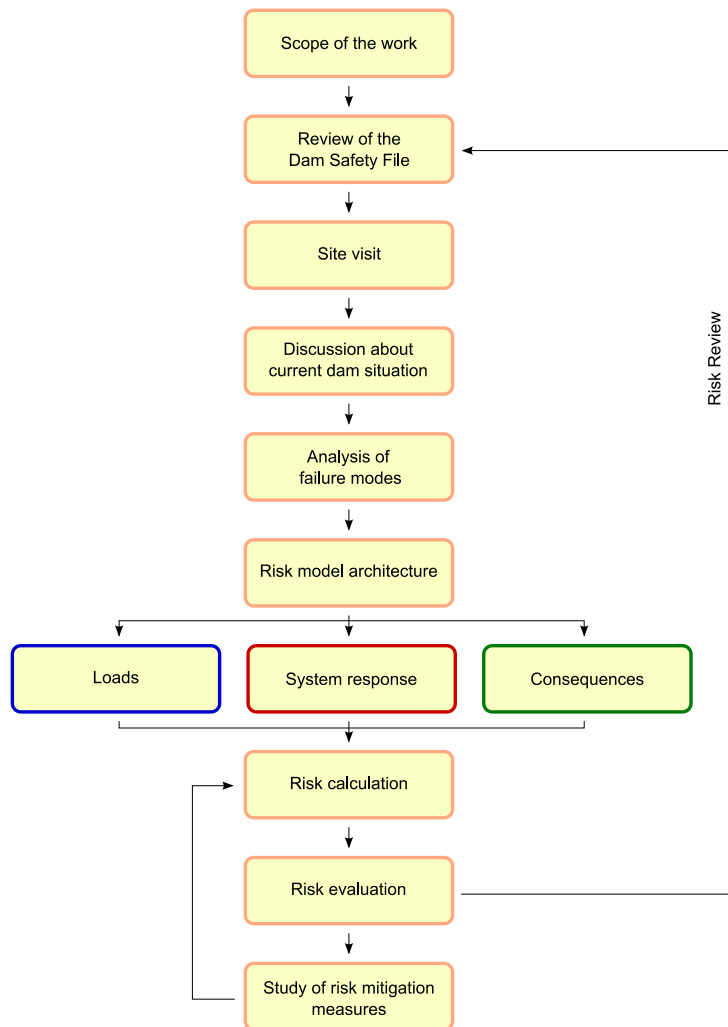


Figure 2-6: Generic Structure of Processes for Risk Analysis. Source: SPANCOLD 2012.

The following similarities and differences can be found in comparison with the general methodology for flood risk assessment proposed in [12] and shown previously in Figure 2-1:

The process in Figure 2-6 starts with data and information gathering and analysis and a technical visit to the dam to analyze its current situation, a stage that corresponds to the *System Definition* in Figure 2-1. In [22] the qualitative phase is introduced as a *Failure Mode Identification Session*. Here, after an individual deliberation, experts and infrastructure managers identify together the potential failure modes that will be introduced in the quantitative risk model. Next, the quantitative analysis is achieved by the definition of a risk model, which should include the required data on loads, failure probabilities, and consequences, in a structured model as shown in Figure 2-5 (example of a generic influence diagram). Finally, the risk results are evaluated based on international tolerability recommendations and are used to establish potential risk reduction measures, analyzing their efficiency and utility.

Both methodologies are conceptually similar, following the same conceptual stages along the processes. Nevertheless, the methodology proposed in [22] is, of course, focused on dam infrastructure and introduce two concepts that are key within the whole analysis process: the *Failure Mode Identification Session* and a *Generic risk model architecture* that should be adapted consequently for every case of study.

SUFRI Methodology

The SUFRI (*Sustainable Strategies of Urban Flood Risk Management*) methodology [1] can be used for the assessment of any source of flood hazard, but it has been developed in detail for river and pluvial flooding. Its intention is to improve flood risk management in case of flood disaster, with special focus on non-structural measures. The overall scheme proposed by the SUFRI methodology to assess flood risk is presented in Figure 2-7.

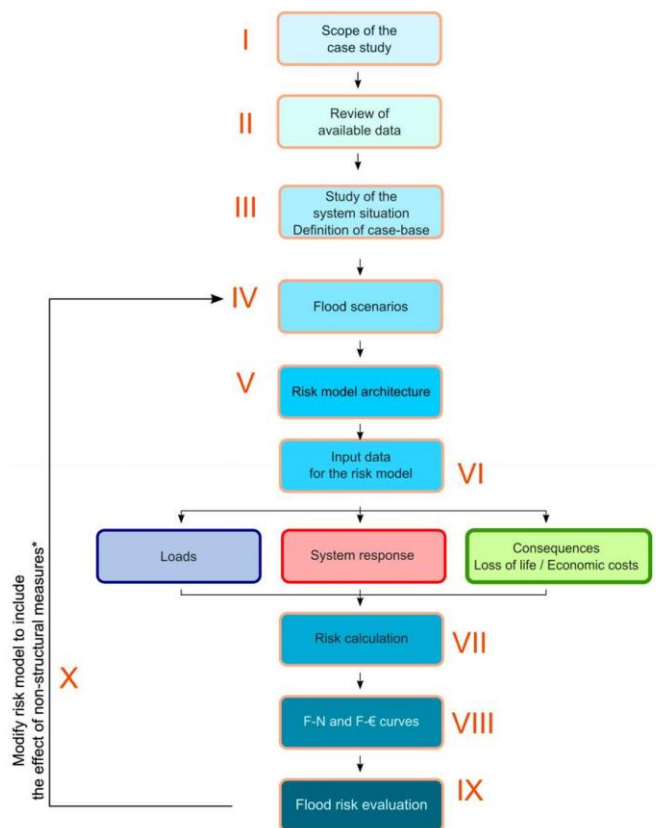


Figure 2-7: Overall scheme proposed by the SUFRI methodology to assess flood risk

For detail information of how to approach each of the SUFRI stages one can refer to [23]. In the following, the method phases are summarized and compared with the other methodologies already presented.

- First, the *scope of the study* should be established, determining the scale of the project (National, Regional, Local), the required level of detail and data and time requirements.
- The *review of available data* aims to define aspects such as the study units, time categories or land use categories. The following step is to define a risk-model for the *base-case scenario*, which will allow for further comparison of different flood risk scenarios and alternatives.
- Definition of *flood scenarios* will determine the range of potential events and damages. Each flooding scenario is identified by a flow rate at the study site Q_f (m^3/s) and a return period T (*years*).
- In the *risk model architecture* step three parts can be distinguished: (1) Loads, (2) System Response and (3) Consequences. The *input data for the risk model* is a critical step in the procedure, as the final results highly depend on data quality and uncertainty.
- For Loads, hydraulic magnitudes (Return Periods, hydrographs, peak flows, and annual probabilities of exceedance) are obtained from hydrological studies. Input data for system response should include all potential failure modes, conditional probabilities for each loading scenario defined by its hydraulic parameters (such as flooded area, depth, velocity, arrival time) which are obtained from hydraulic models.
- Finally input data for *Consequences* normally require information regarding potential loss of life and economic losses. For loss of life estimation, SUFRI methodology proposes an adaptation of the Graham method [24]. For economic losses estimation, SUFRI methodology suggests to use damage-water depth curves as shown in Figure 2-8.

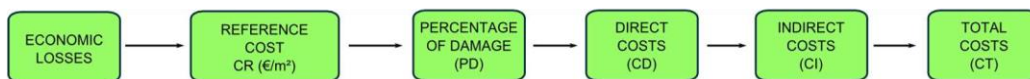


Figure 2-8: SUFRI methodology to assess economic losses.

The aim of the *risk calculation* phase is to combine every possible combination of probability and consequences and to provide values of societal and economic risk for every scenario. The representation in *F-D Curves* enables to evaluate flood risk and provide a useful tool for results comparison.

Within the *Flood Risk Evaluation* phase, results are compared with tolerability criteria on flood risk. Finally, *non-structural measures* such as emergency plans, warning systems, new communication systems, and protocols are analyzed to reduce flood risk at the area under study.

As can be inferred from the previous summary, SUFRI methodology gives extensive information on how to develop a quantitative flood risk assessment, in which the conceptual background and different stages are conceptually similar to the ones found in [12] and [22], shown previously in Figure 2-1 and Figure 2-6 respectively.

However, SUFRI is developed to be used for river flooding in urban areas in which the hazard assessment step does not depend on the affected infrastructure, adapting to any source of flood hazard, explaining how to define the different flood scenarios, what the typical input data requirements are and how to link them to a specific risk model architecture proposal. It also proposes specific methods for consequence estimation, a risk representation in FN curves and focus on different non-structural measures to mitigate flood risk at project area. On the opposite, less focus is given to the *Failure mode analysis*, which was a key part of the process in [22].

At this point of the literature review, the author considers that the overall process proposed in the SUFRI methodology could be adapted to a flood risk analysis of a road segment infrastructure affected by river flooding.

An integration with the methodology proposed in [22] could be achieved by introducing an intensive *Failure Mode Identification* session in the qualitative phase, involving infrastructure managers and multidisciplinary experts. More importantly, the main difference with respect to an urban-oriented flood risk approach comprises the nature of the potential failure modes involved and the consequence assessment, which should be adapted especially to road type infrastructure. Thus, the concepts of transportation system response to river flooding and road vulnerability are treated separately in the following sections.

2.3. Road infrastructure response to river flooding: A probabilistic approach

Roads, being lineal-type infrastructure up to lengths of hundreds of kilometers, normally have to go across valleys and mountainous landscapes, where the road axis is frequently intersected by river streams or run parallel to the river course. Extreme weather conditions or other natural phenomena such as hurricanes or river flooding can make large part of the road network impassable, resulting in potential huge repair costs and indirect losses of travel time by traffic congestion or delays [25] [6].

As stated in a recent study [26], road vulnerability after a flood event has been already taken into account in several researches, however, there is still a gap in the literature regarding road risk assessment after a flood as a key criterion.

In this Msc thesis, the focus is given to pluvial and river flooding-induced hazards, which constitute a main problem for road segments within bigger road networks. Inside this section, the aim is to perform a review of how to determine the likelihood and susceptibility of the main potential road failure modes (FM). Of course, it is possible to think of uncountable different road failure modes after a flood event; however, specific variables for each project such as location site or the infrastructure characteristics will ultimately determine the failure modes that should be included in a quantitative risk analysis.

Considering the specific characteristics of the case study presented, and the conclusions found after the Failure Mode session held along this graduation work (more information can be found in following sections), the main potential failure modes that will be considered for a road risk analysis are: pavement damage due to flooding and hydrodynamic failure of bridges (deck-pier connection and scour-induced instabilities).

2.3.1. Pavement response in case of flooding

Recent natural disasters such as hurricanes Katrina in 2005, I and H in Country Z in 2008, Sandy in 2012 in the USA or flooding in Australia in 2010-11 and 2013 have severely impacted road infrastructure and increased the awareness towards assessing the response of pavements after a flooding event. A flooding event could lead to a total reconstruction of the road segment due to severe damage or, on the other hand, the road segment may still be in service but inundated for several days, which could affect to the base and sub-base functional and structural condition [27].

The impact of flooding on pavement structure and performance has been addressed by several authors. Initial studies [28] identified that moisture intrusion causes losses in the resilient modulus, at granular and subgrade layers, *leading to increased pavement deflections and reductions in pavement life*. In this same line, the road performance after the effect of Katrina Hurricane in the USA in 2005 was studied [29], showing that flooded sections increased deflection values up to a maximum of 7 times in comparison with the initial ones. Similar researches [30] revealed that the pavement strength losses and subgrade modulus due to flooding were 18 and 25 percent respectively. Moreover, [31] when evaluating Hurricane Katrina data, found that no damage was found in rigid and composite pavements or that flooding duration beyond 7 days did not have any further damaging effect on pavements.

Moving specifically towards the field of road risk assessment, understanding risk as the likelihood of an event and its consequences, only limited studies are found in the literature that have dealt with the topic within a pavement management system (PMS). The introduction of risk as a factor in life-cycle cost study for project level was achieved [32] but a proper risk assessment was not performed. Others [33], relied in engineering judgments to define likelihoods of road failure and consequences. For instance, a semi-quantitative risk analysis was performed for unbound granular materials using a fault tree methodology and found reasonable agreement with actual road data [33]. However, one can find limitations in the fact that the method is subjective when quantifying risk ratings and only applicable to low traffic volume roads [26].

The analysis performed by [34] where a deterministic model was developed to assess the time-variation of structural deterioration of pavements after flood, proved that the use of a probabilistic model for this matter is more justified due to resembled uncertainties in the results.

Trying to improve the flood risk evaluation of roads towards a more detailed and reliable assessment, a semi quantitative flood risk analysis is proposed to address pavement performance after a flood [26]. The road pavement condition is evaluated according to the international roughness index (IRI), proposed by World Bank experts (UMTRI, 1998), and that represents driving comfort by simulating the movement of the accumulated vehicle suspension through a specific road profile length of the x and is expressed in (m/km). For example, if IRI > 16 m/km, the road condition will correspond to a deteriorated unpaved road (See Figure 2-13).

The IRI is used to calculate flood consequences on pavement and risk scores [26], validating the results with historical data and showing an acceptable agreement. In this study, risk is based on the likelihood and consequences of an event. The likelihood of a flooding event is defined by its return period and the consequences score by the impact on pavement performance in terms of estimated change of IRI after the flood. The consequences are classified in a semi-quantitative risk matrix [26] presented in Table 2-1:

Frequency/ ΔIRI	1 in 2 years	1 in 5 years	1 in 10 years	1 in 50 years	1 in 100 years
< 2.0	Low risk				
[2.0 - 3.0]	Moderate risk				Low risk
[3.0 - 4.0]					
[4.0 - 5.0]	High risk			Low risk	
> 5.0					

Table 2-1: Semi-quantitative risk matrix to address pavement performance after a flood. Source: [26]

The methodology was applied to a main road network in Queensland (Australia), for 27 road groups considering pavement types, strength and traffic volume. From the results obtained [26], the proposed methodology proved to be useful for evaluating which road groups performed better after a flooding event (had lower risk scores). As concluded in the study, *these results should be helpful in the upgrading from flood damaged roads to flood resilient pavements*, however, for a full-quantitative flood risk assessment, consequences should be measured in a quantifiable monetary metric and not only in an index form.

From the previous analysis [26], the IRI (international roughness index) have proven to be a *representative index in measuring pavement condition (i.e. deterioration against time)*, which, as it will be shown in Section 2.4.2 is also linked with vehicle operating costs, travel time costs and accidents [35] [36]. However, it still not a good index to measure the structural integrity of the road, which will be assessed using flood damage curves as will be shown later in this report.

Another important contribution to the field of road risk assessment is provided by [27] [37] with the introduction of probabilistic road deterioration (RD) models. In his analysis, the author developed probabilistic roughness-based and rutting-based road-deterioration (RD) models, used to predict pavement performance over its life cycle, accounting for flooding strategies (both pre- and post-) and applied it to a case study in Queensland's main road network. In [27] pavement performance (structural and functional) conditions are represented by

two main factors: Roughness (IRI), directly related with vehicle operating costs, accidents and comfort; and rutting, which relates to structural resistance and accidents.

The methodology in [27] generates RD models by Montecarlo simulation with non-homogeneous Markov chains using a percentage transition method and real data for both roughness (IRI, international roughness index) and rutting variables. Therefore, the development of RD models for a specific road segment, with IRI and rutting versus time graphs as main outputs, requires a certain amount of gathered data. The results concluded that these RD models are useful to predict pavement performance for different flooding probabilities, showing consistency and similar trends between observed and modeled data and an increasing deterioration of pavements with higher probabilities of flooding. In addition, the RD models proved to be helpful to select optimal measures to rehabilitate a flood-damaged road and to ensure cost-effective preservation after flooding events, which is a main goal of Pavement Management Strategies (PMS).

For developing countries, where transportation network is a key asset and suffer frequently from flood related issues, lack of reliable and available data is an undeniable reality that could prevent the application of useful and proven probabilistic methodologies such as the one proposed in [27] [37]. However, the extended use of IRI as a pavement performance indicator in several worldwide road infrastructure projects added to an experienced engineering judgement should be enough to propose a safe guess of the IRI index for pre- and post- flood scenarios.

As far as the author's knowledge reaches, none of the road risk assessments consulted have transformed the changes in the IRI after flood into indirect economic consequences, being the latter's linked to vehicle operational costs and travel time costs. So far, only semi quantitative approaches by using subjective indicators as in [26] appear in the literature.

From the previously gathered information, a goal of this graduation Msc thesis is to bring a new approach to improve quantitative road risk assessment by considering pavement response to flooding events. To do so, the author will incorporate part of the existing methodologies by following an event tree approach for risk assessment used in [33] and in dam risk assessment [1] [22]; the use of the IRI as a pavement condition indicator as in [27] [26] ; and will also incorporate new approaches such as the transformation of IRI changes due to flooding events into indirect economic consequences of travel time costs, as will be described in the Section 2.4.2 of this report.

2.3.2. Bridges response in case of flooding

River flash floods after strong and intense precipitation events such as hurricanes or tropical storms are known to be a common cause of bridge failure. Especially when the bridge deck is completely or partially submerged, the structure is not able to withstand the external hydrodynamic loads and ultimately collapse.

Numerous examples of river bridge collapses have occurred in the past due to extreme hydrological events. For example: in 2005 some of the main bridges in Louisiana were affected during Katrina hurricane [38]; the Yabitsu bridge in the Yabetchi river (Japan) suffered a collapse during a flood in August 2013 [39]; or several damages in some of the bridges and infrastructure along the X road (Country Z) were noticed after the 2008 I and H hurricanes [40].

A bridge failure normally implies severe consequences in economic terms, such as high direct reconstruction costs and intangible indirect costs due to travel time loss and isolation of populated areas during an emergence episode. For those reasons, the topic of bridge response during river floods has been of wide interest for researchers in the past. A majority of the state of the art in the topic deals with the calculation of flow forces on the deck superstructure and piers, where numerical calculations and experimental models are used to predict flow depth, velocity and turbulence as key variables. In this context, a recent and extensive literature review in the field of hydrodynamic forces on bridge structures is given in [39] or [41]. Other authors have addressed

the topic of scour around piers as a potential failure mode for river bridges. In this context, the [42] provide a technical guide that is a reference in the literature.

Hydrodynamic loading on submerged bridges

The magnitude of the load on bridges due to hydrodynamic forces depends on flow conditions and bridge characteristics. The main hydrodynamic forces that should be considered in a stability analysis [42] are represented in Figure 2-9. The component of the resultant of shear and pressure forces (due to viscosity and turbulence) in the flow direction is known as the drag force and the component that acts normal is known as the lift force.

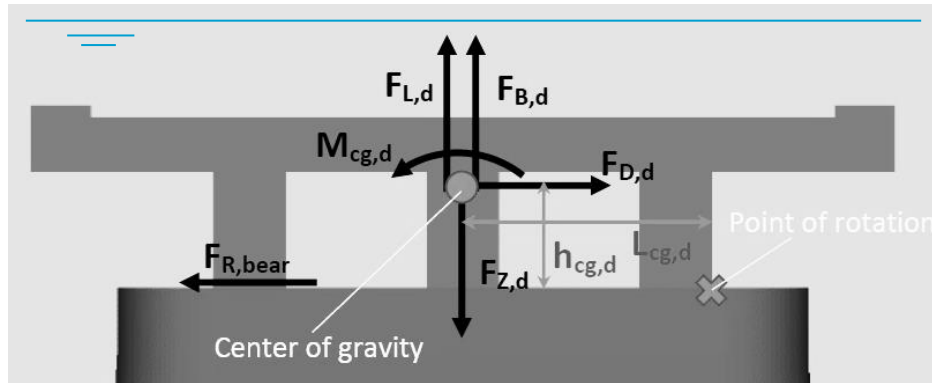


Figure 2-9: Acting forces on a submerged bridge-deck. Source: [39]

Normally, forces in bridge structures are expressed in terms of several ratios. The inundation ratio depends on the upstream inundation depth, elevation of the bridge and deck thickness, and was used in several researches such as [42] [43] and [44].

$$h_* = \frac{(h_u - h_b)}{s} \tag{2-4}$$

Where, h_u is the water depth; h_b is the height until the base of the deck and s is the deck's width (vertical direction).

The blockage ratio (B_r) and the proximity ratio (P_r) [45] are also widely used and are expressed as:

$$B_r = \frac{s}{h_u} \tag{2-5}$$

$$P_r = \frac{h_b}{s} \tag{2-6}$$

This said, the drag forces are normally expressed as:

If inundation ratio is greater than one ($h^* > 1$):

$$F_D = 1/2 * C_D * \rho * V^2 * s * L \tag{2-7}$$

If inundation ratio is lower than one ($h^* < 1$):

$$F_D = 1/2 * C_D * \rho * V^2 * (h_u - h_b) * L \quad (2-8)$$

Where F_d is the drag force in N; C_D is the drag coefficient (non-dimensional); ρ is the density of water (kg/m³); V is the free stream velocity in m/s; h_u is the flow depth from river level (in m); h_b is the distance from the ground to the bottom of the deck's girder (in m); and L is the bridge length (in m).

Moreover, the superstructure stability in the vertical direction depends on the lift forces acting perpendicular to the flow directions, which are expressed as:

$$F_L = 1/2 * C_L * \rho * V^2 * W * L \quad (2-9)$$

Where F_L is the lift force in N; C_L is the drag coefficient (non-dimensional); and W is the bridge width (in m).

The moment around the center of gravity M_{cg} (in KNm) is expressed as:

$$M_{cg} = 1/2 * C_M * \rho * V^2 * W^2 * L \quad (2-10)$$

Where C_M is the momentum coefficient (non-dimensional).

In the literature, most of the authors agree in the use of the above expressions to calculate the hydrodynamic forces. Nevertheless, there is not such an agreement when determining the value of the non-dimensional coefficients (C_D , C_L , C_M), which constitute key variables in the above equations.

In [44] is stated that the non-dimensional force coefficients are related to the inundation ratio (h) and Froude number (F_r) when assuming a time-averaged steady state flow.

$$C_F = f(h^*, F_r) \quad (2-11)$$

where

$$F_r = \frac{U_u}{\sqrt{g * h_u}} \quad (2-12)$$

Where U_u is the average flow velocity along the river sections upstream the bridge.

In [44] the construction of a scale model and measurements with dynamo-meters allowed to estimate the magnitude of the force coefficients as a function of both variables (F_r and h^*). A peak value of 3.4 was estimated for drag coefficient (C_D) around $h^*=1.2$. On the opposite, the lift coefficient (C_L) showed only negative values with a -10.0 peak value independent of the Froude number.

Another important research on the topic was carried out by [45], where several experiments were performed to assess the effect of the Froude number, the inundation ratio and the superstructure's proximity ratio on the hydrodynamic loading of the bridge structure. To that end, different bridge and pier geometries and flow configurations were tested. The outputs of the experiments (more than 500) are given in tables and design figures, where the dependencies of the force coefficients on the different variables are shown. Following the same approach, [43] also included the effect of proximity ratio and inundation ratio when providing design values for hydrodynamic loading on bridge superstructures.

Similarly, [42] studied the effect of hydrodynamic forces on inundated bridge decks, introducing a combination of physical experiments with numerical modeling techniques using Computational Fluid Dynamics software. The experiments and calculations were performed for different Froude numbers, three bridges configurations and different values for the inundation ratio. Opposite to [45], the effect of the proximity ratio was not considered.

The results for drag coefficient (C_D) showed positive values, increasing with F_R and a peak value of 2.0 when $h=1.5$. Similar to the results found in [44], the lift coefficient (C_L) was negative for all inundation ratios and Froude numbers tested. The moment coefficient peaked at $h^*=0.8$ and approached a constant value while the ratio increased, with an observable tendency to rotate in the flow direction sense.

Following the approach found in [42], in a recent study by [41] physical experiments were performed to validate numerical simulations in order to quantify the loads on rectangular bridge cross sections and provide design countermeasures to reduce the probability of bridge failure. To this end, more than 700 simulations were performed, accounting the effect of several variables for bridge configuration and flow conditions. Values for lift, drag and moment coefficients are provided as a function of the studied variables, and showed a reasonable agreement with the results from researches already presented on this matter. An important contribution in is the performance of an incipient failure analysis, which main output are the contour lines of the threshold of a rectangular-cross-section-bridge failure. This method claims to be more reliable than traditional methods which only assume constants values for drag and lift coefficients.

Another study on hydrodynamic failure of river bridges is presented by [39] where a post-failure analysis of a typical bridge on spread footings is performed. In this study, flume experiments are completed to simulate steady-state hydrodynamic forces on the bridge, with Froude number, flow depth and debris load as main variables. The experiments were compared with predicted values of the hydrodynamic forces by using values found in for the hydrodynamic coefficients. Significant differences were found between the predicted and experimental results, mostly due to an overestimation for the debris effect in the predicted values. Also, discrepancies were noticed between the predicted values in [42] for the drag coefficient and the ones found in the experiment results. From the results, the main conclusion is that the hypothesis of a combined deck-pier failure (bridge as a whole) is disregarded for any of the hydraulic conditions that were tested. Also, the hypothesis of a subsequent failure of deck and pier was corroborated; however, it only occurred when debris loads were considered in the experiments. The threshold for deck movement was set for inundation ratios greater than 2.0 and Froude numbers in the range of 0.14-0.32. Piers failed at Froude numbers greater than 0.34 when flow over-topped the pier's height.

In conclusion, several experimental and numerical simulation results and recommendations for adequate design values for the hydrodynamic coefficients have been presented, however, the results are not always aligned and the existing uncertainties suggest the need to describe these variables as stochastic and not in the traditional deterministic way.

To this end, available results from [41] [42] and [45] will be used to find adequate probability distributions to describe the hydrodynamic coefficients stochastically and to incorporate them into the limit state equations for bridge failure under hydrodynamic loading. The proposed approach is explained in detail in Chapter 3: Intended approach.

Probabilistic approach

So far, a review of what are the main hydrodynamic forces that should be considered in a bridge stability analysis under flood conditions and their estimated values as a function of flow conditions and bridge configuration have been performed.

Now, the interest is put on the probabilistic approach to assess the likelihood (i.e. failure probability) of bridge collapse once the hydrodynamic forces are known. However, little is found in the literature regarding specific methodologies to assess the failure probability of bridge collapse due to river flooding. Only a first insight is presented in [39] where the use of a limit state function is explained Eq. (2-13) where R stands for restoring forces and S for soliciting, could be a valid method in combination with a Monte Carlo simulation.

$$Z = R - S \quad (2-13)$$

Correlating a certain probability distribution to each of the forces on Eq. (2-13), the probability of failure can be calculated by finding the ratio of simulations in which $Z < 0$ to the total number of simulations performed. Even if during his experimental research [39], only deterministic calculations were performed and the probabilistic approach was left aside, the limit state functions, for vertical and horizontal forces and overturning moments, remain the same for further work on this topic.

The restoring forces will ultimately depend on the gravitational force, which at the same time depend on the bridge (deck and pier) geometry/material and the capacity of the connection between deck and pier. Normally, the bridge geometry and material characteristics are known, and little uncertainty is expected in this matter. For the capacity of the connection, a detailed analysis is made in [39] for a typical elastomeric bearing often used for short-span, reinforced or pre-stressed concrete bridges after analyzing several potential failure modes that could govern the deck-pier connection failure.

From the previous, it can be stated that most of the undergone research work has focused on the determination of values for the hydrodynamic coefficients in order to calculate the loading forces exerted by the water flow to the bridge. Multiple experimental tests and numerical simulations have been performed in order to give valid design values to use in hydrodynamic calculations depending on bridge geometry and flow conditions. However, there is still a significant uncertainty regarding which values should be used in the calculation, as shown by the discrepancies between experimental results and predicted values found in [39].

Thus, a stochastic approach based on the available results from the existing studies will be used in order to choose adequate probability distributions to define the hydrodynamic coefficients and other key variables involved in the calculation of bridge stability, in order to find fragility curves that could be incorporated into a risk model to assess the quantitative risk of bridge failure under hydrodynamic loading.

Evaluating scour at bridges

The scour development in a bridge foundation has been studied in detail in the literature. A reference document which presents a complete manual for the design and evaluation of bridge foundations against scour during rivers floods is [46]. Three scour types are analyzed: long-term scour/aggregation processes, contraction scour and piers scour.

The magnitude of the long-term scour/aggregation processes is usually due to a problem of river channel instability by modifications in the river or in the upstream basins (dams constructions, canalizations, mining and aggregates extraction), causing river degradation/sedimentation until a new equilibrium is reached. Several methods for estimating long-term erosion/sedimentation are found in [46], and their study, as not being directly related to a flood-induced scour issue, are not part of the scope of this graduation work.

Contraction scour occurs when the flow area in the section where the bridge is located is reduced by a construction of a bridge, resulting in a decrease in the original river bed elevation to the width of the bridge opening. The equations that determine contraction scour are based on the principle of conservation of sediment transport and two types are discerned: *Live-bed* scour when there is river bed material transport from the upstream sections of the bridge and *Clear-water* scour when there is no river bed material transported from the upstream sections of the bridge. Due to potential "armoring" processes that may occur (larger particles are placed over smaller sizes limiting their transport), the values are usually calculated for both cases and the smallest value is used [46].

The recommended equation for predicting potential "Live-Bed" erosion is expressed as:

$$\frac{y_2}{y_1} = \left(\frac{Q_2}{Q_1}\right)^{\frac{6}{7}} * \left(\frac{W_1}{W_2}\right)^{k1} \quad (2-14)$$

$$y_s = y_2 - y_0 = (\text{contraction scour})$$

$$k_1 = f(V^*, T); V^* = (g * y_1 * S_1)^{0.5}; T = f(D_{50})$$

Where y_1 is the flow depth in the upstream section of the bridge (in m), y_2 is the flow depth in the contracted section (in m), y_0 is the flow depth in the contracted section before erosion (in m), Q_1 is the flow rate in the upstream section (in m³/s), Q_2 is the flow rate in the contracted section (in m³/s), W_1 is the width in the upstream section (in m), W_2 is the width in the contracted section (in m) and K_1 is an empirical coefficient that takes the following values according to the shear Speed (V^*) and the suspended material speed (T).

V^*/T	K	Transport mode
< 0.5	0.59	River bed material
0.5 to 2.0	0.64	Some suspended material
> 2.0	0.69	Most of suspended material

Table 2-2: K_1 values. "Live-Bed" contraction scour.

The recommended equation for estimating potential "Clear-Water" scour is as follows:

$$y_2 = \left[\frac{K_u * Q^2}{D_m^3 * W^2} \right]^{\frac{3}{7}} \quad (2-15)$$

$$y_s = y_2 - y_0 = (\text{contraction erosion})$$

Where y_2 is the flow depth in the contracted section after erosion (in m), y_0 is the flow depth in the contracted section before erosion (in m), Q is the flow rate in the contracted section (in m³/s), D_m is the diameter (in m) of the smallest non-portable particle ($1.25 D_{50}$), W is the width in the contracted section (in m) and K_u is an empirically determined exponent and which takes the value of 0.025 in SI units.

Localized scour in the bridge piers is function of the material characteristic which conforms the riverbed (granular, non-granular, cohesive, non-cohesive, erodible or non-erodible rock), the flow characteristics (speed, flow depth and angle of attack), pier/foundation geometry (singular column, several columns, rectangular or circular shape, etc).

The HEC-18 equation is recommended for the study of the maximum scour depth estimated in the bridge piers foundation for simple substructure configurations and fluvial flows in alluvial sand beds. The equation takes the following form:

$$\frac{y_s}{y_1} = 2.0 * K_1 * K_2 * K_3 * \left(\frac{a}{y_1} \right)^{0.65} * F_r^{0.43} \quad (2-16)$$

Where y_s is the depth of erosion, y_1 is the flow depth immediately upstream of the studied pier, K_1 is a correction factor for the pier shape, K_2 is a correction factor for the angle of attack of the river flow, K_3 is a correction factor for the riverbed condition, a is the width of the pile (in m), L is the length of the pile (in m), Fr is the Froude number immediately upstream of the pier (dimensionless).

The following tables show the different K correction coefficients values for in the HEC-18 equation for maximum scour hole near the bridge's piers

Pier shape	K_1
Squared	1.1
Rounded	1
Circular	1
Group of cylinders	1

Sharpen 0.9

Table 2-3: K₁ Correction factor.

Angle	L/a = 4	L/a = 8	L/a = 12
0	1	1	1
15	1.5	2	2.5
30	2	2.75	3.5
45	2.3	3.3	4.3
90	2.5	3.9	5

Table 2-4: K₂ Correction factor.

River condition	Dune height	K ₃
Clear-water scour	-	1.1
Plane bed	-	1.1
Small dunes	[0.6 3]	1.1
Moderate dunes	[3 10]	1.2
Big dunes	> 10	1.3

Table 2-5: K₃ Correction factor.

As stated in [46], the report presents the state of knowledge and practice for the design, evaluation and inspection of bridges for scour, and therefore, its procedures and recommendations for estimating bridge scour and consequent failure will be adopted during this graduation work.

2.4. Road vulnerability

Despite its critical importance for society, the study of road vulnerability has not been a focus of interest until recent years [47]. As stated by [4] not even a general agreement has been reached between researchers regarding the definition for road vulnerability.

When dealing with the general subject of vulnerability in engineering systems, terms such as robustness, redundancy, resiliency or reliability may come to mind. The latter, meaning the probability that a system performs within predefined standards during the period of time intended} [48], is found to be of special importance in the road transportation system, and it was used [2] to build an initial theoretical basis upon road vulnerability. As stated recently [4], transportation network reliability has been a growing field of study and, thus, is elaborated separately.

In the following, the basic concepts and definitions regarding road vulnerability that have been addressed so far by researchers are presented. In addition, several approaches/methodologies applied to this field are presented, in order to establish a solid and robust framework for the estimation of consequences due to road-damage that will be tackled during this graduation project.

2.4.1. Transportation Network Reliability

Natural disasters and dependency of developing countries on their transportation network increased the need for a framework to assess the planning of both, urban and inter-urban road systems [25] [26]. This need has recently been addressed by transportation reliability studies [49] [50].

The analysis of transportation system reliability integrates two aspects [51]: (1) the infrastructure, which consists in roads, bridges, tunnels, drainage, etc, and (2) the users responses to system behavior, grouping reliability studies in the transportation network in three fields: vulnerability, connectivity reliability and performance reliability [52]. While the latter has been applied mostly to urban-networks dealing with the impact of capacity and travel-time variability, connectivity reliability have been more focused on inter-urban road

networks [4]. In addition, the vulnerability concept is highly related to the consequences of link failure and has been analyzed thoroughly in recent years [53] [54]. In the following, the connectivity reliability and vulnerability concepts are treated separately due to their importance during this graduation work. Performance reliability is left aside as the risk assessment of urban-networks is not under the scope of this study.

Connectivity reliability

Several authors [55] [48] [52] have dealt with the concept of connectivity reliability, which can be defined as *the probability that the network nodes remain connected when one or more links of the network have been removed* and is, thus, determined by factors such as road structure, condition and disaster severity [56].

The literature regarding connectivity reliability is classified in two groups [4]: The first group (1) presents a statistical/probabilistic approach to assess network reliability by the use of complex algorithms [57] [5], the second group (2) uses other less common approaches such as complex network theory or risk analysis to address the issue [56] [58]. If a data-record of adequate length regarding days of road-closure are available, a simple but powerful method to assess connectivity reliability is given by [4]. In his work based on inter-urban transportation networks in Colombia, the number of failures of a specific link is assumed to follow a Zero Inflated Poisson Distribution. For more detail related to the current connectivity reliability of road-network's literature one can refer to [59].

While the above is strongly focused on road reliability at a network's level, in the case of this graduation work, the focus is given to the basic road-segment level. In other words, the aim is to assess the connectivity reliability (or probability of disruption) between two single nodes that are part of a more complex network. In the absence of reliable data regarding the number of days with failure in the road-segment of interest (from which a statistical analysis could be undertaken), it seems logical to focus on the physical structure of the road and the related potential failure modes that could lead to road closure. An example for this approach is given by [10], where, as a part of a more complete probabilistic risk assessment, the susceptibility of road closures in New Zealand due to different natural/anthropological hazards (snow storms, seismic activity and traffic accidents) is studied.

For the case of this Msc thesis, the absence of reliable road closure data brings the author to follow a similar approach to the one found in [10]. Thus, the connectivity reliability issue will be treated by calculating the failure probability of the road segment for each of the failure modes described previously in this literature review (road pavement damage and bridge collapse). To this end, by the means of a hydrological/hydraulic model, flow depths and velocities can be calculated in each of road sections of interest and for each return period. Finally, the use of flood-damage curves for road pavement and the calculation of fragility curves for bridge collapse will give the failure probability as a function of the loading conditions and expected damage.

Vulnerability

Unlike reliability, that measures the probability linked with the functioning or non-functioning of a network segment, vulnerability is more related to network weakness and the consequences of failure once they occur [60]. However, vulnerability is a still developing field of study within transportation infrastructure area of knowledge and a precise definition has not been widely accepted.

Firstly, some authors interpreted road vulnerability as a small incident that can cause a major damage to the road system. However, recent definitions accentuated the function of road systems by relating the concept to reduce levels of accessibility/serviceability because of network failure or degradation. Accessibility [4] is generally understood as the "ease of reaching", meaning the potential to move of an individual by means of public/private transport (demand side). On the other hand, the serviceability term describes the possibility to use that link/route during a given time of period (supply side). When analyzing vulnerability, it is of special interest to focus on events that cause disturbances on traffic. These events, so called incidents, can range from extremely adverse weather to physical failures or traffic accidents, each of them varying in categories of

frequency, predictability, geographical extent, etc.. Vulnerability in the road system is defined as *susceptibility to incidents that can result in considerable reductions in road network serviceability* [2].

Various researchers tried to link vulnerability and the concepts of risk [61] [62] [54] integrating both: (1) the probability of occurrence of an incident causing degradation/disruption, and (2) the resulting consequences once the incident has occurred. As stated in [2], the above mentioned potential incidents cover a wide range of combinations where probabilities and consequences are concerned: from minor accidents that occur in a daily basis to less prone failures (such as a bridge collapse) that result in more catastrophic consequences. This range of possibilities, combining susceptibility and consequences, increases effort and difficulties when dealing with a road risk assessment. A pioneer study in this matter is found in [10], where a probabilistic risk assessment is used to study the potential consequences of road closures in New Zealand due to different natural/anthropological hazards (snow storms, seismic activity and traffic accidents).

By addressing the above concepts presented (incidents, serviceability, vulnerability, risk) in order, vulnerability reduction is seen as a risk reduction involving a wide range of incidents. This could be achieved by two perspectives: (1) a fail-safe way such as the reduction of the probability of a road/bridge to fail, (2) a safe-fail approach, by reducing the consequences extent once the failure has occurred. Figure 2-10 illustrates the above in a Concept Wheel [2].



Figure 2-10: Concept wheel for road risk assessment. Source: [2].

In addition, a great research-effort has been given to the study of vulnerability of whole road networks, trying to find reliable methods for the detection of critical links/infrastructure in the road network. For a thorough review in this matter, the reader is referred to [63]. In this context, [64] proposed a classification of literature referring to link-level vulnerability: A first group (1) referring to full calculation methods, in which the capacity is modified for each link separately and all possible network states should be simulated in order to find the most critical one, and a second group (2) referring to link measures to search for the most vulnerable links within the network.

Within the first group of the above mentioned calculation methods, [61] stated that a reasonable measure of reduced serviceability/accessibility should be the increase in generalized cost of travel and they applied it to a case-of-study of a road network in northern Sweden. Also, other examples of the application of full calculation methods can be found in [62] and [4].

Regarding the second group, several authors determined vulnerability by the application of accessibility-based indicators. The ARIA remoteness index [65] is introduced to determine the most critical location in rural and remote areas. A similar work was developed [66] [53], calculating vulnerability by applying the ARIA and Hansen integral accessibility index in Australia's highway network. In [67], the travel time cost increase is again used as a link-measure to evaluate the critical importance of a given highway segment to the overall system by the calculation of the NRI (Network Robustness Index).

In a quantitative consequence estimation context, the first group of vulnerability calculation methods seems to be more appropriate, as it gives a quantitative metric (increase in generalized cost of travel) to measure vulnerability in a road infrastructure segment.

2.4.2. Measuring Vulnerability

Direct consequences

Natural hazards such as flooding, earthquake or landslides can infer large direct damages in the form of infrastructural repair costs that should not be disregarded when developing a quantitative risk assessment. There are numerous references in the literature that address *Flood Damage Assessment* issue, mainly focusing on the residential losses after urban flooding. As it is far from the scope of this report to do a thorough literature review in the topic of residential damage due to flooding, the reader is referred to the state of the art review provided by [68].

Focusing on direct flood damage assessment in road infrastructure; [68] provides an overview of maximum damage values that have been used in the assessment of tangible damage consequences regarding various case studies. In [69] method that uses depth-damage curves based on analysis of past flood events and on expert judgment to evaluate the economic consequences after flooding of transportation infrastructure is proposed. The methodology [69] is presented in Figure 2-11:

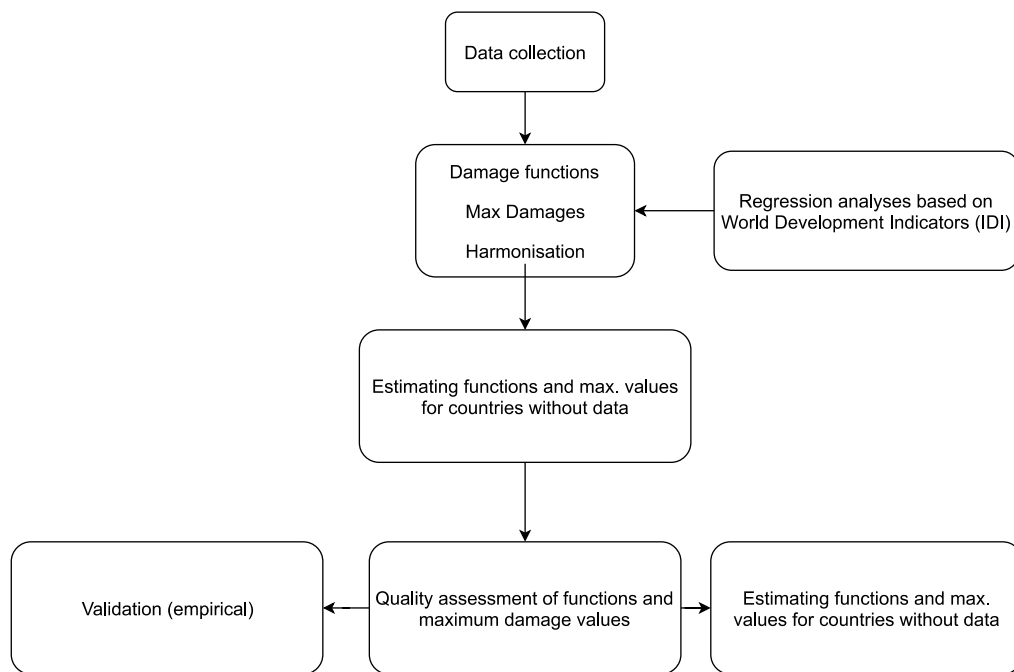


Figure 2-11: Methodology to evaluate economic consequences after flooding and calculate depth-damage curves. [69]

Data was collected for five continents (Africa, Asia, Oceania, North America, South and Central America) and for different damage classes (Residential buildings, Commerce, Industry, Roads and Agriculture). In their report, it is claimed that damage functions for transportation infrastructure are difficult to find and, when they are available, they are quite similar and with limited share in the total (recorded) damage. From the previous statement, they conclude that the application of one global function for paved roads (global meaning valid for any project location globally), based on the average continental functions, is feasible. For unpaved roads, the depth-damage curves estimated for the case of Bangladesh, where the poor economic situation leads to poor infrastructure services, can be chosen as representative. The latter is of course a simplified approach towards road flood damage assessment, as the level of damage will be strongly related to the pavement type; materials

use the structure profile and particular project conditions. However, for a first approach to calculate the pavement response and consequences in project locations with little available data they can be applied.

The propose damage-depth function for both, paved and unpaved roads are shown in Figure 2-12.

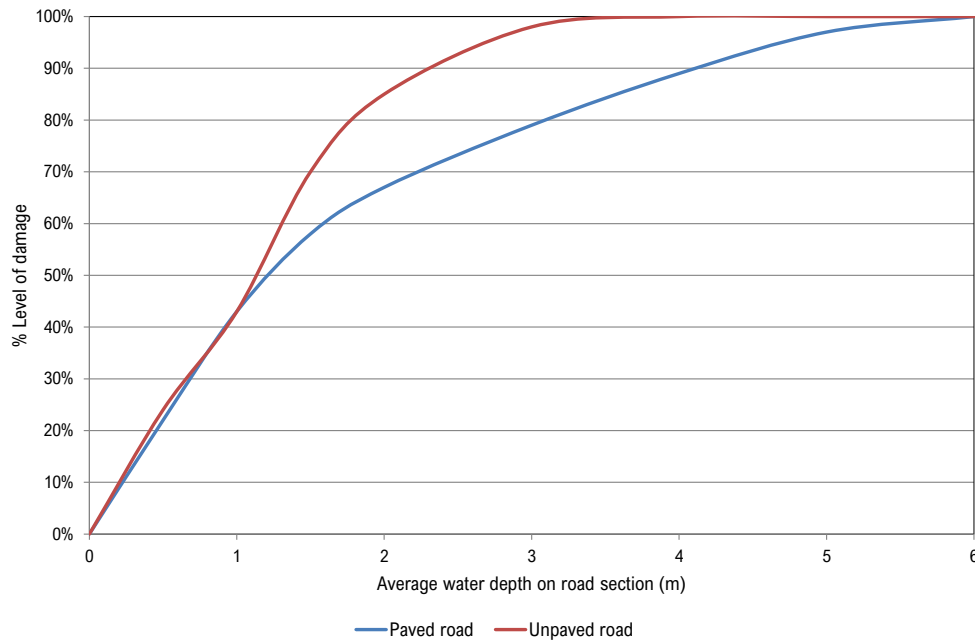


Figure 2-12: Damage-depth function for both, paved and unpaved roads. Source: [69].

However, in spite of the general and useful applicability of Figure 2-12 one still need recorded data from previous local flood-events to quantify and validate the flood damage function for the region of interest. In the case of this graduation work, this information is provided by [40]. The proposal for adjustment and validation procedure of this curve is presented in the INTENDED APPROACH section (Chapter 3) of this report.

Indirect consequences

So far, road vulnerability has been analyzed from a perspective that only accounts for direct consequences after road failure. However, road failure can also impact local economies through indirect damage caused by transportation disruption [4]. The increase in generalized travel cost is often used as a measure of the indirect consequences of road failure [10] [53] [61]. This approach can reflect two different perspectives depending on the political judgment [61]: (1) *equal opportunities* if the roads are treated as equally significant and (2) *social efficiency* if the roads are treated differently depending on their individual traffic demand.

In [55], [61], travelers are assumed to behave by the users equilibrium principle, i.e., choosing the route that minimizes their travel cost (in \$). Denoting the cost of travel from demand node i to demand node j $c_{ij}^{(e)}$ when element e has failed and representing the cost of travel in the initial network by $c_{ij}^{(0)}$, the basis to derive indirect consequences due to road failure is Equation (2-17).

$$\Delta c_{ij}^{(e)} = c_{ij}^{(e)} - c_{ij}^{(0)} \quad (2-17)$$

In addition, when an element e is disrupted, the travel time between nodes in different parts of the network may become infinite. To measure this inability to travel [61] introduces the concept unsatisfied demand u_{ij} , in Eq. (2-18), where x_{ij} is the travel demand from node i and node j . However, how to value unsatisfied demand is still an open question.

$$u_{ij} = \begin{cases} x_{ij} & \text{if } c_{ij}^{(e)} = \infty \\ 0 & \text{if } c_{ij}^{(e)} < \infty \end{cases} \quad (2-18)$$

A link that causes increases in travel cost when cut is call a non-cut link, and the set of non-cut links is denoted as E^{nc} , while the set of cut links is denoted as E . Focusing on the case where a single link is closed, the importance of a link k with regard to the total network is represented by Eq.(2-19).

$$Importance_{net}(k) = \frac{\sum_i \sum_{j \neq i} w_{ij} (c_{ij}^{(k)} - c_{ij}^{(0)})}{\sum_i \sum_{j \neq i} w_{ij}}, k \in E^{nc} \quad (2-19)$$

The potential for natural hazards to close a road is studied in [10], establishing the probabilities with which this hazards are likely to damage a road in New Zealand, establishing ways to find both the frequency of occurrence and potential consequences of the events. A systems model is developed using this information, to predict the total risk of closure of the road.

In the context of this study, the consequences of the hazard events have been expressed in terms of the duration of road closures that result. Some hazard events have the potential to close more than one road link at any one time, increasing the impact of the hazard. The consequences of an event can be expressed in terms of the closure duration of every road involved in the network under analysis. To make all of the closure scenarios comparable, the consequences are expressed in terms of the cost imposed on the country economy.

Cost of travel time: Vehicle operational costs and Costs of vehicle occupant time

The costs imposed on the economy because of any closures, will be dependent on how travelers respond to the reduction in route options. Travelers will always use the route that they perceive has the minimum cost associated with it. This implies that when all routes are available for use, travelers will choose a route that minimizes their costs. When some of the road links in the network are closed, trips then have to be redistributed to other routes through the network.

The additional travel cost to each road user is then the difference between the cost of travel when links are closed, minus the cost of the trip if all roads were open. The cost to the economy will be the sum of these differentials for all travelers on the network is shown in Equation (2-20) [59], where C_T is the total travel cost of the road closure, c_{af} is the cost of traveling on link a when a road is closed, c_{al} is the cost of traveling on link a when all links are open, and F_a is the flow on link a for each of the scenarios.

$$C_T = \sum c_{af} F_{af} - \sum c_{al} F_{al} \quad (2-20)$$

The cost of road closures can be assessed using the value of time a function of the costs of making the trip both vehicle operating costs and the costs of vehicle occupant time [70] [71]. In [10] the costs of travel on the road network have been defined in accordance with the recommendations laid out in the Economic Evaluation Manual (EEM) published by New Zealand [71].

The cost of vehicles exploitation (VEC) depends on the road condition [72] . There are three factors that imply an increase of vehicles operational costs in case of pavement deterioration: lower productivity of vehicles due to a lower speed, the increased consumption of fuel due to movement resistance and higher costs of maintenance due to greater damage of the vehicles components (tires, shock absorbers...).

The road condition is evaluated according to the international roughness index (IRI), proposed by World Bank experts and that represents driving comfort by simulating the movement of the accumulated vehicle suspension through a specific road profile length of the x and is expressed in (m/km). Figure 2-13 shows indicative IRI values according to the road type, and firm condition [73].

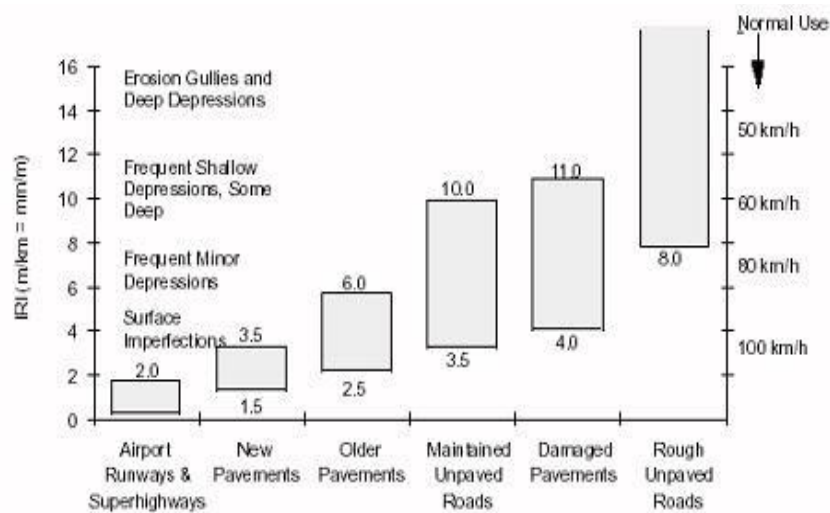


Figure 2-13: Indicative IRI values according to the road type, and firm condition. Source: [73]

Values that link the costs of exploitation of vehicles (in \$/ km) to the vehicle category and the road conditions (IRI) are shown for the case of Country Z [72]. Other references can be found in [71]. Regarding average cost of vehicle occupant time per person/worker, several studies have made estimations for both developed [71] and developing countries [74].

In [74] methodology to derive the cost of time for developing countries is developed and empirically examined for transportation/accessibility projects evaluation, taking as a case study the region of Jessore (Bangladesh), where there is predominance of terrestrial transport, the roads are mostly unpaved, and agriculture is the major income source (similarities with Country Z). The application of the methodology resulted in the following estimates cost of time (See Table 2-6). Where Tk/hr is Taka per hour (Bangladesh coin) and 1 Taka equals to 0.017 US\$.

Base value for cost of time (C_{time}) in Bangladesh				
Base value	3.5	Tk/hour	0.06	\$/hour
Uncomfortable trip	2.29		0.04	
Market day	1.47		0.02	
Employed	14.72		0.25	
Load trip	0.48		0.01	
Max Cost of time			0.40	\$/hour

Table 2-6: Cost of time value for Jessore region (Bangladesh). Source: (Department for International Development, 2002)

In [71] base values to estimate the cost of travel time are proposed for a normal user depending on the type of road and working day / non-working. As shown in Table 2-7, the cost of time values are much higher than expected for least developed countries.

Base value for cost of time (C_{time}) for rural roads in New Zealand	
Labor day	25.34
Non labor day	19.21
Time cost	23.25 \$/hour

Table 2-7: Cost of time value for New Zealand. Source: (NZ Transport Agency, 2016)

From the above, the assessment of indirect consequences due to road failure will be evaluated by means of the increase in generalized travel cost (cost to make a trip) during the time the road is disrupted during and after a flood event using two different parameters:

- The traveler's cost of time during road closure due to a flood event, as suggested in [10].
- The incremental vehicles exploitation cost due to circulation on a deteriorated pavement during reconstruction time after the flood event, as proposed in [71].

2.5. Literature review conclusions

As stated by [4], vulnerability is a widely accepted metric in both urban and inter-urban networks subjected to disruption or degradation. From the above, it can be inferred that a great effort has been focused in the study of vulnerability of road networks, trying to find reliable methods for the detection of critical links, weak spots or critical infrastructure in the road network to maintain its robustness.

The above global network-approach it is, indeed, a useful tool for urban and inter-urban transport planning, dealing with complex transport networks (in terms of road-segments number and traffic behavior) in order to gain insights on the transportation system and to increase its global efficiency. Nevertheless, for the vast majority of the probabilistic methods proposed in the literature regarding this specific topic, a large amount of historical data for road closure days is required, which are not always available, especially for the case of road projects in developing countries.

How to deal with road vulnerability and risk assessments in project locations where historical closure data is not available seems to be a topic that has not been fully analyzed yet. Looking at what has been done in other civil infrastructure, an answer may be given by looking from a designer/ manager perspective, dealing directly with the specific road-segment under hydro-logical threat and shifting the interest to a more detailed comprehension of the hazards likelihood of occurrence, the road segment infrastructure and design alternatives response, the potential failure modes involved and the expected consequences derived from a failure. In other words, to a detailed and specific risk characterization from the most basic level (which is the road segment), in order to support decision making and prioritization of road improvement and risk reduction actions.

For the case of typical road segment, the main failure modes will be studied and incorporated to the risk model. First, the pavement response to large scale flooding in case of increasing river levels, where each level of damage due to flooding will be associated to direct reconstruction costs by the use of global accepted flood-damage curves, an associated time of road closure following the approach in [10] and a variation of the IRI index, a widely accepted metric to measure pavement deterioration, in order to incorporate indirect economic consequences into the analysis. Second, the bridge structural response to hydrodynamic loading, where fragility curves will be constructed in order to overcome the commonly used deterministic approach to assess the bridge stability under river flooding conditions, both considering the deck-pier connection stability and piers erosion induced-failure.

For the work that will be developed during this graduation work, the main focus should be established into applying an integral risk assessment methodology, by adapting the general concepts presented for flood defense infrastructure and river flooding in urban areas. From potential failure mode identification to risk quantification, a risk-informed methodology will be applied to a case study to illustrate the whole process, ending up with management and design recommendations to support decision-making in the road-segment design affected by recurrent river flooding.

PART II. INTENDED APPROACH

3. INTENDED APPROACH

After the literature review, it was concluded that the overall process proposed in the SUFRI methodology could be adapted for flood risk analysis of a road segment infrastructure affected by river flooding, by introducing an intensive *Failure Mode Identification* session in the qualitative phase, and studying in detail the nature of the critical potential failure modes involved and adapting the system response to a flood event and the consequence's assessment to the road type infrastructure.

To reach the goals described in the introduction to this graduation work, the proposed methodology that is intended to be followed regarding the road flood risk analysis process is now presented in Figure 3-1.

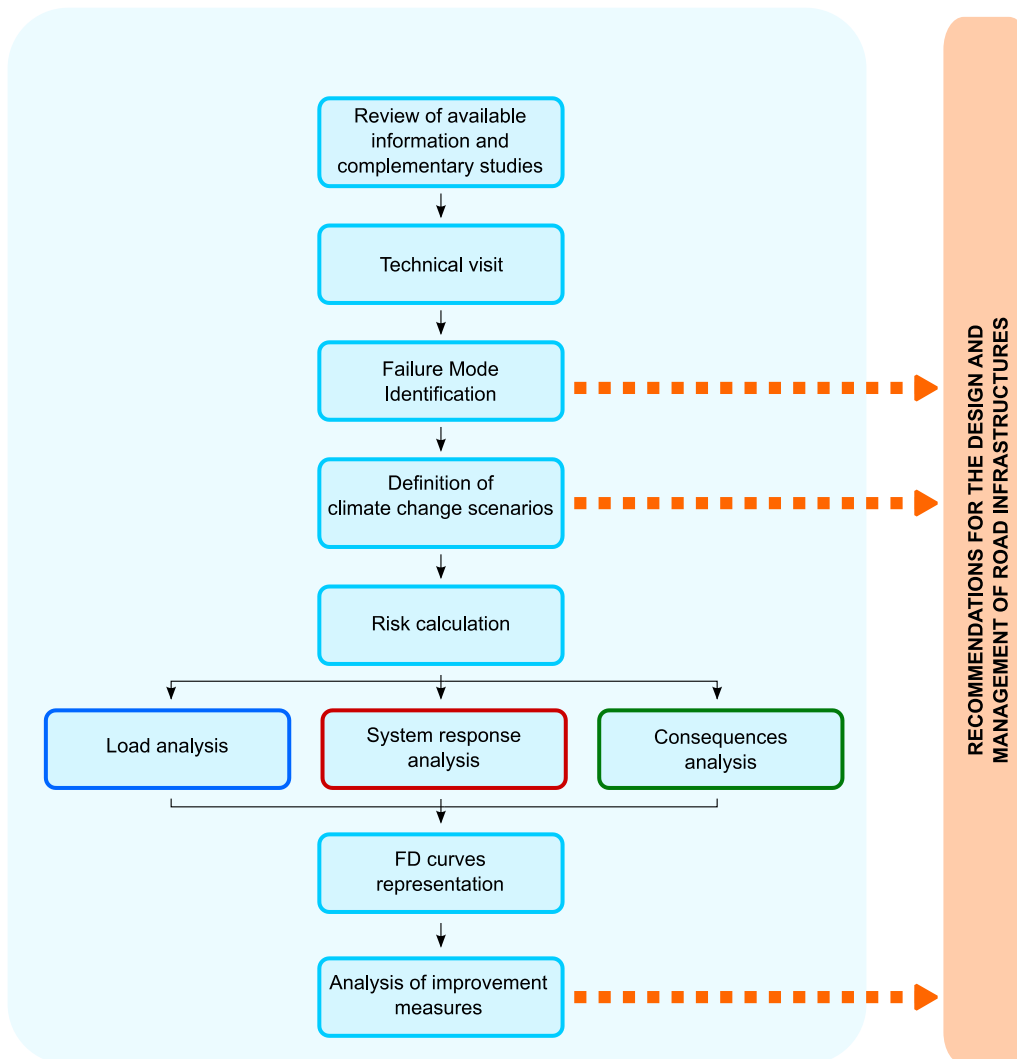


Figure 3-1: Proposed methodology for road risk analysis, adopting SUFRI methodology fundamentals.

The main stages of the methodology are now summarized:

- The first step of this methodology consists in the detailed review of the available information regarding the project characteristics and location and the elaboration of a complementary hydraulic and hydrological model to improve the knowledge relative to the road exposure against flooding.

- The next step consists in conducting a technical field visit to the region of study. This visit will allow observing potential vulnerabilities of the road and gathering useful information for the Failure mode identification sessions.
- The third step is the potential failure mode identification for the Natural Risk Assessment that has allowed to globally characterize the risks in the project location, including the climate change potential impact into the hydrological conditions of the watershed. These failure mode sessions were performed in a group workshop organized in Port Prince (Country Z).
- The failure modes identified are a valuable input for the new design of the projected infrastructure. The failure mode identification allows detecting further needs in research and studies, support for a better planning and management of the structures maintenance and improving the knowledge of the risk management system. From this failure mode identification, several climate change scenarios will allow to estimate risk for the base case and for different proposed alternatives to improve the road infrastructure.
- Risk calculation will be achieved by a quantitative risk model that simultaneously analyses the probability of occurrence of flood hazards, the vulnerability of the road once the hazard occurs and the consequences for different failures mechanisms.
- The quantitative risk results are represented using FD graphs that will allow the analysis of different alternatives for the protection and road improvement and potential recommendations for the design and further road management.

3.1. The Failure Mode Identification Process

3.1.1. Failure Mode Identification

Previous to define the risk model architecture, the first step in performing the quantitative risk model is to identify and define the failure modes that will be present in the model. Thus, within the Risk Analysis, the failure mode identification is a key part in the whole process.

In the present graduation work, a failure mode is defined as the particular sequence of events that may result in failure or mission disruption of the road system (or a part of it). This series of events is associated with a given load scenario and has a logical sequence, which consists of an initial trigger event, a series of events of development or propagation, and ends with dam failure, as shown in Figure 3-2:

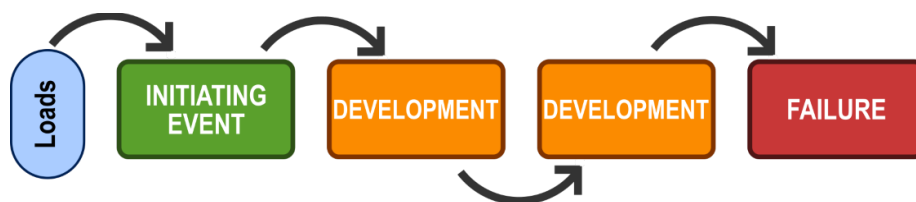


Figure 3-2: Generic diagram for a Failure Mode

This failure mode identification has considered the risk management system from a global perspective and thus, it includes potential failures that affect the road infrastructure (pavement, foundation, slopes...), failures affecting the singular works (longitudinal drainage, transversal drainage...) and failures regarding the risk management system (communication, evacuation...) towards natural hazards (floods, earthquakes and landslides). Thus, every failure mode that will potentially produce damages of any type (economic, loss of life, environmental...) it is included in the analysis.

Generally, the failure modes are related to a load scenario, defined for the natural events that affect the management system due to external actions. In a failure mode analysis regarding natural hazards, two scenarios are defined.

- **Hydrological Scenario:** Within this scenario, every hydrologic event that produces discharges with potential to produce floods is considered, occasionally implying loads on bridges, drainage works or other existing infrastructure within the road system.
- **Management Scenario:** It is considered within this scenario, any load event derived from the ordinary risk management, including routine exploitation and inspection operations.

The process that will be followed to perform this failure mode identification is shown in Figure 3-3.

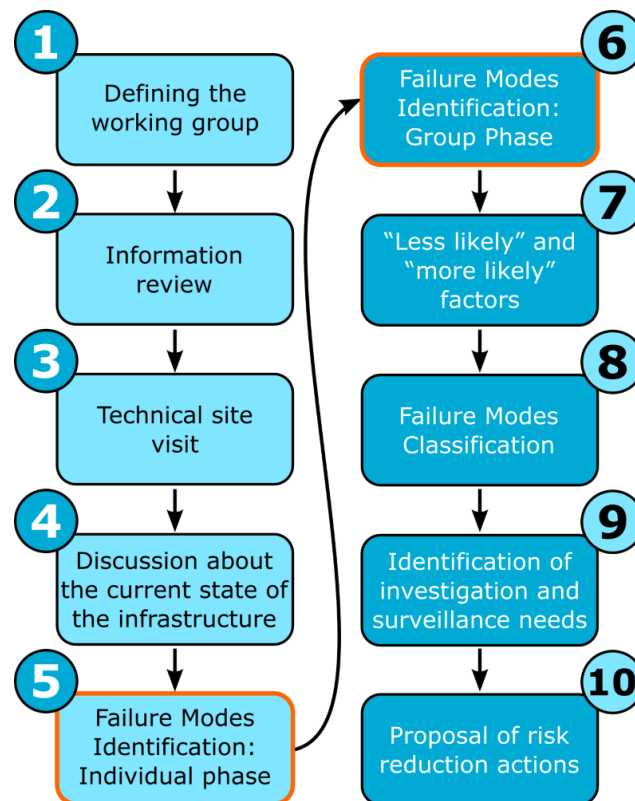


Figure 3-3: Failure Mode Identification process.

First, an introduction to the system characteristics and a review of available information regarding the project and analyzed infrastructure is performed. The next step consists of an individual failure mode identification phase. Within this step, an individual proposal is performed regarding the possible failure modes that could potentially develop in the system. The individual proposals should be gathered together with the aim of avoiding redundancies and to obtain group failure modes. In addition, for each of the identified failure modes, “more likely” and “less likely” factors regarding its occurrence shall be discussed. Finally, from the failure mode identification, the participants should propose improvements to the risk management system.

3.1.2. Failure Mode Classification

Once the potential failure modes that can potentially affect the infrastructure are identified is necessary to make a classification to determine the relevance degree of each of them and their subsequent inclusion (or not) in the quantitative phase of project.

Following the recommendations and risk factors identified in the working session for failure mode identification in Port-au-Prince (Country Z), and after reviewing recommendations developed by international organizations related to civil infrastructure safety [22] the identified failure modes are classified based on the following categories:

- **Grade A:** The failure mode directly affects infrastructure that have, within its main functions, the protection against natural hazards. The reduction of the probability of this failure mode is one of the main missions of the planned infrastructure. The occurrence of failure mode involves high social, environmental and economic consequences. This type of failure mode requires quantitative risk analysis to justify the proposed works/design on the basis of the potential economic and social consequences avoided.
- **Grade B:** The failure mode occurrence is considered probable for the intended design of the infrastructure; its occurrence can generate a complete and widespread destruction or complete loss of function of the infrastructure for a long time. The occurrence of failure mode involves high social, environmental and economic consequences. In this case, risk analysis may introduce significant changes in the infrastructure design or consider the need for additional measures.
- **Grade C:** The failure mode occurrence is considered probable for the intended design of the infrastructure, but its occurrence can generate only partial and located damage in infrastructure without causing high (social, environmental and economic) consequences. A quantitative risk analysis for these failure modes is not considered necessary as the failure modes qualitative phase already allows to make small changes in the design of infrastructure and/or establishing recommendations concerning additional checks and/or maintenance of the infrastructure.
- **Grade D:** The failure mode is not feasible, and its appearance is not considered reasonable for the current design of the infrastructure or its consequences are very low. For these modes of failure, it is not necessary to perform quantitative risk estimates. However, it is still necessary to document them and explain the reasons considered to classify them. The fact that a potential failure mode has not been considered relevant in the past does not mean it should be ruled out in each reassessment. In any case, the failure mode identification can serve to make recommendations on monitoring and maintenance.
- **Grade E:** Modes of failure for which the available information is insufficient to determine the feasibility of the failure mode but they cannot be ruled out if its occurrence had high social, environmental and economic consequences. The recommendations related to this type of failure modes are based on new campaigns of investigation or further studies in order to better characterize the feasibility of its occurrence.

Once the failure mode classification is performed, the failure modes identified as A or B are studied in detail in order to incorporate them in a quantitative risk model that will allow to give risk-informed recommendations for the infrastructure design and management. In addition, at this point, it is also possible to give qualitative-based recommendations and proposals for risk-reduction actions to the failure modes classified as grade C, D or E, based on the outcomes from the failure mode identification session.

3.2. Definition of Climate Change Scenarios

The impacts of disaster and climate change risk are growing concerns as they reduce the predictability of future infrastructure needs and increase the vulnerability of populations and assets. As part of sustainable planning, development projects should consider current and future risk and resilience opportunities in the design, construction, and operation phases (IDB & IDB Invest, 2018).

Every new road design in flood-prone areas that is intended to last for the next decades should include a quantitative analysis regarding the climate change effect on the infrastructure risk, mainly by defining the impact on future storm events in the project area.

Thus, an important step within the quantitative risk analysis methodology to be developed is to define the different climate scenarios that will allow estimating risk for the current situation and future scenarios and designs.

3.2.1. Mathematical models used for Climate Change prediction

The predictions related to climate change that are presented are based on the analysis of Greenhouse Emission Scenarios using two types of mathematical models: GCMs and RCMs.

Global circulation models (GCMs) are a mathematical tool for the representation of physical and dynamic processes present in the atmosphere, oceans and land surface. Their consistency in the representation of current and past weather conditions, make them a very useful tool to simulate future climate under different emission scenarios.

The main drawback of GCMs is its poor resolution on the scale of the information required at design level. The size of a wide-region (i.e. Country) concerning the GCMs mesh resolution implies that nationwide is only represented by a few "rectangles of calculation". Through the development of downscaling techniques, Regional Circulation Models (RCMs) allow to obtain more specific information for inside regions without devaluing the information obtained from GCMs.

RCM and GCM models for Country Z have scenario-based simulation on the proposed RCPs (Representative Concentration Pathways), which represent a set of mitigation scenarios and are selected according to different objectives in terms of atmospheric radiation by 2100: (2.6, 4.5, 6.0 and 8.5 W/m²).

- **RCP2.6:** Radiation peak of 3 W/m² before 2100 and decrease to 2.6 W/m² in 2100.
- **RCP4.5:** Radiation stabilization without exceedance in 4.5 W/m² after 2100.
- **RCP6.0:** Radiation stabilization without exceedance in 4.5 6.0 W/m² after 2100.
- **RCP8.5:** Radiation stabilization without exceedance in 4.5 8.5 W/m² after 2100.

These scenarios are not directly based on socio-economic trends and, because of his rank in the forecast; it may be representative of global policy regarding greenhouse gases emission. Figure 3-4 shows the projection for the atmospheric radiation and CO₂ emission evolution for every RCPs scenarios and horizon 2000-2100. For more information about the scenarios of emission RCPs the reader is referred to [75].

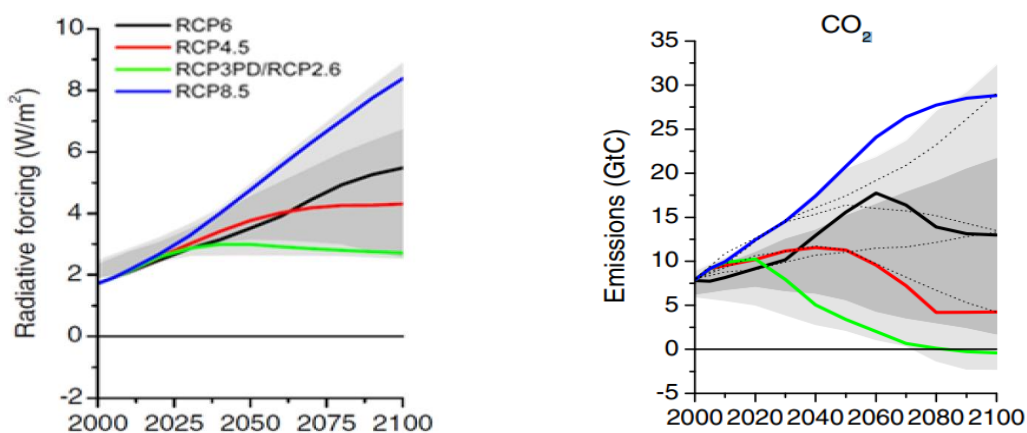


Figure 3-4: Screening of the evolution in atmospheric radiation and emission of CO₂ for the four RCPs scenarios and Horizon 2000-2100.

3.2.2. Methodology proposed

The climate change predictions regarding future behavior of storm events in the project area that are presented in this report are based on climate model GCM Canadian Earth System Model (CanESM2), which provides worldwide simulations of daily rain for historical, RCP 2.6 RCP 4.5 and RCP 8.5 scenarios. Data from model simulations must be subsequently validated with data from historical records to obtain valid predictions for the study area.

The methodology used for the calibration and adjustment of the simulated rainfall with historical data is shown in Figure 3-5.

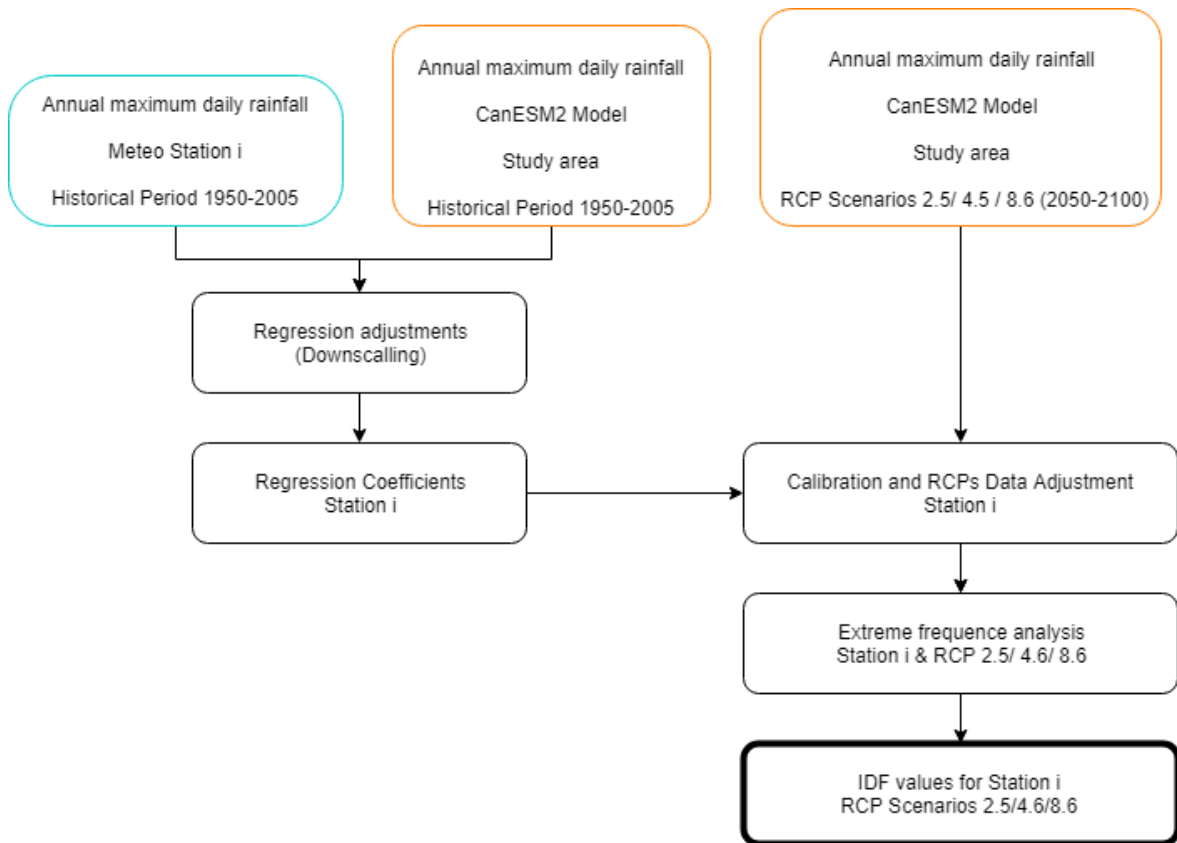


Figure 3-5: Methodology for obtaining rainfall IDF values for a climate change scenario.

First, the simulated data of climate model (CanESM2) is downloaded for: the historical period corresponding to available precipitation records; and coordinates close to the study area.

The downloaded simulated data values will not coincide with those observed in the same period for different weather stations in the study area, as the location from which the simulated data is obtained will hardly coincide with the coordinates of meteorological stations under study. Therefore, a downscaling technique adjustment is required.

The adjustment will be done by using a polynomial regression, comparing observed data at stations with simulated data in the model, for the same historical period. The adjustment process can be seen in Chapter 7 of this report.

As an example, Figure 3-6 shows the regression estimated for B meteorological station (Country Z).

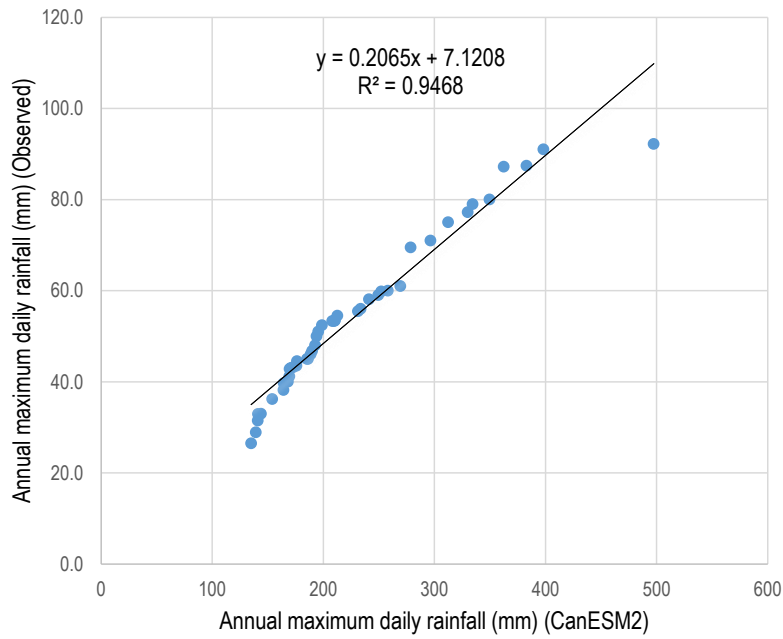


Figure 3-6: Example of regression adjustment (simulation CanESM2 vs observed data).

Once the adjusted data set is obtained for each trend-based scenario (RCP2.5, RCP4.6, and RCP8.6) and each weather station, an extreme frequency value analysis should be performed to obtain the IDF (Intensity Frequency Duration) storm values for each of the stations analyzed in the future climate-trend scenarios.

An example of the frequency of rainfall extreme values analysis for a meteorological station and climate scenario is shown in Figure 3-7.

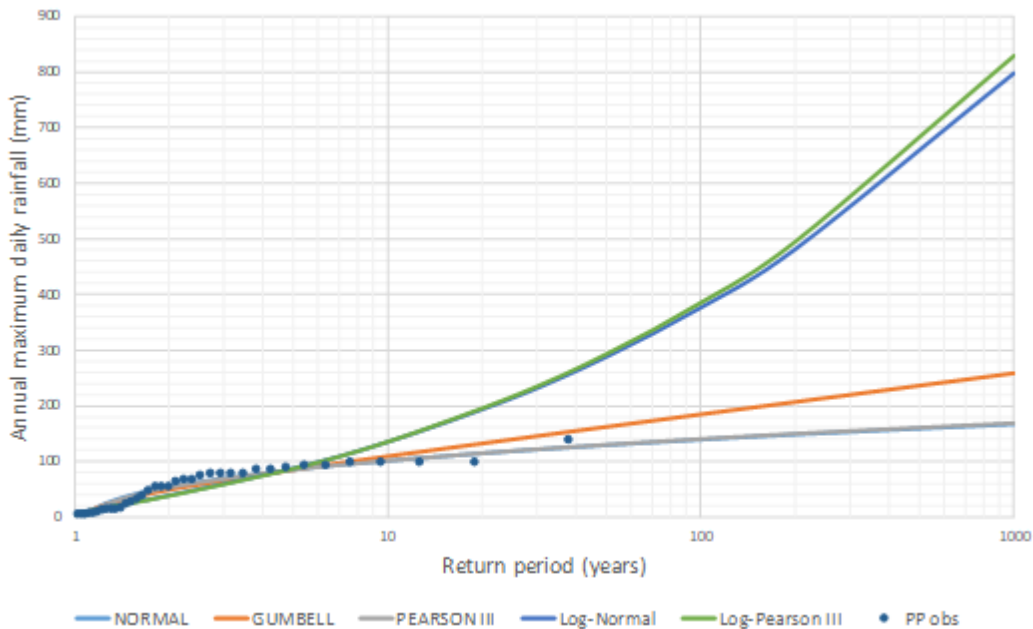


Figure 3-7: Example of frequency of extreme values analysis (Several probability distributions).

The results from the application of the proposed methodology are shown in Chapter 7 of this report.

3.3. Quantitative Risk Calculation

Any risk assessment is mainly driven by its purpose, the question it hopes to answer, and the information it wishes to provide [10]. Therefore, it is very important to clearly state the objective for the analysis. Only by comparing the end-product with these objectives the assessment success could be judged.

In the case of this case study, and after performing an exhaustive failure identification process, the following objectives have been set.

- To analyze quantitatively the risk by large scale river flooding in the critical road stretches considering the pavement response and the effect of climate change. The goal is to characterize the hydrological risk in the form of FD curves and obtain the expected annual economic costs by flood, in order to justify the need to include design and management alternatives.
- To analyze quantitatively the risk in road bridges considering the effect of climate change on the hydrological conditions of the river streams. The objective is to compare the current risk of failure by hydrodynamic forces and erosion with that same risk in climate-trend-based scenario. For each return period of the flood event, the probability of the bridge failure along with the consequences associated with that failure shall be calculated. Comparing the current risk (consequence) with the trend-based scenario risk, will provide the background to evaluate if the bridges are correctly designed and if any measures are needed to improve the infrastructure safety.

However, the integral risk-informed methodology presented in this graduation work is intended to serve for the assessment of any other failure mode that could entail risk (derived from river flooding hazards) to the road infrastructure system.

3.3.1. The risk analysis process

In this graduation work the risk term is defined as the combination of three concepts: what will happen, how likely it is to happen and what are its consequences. Applying to the case of a road affected by natural hazards, *what will happen* refers to the failure of any part of the road infrastructure. *How likely it is to happen* to the combination of the probability that a certain natural hazard occurs and the conditional probability of failure of the road/bridge once the threat is produced (also known as system response). Finally, the *consequences* are those arising from the failure of the infrastructure including economic consequences (direct and indirect), if it were the case.

The quantitative flood risk calculation will be performed using *iPresas software developed by iPresas Risk Analysis (a spin-off company of the Polytechnic University of Valencia)*. The risk analysis process has 3 parts as shown in Figure 3-8

- **Load analysis:** Definition of the probability of loading scenarios. Loading scenarios include flood events, or any other event which can pose a risk to the road infrastructure.
- **System response analysis:** Definition of the failure probabilities (given a loading condition), for all the failure modes.
- **Consequence analysis:** Estimation of the consequences that would happen in all the considered scenarios.

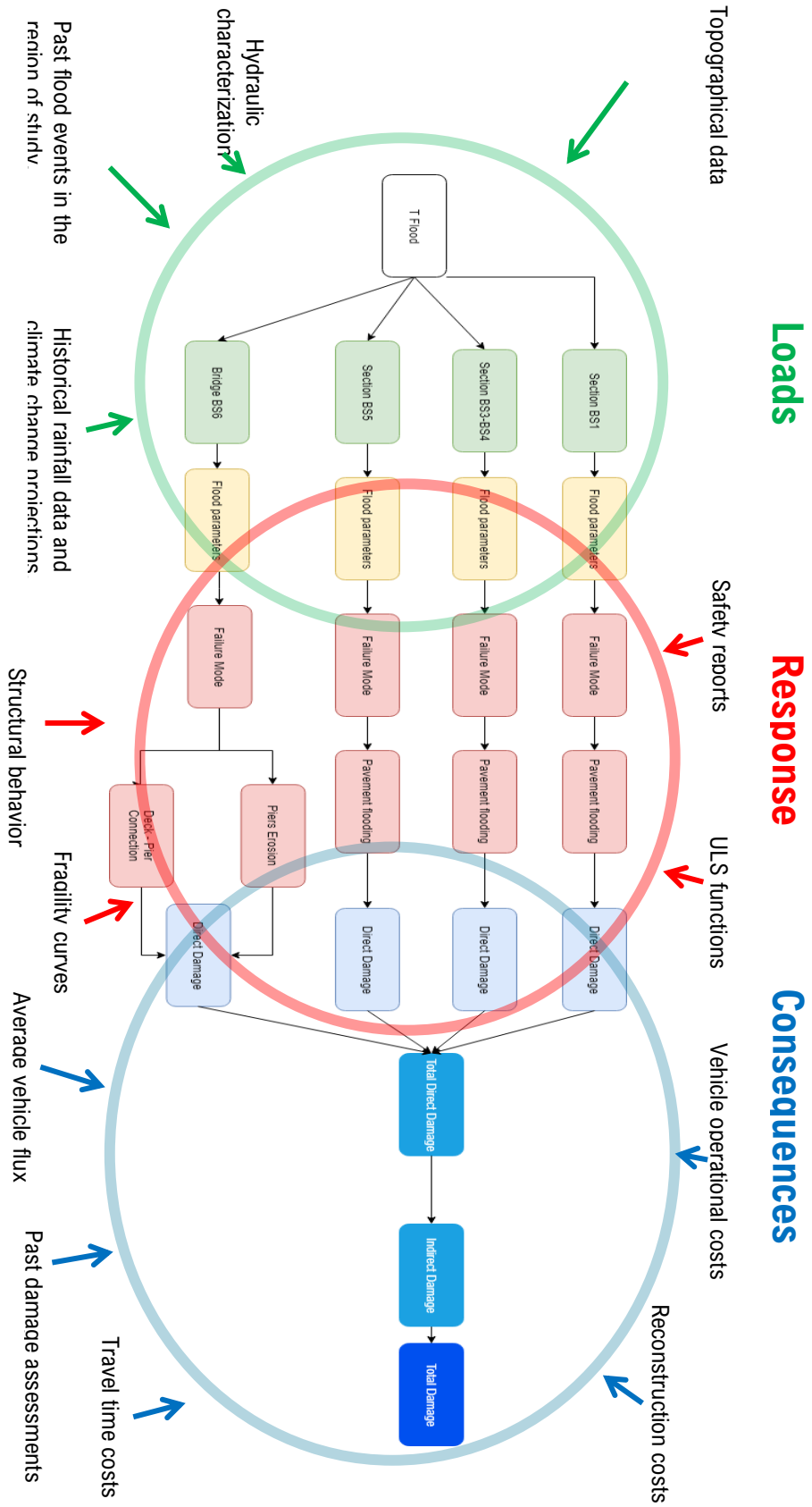


Figure 3-8: The road flood risk analysis process.

As observed in previous figure, *iPresas software* is based on the use of event trees for its calculations and, for a more compact representation, data input is made through influence diagrams. An event tree is a representation of a logical model that includes all possible chains of events resulting in a failure from an initial event. As its name suggests it is based on the mathematical structure known as tree and which is widely used in many other fields.

Each node represents an event. The root node is called the initial event. The branches that depart from an event represent the possible outcomes of the respective event. In general, these branches must represent mutually exclusive and collectively exhaustive events. Therefore, the result of an event always will be reflected in one (and only) branch. So, if each branch is assigned a probability, the sum of the probabilities of all the branches that depart from any node will be 1.

Influence diagrams are a compact conceptual representation of the logic of a system. In its most generic form, an influence diagram is any representation that includes the relationships between events, States of the environment, system States or subsystems, and consequences.

An influence diagram provides a visual representation of a risk model. In it, each system variable is represented by a node and each relationship with a connector. From an influence diagram, it is possible to build the tree of events that can then be used to carry out the calculation as shown in Figure 3-9.

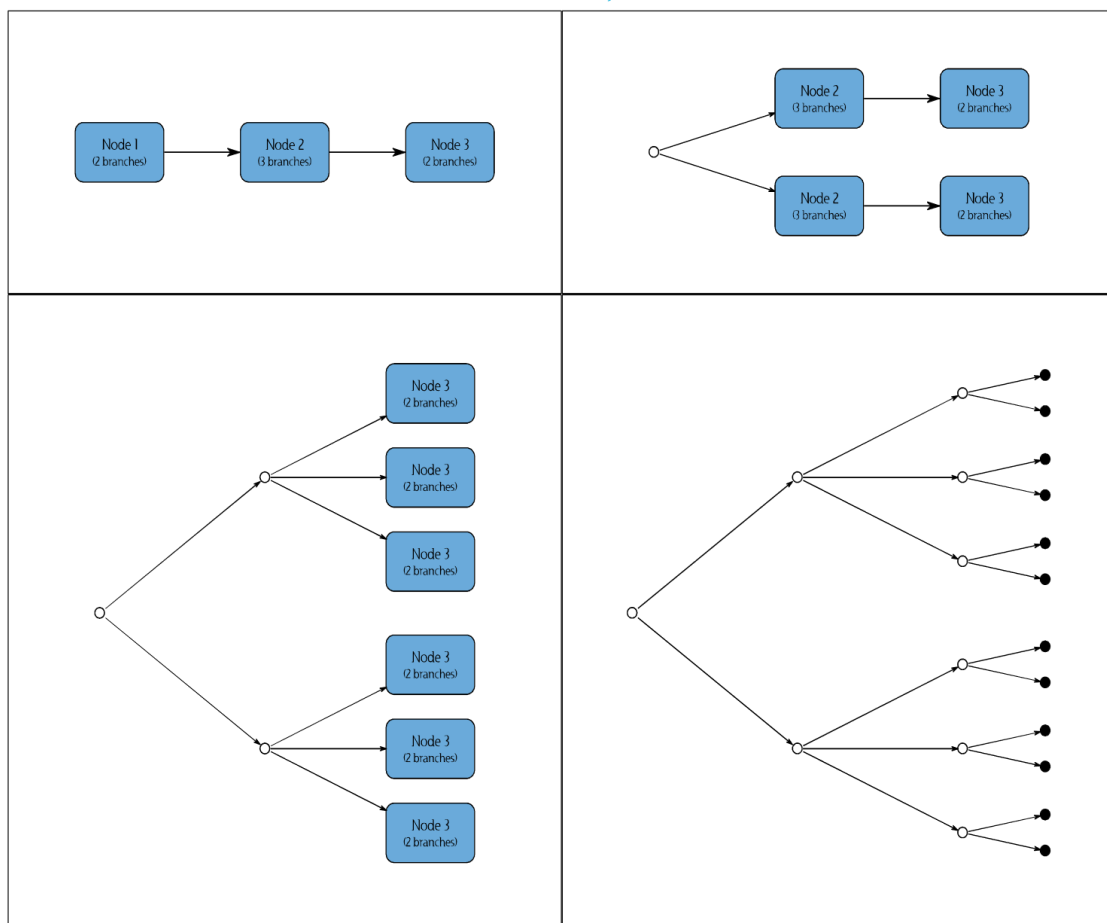


Figure 3-9: Relationship between influence diagram and event trees. Source: [76]

3.3.2. Load analysis

The review of the available information is fundamental to ensure the robustness of the works and acquires special relevance as it is prior to the failure mode identification and the quantitative analysis of the risk of flooding in the region under study.

At least, the following information should be gathered and review in detail prior to the start of any risk hazard assessment:

- Natural risks present in the region of study.
- Historical rainfall data and climate change projections.
- Land use in the region under study.
- Topographical data (site DEM) and road infrastructure main characteristics.
- Recent damage assessment reports from previous infrastructure failure Load analysis.

Flood Hazard Assessment

The Flood Hazard Assessment deals with to two risk concepts presented above: *what will happen* and *how likely it is to happen*. Thus, it corresponds to the characterization of hydrologic-hydraulic behavior in the watersheds that surround the road under study, including the analysis of the most critical points and estimated flow rates and expected flood depths. The main object during this phase will consist in performing a diagnosis, identifying potential flood events and their corresponding affection to the road under analysis.

The methodological procedure for hydrological-hydraulic characterization is shown in Figure 3-10 and is summarized in three fundamental stages:

- (1) Analysis of available information and data acquisition, including past storms and flood events.
- (2) Hydrologic characterization, identifying the critical flood-prone road areas and their associated watersheds, defining the main geo-morphological characteristics and obtaining the flood hydrographs in the river-road critical intersections.
- (3) Hydraulic characterization of flood events resulting from design storms and flood hydrographs based on outcomes from the hydrologic model, obtaining the required hydraulic parameters (flow depth, flooded areas...) to be introduced in the quantitative risk model.

Finally, results of the flood hazard assessment will represent:

- (1) A basis for failure mode identification sessions to be carried out as part of the first phase of the work.
- (2) A fundamental input for the quantitative risk model to be developed.

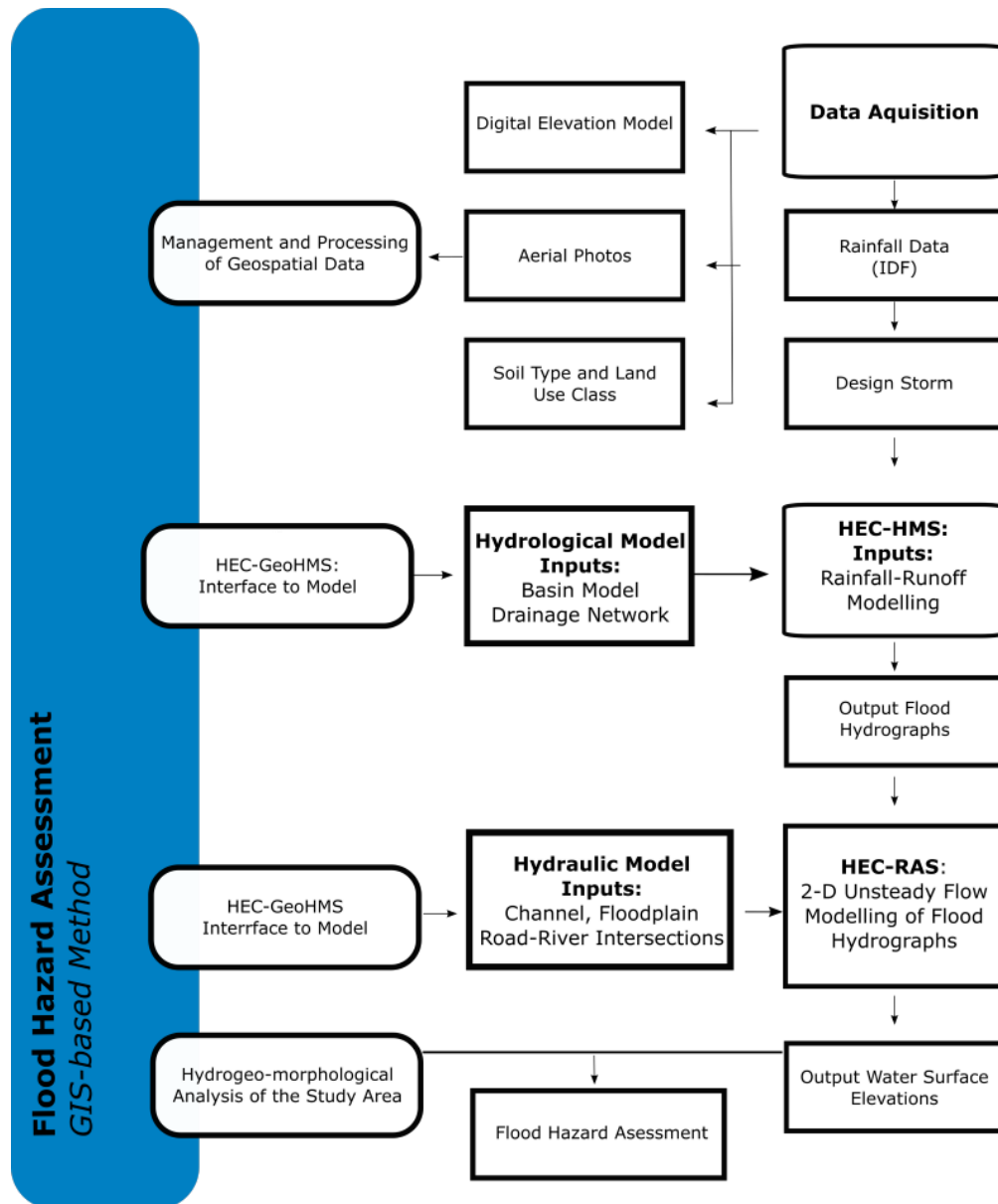


Figure 3-10: GIS-based methodological procedure for hydrological-hydraulic characterization.

Hydrological Characterization of Flood events

The first step is to determine the watersheds and river streams draining towards the road, their main characteristics and geo-morphological parameters, as well as locate critical points (stream-road intersection points) susceptible to cause flood-related issues for further analysis in a hydraulic model.

The hydrological characterization will be performed with the aid of a GIS support (Geographic Information System) and a Digital Elevation Model (DEM) from the area under study. From this GIS analysis, the expected outcomes are related to the geometrical parameters of the watersheds: Location, Maximum flow path length, watershed area and perimeter, watershed slope and watershed elevation (max, min, mean and standard deviation).

Once the watershed's geometry is defined, the following step in the hydrological characterization is to define the design storm. A *design storm* is a precipitation pattern defined for the use in the design of a hydrologic system [77]. Design storms can be based upon historical precipitation data at a site or can be constructed using the general characteristics of precipitation in the surrounding region.

In case daily rainfall data of historical records are available, a frequency distribution analysis should be carried out, in order to obtain the maximum daily rainfall (mm in 24 h) associated with different return periods and climate scenarios for each one of the stations considered in the analysis.

Once the values of maximum daily rainfall (mm in 24 h) expected at each meteorological station and for different return periods are known, the following step is to build a design storm for the chosen sub-basin and return period. The US Department of Agriculture, [77] developed synthetic storm hyetographs for use in the United States for storms of 6 and 24 hours. For the case study in the present report, the type III (Figure 3-11) is of special interest, as it was developed for areas, “where tropical storm result in large-24 hour rainfall amounts”.

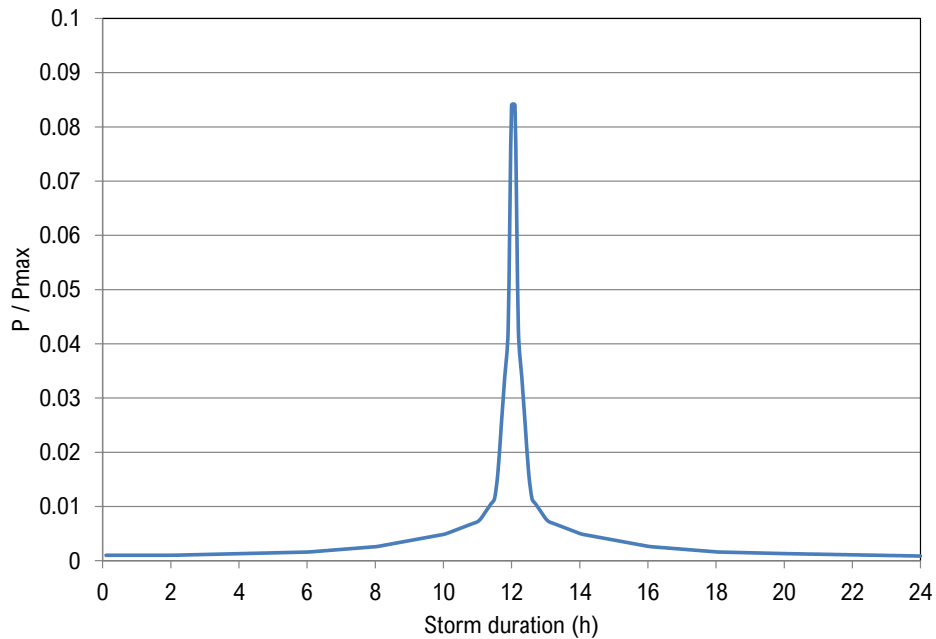


Figure 3-11: SCS type III hyetograph. P / Pmax in 24h vs storm duration.

In order to know the estimated rainfall in each watershed from the data of the nearby stations, the Thiessen polygons method is applied through GIS tools. The method delimits the sub-regions of influence corresponding to each pluviometer. Once the zones of influence are delimited, and their areas within the watershed A_i calculated, the spatial average precipitation for a specific watershed is obtained according to the following expression Eq. (3.1):

$$\bar{P} = \sum_{i=1}^n \left(P_i * \frac{A_i}{A} \right) \tag{3.1}$$

Where \bar{P} is the average precipitation in the watershed; P_i is the precipitation obtained for each pluviometer; A_i : is the influence area of pluviometer i in the watershed under analysis A : is the total area of the watershed.

The hydrological model is elaborated using the HEC-HMS software (**¡Error! No se encuentra el origen de la referencia.**), developed by USACE (United States Army Corps of Engineers). The Curve Number method, proposed by the United States Department of agriculture [78] and globally used, is used in the hydrologic model. The curve number (CN) from the basin determines the precipitation-runoff ratio and depends mainly on the use and the type of soil present in the area under study.

The CN values are determined for each of the watersheds from the 500m –resolution global maps facilitated by MODIS (*Moderate Resolution Imaging Spectroradiometer*) according to the classification by IGBP (*International Geosphere Biosphere Program*), depending on the type of soil and the soil's hydrologic condition. The different land uses types referred to in this classification system are shown in Table 3-1.

MODIS land cover classification		CN for different HSG			
ID	IGBP land cover type	A	B	C	D
0	Water	N/A	N/A	N/A	N/A
1	Evergreen Needleleaf Forest	34	60	73	79
2	Evergreen Broadleaf Forest	30	58	71	77
3	Deciduous Needleleaf Forest	40	64	77	83
4	Deciduous Broadleaf Forest	42	66	79	85
5	Mixed Forest	38	62	75	81
6	Closed Shrublands	45	65	75	80
7	Open Shrublands	49	69	79	84
8	Woody Savannas	61	71	81	89
9	Savannas	72	80	87	93
10	Grasslands	49	69	79	84
11	Permanent Wetlands	30	58	71	78
12	Croplands	67	78	85	89
13	Urban and Built-Up	80	85	90	95
14	Cropland/Natural Vegetation Mosaic	52	69	79	84
15	Snow and Ice	N/A	N/A	N/A	N/A
16	Barren or Sparsely Vegetated	72	82	83	87
255	Fill Value/Unclassified	N/A	N/A	N/A	N/A

* Hydrological condition assumes for both hydrologic surface condition

Table 3-1: CN values depending on hydraulic condition of soil (A, B, C, D) and land-use type according to the classification by IGBP

The parameters necessary to carry out hydrologic modeling for each of the sub-basins are obtained from a DEM spatial analysis from the region under study and they are: (1) Maximum flow path length, (2) Watershed area, (3) Flow path average slope, (4) Concentration time and (5) Lag-time.

The time of concentration (T_c) is defined as the minimum time required for all points of a watershed to simultaneously provide water-runoff to the basin outlet. Its calculation is normally based on empirical methods and there are various formulations in the literature. A common practice is to use several of these existent expressions and take the average value without considering the maximum and the minimum outputs. The following formulations are considered: (California, Kirpich, SCS, Williams, Temez, Rivero, Pilgrim, Valencia y Zuluaga y *Spanish General Road Management*). The formulae and results from its application are shown in the Appendixes the present report.

The lag-time (T_{lag}) is defined as the time elapsed since the hyetograph centroid and the peak flow generated at the outlet. According to NRCS [78], the lag-time can be approximated as expressed in Eq (3.2).

$$T_{lag} = 0.6 * T_c \quad (3.2)$$

The initial abstraction or initial threshold ($A_{initial}$) is defined as the amount of initial precipitation that does not produce direct runoff. The Soil Conservation Service, proposed the following expression depending on the curve number (CN) value:

$$(3.3)$$

$$A_{initial} = 0.2 * S = 0.2 * \left(\frac{25400}{CN} - 254 \right)$$

Finally, within the HEC-HMS model, a meteorological model with specific rainfall data to each of the sub-basins of the study area is considered, **where every sub-basin experiences the same hydrological event at the same time (i.e. associated storm event return period)**, and design storms are calculated from: the SCS type III proposed by the NCRS for the Atlantic coastal areas subject to storms tropical (case of Country Z), the maximum daily rainfall values (mm in 24 h) estimates for several metrological stations, return periods, climate scenarios, and Thiessen coefficients in the area of interest.

The model considers a 24 hours precipitation event and the modeling time is set as 48 hours with an 10 minutes interval.

The main outputs that are obtained from hydrological modeling are:

- Watershed delineation and critical points (river-road intersection) identification.
- Flow hydrographs (River discharge vs time) for each critical point (river-road intersection) and for each flood event return period and climate scenario considered in the analysis.

Specific considerations and results from hydrologic modeling applied to the case study are presented in detail in Appendixes of this report.

Hydraulic Characterization of Flood Events

The hydraulic model will be performed using HEC-RAS software, developed by USACE (United States Army Corps of Engineers). Two-dimensional simulations are performed in non-permanent flow regime in order to obtain flood maps associated with climate scenarios and different flood events.

A DEM (Digital Elevation Model) with adequate resolution from the region under study is required. A calculation mesh should be established along the axis of the road, leaving sufficient margin on each side for the study of wave propagation. From the model, calculation meshes are elaborated regarding each watershed present in the study area. The Manning coefficient employed in the calculation mesh is considered uniform in the whole area.

The boundary conditions for the calculation mesh are divided into:

- An **input condition** defined by flow hydrographs (Q vs time) for each of the river channels entering the mesh grid;
- An **output flow condition**, related to energy slope (Friction Slope) at every mesh geometry exit.

Flow entry points should be established upstream of the location of the identified critical points (stream-road breakpoint). Figure 3-12 shows an example of the calculation mesh used in the hydraulic modelling of a watershed from the case study presented in this report:

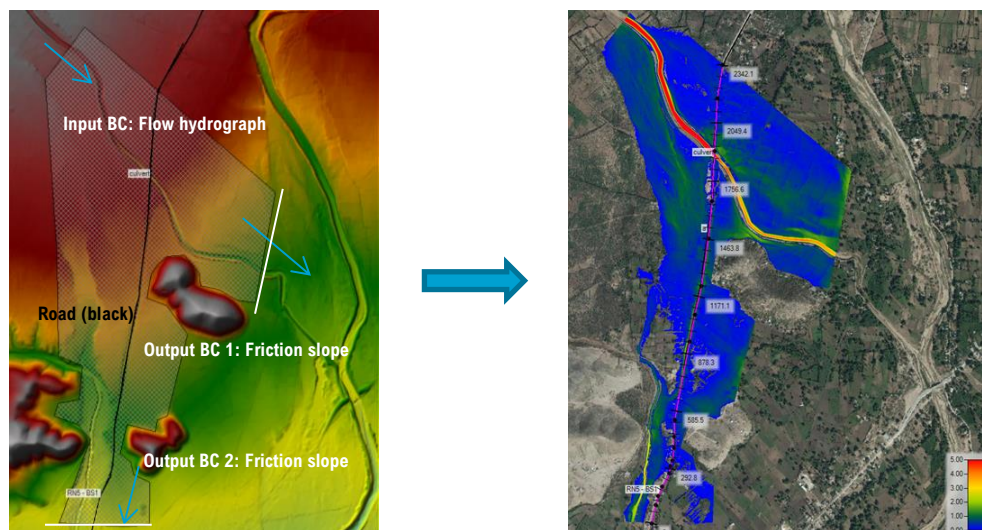


Figure 3-12: Calculation mesh and boundary conditions example. HEC-RAS 2D model. Case study: Watershed BS1

The flow hydrographs introduced in the model are obtained previously by means of hydrologic modeling and should be included with an adequate time interval. Also, an adequate time-step for the model calculation and total simulation time should be established. A balance should be made between computational efficiency and result precision.

The main outputs that are obtained from hydraulic modeling are (for each flood event return period and each climate scenario):

- Flood maps for each identified critical section.
- Average and maximum flow water depths over the road within the road flooded section.
- Maximum flooded length and area within the road flooded section.
- Maximum river water depth/level at bridge location during peak flow.
- Cross section averaged flow velocity at bridge location during peak flow.
- Cross section averaged Froude number at bridge location during peak flow.

Specific calculation considerations and results from hydrologic modeling applied to the case study are presented in detail in Appendixes of this report.

3.3.3. System response analysis

The system response to each of the loading scenarios is calculated once the loads for the risk model are defined, trying to give response to the following questions:

- Will the bridges fail for the hydrodynamic forces calculated for each frequency period?
- What will be the scour magnitude at the foundation after a flood? Will the bridge fail due to scour?
- What will be the pavement damage in case of large-scale flooding on top of the road axis?

Fragility curves for bridges under hydrodynamic loads

Following the approach suggested in [39], a method to assess the failure probability of the bridge is proposed by the use of limit state functions and probability distributions for each of the stochastic variables present in the equations, mainly, for the non-dimensional hydrodynamic coefficients that define the hydrodynamic loading of the bridge (C_D , C_L , C_M).

In the case of this report, the interest is focused on the bridge collapse, so only ultimate limit state (ULS) functions will be defined. Three limit state functions are defined based on the 2D directions of force stability

(vertical, horizontal and moment stability). The appropriate distributions to each of the variables involved are chosen based on different loading scenarios. Then, a Monte-Carlo simulation is performed to calculate the failure probability of the bridge for each loading scenario. Once this is achieved, fragility curves for bridge failure under hydrodynamic loading will be created, representing the failure probability against hydrodynamic loading (inundation ratio, proximity ratio and Froude number). The fragility curves define the system response to a river flooding event and can be used later within a risk model to calculate the quantitative risk of bridge collapse under study.

System definition: Bridge geometry and critical variables

Following the previous work in [39] and considering the fact that the bridge present in the region under study corresponds to a typical 3-girder bridge with concrete deck, Figure 3-13 shows the most relevant geometrical characteristics to be defined:

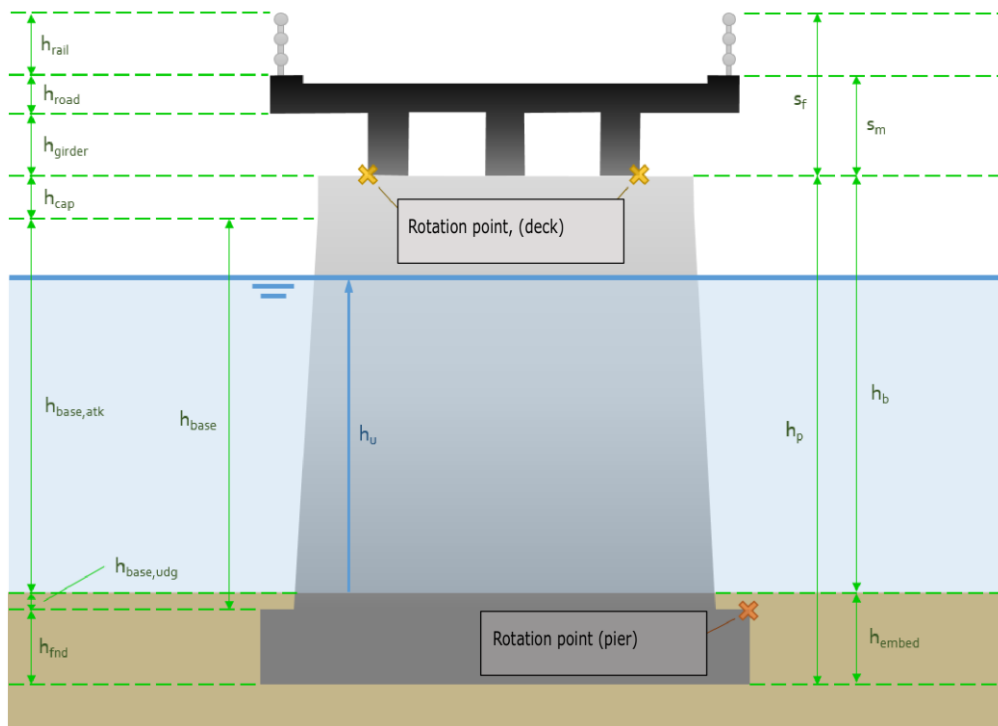


Figure 3-13: Typical geometrical parameters for a 3-girder bridge with concrete deck. Source: [39]

In Table 3-2 the definition for each of the parameters shown in Figure 3-13 is presented. Apart from the above geometrical parameters, other critical variables such as the water depth h_u , the specific weight for the bridge materials, mainly steel ρ_{steel} and concrete ($\rho_{concrete}$), or the friction coefficient between the deck and pier (μ) should be defined appropriately.

Pier dimensions		Deck dimensions	
h_{base}	Pier height	L_{deck}	Deck length (for one pier)
$h_{base, atk}$	Pier height without cap	W_{road}	Road width
$h_{base, udg}$	Foundation depth	W_{deck}	Total deck width
h_{cap}	Pier height cap	$W_{deck, sides}$	Deck sides width
h_{embed}	Imbedded foundation	h_{girder}	Girder height
h_{fnd}	Height from rotation point	W_{girder}	Girder width
h_p	Total pier height	$N_{girders}$	Girder numbers
$W_{pier, base}$	Base pier width	$D_{girders}$	Distance between girders
$W_{pier, cap}$	Cap pier width	$D_{gird, deck}$	Distance to deck edge from girders
W_{cim}	Foundation width	h_{rail}	Rail height
$L_{minpier}$	Min length base pier	h_{road}	Road-layer height
$L_{maxpier}$	Max length base pier	s_f	Total deck height (with rail)
$L_{medpier}$	Average length base pier	s_m	Total deck height (no rail)
L_{cim}	Length foundation		
h_b	Distance from riverbed to bottom deck		

Table 3-2: Definition of typical geometrical parameters for a bridge

In the next section, the expressions to calculate the hydrodynamic forces are presented, for both resisting and destabilizing loads, along with the limit state functions that will be used to calculate the fragility curves.

Hydrodynamic forces

For a submerged bridge deck, the acting forces are represented in Figure 2-9 in Chapter 2.3.2. Six main forces require to be calculated: F_z as the gravitational force and main resisting force (i.e. weight), F_d as the drag force, F_b as the buoyancy force, F_l as the lift force and F_r as the frictional force.

As explained during the literature review, the magnitude of the loading on bridges due to hydrodynamic forces depends on flow conditions and bridge characteristics.

The gravitational force (i.e. weight) exerted by the bridge deck is expressed as a function of several geometrical parameters and material's specific weights, as shown in Eq. (3.4):

$$F_{xd} = W_{deck} * h_{road} * L_{deck} * \rho_{deck} + W_{girder} * h_{girder} * L_{deck} * N_{girder} * \rho_{girder} \quad (3.4)$$

The buoyancy force exerted by the water on the bridge deck is expressed as a function of the submerged deck volume and water specific weights, as shown in Eq.(3.5):

$$F_{Bd} = V_{sub,d} * \rho_w * g \quad (3.5)$$

The resultant component of shear and pressure forces (due to viscosity and turbulence) in the flow direction is known as the drag force, which is calculated as:

$$F_D = 1/2 * C_D * \rho * V^2 * s * L \quad (3.6)$$

Where F_d is the drag force in N; C_d is the drag coefficient (non-dimensional); ρ is the density of water (kg/m^3); V is the free stream velocity in m/s; h_u is the height of water from the ground in m; h_b is the distance from the ground to the bottom of the girder in m; and L is the bridge length in m.

The superstructure stability in the vertical direction depends on the lift forces acting perpendicular to the flow direction, expressed as:

$$F_L = 1/2 * C_L * \rho * V^2 * W * L \quad (3.7)$$

Where F_L is the lift force in N; C_L is the drag coefficient (non-dimensional); and W is the bridge width.

Finally, the instabilities caused by the hydrodynamic loads create a moment around the center of gravity M_{cg} that is expressed as:

$$M_{cg} = 1/2 * C_M * \rho * V^2 * W^2 * L \quad (3.8)$$

Where C_M is the momentum coefficient (non-dimensional).

Table 3-3 shows the most important variables that play a role regarding the calculation of each of the main acting forces.

Forces	Variables
Gravitational force	$W_{deck}, h_{road}, p_{road}, W_{gird}, h_{gird}, N_{gird}, p_{gird}, h_{rail}, W_{rail}, p_{rail}$
Buoyancy force	$W_{deck}, h_{road}, W_{gird}, h_{gird}, N_{gird}, h_{rail}, W_{rail}, p_{water}$
Lift force	$C_L, U, p_{water}, S_f, W_{deck}, L_{deck}$
Friction force	$W_{deck}, h_{road}, p_{road}, W_{gird}, h_{gird}, N_{gird}, p_{gird}, h_{rail}, W_{rail}, p_{rail}, \mu_{fricc}$
Drag force	$C_D, U, p_{water}, S_f, h_u, h_b$
Moment Force	$C_L, U, p_{water}, S_f, W_{deck}, L_{deck}$

Table 3-3: Variables that influence the main resisting and soliciting forces on submerged bridge deck.

The associated magnitudes to the variables in Table 3-3 are defined when the bridge dimensions/materials and the flow conditions (water depth h_u and flow velocity U) are known. However, there is still a need to specify which values should be used regarding the non-dimensional hydrodynamic coefficients present in the equations for determining the drag, lift and moment forces.

Several researches already presented in the literature review have performed experimental tests and numerical simulations for various flow conditions and bridge configurations, giving design values to be used in the above expressions for the hydrodynamic forces. However, there are still uncertainties surrounding those magnitudes and not always an agreement is found between the design values in the literature and experimental tests.

In order to cope with those uncertainties, the analysis of the published experimental results for a typical 3 girder bridge with concrete deck found in [42] and [45] are used to propose probabilistic distributions that will be later introduced in the limit state functions, building the foundations for a probabilistic approach to assess the failure probability of bridge instead of the normal deterministic approach.

Hydrodynamic coefficients: Sensitivity and probabilistic analysis

As seen during the literature review, there are several experimental and numerical simulation results and recommendations for adequate design values for the hydrodynamic coefficients that are not always aligned. Even in the laboratory, given a specific set of hydrodynamic loads and bridge configurations, the expected values for the different hydrodynamic coefficients might suffer from slight variations and, thus, in this graduation thesis it is suggested to be treated stochastically and not in the traditional deterministic form.

To define a stochastic variable, a probability distribution is needed. Normally, the probability distribution for a specific variable is defined based on pure statistical analysis of gathered data, both in field and in laboratory conditions. The methods to fit probability distributions to a data record are widely known and extensive information could be found in the literature. It is out of the scope of this thesis to perform this type of tests; however, available results from already undertaken experimental tests performed in laboratory could be used to define an appropriate probability distribution of values for the coefficients as a function of the flow conditions and bridge configurations.

As mentioned during the literature review, the results from [41], [42] and [45] will be analyzed in order to define adequate probability distributions for the hydrodynamic coefficients and finally elaborate the intended fragility curves for a typical three concrete girder bridge. A summary of the three studies that will be used along this section is now presented.

- In [41], physical experiments were performed to validate numerical simulations in order to quantify the loads on rectangular bridge cross sections. To this end, more than 700 simulations were performed, accounting the effect of several variables for bridge configuration and flow conditions. Values for lift, drag and moment coefficients are provided as a function of the studied variables.
- In [42] the effect of hydrodynamic forces on inundated three girder bridge with concrete deck is studied, by means of a combination of physical experiments and numerical modeling techniques using Computational Fluid Dynamics software. The experiments and calculations were performed for different Froude numbers, three bridges configurations and different values for the inundation ratio.
- In [45] several experiments were performed to assess the effect of the Froude number, the inundation ratio and the superstructure's proximity ratio on the hydrodynamic loading of the bridge structure. To that end, different bridge and pier geometries and flow configurations were tested. The outputs of more than 500 experiments are given in tables and design figures. In addition, design criteria that considers maximum loads on bridge piers and superstructures caused by debris is presented.

The results found in the bibliography have been analyzed to define a range of potential values that can be used in the stability analysis of the deck-pier connection against hydrodynamic thrust. Table 3-4 shows the minimum, mean and maximum estimates for coefficients according to the bridge proximity ratio and two hydraulic parameters (Froude number and inundation ratio), which should be previously calculated by means of hydraulic modeling for each return period. Only the values associated for proximity ratio equal to 3.5 is shown, being the case study bridge's proximity ratio.

Proximity ratio = 3.5							
Froude	h*	CD-	CD+	CL-	CL+	CM-	CM+
0.15	0.5	1.1	1.5	-6.0	2.5	-6.0	0.2
	1	0.9	1.5	-6.0	-0.5	0.1	1.5
	2	1.5	2.2	-4.5	-1.5	-0.1	4.5
	3	1.6	2.2	-1.0	0.0	-0.1	4.5
0.3	0.5	0.6	1.4	-6.0	0.5	-1.1	2.0
	1	1.2	2.3	-7.0	0.0	-1.6	1.5
	2	1.9	2.2	-5.5	0.0	-1.7	4.5
	3	1.8	2.2	-2.0	0.0	-1.7	4.5
0.5	0.5	0.7	0.9	-1.1	0.5	0.0	1.3
	1	1.5	1.9	-8.0	0.0	-0.2	1.5
	2	2.2	2.2	-6.5	0.0	-0.2	4.5
	3	2.1	2.2	-3.0	0.0	-0.2	4.5
0.8	0.5	0.8	1.5	-1.8	0.5	0.3	1.3
	1	1.5	1.6	-1.7	0.0	0.3	1.5
	2	2.0	2.2	-1.7	-0.8	0.4	4.5
	3	1.9	2.2	-1.3	0.0	0.2	4.5

Table 3-4: Minimum and maximums values estimates for hydrodynamic coefficients as a function of proximity ratio, inundation ratio and Froude number. Source: [41], [42], [45]

From the above information it is possible define the hydrodynamics coefficients as a stochastic variable.

A Uniform distribution is suggested defined by the largest range in which the coefficients expected values may shift as shown in Table 3-4, prior consideration that any value for hydrodynamic coefficients can occur with the same probability within the established range.

Limit state functions for deck-pier connection stability

Considering F_Z the gravitational force, F_D as the drag force, F_b as the buoyancy force and F_L as the lift force, the equations for the different limit state functions (LSF) regarding deck stability are given in [39]:

Eq. (3.9) shows the vertical stability Limit State Function that is used in the vertical deck-pier connection stability assessment.

$$Z_{vert,d} = R_{vert,d} - S_{vert,d} = F_{Z,d} - (F_{B,d} + F_{L,d}) \quad (3.9)$$

Where $Z_{vert,d}$ is the resistance against vertical movement of the deck; $R_{vert,d}$ the vertical restoring force of the deck and $S_{vert,d}$ is the vertical soliciting force of the deck. All forces expressed in N.

Eq. (3.10) shows the horizontal stability Limit State Function that is used in the horizontal stability assessment of the deck-pier connection.

$$Z_{hor,d} = R_{hor,d} - S_{hor,d} = F_{R,bear} - F_{D,d} \quad (3.10)$$

where

$$F_{R,bear} = F_F = \mu * Z_{vert,d} \quad (3.11)$$

Where $Z_{hor,d}$ is the resistance against horizontal movement of the deck, expressed in N; $R_{hor,d}$ the horizontal restoring force of the deck; $S_{hor,d}$ is the horizontal soliciting force of the deck; $F_{R,bear}$ the restoring force exerted on the bridge deck by the bearing; and F_F the frictional force. All forces expressed in N.

For the friction force, the friction coefficient (μ) between the elastomeric material and steel plate is determined by the manufacturer. The range can vary between 0.20 and 0.33 (Bearings, 2018) (Trelleborg Engineered Products., 2018). In this case, a friction coefficient of $\mu = 0.2$ (less favorable scenario) is assumed.

Eq. (3.12) shows the rotation stability Limit State Function that is used in the rotation deck-pier connection stability assessment.

$$Z_{over,d} = R_{over,d} - S_{over,d} = F_{Zd} * L_{cgd} - [(F_{B,d} + F_{L,d}) * L_{cgd} + F_D * h_{cgd} - M_{cgd}] \quad (3.12)$$

Where $Z_{over,d}$ is the resistance against rotation movement of the deck, expressed in N; $R_{over,d}$ is the restoring moment of the deck and $S_{over,d}$ is the overturning of the deck; L_{cgd} is the horizontal distance from the center of gravity to the point of deck's rotation; h_{cgd} is the vertical distance from the center of gravity to the point of rotation. All forces expressed in mN.

Deck-pier stability evaluation

As stated during the literature review, by the use of a limit state function Eq. (3.13) where R stands for restoring forces and S for destabilizing forces:

$$Z = R - S \quad (3.13)$$

The bridge stability evaluation against hydrodynamic forces is based on the following principle:

If any of the three ULS functions is less than 0, which implies that the destabilizing forces are greater than the resistant forces, then the pier-deck connection fails causing bridge deck collapse.

Based on the range of values for the hydrodynamic coefficients (Table 3-4), values for the hydraulic parameters (Froude number and inundation ratio) obtained after hydraulic modelling and bridge geometry configuration the three functions ULS already presented are evaluated.

The results are displayed in the form of sensitivity analysis, since the values of the hydrodynamic coefficients vary depending on the consulted study, presenting a range of potential values for each limit function, each return period of flooding and each climate scenario.

Considering that any value for hydrodynamic coefficients can occur with the same probability within the range established (what would equal to a Montecarlo simulation where the hydrodynamic coefficients follow a uniform distribution between the proposed range values), the failure probability of the deck-pier connection is calculated using the ratio between values that fall below zero and the values that are greater than zero

Finally, fragility curves are constructed, where the x-axis will be represented by the flow peak at the bridge location (which is directly linked with a water depth and Froude number for a specific bridge cross section) and the y-axis by the failure probability.

For an example of the application of the above methodology to a bridge case of study, the reader is referred to A11.6 section of Appendixes of the present report.

Bridge-scour response under flooding

As seen during the literature review, the recommendations and procedures given by [46] presents the state of knowledge for the evaluation of bridges for scour, and therefore, its guidelines will be adopted during this graduation work. The general procedure proposed in this document to evaluate erosion in the bridge-type of study can be summarized in the following stages:

- Choosing the range of flood events that are estimated to produce severe erosion conditions in the foundation.
- Application of a hydraulic model to calculate the hydraulic parameters necessary to estimate the scour development for each of the flood events defined in the previous step.
- Estimation of the total scour for the hydraulic conditions defined above by the following steps:
 - The review of available information allows to obtain the required variables for scour evaluation: Gradation, distribution and size of the river bed granular material, cross section at bridge location including the main channel and flood plains, Watershed characteristics historical scour data in other bridges close to project area, longitudinal riverbed slope, historical flood events, location of other bridges close to the study area, river characteristics (permanent, torrent, gradual flow peaks) and geomorphology of the study area.
 - Determine the magnitude of the long-term scour/sedimentation processes.
 - Determine the magnitude of scour by section contraction.
 - Determine the magnitude of the local scour in the bridge supports/piers.
 - Determine total erosion and evaluate the design of the bridge foundation.
- Evaluation of the results reliability by expert judgement based on a multidisciplinary team that includes hydraulic, geotechnical and structural engineers.
- Evaluate the bridge foundation's failure based on the results obtained. For foundations on spread footings in granular soils, any scour situation is considered unstable if: the lower foundation footing level is above the final level of the river bed after the flood event.

Here, some of the considerations made for the case of study are shown.

- The range of flood events considered for the study of this failure mode is identical to the one used in the study of the other failure modes analyzed in this report (general pavement deterioration due to

river flooding and bridge collapse by hydrodynamic thrust). A range of flood return periods of 2 to 500 years is selected.

- The hydraulic model used for the study of the bridge scour is identical to the one been applied for the study of the other failure modes analyzed in this report (i.e. general pavement deterioration due to river flooding and bridge collapse by hydrodynamic thrust). The hydraulic characteristics are determined using the HEC-HMS and HEC-RAS software as explained in detail in Chapter 3.3 of this report. It is particularly important to obtain: the maximum flow depth (m); and the maximum flow velocity (m/s) during flood peak at bridge location.
- The system definition (i.e. piers foundation) is considered as a spread footing foundation. Piers are not groups and have a rounded hydrodynamic shape. Therefore, all of the scour calculation should be performed for this foundation and piers type.
- The magnitude of the long-term erosion/sedimentation processes is usually due to a problem of instability of the channel by modifications in the river or in the upstream basins (construction of dams, canalizations, mining and extraction of aggregates), causing degradation/sedimentation until equilibrium is reached. Methods for estimating long-term erosion/sedimentation are found in (FHWA, 2012). This example assumes that the considered section is in equilibrium.
- Scour will be calculated considering the sum of contraction scour and localized pier scour.
- The failure of the bridge by destabilization is governed by the following principle: The base of the foundation must never be left above the final level of the river bed once the flood event and induced-scour has occurred.
- Following the previous principle, if the total scour is greater than total foundation depth, the probability of failure of the bridge will be high ($\cong 100\%$). If the scour depth is below the foundation depth, probability of failure will be equal to zero.

Road pavement response under flooding

The road pavement response under flooding will be assessed following the next steps:

- The following main outputs are obtained from the hydrological/hydraulic model: the identification of critical road stretches where large-scale flooding is expected due to increasing river levels, including the water depths (in m) and flooded areas (in m^2) for each return period considered in the analysis.
- The probability of road failure due to pavement flooding is given by the frequency (i.e. return period) from which water depths are expected to occur on the road axis. Once there is more than 0.3 cm of water depth on top of the infrastructure [79], the road will be considered closed for normal vehicle traffic and failure probability will be 1.
- The level of pavement damage is estimated by the use of a global depth-damage curve based on analysis of past flood events and on expert judgment to evaluate the economic consequences after flooding of transportation infrastructure. The propose damage-depth functions are given in the Literature Review of this report (Section 2.4.2). Two different depth-damage curves are used to differentiate paved and unpaved roads.
- The level of damage should be transferred to quantifiable metrics to allow for a better consequence estimation.
 - For direct consequence estimation, the maximum value of damage ($\$/m^2$) is used to quantify the proposed damage-depth curves for paved and unpaved roads and its value is estimated by analyzing the information from the damage assessment report presented by [40].

- For indirect consequence estimation two metrics will be used: Road closure time and cost of economic disruption during that time; Road rehabilitation time and incremental vehicle operational cost due to road pavement deterioration (measured by IRI index) during repair works.
- Specific expressions and case-study considerations for (direct and indirect) consequence estimation are presented respectively in chapter 3.3.5 and Appendixes of this report.

3.3.4. Consequence Estimation

Direct consequences

The methodology used to estimate the direct consequences is now described and is based on the combination of the flood hydraulic characteristics and the estimated values for the pavement and road infrastructure reconstruction costs along with the depth-damage curves [69] proposed for paved and unpaved roads, which were presented in the literature review (Section 2.4.2).

For the assessment of the direct consequences regarding the road pavement damage due to river flooding, the damage-depth curves [69] require to be quantified by means of a maximum damage value in case of road failure. The expression to calculate the direct reconstruction cost for a specific road section is shown in Eq. (3.14).

$$R_{\text{cost}} = A_{\text{flood,road}} * LOD_{\text{road}} * D_{\text{max,value}} \quad (3.14)$$

Where R_{cost} is the total direct reconstruction cost in €, A_{road} is the flooded area of the road section considered, LOD_{road} the level of damage of the road section given in % and D_{max} the maximum damage value for the road section in €/m².

The flooded road-section area (A_{road}) is obtained as an output of the hydrological-hydraulic modelling with HEC-HMS and HEC-RAS 2D software's.

The level of road damage (LOD) due to a flood event is calculated using the damage-depth curves proposed for both, paved and unpaved roads (See Figure 2-12).

The maximum damage value (D_{max}), normally expressed in €/m², is specific for each project location and construction material conditions. In the case of this graduation project, the maximum flood-induced damage-cost for the road (in €/m²) will be obtained by analyzing the information from the damage assessment report prepared by [40]. Detailed calculation process and considerations made to obtain $D_{\text{max,value}}$ can be found in Appendixes of the present report.

For the assessment of bridge reconstruction cost, in absence of reliable data, an expression is proposed by [10], which relates the mean structural value ($R_{\text{cost,bridge}}$ in \$ 1994) of a bridge with the length (m) and is based on a statistical analysis of a wide bridge structural values record. These construction costs are in 1994 dollars, and need to be adjusted to present dollar value.

$$R_{\text{cost,bridge}} = 20000 + 8000 * L_{\text{bridge}} \text{ (in 1994 \$)} \quad (3.15)$$

Indirect consequences

As concluded from the literature review, the assessment of indirect consequences due to road failure is usually evaluated by means of the increase in generalized travel cost (cost to make a trip) during the time the road is disrupted during and after a flood event. In this graduation work, two different metrics are used for this matter:

- The traveler's cost of time during road closure due to a flood event, as suggested in [10].
- The incremental vehicles exploitation cost due to circulation on a deteriorated pavement during reconstruction time after the flood event, as proposed in [71].

Considering that travelers are assumed to behave by the user's equilibrium principle, i.e., choosing the route that minimizes their travel cost, the basis that will be used along this graduation work to derive indirect consequences due to road failure is derived from Eq. (2-17) [55]. Including the indirect damage due to road closure cost of time and incremental costs of vehicle circulation in a deteriorated road it stays as shown in Eq.(3.16).

$$C_{ind} = T_{clos} * (C_{travel,flood} - C_{travel,norm}) + T_{rehab} * (CVO_{rehab} - CVO_{norm}) \quad (3.16)$$

Denoting the indirect consequences by C_{ind} (in \$), T_{clos} as the total time of road closure (in days); $C_{travel,flood}$ as the total daily cost of traveling during the flood scenario (in \$/day), $C_{travel,norm}$ as the total daily cost of traveling during the base-case scenario (\$/day); T_{rehab} as the total time of road rehabilitation (days), CVO_{rehab} as cost of vehicle exploitation during rehabilitation works and CVO_{norm} as cost of vehicle exploitation during normal road use before flood.

If during a flood, there are no real route alternatives to the desired destination regardless the road under analysis it is therefore not possible to calculate the increase in travel time during the flood event for travelers choosing an alternative way as they are no substitute paths. It is then assumed the indirect costs during closure (C_1) equals to the total cost of lost working time due to road closure, which is expressed as the average cost of time of a normal worker (C_{time}), multiplied by the expected daily traffic flow expected F_{veh} , the number of closure days T_{clos} and the average workday duration T_{work} .

When Eq.(3.16) is updated, the expression changes into:

$$C_{ind} = C_1 + C_2 = T_{clos} * F_{veh} * C_{time} * T_{work} + T_{rehab} * (CEV_{rehab} - CEV_{norm}) \quad (3.17)$$

Equation (3.17) allows to link pavement deterioration to indirect consequences after a flood event, as the cost of vehicles exploitation (VEC) depends on the road condition [71].

As stated during the previous chapter, pavement condition after flood is normally evaluated according to the international roughness index (IRI), which represents driving comfort by simulating the movement of the accumulated vehicle suspension through a specific road profile length of the x and is expressed in (m/km).

Figure 3-14 shows the relation between the road pavement condition (IRI) and vehicle operational costs that will be used for the case study, based on a report conducted for Country Z's roads. Other reference, in absence of specific project data can be found in [71].

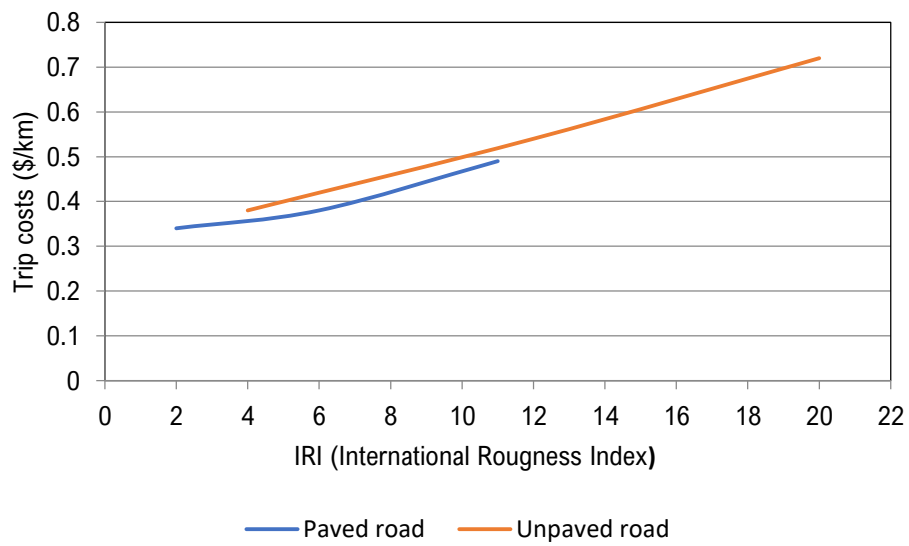


Figure 3-14: Relation between the road pavement condition (IRI) and vehicle operational costs for the case study.

The closure/reparation time of the road during/after a flood event is normally calculated based on past flood-damage assessments. For the case study, road closure values will be estimated based on the life-cycle duration of past hurricanes in the project area and road reparation times will be estimated based on current values (10 years after last important flood event in the road).

The estimate of the average cost of time per person/worker (in \$/ h) has been carried out on the basis of two studies [74] [71].

The detailed calculation process and assumptions to obtain value's estimations for the above variables for the case-study are explained in detail in Appendixes of this report.

PART III.CASE STUDY

4. REVIEW OF AVAILABLE INFORMATION

The first phase of the methodology consists in the review of the existing information (see Figure 4-1) to improve the knowledge regarding road vulnerability against floods, prior to the failure mode identification session.

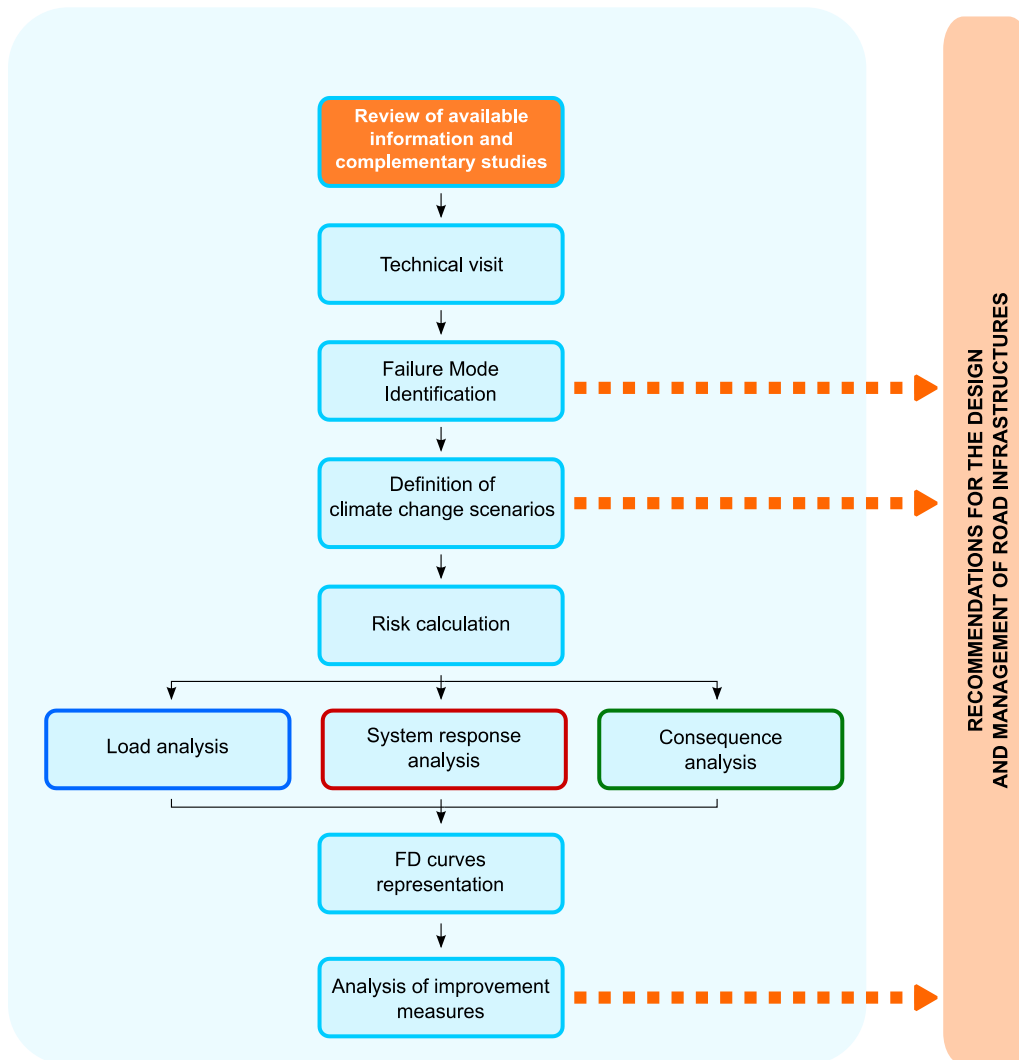


Figure 4-1: Proposed methodology for road risk analysis. Phase 1: Review of available information and complementary studies

The case study is based on the consultancy work; however, the assumptions and results hereby presented have been modified explicitly for the graduation work purposes and do not represent, in any case, a rigorous representation of the real case project.

However, the Case Study may contain sensitive professional information for the company and client interest and the Review of available information was decided to be classified for the public

5. TECHNICAL VISIT

5.1. Introduction

The next step of the methodology, prior to the failure modes identification session, is a technical visit to the road (X). This phase is a source of valuable information as it allows checking the current conditions of road infrastructure and the correspondence with the hydrological model. On the other hand, it also allows detecting peculiarities which, by its nature, or simply by constant changes affecting the structure over time, are not detailed in the documentation.

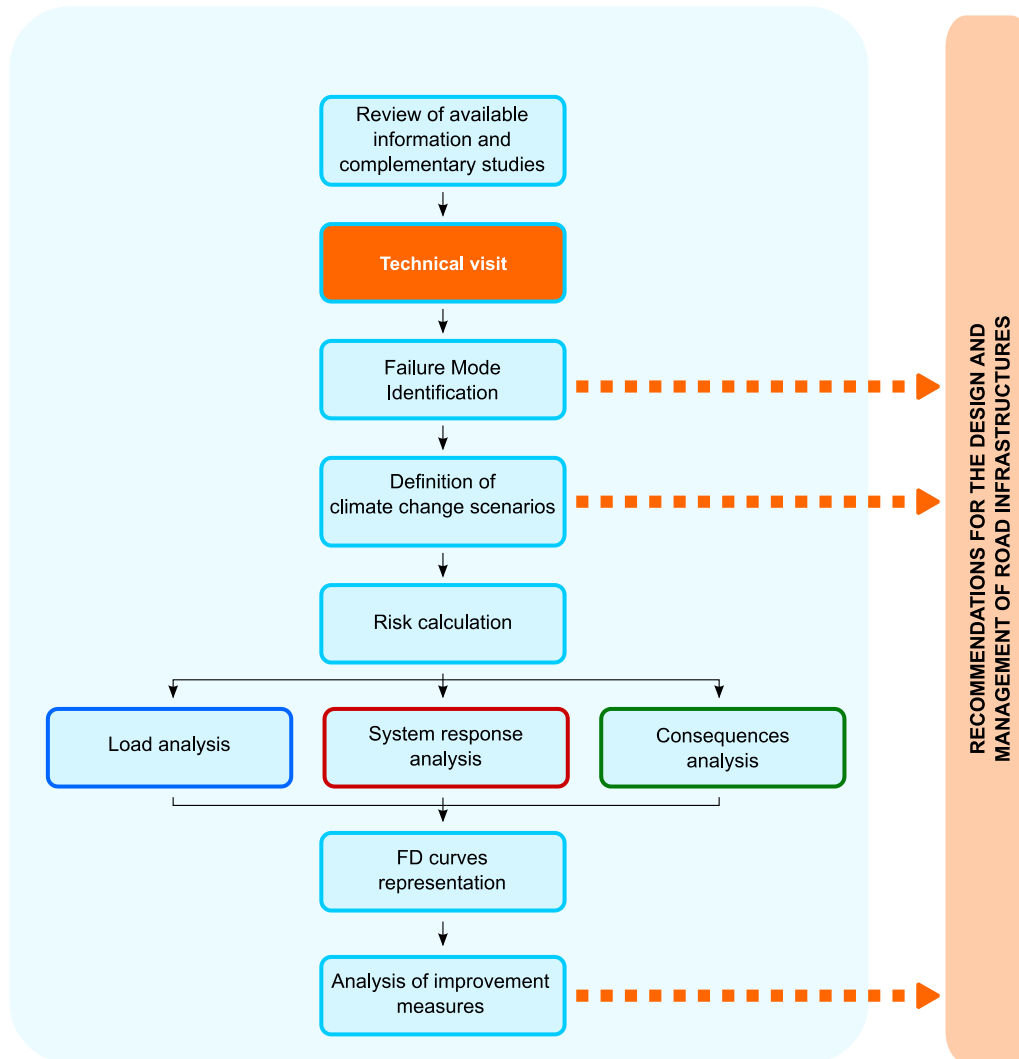


Figure 5-1: Methodology for the analysis of natural hazards on the X highway. Phase II: Technical visit.

The case study is based on the consultancy work; however, the assumptions and results hereby presented have been modified explicitly for the graduation work purposes and do not represent, in any case, a rigorous representation of the real case project.

However, as, the Case Study may contain sensitive professional information for the company and client interest and the the Technical visit was decided to be classified for the public.

6. FAILURE MODE IDENTIFICATION

Within the process of flood risk analysis, identification of failure modes is a key part of the process, since it is the preliminary step towards the definition of the architecture of the quantitative risk model to calculate the risk in the current situation and after implementation of the projected measures.

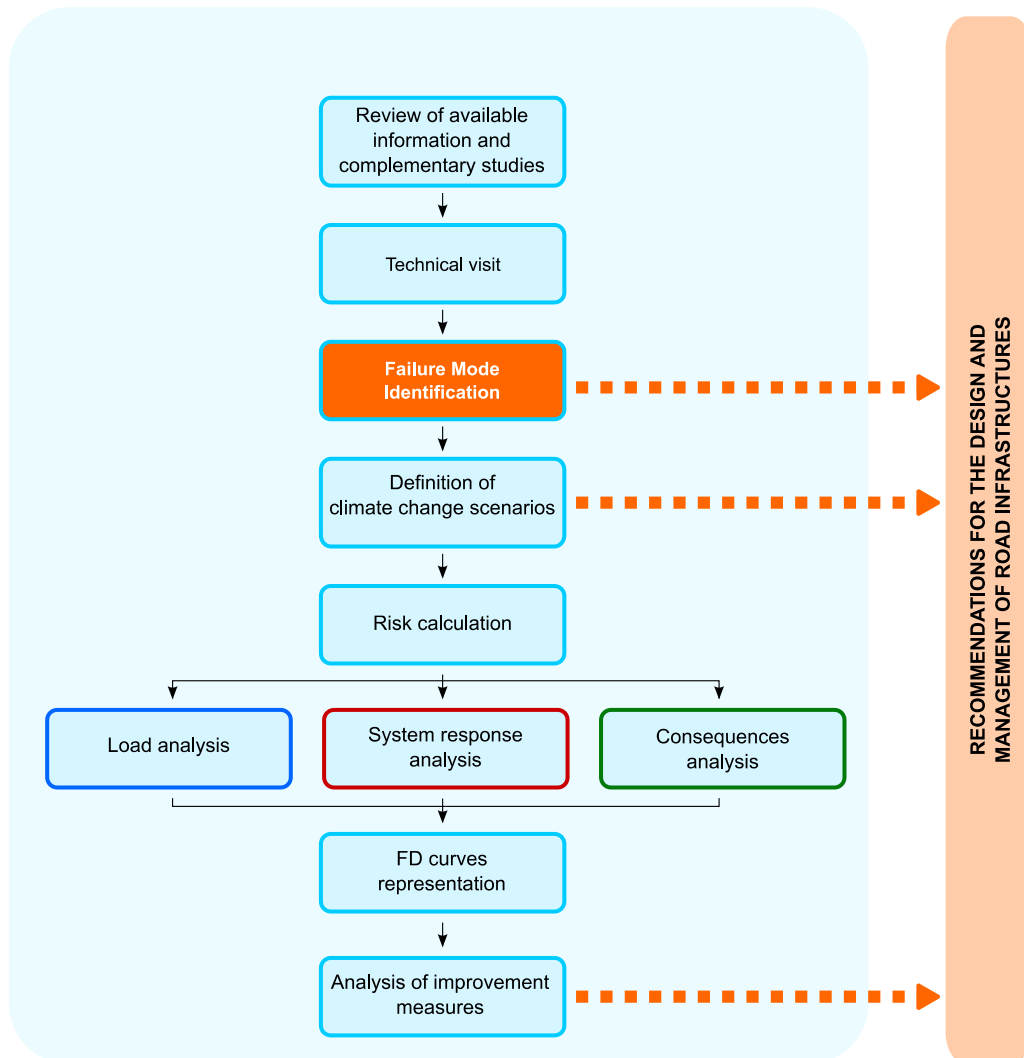


Figure 6-1: Methodology for the analysis of natural hazards on the X highway. Phase III: Failure Mode Identification

As explained in the Chapter 3.1 to this report, a failure mode is a particular sequence of events that may lead to a risk management system failure. This series of events is associated with a particular load and have a logic sequence, which consists of an initial trigger event, subsequent development and system failure, as shown in Figure 6-2.

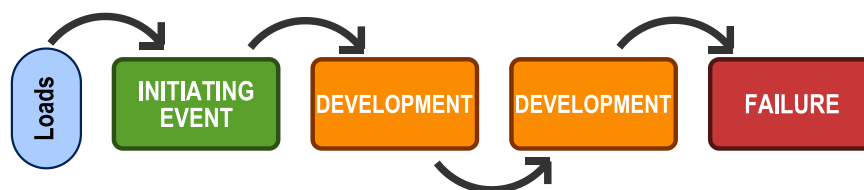


Figure 6-2: Generic structure for a failure mode

6.1. Failure Mode Classification

Once the potential failure modes are identified, a classification is required to determine their relevance and their subsequent inclusion (or not) in the quantitative phase of the project. The classification criteria are explained in Chapter 3.1.2 of this report.

Table 6-1 shows the Failure Mode Classification for the X road in Country Z. The considerations that have been made for the classification of failure modes are presented in Appendix 1 (Section A1.6) of this report

Failure Mode	Level
A1: Large scale flooding and generalized damage to pavement	B
A2: Pavement erosion by run-off on steep road slopes	C
A3: Road settlement due to foundation wash out of fine particles	D
A4: Liquefaction in case of an earthquake	D
A5: Road settlement by karst formation	D
B1: Clogging of the longitudinal drainage by sediments	C
B2: Clogging of the transversal drainage by sediments / trunks	C
B3: Drainage failure due to erosion at foundation level	C
B4: Clogging of the transversal drainage due to insufficient capacity	C
C1: Scour piers/abutment foundation and bridge collapse	E
C2: Deck-pier connection failure and bridge collapse	E
C3: Failure due to a seismic load	E
D1: Land-slide under the road	C
D2: Land-slide over the road	C
D3: Rock falling over the road pavement	D
D4: Slope erosion due to river load	C
D5: River bank protection failure due to river load	C
E1: Informal population settlements	E
E2: Not leaving of properties in case of flooding	E
E3: Failure in the alert system	C

Table 6-1: Failure Mode Classification. X road (Country Z).

In the following figures, the three FMs classified for quantitative risk calculation (Level B) are presented and described. The rest of the identified failure modes schemes and the main factors that increase or decrease the probability of occurrence are detailed in Appendix 1 of this report.

Failure Mode A	
Name	Large scale river flood and structural pavement deterioration
Description	
<p>In hydrological scenario, a river level increase by a flood until exceeding the road level. The water depth on the pavement causes scour, that develops until finally producing the removal of the pavement layer, leaving it totally or partially impassable, isolating local populations in cases of flood emergency.</p>	
Graphical Scheme	
More likely factors	Less likely factors
<ul style="list-style-type: none"> ▪ Most of the route is unpaved, which favors deterioration for a river flooding event. ▪ The route runs parallel to the river channel in several sections with small difference between the river and the road level, without flood defense works to protect against river flooding. ▪ There are blockages in some longitudinal drainage sections that increase the water level and duration on the road after a flood or storm event. ▪ Climate change is expected to increase rainfall intensity and flood levels for a certain return period. ▪ Isolation of populations during emergencies in case of impassable route. ▪ Deforestation problems of the watershed, which generates erosion, debris occurrence, higher flood peaks and lower concentration times. 	<ul style="list-style-type: none"> ▪ The design of a new route could avoid some of the zones that run parallel and close to the river channel (less flood-prone potential). ▪ In several points, bridges section seems to be enough to allow river flows and to avoid the flood by increasing river levels at the river-road intersections.

Figure 6-3: Failure Mode A1. Description and “less likely” and “more likely” occurrence factors.

Failure Mode B	
Name	Deck-pier connection failure and bridge collapse
Description	
<p>In hydrological scenario, if river flood reaches a sufficient magnitude it can overtop the bridge deck causing a hydrodynamic force on the deck-pier connection. If the destabilizing force is large enough it can exceed the friction force between deck and pier producing the failure of the connection.</p>	
Graphical Scheme	
More likely factors	Less likely factors
<ul style="list-style-type: none"> ▪ The extraction of aggregates in the river channel area can increase flow velocity and, thus, the hydrodynamic force on the deck-pier connection. ▪ Climate change is expected to increase the rainfall intensity and the flood level for a certain return period. ▪ Isolation of the population in case of bridge failure during a flood event. ▪ There are not always alternative routes in case of bridge failure. ▪ Narrow river channels have higher levels and flow velocities and are more likely to suffer from this type of failure. 	<ul style="list-style-type: none"> ▪ In several bridges, the riverbed is sufficiently wide and it seems unlikely that the river can suffer such large elevations to cause overtopping of bridge deck.

Figure 6-4: Failure Mode C2. Description and “less likely” and “more likely” occurrence factors.

Failure Mode C	
Name	Scour piers/abutment foundation and bridge collapse
Description	
<p>In the hydrological scenario, if the flow velocity is sufficiently high, the natural granular terrain surrounding the foundation can be eroded producing a scour hole. The scour can lead to the settlement of the entire infrastructure and loss of support. The loss of support ends up causing instabilities and final collapse, if the river level ends up below the lower part of the piers foundation.</p>	
Graphical Scheme	
<p>2. Flow velocity increases due to floods, climate change, watershed deforestation and aggregate extractions.</p> <p>1. Unrestricted aggregates extraction in the riverbed</p> <p>3. Scour holes close to foundation level induces settlements and infrastructure instabilities</p>	
More likely factors	Less likely factors
<ul style="list-style-type: none"> ▪ Extraction of aggregates in the channel area can increase the flow velocity and the risk of erosion. ▪ Climate change, which is expected to increase the rainfall intensity and floods level for a certain return period. ▪ Isolation of population in case of bridge failure during a flood event. ▪ Presence of non-cohesive and easily eroded materials in the river bed and in the piers foundation. ▪ There are no alternative routes in case of bridge failure. 	<ul style="list-style-type: none"> ▪ In dry season most piers are visible and scour problems can be detected and corrected. ▪ After the field visit it was observed that most of the large bridges are generally in good condition and there are no visible signs of scour problems. ▪ The failure is gradual and localized and does not have serious consequences of loss of life or complete loss of function of the infrastructure.

Figure 6-5: Failure Mode C3. Description and “less likely” and “more likely” occurrence factors.

7. DEFINITION OF CLIMATE CHANGE SCENARIOS

This chapter refers to the effect of climate change on natural hazards (mainly floods) that directly affect the road infrastructure under study and a description of how should be considered when implementing a new road design, so it is directly related to the fourth point in the process (in Orange in the figure). The definitions of these scenarios of calculation allow obtaining recommendations for infrastructure design, which are detailed in this report.

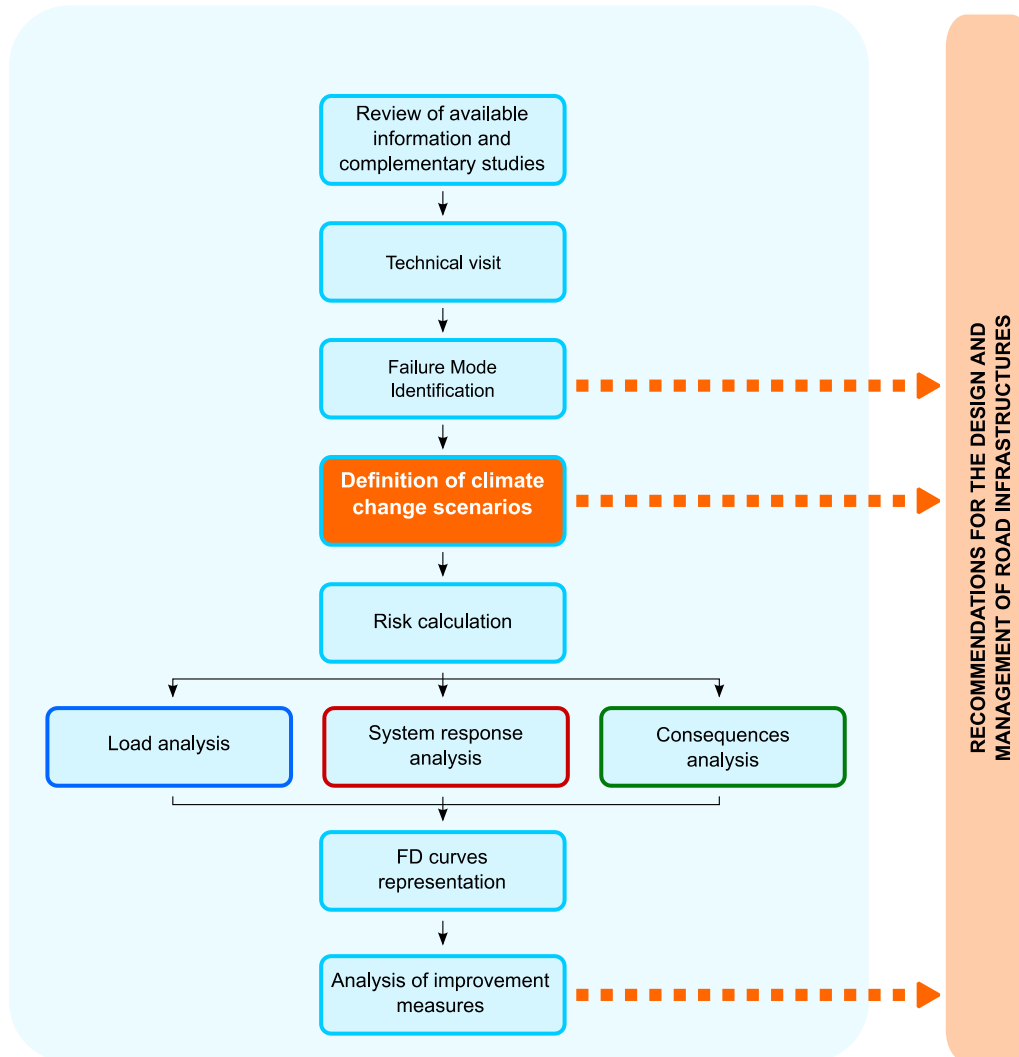


Figure 7-1: Methodology for the analysis of natural hazards in the X. Definition of future climate change scenarios

The climate change scenarios that will be studied in this report and the proposed methodology to obtain associated IDF storm values is explained in Chapter 3.2 of this report. In this chapter, the results from applying the proposed methodology are shown and a representative climate change scenario for updating the hydraulic modeling will be selected.

7.1. Recommendations to include the effect of the CC: Design storms

In general, the projections for Country Z reveal a general reduction on the annual precipitation volumes and an increase of temperatures in the region. In contrast, precipitation rates during tropical storms are prone to increase.

The following figure shows the proposed methodology explained in Chapter 3.2 of this report to assess the climate change effect on precipitation regimes (maximum daily rain expected) in the project area.

Figure 7-2 shows the average percentage increase expected with respect to the historical maximum daily rainfall expected for three trend scenarios of climate change (RCP2.6, RCP4.5 and RCP8.5) and 7 return periods (2 to 500 years) The results are not specific to a weather station, representing the mean increment with respect to the four meteorological stations analyzed.

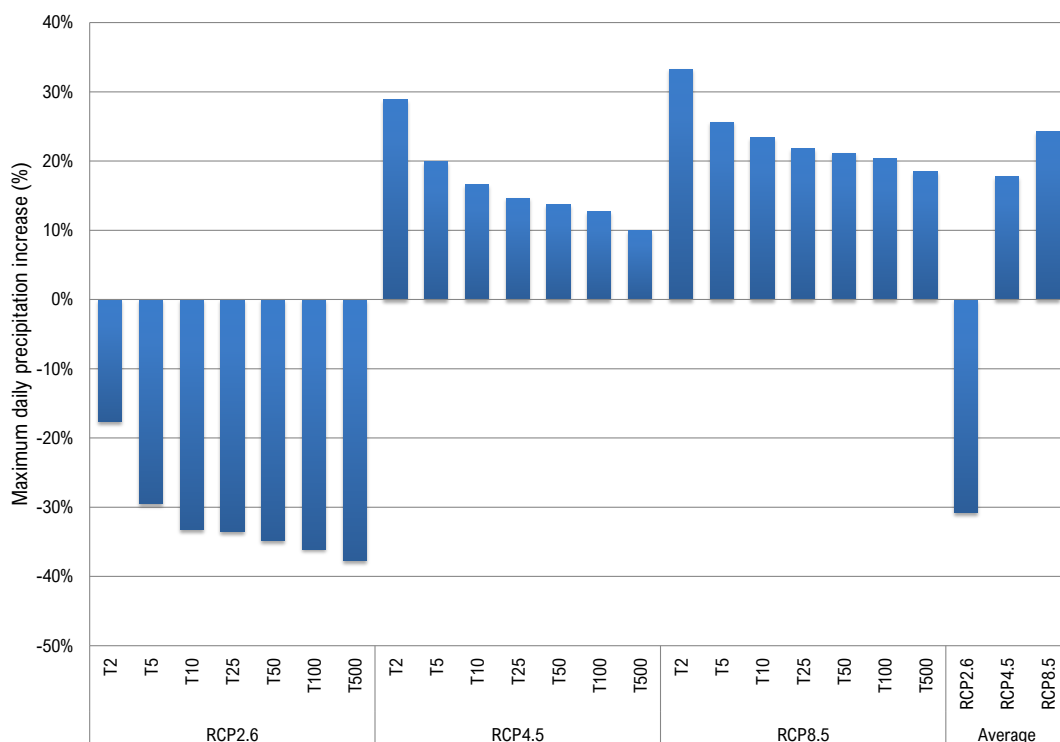


Figure 7-2: Increase (in %) with respect to the historical data for maximum daily rainfall (mm in 24 h) expected for three climate-trend scenarios (RCP2.6, RCP4.5 and RCP8.5), 7 return periods.

Based on the results, a climate trend-based scenario is selected to perform and update the hydrological and hydraulic simulations prior to quantitative analysis of risk for the study area.

The climate trend-based RCP8.5 scenario, representing an average increase of around 25% of the annual daily maximum precipitation with respect to the historical setting (see Figure 7-2), which results to be the most conservative scenario, will be considered as representative for the hydraulic and hydrologic simulations prior to quantitative risk analysis.

7.2. Recommendations to include the effect of the CC: Land – use cover

The land-use cover distribution in the sub-basins has been determined from global maps provided by MODIS as explained in Chapter 3.3.

Based on a desertification forecast due to climate change in the study area, is suitable to think about a future soil degradation and a change from a soil hydrological condition of type C to type D, with higher values of the CN. Considering a poor hydrological condition of the soil, CN values have been determined for each of the basins according to the classification by IGBP and GIS software tools.

Figure 7-3 shows the results of applying the methodology explained above, presenting the CN values for each sub-basin and climate trend-based scenario.

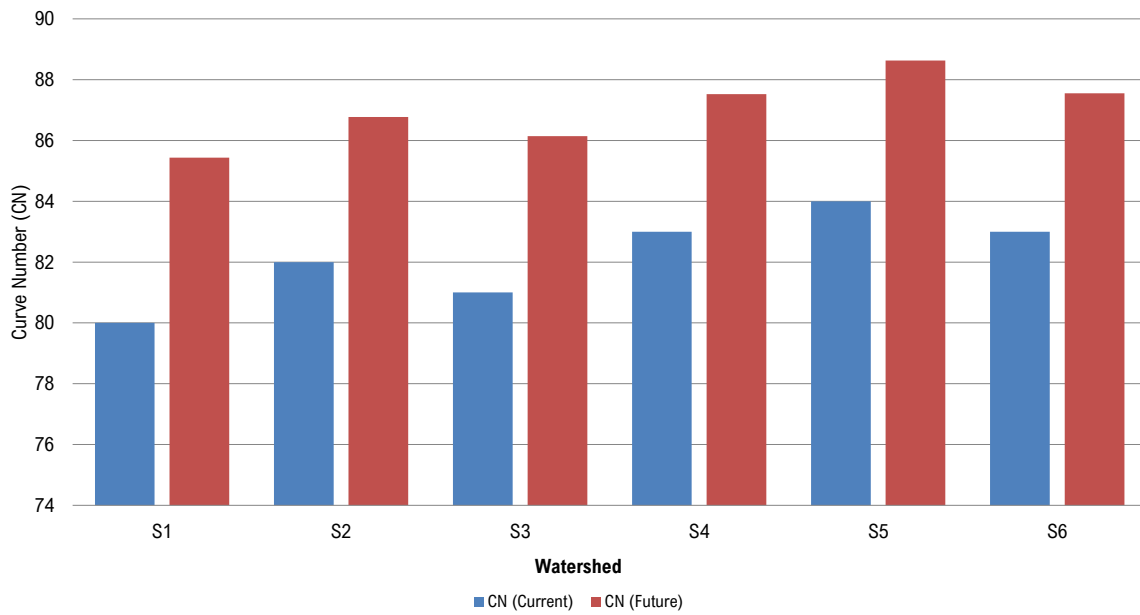


Figure 7-3: Values of the CN for each sub-basin and climate trend-based scenario.

8. LOAD ANALYSIS: HYDROLOGICAL & HYDRAULIC MODELING

8.1. Watersheds and land use

For the watersheds definitions, the DEM used in this analysis has been obtained from the database of the Web Open Topography, with a resolution of 30 m x 30 m. From the DEM, and using the corresponding GIS tools, the main 6 watersheds and river channels that intercept the different road sections have been determined.

The parameters relating to the morphometry of each of the sub-basins are presented in Chapter 4.3.3 of this report showing the values for: the area, the length of the main channel, the Elevation the slope of the basin, obtained after the spatial analysis of the MDT of 30 m resolution.

8.2. Historical rain data and design storms

For this project, daily rainfall data of historical records for several stations close to the X road was available. Table 8-1 shows the period of historical registration for each of the stations that have been studied.

Station	Record length (years)	Maximum Daily Precipitation (mm)
A	51	99.5
B	33	138
C	27	132
D	39	252
E	76	412

Table 8-1: Daily rainfall data of historical records for several stations close to the X road.

From the annual maximum historical data of daily rainfall (in mm), a frequency distribution analysis is carried out, in order to know the maximum daily rainfall associated with different return periods for each one of the stations considered in the analysis.

After the statistical analysis, where an adjustment with different probability distributions (Normal, Pearson III, log-normal, log-Pearson III, Gumbel) has been tested, it has been observed that the best fit for all stations is the Gumbel distribution.

Table 8-2 shows the maximum daily rainfall for different return periods.

	Return period (years)						
	T2	T5	T10	T25	T50	T100	T500
A	92	158	201	256	297	337	430
B	77	127	160	201	232	263	333
C	64	92	111	135	152	169	210
D	58	92	115	143	164	185	233
E	51	67	78	92	102	113	136

Table 8-2: Maximum daily rainfall for different return periods. Several meteorological stations within the project area.

Once the values of maximum daily rainfall (mm in 24 h) expected at each meteorological station and for different return periods are known, the following step is to build a design storm for the chosen sub-basin and return period.

In analysis the design storm type III proposed by NRCS (Natural resources Conservation Service of the USA) has been used, which is valid for coastal areas in the Atlantic, where tropical cyclones result in storm durations of 24 hours [77].

In order to know the estimated rainfall in each watershed from the data of the nearby stations, the Thiessen polygons method is applied through GIS tools. The method delimits the sub-regions of influence corresponding to each pluviometer.

From maximum daily rainfall values (mm in 24 h) estimated, the form given by the design storm proposed by the NCRS and the Thiessen coefficients in the area of interest, it is possible to construct the storm design for a 24 h storm duration for each of the 19 watersheds of interest. As an example, the design storm for the S1 Basin, return periods of 100 years, is included below.

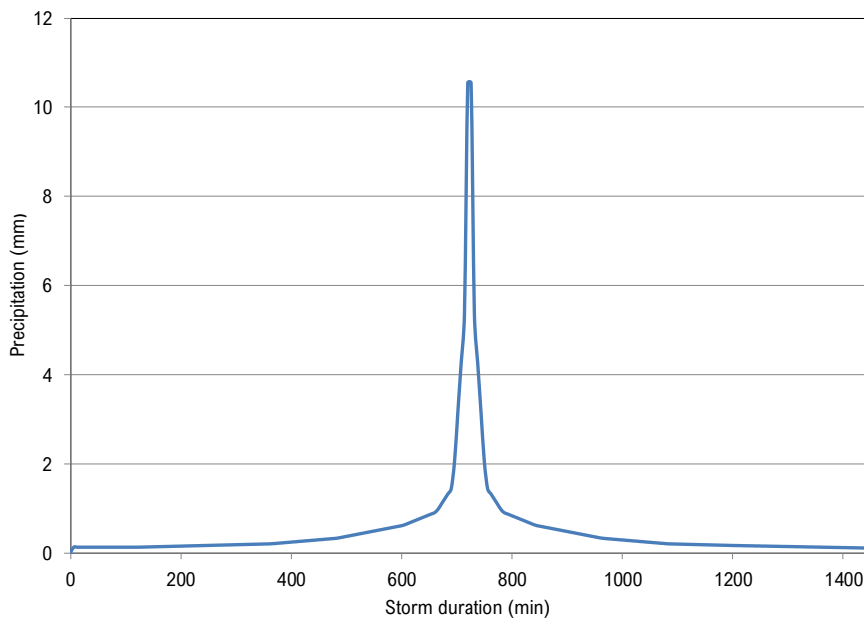


Figure 8-1: SCS type III design storm for case study. S1 basin, 100 return period and current climate conditions.

8.3. Hydrological model results

The hydrologic model was build using the HEC-HMS software, developed by USACE (United States Army Corps of engineers). A total number of 6 watersheds were modelled; whose river channels affect the X road at different points.

The curve number method globally used and proposed by the United States Department of Agriculture was incorporated in the hydrologic model. The curve number (CN) for each basin determines the precipitation-runoff ratio in the model and depends fundamentally on: the land use and the soil present in the study area.

Taking as reference the specified by [83], the watersheds are taken as a soil formed mainly by lixisols and vertisols and, therefore, belonging to group C. Considering an average hydrologic condition of the soil, the following CN values have been determined for each of the watersheds from the global maps facilitated by MODIS according to the classification by IGBP, depending on the type of soil and the soil’s hydrologic condition.

The parameters required to carry out a hydrological modeling for each of the sub-basins are presented below in the Table 8-3. The area, the length of the main channel and the median slope of the basin have been obtained from the spatial analysis of a 30m resolution DEM (source: OpenTopography).

Watershed	Maximum channel length (km)	Area (km ²)	Average slope (m/m)	Concentration time (h)	Lag time (h)	Curve number
S1	14.91	57.40	0.065	2.76	1.65	80
S2	49.25	233.09	0.021	7.77	4.66	82
S3	13.76	39.07	0.067	2.56	1.53	81
S4	17.98	61.76	0.055	3.12	1.87	83
S5	14.83	18.11	0.063	2.47	1.48	84
S6	44.78	291.16	0.021	7.46	4.48	83

Table 8-3: Parameters required to perform a hydrological modeling for each of the sub-basins.

The design storms introduced to the model consider a rainfall event of 24 h. The modeling time is set to 48 hours with an interval of 10 minutes.

Considering 6 Watersheds, 7 return periods (2, 5, 10, 25, 50, 100 and 500 years) it results in a total of 42 Flood Hydrographs at the points identified as critical and that will be considered in the hydraulic analysis. As an example, the hydrographs for the S6 Basin are presented in the Figure 8-2. The rest of the flood hydrographs can be consulted in the Appendixes.

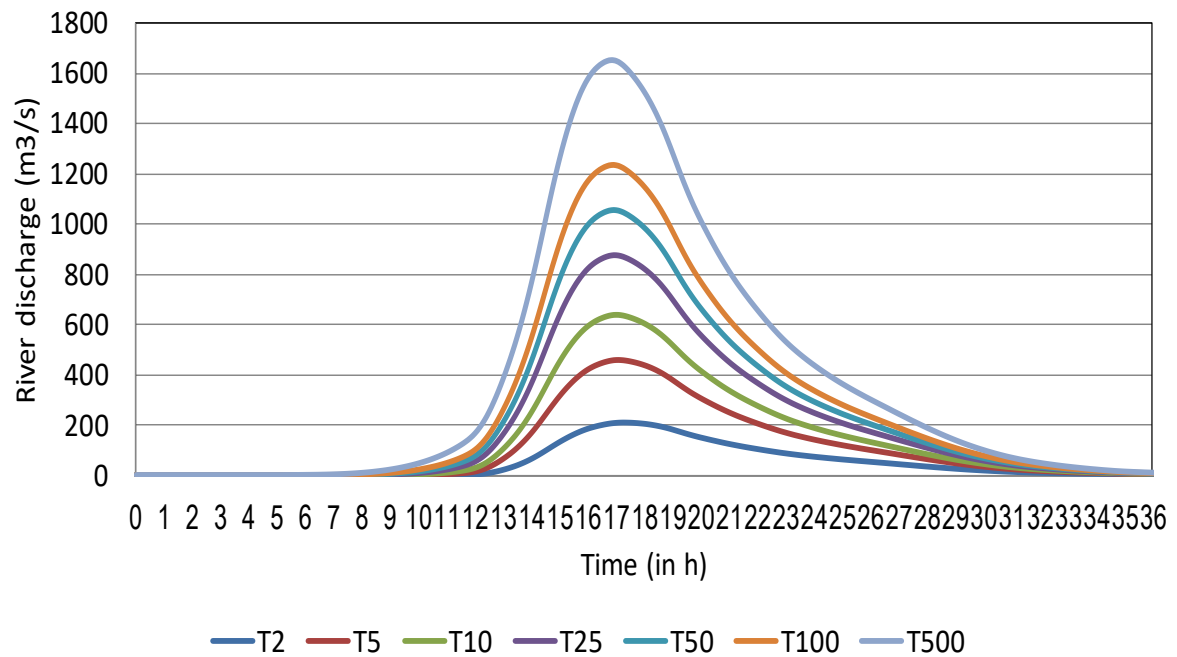


Figure 8-2: Flood hydrograph (Design storm 24h). Basin S6.

Figure 8-3 shows a summary of the results obtained from the hydrologic model in terms of flow rates peak at every river-road intersection (critical point).

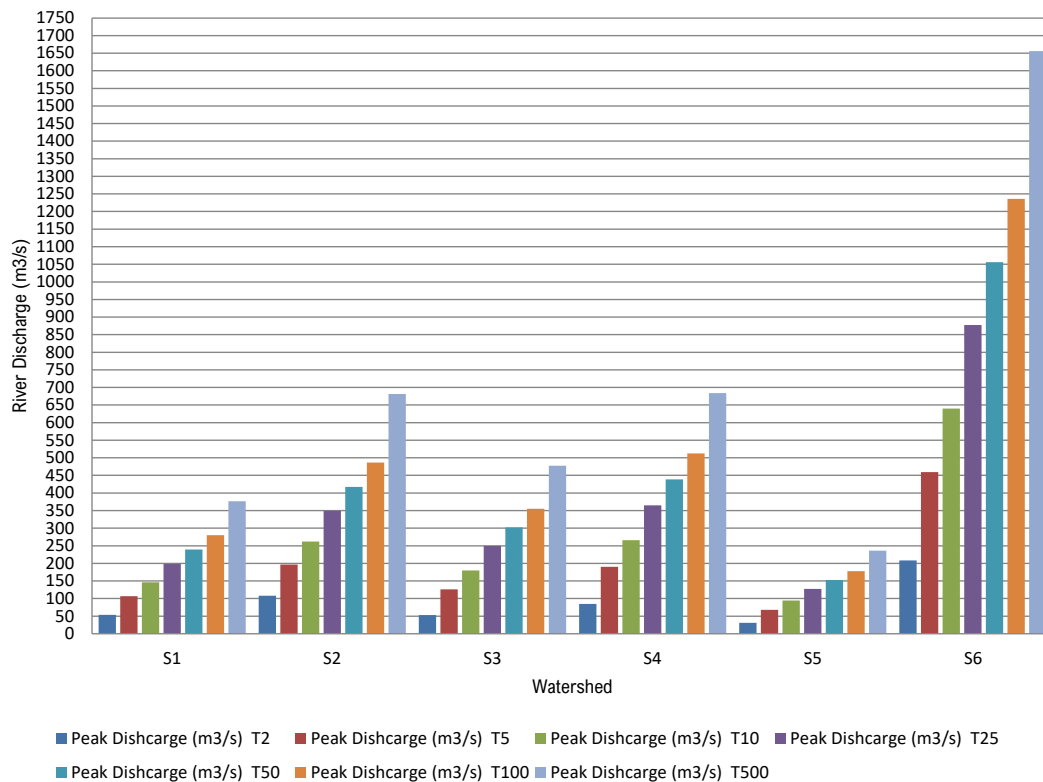


Figure 8-3: Summary of the results for the peak flow rate (in m3/s). 6 basins and seven return (2 to 500 years) periods.

8.4. Hydraulic model results

The hydraulic model was built using HEC-RAS software, developed by USACE (United States Army Corps of Engineers). 2D simulations have been performed in non-permanent flow regime in order to obtain flood maps associated with climate scenarios and different flood return periods.

The flood hydrographs (Q vs t) introduced in the model were previously obtained by means of hydrological modeling with HEC-HMS software. For the elaboration of the model a DEM (Digital Elevation Model) was obtained for the study area with a 1.5 m x 1.5 m resolution. A 2 x 2 m mesh resolution was established along the axis of the road, leaving sufficient margin on each side for the study for flood wave propagation.

¡Error! No se encuentra el origen de la referencia. shows an example of the calculation mesh and the interface of the HEC-RAS 2D model for the road-river intersection (BS3 - BS4 basins).

Two flood risk situations are identified:

- Road sections where there is a general flood over the road axis, where the river overflows and inundates part of the road pavement.
- Road-river intersection, usually with drainage works (culverts) or bridges, where hydrodynamic forces may cause erosion problems and collapse of infrastructure.

In ¡Error! No se encuentra el origen de la referencia. the modelling results are shown for one of the main river- road intersection points (BS3-S4 basins). The figure shows the 500-T flood map of water depths for the current climate scenario.

From the road profile indicated in ¡Error! No se encuentra el origen de la referencia., cross section results of water depths and flow velocities can be obtained for the specified road stretch and flood map. The results are analyzed in order to obtain cross sectional average and maximum values for water depths, flooded areas and

velocities to compute road response (flood-damage curves and fragility curves) and derived failure consequences (reconstruction costs and traffic disruption costs), as explained in Section 3.3.

A summary of the hydraulic modelling results for the current climate scenario and seven return periods is presented. The results are grouped into three types of hydraulic parameters: the maximum flow depth reached on top of the road pavement (in m); the total flooded length of the road (in m); and the deck's inundation ratio (for bridges) (see definition in Section 2.3.2).

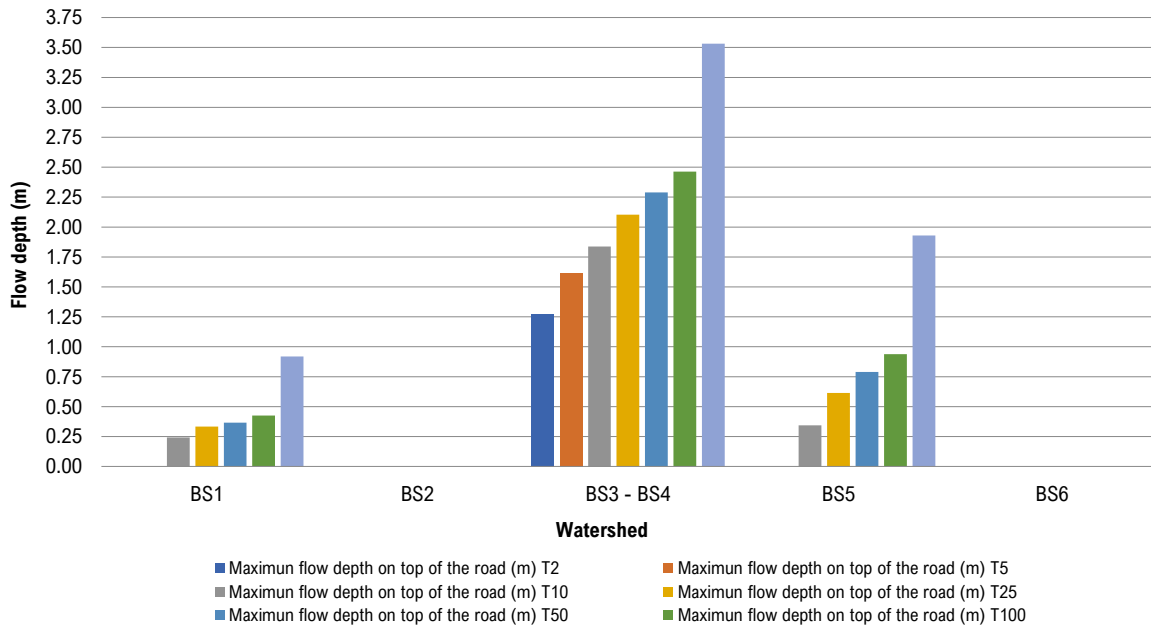


Figure 8-4: Summary results of hydraulic modelling. Current climate scenario. Maximum flow depth on top of the road axis at each road-river intersection.

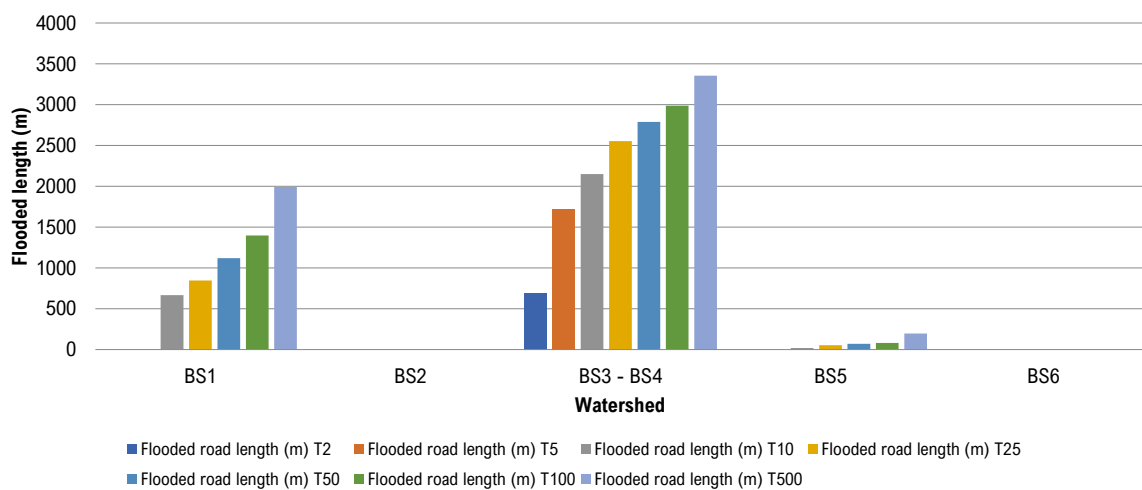


Figure 8-5: Summary results of hydraulic modelling. Current climate scenario. Flooded road length on top of the road axis at each road-river intersection.

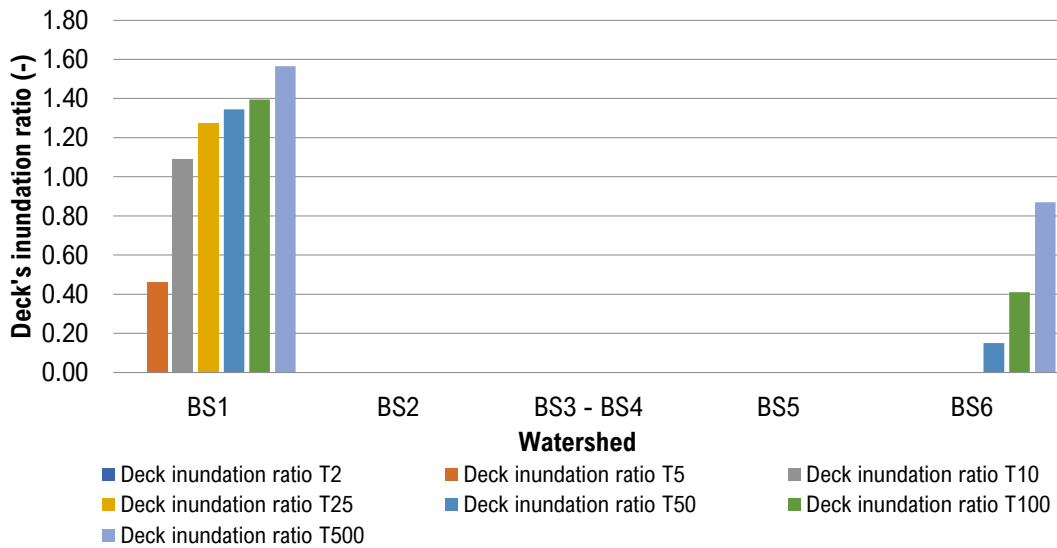


Figure 8-6: Summary of hydraulic modelling. Current climate scenario. Inundation ratio for culvert (BS1) and Bridge (BS6).

8.5. Hydrologic and hydraulic characterization update with CC effect

The climate-trend scenario that will be incorporated into the analysis (RCP8.5 scenario) was defined in Chapter 7. Here, the hydrologic and hydraulic characterization of the watersheds (Chapter 2.4) is updated to consider quantitatively the effect of climate change in the study.

After applying the proposed methodology explained in Figure 3-5 (Section 3.2) for the chosen scenario (RCP 8.5) and for five meteorological stations in the area, the values of maximum daily rainfall (in mm) in 24 h projected in current and trend-based scenario is shown in Table 8-4.

Weather station	Climate scenario	Maximum daily rainfall (mm) Storm 24h						
		T2	T5	T10	T25	T50	T100	T500
A	Current	58	92	115	143	164	185	233
	RCP8.5	96	143	175	214	244	273	341
B	Current	51	67	78	92	102	113	136
	RCP8.5	57	74	85	100	111	121	146

Table 8-4: Values of maximum daily rainfall (mm in 24 h) expected for each weather station, range return periods and two climate-trend scenarios (current and RCP8.5).

With data from Table 8-4, the design storm for each basin is built based on the climate-trend scenario and return period using the design storm type III proposed by the NCRS, as described in Chapter 3.3 of this report. In addition, it is required to update the change in land-use at project area as described in 7.2. The new values for the Curve Number in trend-based scenario are shown in Figure 7-3.

Once the design storms and land use values are updated, the same steps described in Chapter 8 are followed for obtaining flood hydrographs for the climate trend-based scenario.

Figure 8-7 present the results from updated hydrologic modelling considering the climate change effect considered as a function of the flood peak-flow (m³/s).

In addition, to allow for a better visualization of the climate change effect in the river flow peaks in the critical points (river – road intersections), the increase (in %) in flow peaks (current vs trend-based scenario RCP 8.5) for each basin and return period analyzed is shown in Figure 8-8.

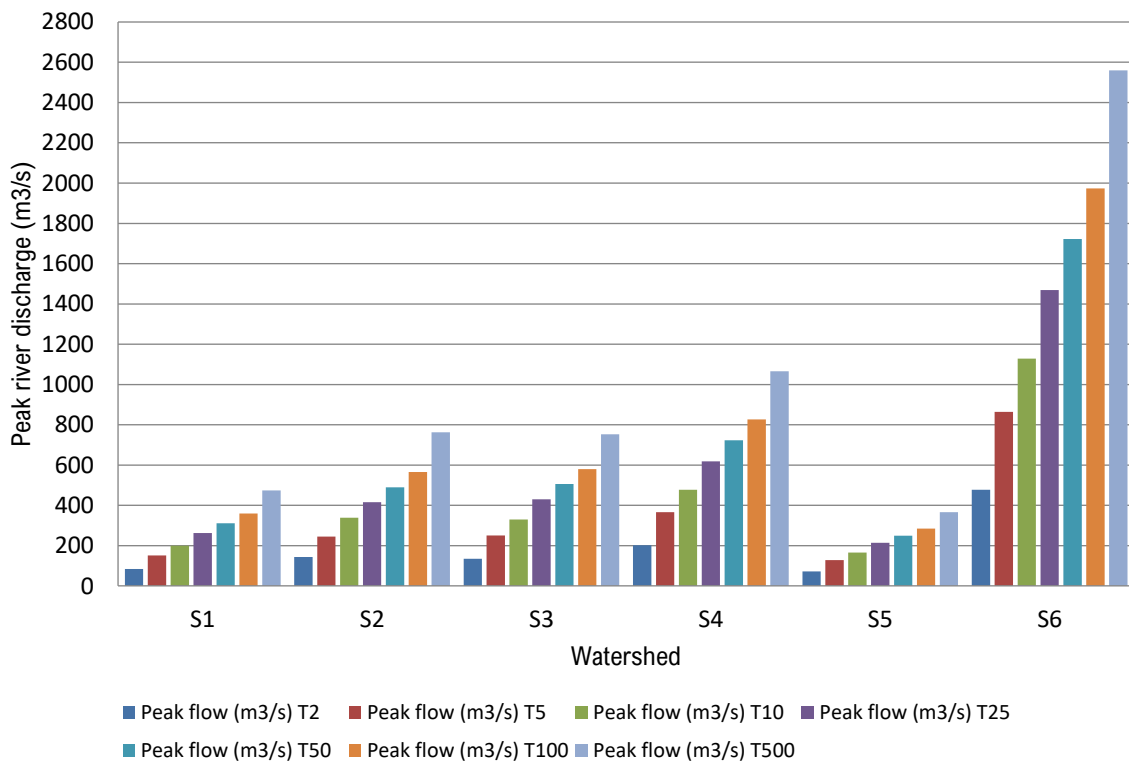


Figure 8-7: Summary results for peak flow rate (in m³/s). 6 basins and seven return periods. RCP8.5 scenario.

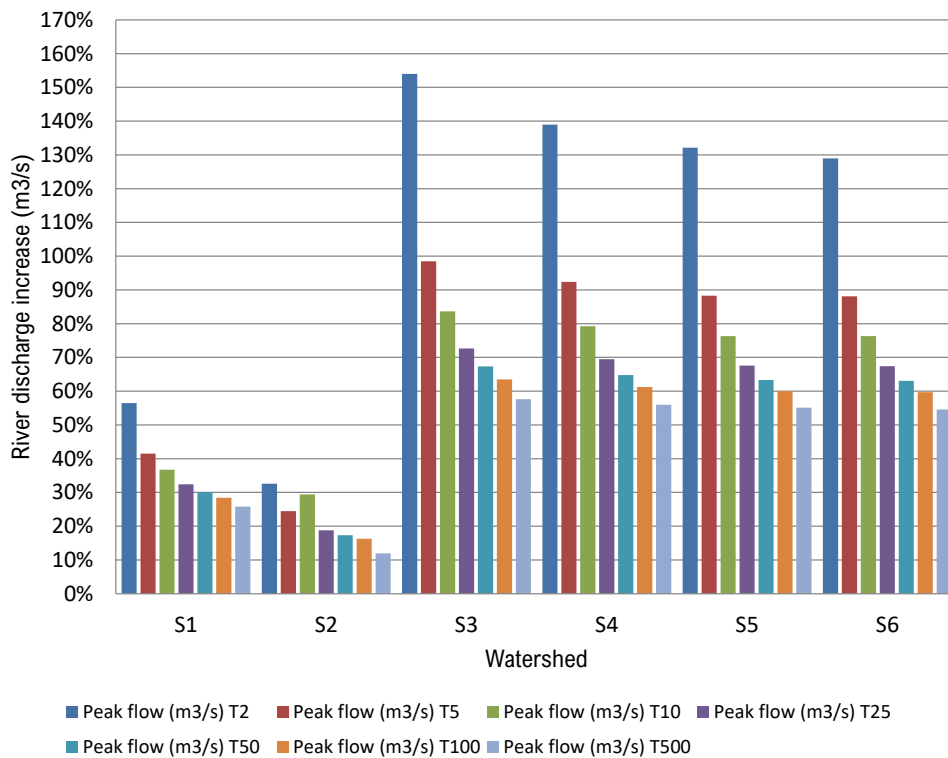


Figure 8-8: Increase (%) Future climate scenario vs current climate scenario. 6 sub-basins and seven return periods.

Next, a summary of the hydraulic modelling results for the climate-trend scenario and seven return periods is presented in several figures. The results are grouped into three types of hydraulic parameters: the maximum flow depth reached on top of the road pavement (in m); the total flooded length of the road (in m); and the inundation ratio (% of the width of flooded deck) for the bridges (if existent).

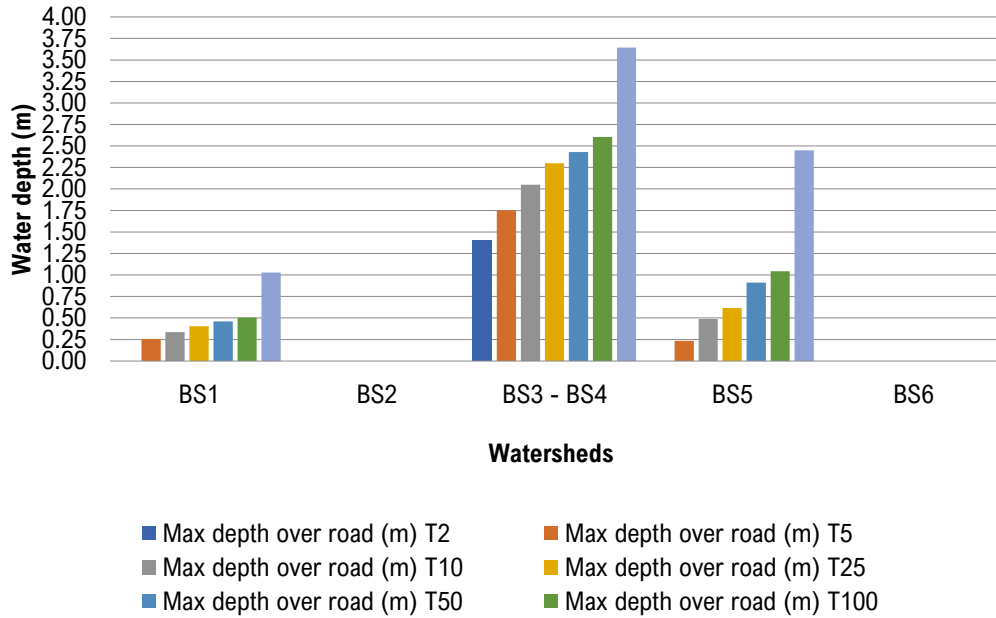


Figure 8-9: Summary of hydraulic modelling results. Max depth on road at each river – road intersection analyzed. Future Climate trend-based scenario.

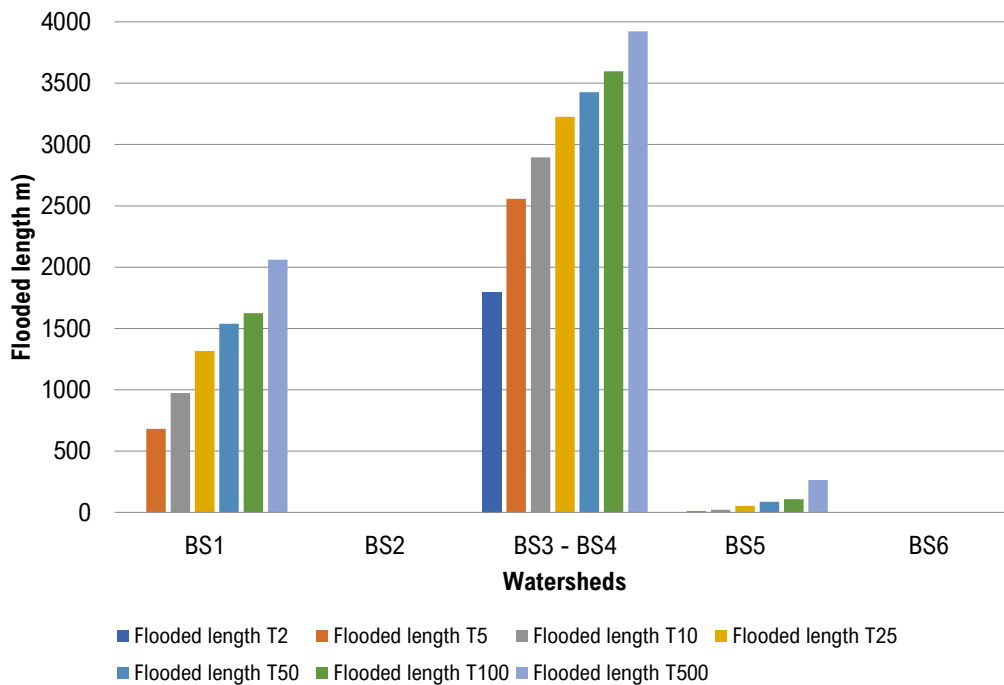


Figure 8-10: Summary of hydraulic modelling results. Flooded length on road at each river – road intersection analyzed. Future Climate trend-based scenario.

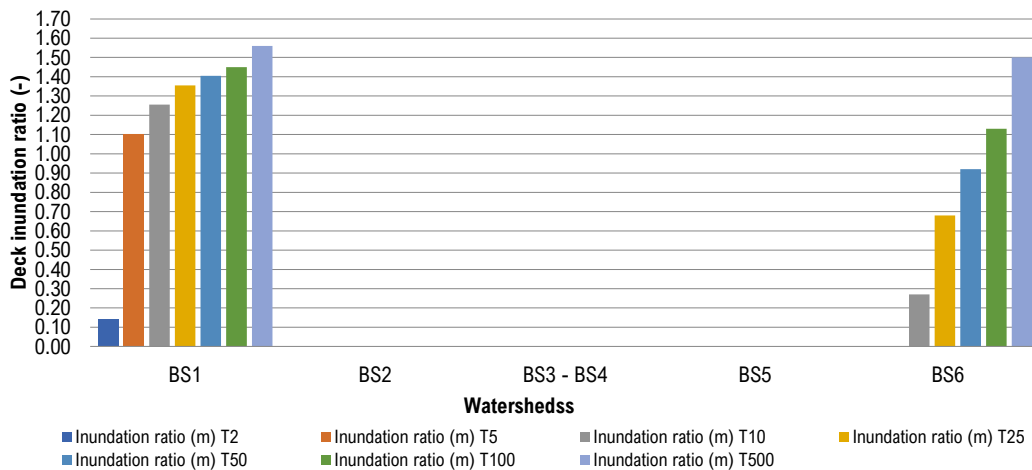


Figure 8-11: Summary of hydraulic modelling results. Inundation ratio on road at each river – road intersection analyzed. Future Climate trend-based scenario.

In addition, to visualize the climate change effect on hydraulic parameters the following figures are presented; showing percentage increases (current scenario vs future climate RCP 8.5) for each basin and return period analyzed for the following three hydraulic parameters: the maximum depth reached on the road (in m); the flooded length on the road (in m); and the inundation ratio on bridge's deck:

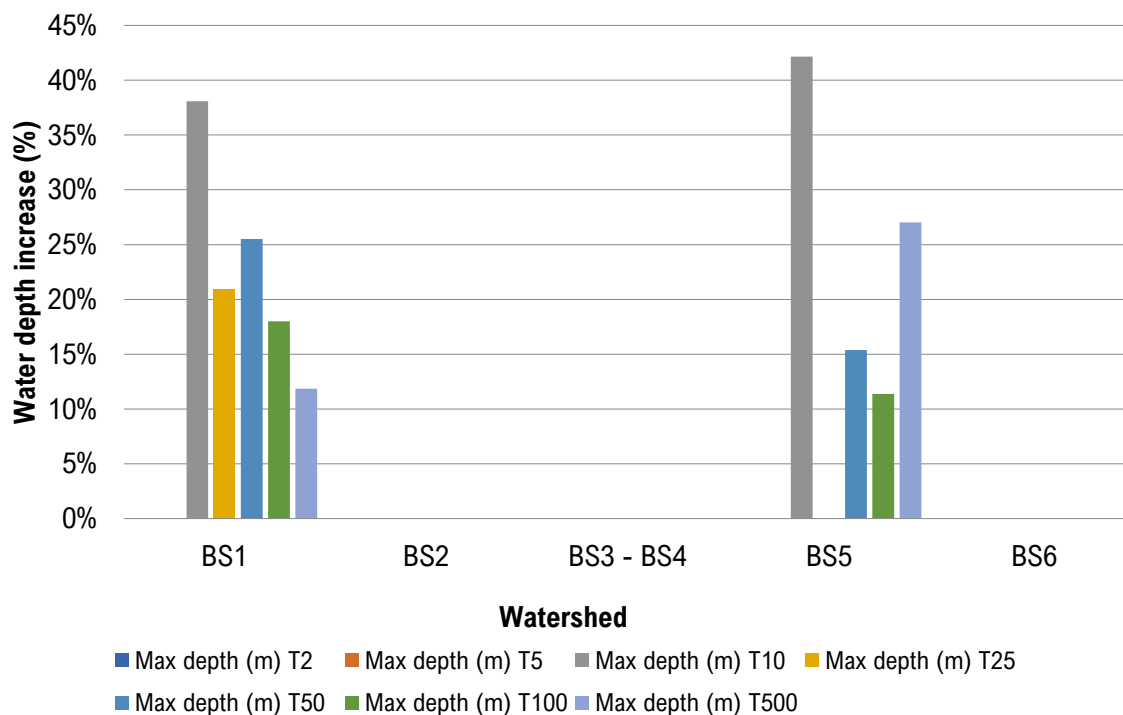


Figure 8-12: Increase (in %) for max depth on road at each river-road intersection analyzed. Future Climate trend-based scenario vs current scenario.

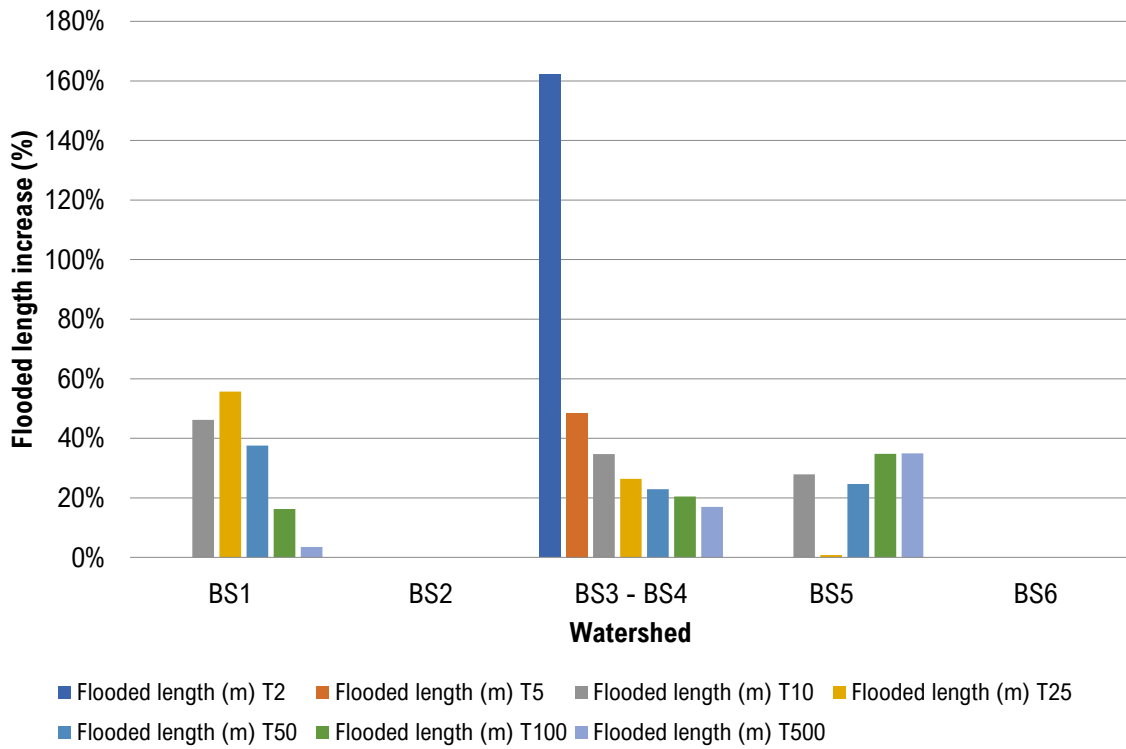


Figure 8-13: Increase (in %) for flooded length on road at each river-road intersection analyzed. Future Climate trend-based scenario vs current scenario.

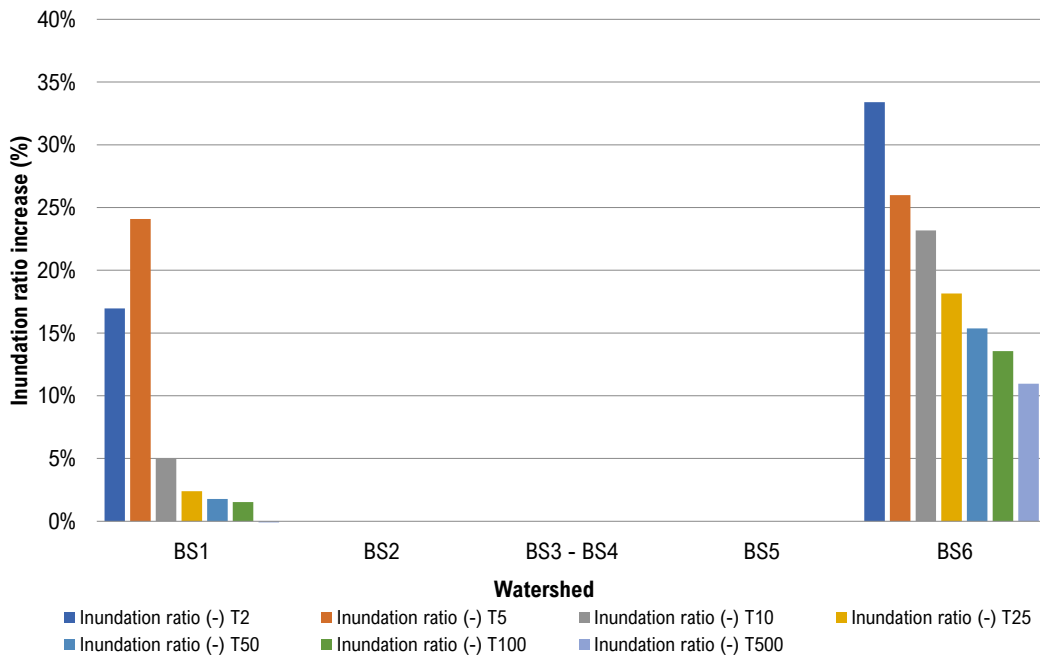


Figure 8-14: Increase (in %) for inundation ratio on bridge deck at each river-road intersection analyzed. Future Climate trend-based scenario vs current scenario.

8.5.1. Conclusions

Finally, the conclusions derived from the analysis performed are summarized:

- The review of the available information has established a preliminary insight of the natural risks in the study area and especially the hydrologic and hydraulic response of watersheds as a starting point for the development of the next steps of the proposed methodology (failure identification session and quantitative risk analysis).
- With respect to the results of the hydrological model, 6 critical areas are identified within the study section. A single current climate scenario has been considered, until the definition of the climate scenarios and the results update after the failure mode identification session.
- With respect to the results of the hydraulic model, the flooded lengths of road stretch and maximum flow depths on top of the road axis were identified in the critical stretches river overflows and inundates part of the road pavement. In addition, the deck's inundation ratios and flow velocities (average and maximum) during peak river discharges were obtained for the in the critical stretches identified as river-road intersections, where bridges and culverts are located.
- The updated results from hydraulic modeling show a general increase in hydraulic parameters during flood due to the impact of climate change on precipitation regime and land use degradation. The increase (in %) of the three hydraulic parameters its specific for each the return period and sub-basin since the methodology used to consider the effect of the CC in the region has been applied to each weather station separately, differentiating the impact in each return period.
- The hydraulic characterization results highlight the road vulnerability both in its current and future situation against flooding in several of the identified critical points, with several sections flooded such as the BS1 and BS3-BS4 road-catchment interceptions for storm events associated to return period of 2-5 years.

In conclusion, Table 8-5 shows potential hydrological threats, observed in each of the critical points.

Watershed	Flood threat	Quantitative risk analysis
BS1	General flood on the road / Culvert overtopping	Yes
BS2	Potential hydrologic hazards are not detected	NO
BS3 -BS4	General flood on the road	Yes
BS5	General flood on the road / There is no risk of bridge overtopping	Yes
BS6	Potential overtopping of bridge deck / Piers erosion	Yes

Table 8-5: Summary of hydraulic modelling results

9. QUANTITATIVE RISK CALCULATION

Figure 9-1 summarizes the proposed methodology to perform a quantitative analysis of the natural hazards that threaten the X road of Country Z, including the analysis of climate change effect and the implementation of failure modes identification process in the study area. In orange, the sections directly related to the risk calculation are shown.

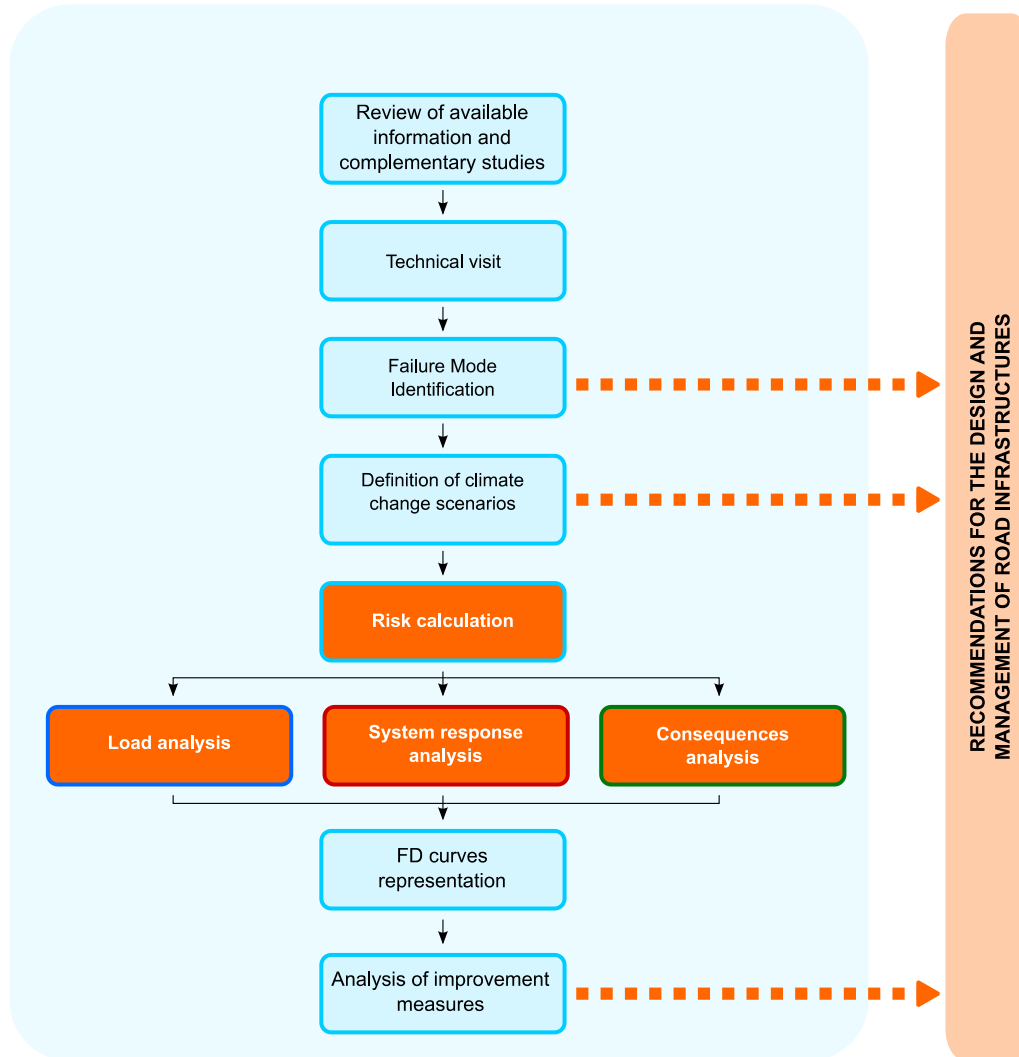


Figure 9-1: Methodology proposed to perform a quantitative analysis of the natural hazards that threaten the X highway of Country Z. In Orange, the stages related to the calculation of risk.

Detailed considerations on quantitative risk analysis are presented in Chapter 3.3, in this chapter the risk model architecture, the input data for the road risk model and risk calculation and evaluation are described.

Input data on loads, system response, and consequences are incorporated into each node of the risk model as described in the Appendixes.

9.1. Risk model architecture

Based on the selected three failure modes in previous stages of the proposed methodology, the risk model architecture has been developed to calculate economic risk (direct, indirect and total).

The risk model architecture has been developed using iPresas Calc software, which uses influence diagrams and event trees to compute failure probability and risk. This software can model any type of loads (hydrologic, seismic, etc.), failure modes and consequences (economic, total, incremental, etc.). The risk model architecture is represented by an event tree. The event tree is a logical mathematical construction which includes every possible chain of events that may lead to flooding and calculates the probability and consequences of each of these branches.

It should be noted that the inputs to the risk model nodes are related to the river - road intersection areas identified as potentially vulnerable after hydraulic modelling, where the risk analysis will be focused since it is the area where rehabilitation works will take place.

Figure 9-2 shows the two type of general risk model architecture used to calculate flood risk in every critical section on the X road, differentiating sections with and without a bridge infrastructure.

To calculate risk, these models combine the **probability of flood occurrence** in a wide range of return periods (blue node), the **critical section** that will be analyzed (green node), the **flood parameters** (flow peak, flow depth over the road, flooded road length, Froude number, inundation ratio) associated with each of these flood events for each section in the project area (yellow), the **failure modes** that can cause road failure (general flood, piers erosion, hydrodynamic failure of bridge – deck connection), the **direct consequences** for reconstruction costs (pink node), the **indirect consequences** related to cost of time during the road closure under flood conditions and the increase in VEC (Vehicle operational costs) due to the use of a damaged road during the repair time (purple node), and **total economic consequences**, sum of direct and indirect damage expressed in economic terms.

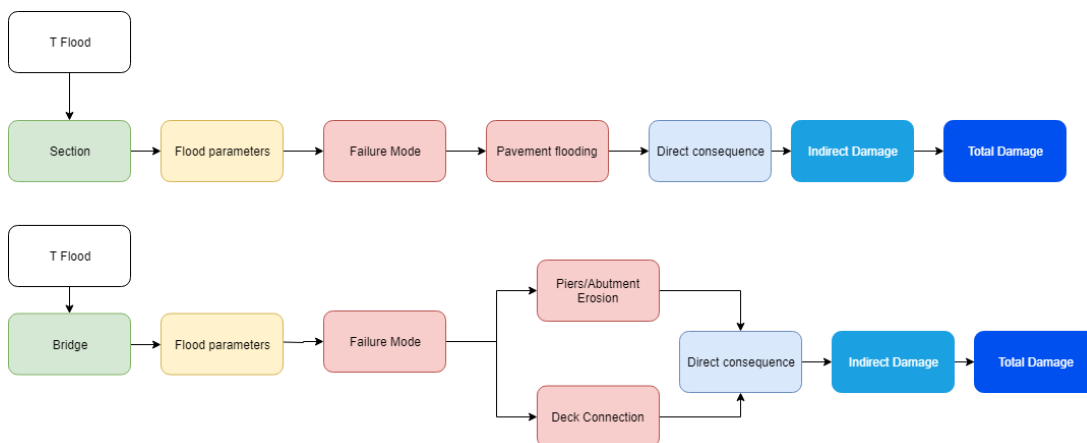


Figure 9-2: General risk model architecture

Considering every section identified as potentially vulnerable during a flood event after the hydraulic modelling, the quantitative risk model for the road system is shown in Figure 9-3:

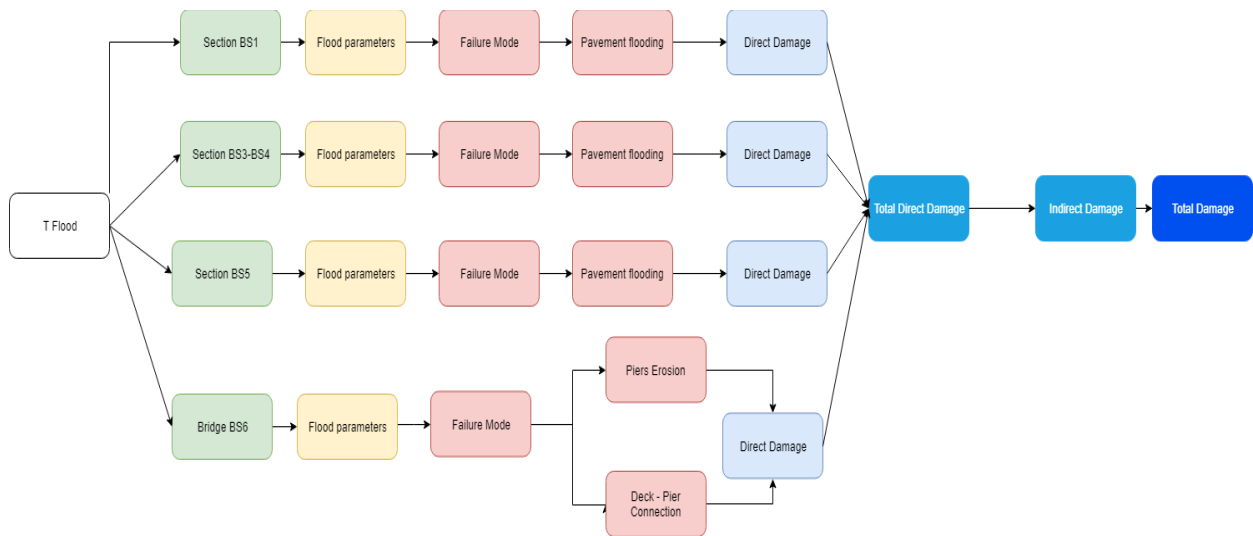


Figure 9-3: Risk model architecture for the X road.

9.2. Risk scenarios

Once the required data for the model is gathered, and it is incorporated into the correspondent nodes within the risk model architecture, economic risk results (direct, indirect and total) are obtained for each considered scenario:

- **“Current climate” scenario A**, which analyzes the current road flood risk: Current climate scenario, not rehabilitated pavement, mismanagement of reconstruction works.
- **“Future climate” scenario B**, which analyzes the road flood risk in 2050-2100 if the rehabilitation works are not implemented and climate change trends continue as established by the RCP8.5 scenario: RCP 8.5 climate trend-based scenario, pavement not rehabilitated, mismanagement of reconstruction works.

In addition, other scenarios are considered, which incorporate the projected improvements on the X road which aim to improve the quality of the transportation infrastructure in Country Z through an increase in the coverage of paved roads and improvement of infrastructure management:

- **“Current climate & new road design” scenario C**, which analyzes road flood risk at current climate conditions after the implementation of projected rehabilitation works: current climate scenario, pavement rehabilitation, traffic volume increase and mismanagement of reconstruction works.
- **“Future climate & new road design” scenario D** which analyzes road flood risk at future climate-trend conditions after the implementation of projected rehabilitation works and without proper watersheds management and reconstruction works: Trend-based climate scenario, pavement rehabilitation, without watershed reforestation, traffic volume increase, and delay in the reconstruction costs.
- **“Future climate & new road design” optimal scenario E** (only for the BS3-BS4 basins) which analyzes the risk evolution to the year 2050-2100 if rehabilitation works are implemented; they are accompanied by better watershed management and reconstruction works; continue with climate change trend and traffic volume increase: climate trend-based scenario, pavement rehabilitation, watershed reforestation, traffic volume increase, optimal management of reconstruction tasks.

9.3. Input data for the road risk model

The influence diagram developed for X road and shown in Figure 9-3 includes 11 nodes. Information included in each node can be classified in three categories: loads, system response and consequences. Nodes referring to loads are highlighted in yellow color in Figure 9-3:

These nodes include the information described in Table 9-1 obtained from the following analyses:

- Analysis of the hydrologic model developed in HEC-HMS.
- Analysis of the hydraulic model developed in HEC-RAS 2D.

Outcomes from listed actions are included in the Appendix 5 along with input data finally included in these nodes.

Node	Description
T Flood	This node includes the range of potential flood events into the road-river intersection and related annual exceedance probabilities (AEPs).
Section	This node includes the probability of a critical intersection being affected when a flood occurs. It is used to define the different critical section that will be analyzed at each stage.
Flood parameters	This node includes the results of the flood (hydraulic modelling) analysis, for all combinations of flood event, and critical sections included. Outcomes from hydraulic modeling analysis included in this node are maximum water depths on the road reached during the flood event, maximum flooded road lengths, peak discharges at bridge/intersection locations, Froude number and deck inundation ratios at bridge locations

Table 9-1: Input data for the road risk model: loads.

Nodes including information on system response are highlighted in red color in Figure 9-3. Each failure mode is divided into different events (which are represented by different nodes in the risk model) and the conditional probability of each event may vary for different flood-related hydraulic parameters.

These nodes include the information described in Table 9-2 obtained from the following analyses:

- Flood hydraulic analysis and potential road overtopping scenarios.
- Bridge stability analysis.

Outcomes from **flood hydraulic analysis and bridge stability analysis** are included in these nodes and described in Appendix 7.

Node	Description
Failure mode	Auxiliary node to define the common cause adjustment technique used to compute failure probabilities.
FMA Pavement flooding	Probability of road/pavement damage due to flooding over the road infrastructure based on the maximum river level resulting from 2D hydraulic analysis.
FMB_Deck connection	Conditional probabilities of failure due to loss of bridge stability based on the maximum Froude number and deck inundation ratio resulting from hydraulic analysis at bridge location.
FMC_Pier Erosion	Conditional probabilities of failure due to loss of stability based on the maximum erosion depth resulting from hydraulic and erosion analysis in the bridge piers.

Table 9-2: Input data for the road risk model: system response.

Nodes including information on potential consequences in case of road and/or bridge failure are highlighted in blue color in Figure 9-3.

These nodes include the information described in Table 9-3 obtained from the following analyses:

- Analysis of the hydraulic model, developed in HEC-RAS 2D.
- Analysis of potential direct reconstruction consequences in case of road failure or bridge failure
- Analysis of potential indirect consequences due to traffic disruption during road closure time and VEC increase during reparation time in case of road failure or bridge failure

Information included in these nodes are described in the Appendix 5.

Node	Description
Direct damage (\$)	Consequences in terms of estimated potential economic costs caused by pavement failure, which mainly includes reconstruction costs, using water depths over the road and depth-damage curves, in Dollars.
Indirect damage (\$)	Consequences in terms of estimated potential economic costs caused by road closure and road deterioration, including cost of time for travelers during closure and incremental cost of vehicle exploitation during rehabilitation using flood characteristics and IRI variations, in \$.
Total damage (\$)	Consequences in terms of estimated potential economic costs caused by road failure, adding direct and indirect consequences, in \$.

Table 9-3: Input data for the road risk model: potential consequences

10. RISK RESULTS: FLOOD RISK MAPS AND FD CURVES

Once the input data necessary for the risk calculation is included in the risk model architecture, risk economic results (direct, indirect and total) have been obtained for each calculation scenario.

To represent these risk results, FD (frequency-damage) curves are used. In the FD charts, the risk situation is represented by a curve where the horizontal axis represents the Economic damage (D) and the vertical axis represents the annual probability of exceedance of each level of potential consequences (F). The FD graphs are monotonously declining due to its cumulative exceedance probability nature.

The main advantage of the use of this type of graphs for risk representation is the representation by a single curve of all events that are producing flood risk, from low probability-high consequence events to high probable but low impact events. Thus, the area under the FD curve represents the average annual economic risk (\$/year).

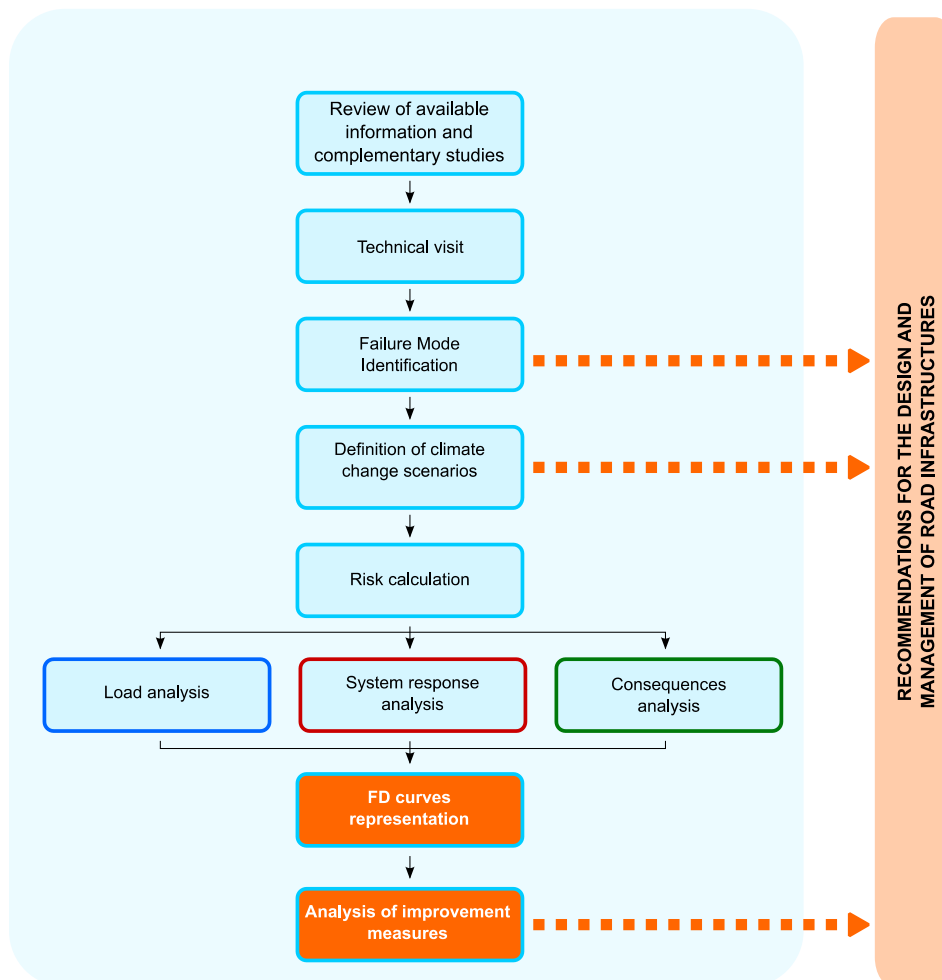


Figure 10-1: Methodology for the analysis of natural risks in the X. Representation in FD curves.

As stated in the previous chapter, five scenarios are considered for risk calculation, two base scenarios without road improvement measures and three design scenarios including road improvement measures.

The Appendixes show the obtained risk results for each scenario in the form of FD curves.

10.1. Global Risk calculation results: F-D curves

The results obtained by combining (in the risk model) the floods and their probability with the potential consequences of system failure for the five considered scenarios are shown in Table 10-1. Results show that flood economic risk is significant, which is consistent with the frequently flood events occurring in this area. Within this analysis the direct damage to the transport infrastructure is included, but also the indirect consequences of the flooding due to traffic disruption and incremental increase of circulation costs through a deteriorated road.

	Scenario A	Scenario B	Scenario C	Scenario D	Scenario E
Direct economic flood risk (\$/year)	187,757	297,075	360,582	553,191	553,191
Indirect economic flood risk (\$/year)	640,905	1,354,166	4,013,640	6,119,282	631,198
Total economic flood risk (\$/year)	828,662	1,651,242	4,374,445	6,672,473	1,198,184

Table 10-1: Economic risk (\$/year) calculation results (Direct, Indirect and Total risk). Five scenarios.

The following figures show the FD charts of all the risk calculations made:

- Figure 10-2 represents the FD curves for direct risk for every scenario.
- Figure 10-3 represents the FD curve for indirect risk for every scenario.
- Figure 10-4 represents the FD curve for total risk for every scenario.

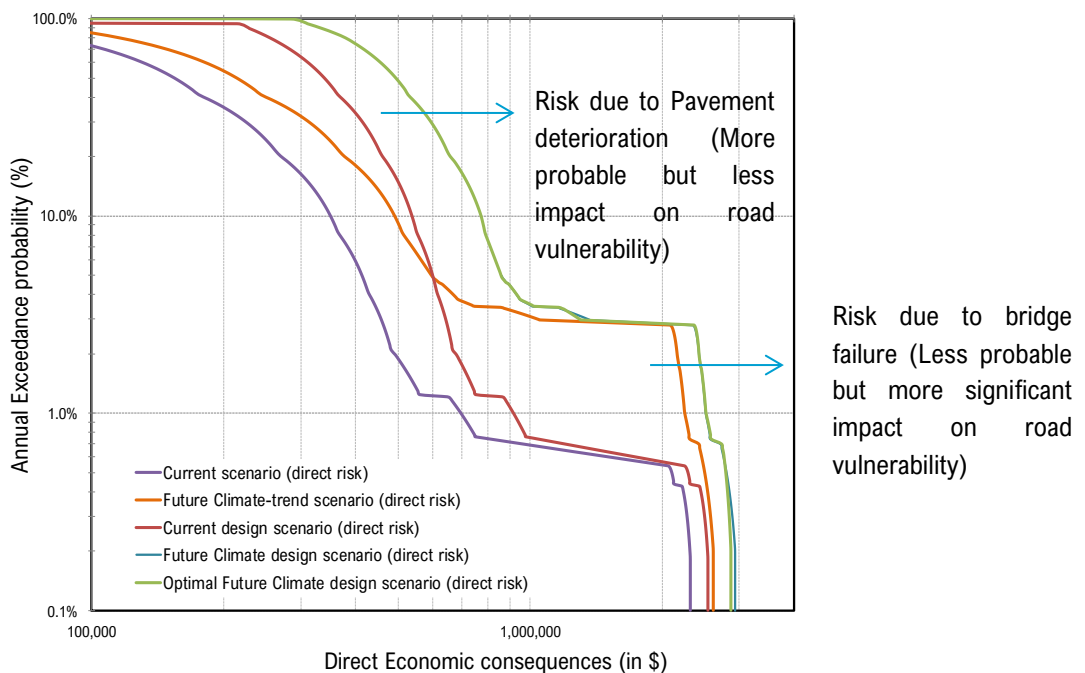


Figure 10-2: FD curve for the different risk calculations. Direct damage.

From Figure 10-4, two different sections are clearly differentiated within the FD curves. A first moderate decreasing curve, which represents direct economic risk due to: Pavement deterioration (FMA) and copes with more probable but less significant consequences. An abrupt horizontal risk variation in the curves, caused mainly by the BS6 bridge failure (due to overtopping and/or scour induced failure), which is less probable (variations dependent on the calculation scenario) but causes more significant direct consequences than pavement rehabilitation.

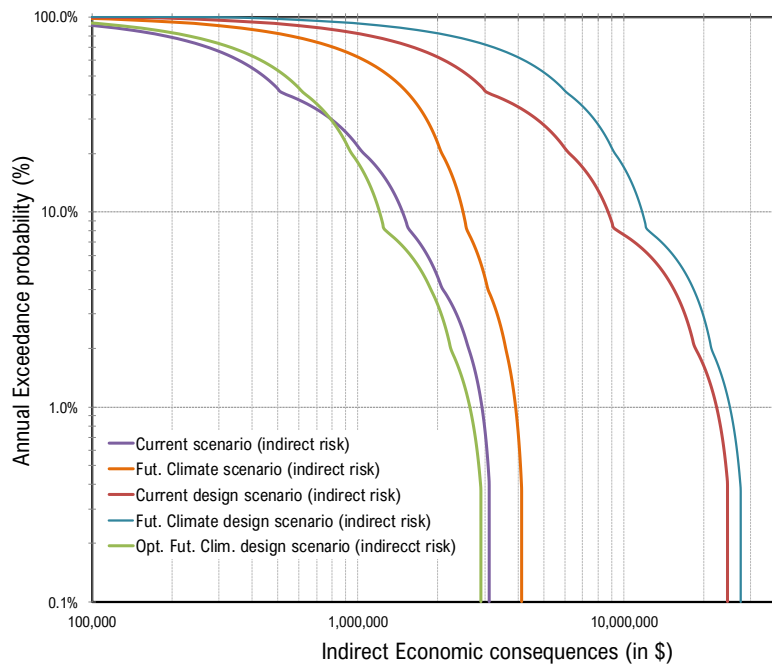


Figure 10-3: FD curve for the different risk calculations. Indirect damage.

From Figure 10-5, the FD curves decrease with small horizontal changes as the effect in the indirect consequences of bridge failure (for road closure) is not as the important as the contribution of indirect damage during road rehabilitation due to incremental vehicle operational costs, which in the specific case of this project is the most critical variable.

Finally, in Figure 10-6, the sum of the previous two figures is shown, presenting the total flood risk of the X road. The FD curves are therefore similar as the ones shown in Figure 10-6 (as the contribution of indirect risk is more significant than the direct risk). However, the abrupt changes in the horizontal direction due to bridge failure influences are noticeable.

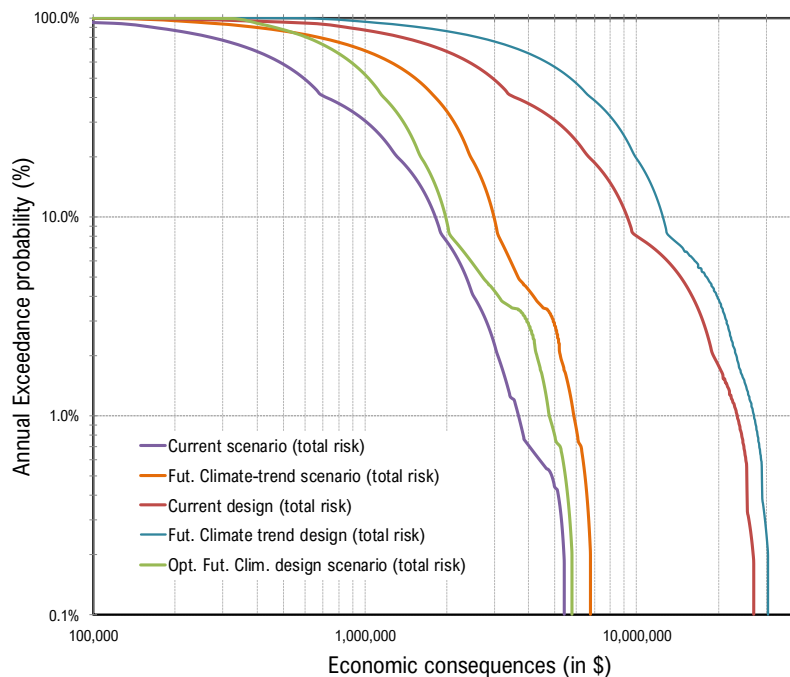


Figure 10-4: FD curve for the different risk calculations. Total damage.

10.2. Analysis of Climate Change and improvement measures on road risk: Comparison between scenarios.

In this chapter, the effect of Climate Change and road improvement measures between scenarios is evaluated. From the FD curves already shown in the previous chapter, the effect of climate change and projected road improvement measures on the road flood risk can be evaluated.

- (Non-optimal) Design scenarios (red and blue curves), where **pavement rehabilitation** is implemented, increases **direct flood risk** in comparison with present unpaved road condition (purple and orange curves), mostly for the smaller return periods (shift from the FD risk curve to the right). This increase is due to an economic reevaluation of a paved road in comparison with an unpaved road. For higher return periods, direct risk variation is similar as bridge collapse risk (horizontal jump in the FD curves) is the same for design (paved) and not-design (unpaved) scenarios. (See Figure 10-2)
- (Non-optimal) Design scenarios (red and blue curves), where **pavement rehabilitation** is implemented without road management improvements, significantly increases **indirect and total flood risk** in comparison with present unpaved road condition (purple and orange curves) for the entire range of return periods (shift from the FD risk curve to the right). This significant increase is mainly attributable to the flood indirect consequences (traffic disruption and incremental vehicle operation costs), which are more appreciable for a paved road design, due to increasing exposure and vulnerability (comparing to the unpaved scenario, the traffic volume will increase, and the IRI variation after flood will be more significant). For example, the total economic consequences expected to be exceeded with a 1% annual probability for the current scenario (purple) are equal to those expected to be exceeded with a probability of approx. 40% in the current design scenario (red). (See Figure 10-4)
- The flood-risk increase due to **pavement rehabilitation** (design scenarios) should be understood as a cost for the benefits derived from the road improvement (not considered in a flood risk analysis), such as a greater utility of the infrastructure, economic development of the connected populations or less time to travel the road once rehabilitated. The increase in flood risk should not be used as an argument against rehabilitation, if not as an extra cost when evaluating the cost-benefit analysis of the investment or comparison of design measures.
- Future Climate-trend scenarios (orange and blue curves), where **climate change** effect is included, increases **direct road flood risk** in comparison with current climate conditions (purple and red curves) due to higher flood peak flows on river-road intersections. The latter implies higher pavement deterioration for the same flood event (shift of the FD curve to the right); and increasing failure probability of bridge collapse due to hydrodynamic forces and piers erosion, which means higher probability of occurrence for the same direct bridge damage (upward shift of the FD curve). (See Figure 10-2)
- Future Climate-trend scenarios (orange and blue curves), where **climate change** effect on watersheds precipitations and land-use coverage is included, **increases indirect and total road flood risk** (shift from the FD risk curve to the right) in comparison with current climate conditions (purple and red curves). The CC effect will increase flood peak flows and pavement deterioration after flood. However, the fact of moving from an unpaved road to a paved road implies higher indirect damage (during the closure and rehabilitation) than that caused only by the isolated CC effect in the study area. (See Figure 10-4)
- The flood-risk increase due to **climate change** effect (Future climate scenarios) should be understood as a direct consequence of a future increase in expected rainfall intensities during hurricanes and land-use coverage deterioration due to draughts and desertification. This highlights the need to include the CC effect on the new design criteria and to review the safety of existing bridges along the X road.
- Optimal Design scenario, (green curve), where an **improvement in the road management** (rehabilitation tasks and watersheds) is included, slightly decreases the direct flood risk results in comparison with Non-Optimal Future design (blue curve), displacement of the FD risk curve to the left. The (BS3-BS4) watershed reforestation, which reduces flood flow peaks in the most critical river-road

intersection, reduces pavement deterioration for the same flood event; however, this effect on risk reduction is small in comparison with other measures such as reduction of road reconstruction times.

- Optimal Design scenario, (green curve), where an **improvement in the road management** (rehabilitation tasks and watersheds) is included, **significantly decreases the indirect and total flood risk** results in comparison with Non-Optimal Future design (blue curve) and for the entire range of return periods (displacement of the FD risk curve to the left). The risk reduction is mainly attributable to the indirect damage decrease due to reconstruction time reduction, which reduces associated costs to vehicle operation through a deteriorated road after flood. For example (See Figure 10-4), the economic consequences expected to exceed with a 10% annual probability for the Future Climate design scenario are not expected to exceed in the Optimal Future design scenario in any case.
- The flood risk reduction due to improvement of road management practices highlights the importance in reducing reconstruction times after a flood, as economic disruption due to road closure and traffic disruption during road rehabilitation are critical factors for the total road flood risk.

11. RECOMMENDATIONS FOR THE DESIGN AND MANAGEMENT OF THE X

The main objective is to carry out a qualitative and quantitative risk analysis of the flood hazards that threaten the X road, analyzing different alternatives of improvement and future scenarios, based on a process of failure modes identification in the study area. This process has led to recommendations for the design of new works on the road, and to carry out more detailed studies of some phenomena analyzed as support to the responsible firm for the road design and management.

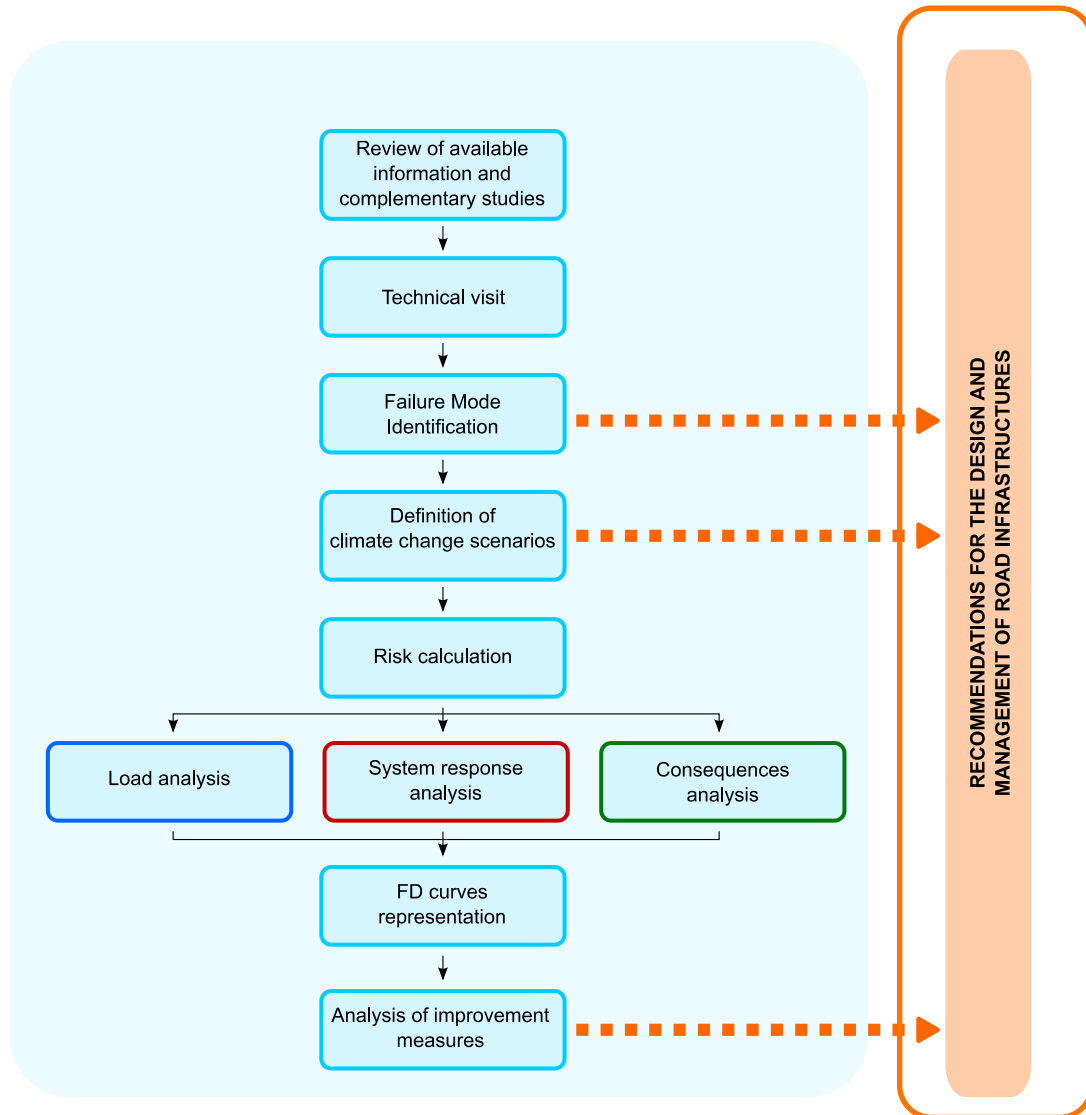


Figure 11-1: Methodology for the analysis of natural hazards in the X road. Recommendations for the design and management.

11.1. Recommendations for the design of the X road

The results of the qualitative and quantitative risk analysis have ended in the following recommendations for road future design regarding natural risks present in the X road:

- The definition of the potential failure modes serves as a main departure point for not to ignore possible calculation scenarios and failures in the new design of the infrastructure.
- From the failure modes identification session, there have been several proposals for improving specific design measures, including:

- The identification and characterization of flood and landslide risk during design and construction processes.
- Paving and asphaltting the X road using flood-resistant materials and avoiding high risk stretches.
- The construction and rehabilitation of longitudinal drainage works.
- New design of transversal drainage works (culverts) to improve the hydraulic capacity.
- Protection with gabions to prevent the erosion of river-road embankments.
- A simple but trustful methodology have been defined along with and several calculation scenarios for the incorporation of the CC to the project in three different areas:
 - Regarding design storms, whereas an increase in precipitation intensities implies an increase in flows peak, relevant for design of bridges and drainage works.
 - At design temperatures, including a higher design temperature to avoid future problems of pavement durability.
 - Land-use and desertification, correcting the NC to estimate the runoff-rainfall ratio in a deteriorated soil.
- A methodology for the hydrological and hydraulic characterization of the new road design, emphasizing procedures for:
 - Obtaining values of daily maximum annual rainfall for different periods of return and climate scenarios.
 - Design storms calculation based on hyetographs proposed for hurricane prone areas.
- There has been an identification of the most vulnerable sections of the X against flood.
 - The outputs of the hydraulic model serve as starting point for redesign of identified critical drainage works and/or bridges.
 - After the flood risk analysis of existing bridges (current and climate scenario) it is recommended to review several of the already existing bridges due to the impact of the CC in future floods, due to lack of hydraulic capacity and scour-induced problems near the foundations.
- The quantification of economic flood risk variation due to the CC has shown the increased risk due to more frequent and severe flood episodes in the future. Therefore, it is recommended to incorporate the effect of CC in the new design of the road and bridges through the agreed methodology.
- The quantification of risk increase due to pavement rehabilitation has highlighted the risk of continuing with the current road path in the new design. These quantitative results can be the basis for studying the economic efficiency of alternative routes.
- It is recommended that flood risk is used as a cost-variable when assessing the global cost-benefit analysis investment of proposed routes alternatives. Thus, the increase of the economic risk for the rehabilitation should be understood as a cost derived from the global benefits of this improvement (and that are not included in a flood risk analysis). An example of these benefits is a major utility infrastructure; the economic development of the populations that will be connected or the less time to travel the road once is rehabilitated.

11.2. Recommendations for the risk management of the X road

The results of the qualitative and quantitative risk analysis carried out have enabled to give the following recommendations for future road management in relation to natural risks of this road:

- The definition of potential failure modes is the starting point for establishing possible calculation scenarios and not to ignore failures in the future management of the new road.
- Several proposals for improving road management from the failure modes session, both for the medium to long term project management are recommended:
 - Short term Project Management
 - Maintenance plan of infrastructure/drainage works by defining responsibilities and funds.
 - Greater socialization of new works and to involve the population in risk management tasks.
 - Emergency alert system plan. Define actions before / during / after Hurricane.
 - Plan and training in waste-management to prevent waste releases into drainage works.
 - Campaign of seismic surveys in the area.
 - Campaign of hydraulic studies to determine the river channel capacity at the intersection with bridges.
 - Long term Natural Hazards Management
 - Hydrological-forestry rehabilitation of watersheds to restore vegetation and reduce peak flow rates.
 - Better planning of urban development to avoid informal settlements near vulnerable areas.
 - Improving the criteria for infrastructure design and consideration of climate change.
 - Improvement in rainfall and hydrometric data-collection system to validate future hydrological and hydraulic models.
- The quantification of flood risk has highlighted the importance of road indirect damage resulting from a flood for the whole of the country and some measures are recommended to reduce its impact in two areas:
 - It highlights the significant economic disruption due to road closure as there is no possible alternative to the X road to reach the points connected by the same. It is recommended to have floating bridge as temporary solution during an emergency.
 - The increase of the vehicles operational cost through a road deteriorated after a flood and during the time of rehabilitation has been quantified. The results highlight the need to reduce reconstruction times through the optimization of reconstruction task, which significantly reduces flood risk in the infrastructure.
- The quantification of the risk reduction due to watershed rehabilitation of the most problematic basins highlights the value of recuperating the vegetation cover, proven to be an effective measure to reduce the risk on the road.
- Finally, it is recommended to continue with this risk analysis (qualitative and quantitative) culture in the country and future projects to reinforce the need for structural and non-structural measures of improvement of infrastructure and/or reduction of natural hazards risks.

12. CASE STUDY CONCLUSIONS

This chapter summarizes the conclusions after the application of the proposed risk methodology to assess flood risk on the road X in Country Z. Regarding the qualitative and quantitative risk analysis results, the following recommendations to the new design and the following conclusions have been drawn:

- The Failure Mode identification process has allowed the identification of **21 Failure modes** that directly affect the road between the A and B population centers. Failure modes were grouped into:
 - 5 FMs for structural failure of the road pavement.
 - 4 FMs for the drainage system.
 - 3 FMs for the bridges.
 - 6 FMs for landslides in road embankments.
 - 3 FMs for risk management system.
- The identified FMs during the qualitative phase are a very valuable input for the design of the road rehabilitation works. The FM identification has allowed defining the main structural and the risk management system problems on the X road and identifying the main opportunities for improvement. Specifically, **12 Proposals for improvement** are given which emphasize the importance of a maintenance plan, a greater socialization of the risk management actions, and the improvement in rainfall and topographic data collection.
- **The Failure Mode Classification** defines a framework based on current standards to classify failure modes in civil infrastructure threatened by natural hazards. **Three failure modes** are considered for **risk quantification** due to its high likelihood of occurrence and high consequences:
 - General pavement deterioration due to river floods.
 - Failure of deck-pier connection due to hydrodynamic failure.
 - Bridge collapse due to piers erosion-induced instabilities.
- **A methodology** has been developed **to incorporate Climate change to the road design** and select appropriate design climate-trend scenarios, including the following aspects:
 - Design storms: Regression downscaling techniques to adjust the CanESM2 (Global Climate Model) to the project area (Regional Climate Model) and predict changes in daily maximum rainfall for different return periods.
 - Land use change and desertification: CN correction to estimate run-off for a soil with poor hydrological condition.
- Performance of a hydraulic and hydrological road characterization **using a GIS-based methodology** to assess flood hazard on the road, using design storms specified for hurricane prone areas, a Digital Elevation Model and 2D hydraulic simulations.
- The results of the road **hydrological and hydraulic characterization** show the high vulnerability against floods in its current design in several sections identified as critical, being flooded for rainfall events of 2-5 years return periods. The results of the hydrologic model have allowed to identify 5 critical areas in the study section, of which 4 sections have been considered of high flood risk potential and have been incorporated in the quantitative risk analysis.
- The quantitative risk analysis and the climate-trend scenarios has allowed to analyze the flood risk variation due to planned rehabilitation works in critical road sections, as well as identifying the potential effect of climate change on the **road flood risk** for five calculation scenarios (Current, Climate-trend, Current design, Climate-trend design and Optimal design).
- These future scenarios allow analyzing aspects such as the effect of climate change, the effect of road pavement rehabilitation, the effect of the road traffic volume increase, the effect of watershed management and infrastructure reconstruction tasks management improvement. The results of the **quantitative flood risk analysis** have derived in the following conclusions and recommendations:

- Climate change will result in a widespread road flood risk increase, resulting from increased rainfall intensity and desertification of soil's land use projected for the study area by the end of the century (temporal horizon 2050-2100). Therefore, this effect should be considered in the new design of all road infrastructures such as bridges and culverts.
- The new pavement rehabilitation works will result in a widespread increase in road flood risk, both for the current climate scenario and for the climate-trend scenario, which is derived from the economic revaluation of the rehabilitated infrastructure, which makes it more vulnerable to possible flood events. Therefore, if the future road follows exactly the current road route, flood risk will increase, since the likelihood of flood occurrence remains but the potential consequences increase.
- The increased economic risk due to rehabilitation works should be understood as a cost for the benefits derived from the improvement. Benefits such as: economic development of the populations connected by the road and less time to travel the road once rehabilitated. The flood risk increase should not be used as an argument against rehabilitation, if not as another cost when evaluating the cost-benefit analysis or comparison between design measures. In this sense, it is recommended to analyze other route alternatives to reduce the flood risk.
- The quantitative risk analysis results have shown the flood-induced indirect damage impact for the whole country, mainly caused by economic disruption during closure and incremental vehicle operation when circulating on a deteriorated road, which are multiplied by the current existing delay to start reconstruction tasks after a natural catastrophe. For this reason, the reduction of reconstruction times after a flood is shown as an effective measure to reduce flood risk on new projected rehabilitation works.
- Historically, there has been a significant degradation of forest coverage in the watersheds draining to the road, which increases hydrologic risks. For this reason, one of the recommendations of this document is to carry out a hydrological-forestry rehabilitation of these watersheds, recovering the vegetation and reducing erosion and desertification processes. These actions would have a significant impact on risk reduction, as shown in the obtained results.

PART IV. MSc

CONCLUSIONS

13. MSc THESIS CONCLUSIONS AND RECCOMENDATIONS

The major finding of this MSc thesis is that the implementation and adaptation of existing quantitative flood risk assessment methodologies for other civil engineering fields (such as dam safety or flood risk management in urban areas) to a critical road stretch to support decision-making within the project-design stage is feasible and useful. Giving special attention to evaluate the road system response during a flood event and the derived consequences, this type of integral flood risk assessment could allow overcoming the complexities that are commonly found when applying traditional global-network road risk/vulnerability assessment methodologies in projects where lack of data and poor developed infrastructure network is a deniable reality.

Next, the main conclusions and further recommendations for further research on the topic are provided.

13.1. Main conclusions

- During the state-of-the-art review performed during this graduation work it was concluded that a great effort has been done in the last years regarding the vulnerability and risk study of road networks focusing on a global-network approach, giving useful tools for the vulnerability assessment of urban and inter-urban transportation infrastructure threatened by natural hazards.
- However, for most of the probabilistic methods proposed in the literature regarding this specific topic, a large amount of historical data for road closure days, origin-destination traffic volume matrix and transport modelling is required, which are not always available, especially for the case of road projects in developing countries.
- The innovative approach described in this Msc thesis is driven by a review of existing bibliography regarding vulnerability assessment of road-related infrastructure and gathering this knowledge together in a unique risk model framework that allowed to calculate risk for every flood-prone section and globally. The integral methodology presented is based on the SUFRI methodology fundamentals, dealing directly with the specific road-segment under natural threat and shifting the interest to a more detailed comprehension of the hazard's likelihood of occurrence, the road segment infrastructure response, the potential failure modes involved, and the expected consequences derived from a failure.
- In this context, a methodology to assess pavement response to flooding has been developed, quantifying proposed flood-damage curves for transportation infrastructure using historical road flood damage assessment reports and including indirect damage during road closure and road rehabilitation time as damage-metrics in the analysis. To do so, cost of time based on countries economies (GDP) and incremental cost of vehicle operation based on pavement deterioration after flooding, which is quantified using the IRI index, are estimated. As far as the author's knowledge reaches, this is the first time these metrics are included in a road flood risk analysis.
- In addition, bridge's stability ultimate limit functions regarding deck-pier connection and piers erosion failure modes are included in the system response analysis. After thorough review of the past bibliography regarding the calculation of hydrodynamic forces, it was concluded that design values for similar flow and bridge configurations are not always aligned. A stochastic approach has been used for probability elicitation of the deck-pier connection failure due to hydrodynamic forces during flood peaks. For pier erosion-induced failure a widespread methodology proposed in the literature is used in combination with expert judgement have yield failure probability assessments.
- The integral approach in combination with an event-tree based risk model allow to simplify risk representation in the form of Flood risk maps and Frequency-Damage curves and expected annual average risk (\$/year). This allow to compare different calculation scenarios and to analyze risk (direct, indirect and total) variation among them, for every separate road section and for the whole road, setting

the foundations to perform cost-benefit analysis of road design improvements or even optimization of specific dimensions for road infrastructure such as culverts or bridges.

- When applying the proposed methodology to analyze risk variation due to road design improvements an increase in economic risk is expected due to economic revaluation of the new infrastructure. The latter should be understood as a cost for the benefits derived from its improvement. Benefits as a greater utility of the infrastructure, economic development of the connected populations or less time to travel the road once rehabilitated. The increase in flood risk due to road design improvements (which increases the infrastructure exposure and vulnerability) should not be used as an argument against its rehabilitation, but as an extra cost when evaluating the cost-benefit analysis of the investment or comparison of design measures.
- Results of successfully applying the methodology to a case study in a road in Country Z, where lack of data and poor developed infrastructure network difficult the application of existing road risk/vulnerability assessment methodologies, highlight the usefulness of promoting this culture of integral risk analysis in developing countries, which are normally the most vulnerable countries in the world against natural hazards and will be affected in the future by climate change impact.
- The qualitative phase of the methodology has a series of beneficial effects derived from its own nature and structure. The review of existing information, the technical visit to the infrastructure and collaborative failure mode identification, allow establishing a first and homogeneous insight for the development of further work. In addition, it constitutes a very valuable input for the design of measures, defining the main structural and road management system problems and identifying the main improvements opportunities.
- The quantitative phase of the methodology combines road load analysis, system response and consequence estimation in a single risk model, and allow for comparison of different calculation scenarios, where road design improvements or risk reduction measures can be directly included, providing a solid framework for cost-benefit analysis of various design alternatives.
- Lastly, the innovative approach described in this MSc thesis, from collaborative work to failure mode identification/classification and to risk quantification, can be applied to other roads and types of natural risks (landslides, earthquakes...) to reinforce the need for structural and non-structural measures for infrastructure improvement and/or risk reduction.

13.2. Further improvements and recommendations

In addition, further improvements and recommendations are suggested on this topic:

- Regarding the road hydrological characterization:
 - Only annual maximum daily rainfall data was available, and, thus, it has not been possible to obtain the whole range of IDF rainfall values normally required for a complete hydrological analysis. In case of having access to more detailed data, it is recommended to extend the frequency extreme value analysis to obtain rainfall intensity values associated to other storm durations different from 24 h.
 - The design storms were constructed based on 24 h synthetic hyetographs proposed by NRCS for hurricane-prone Atlantic coastal areas. It is recommended to extend the study to other storms durations and design storm based on IDF rainfall values (if available), in order to select the one that results in the most conservative flood hydrograph for each watershed.
 - In addition, the hydrological model results should be compared with project specific data (discharge measurements) to validate the model. In this case study, this could not been

performed due to absence of data regarding the river discharges in project area. For similar projects where data is available, this model validation should be included.

- Regarding the climate change impact assessment:
 - The methodology presented to update annual maximum daily rainfall to future RCP's scenarios using the CanESM2 model data use only spatial downscaling techniques for historical data adjustment. Other methodologies that use both spatial and temporal downscaling techniques may be more accurate and reliable. In this context, the Equidistance Quantile Matching Method [88] could be used.
- Regarding the road hydraulic characterization:
 - The hydraulic simulations have been performed using a DEM with 1.5 m resolution, which gives reliable results for general flood on extended areas but it is not optimal to obtain accurate data on specific locations such as culverts or bridges, where the construction could influence the model results.
 - A 2D hydraulic model was developed using HEC-RAS 2D software. The model does not allow incorporating bridge structures in to the interface, and the bridge under analysis was modelled as a culvert-type structure. This leads to inaccuracies regarding the hydraulic loads on substructure and superstructure. For a better assessment of loads in the bridge, numerical simulations with CFDs software are recommended or, if required by the project, physical tests on laboratory scale models can be developed.
 - In addition, the hydraulic model results should be compared with project specific data (past flow depths on the road or flooded areas) to validate the model results. In this case study, this could not been performed due to absence of data regarding past flood characteristics for project area. For similar projects where data is available, model validation should be included.
- Regarding the road system response analysis,
 - For the road pavement response to flooding, two damage-depth curves for paved and unpaved roads are used. In addition, the IRI index is used to quantify road deterioration before and after a flood, which values are estimated based on past (specific-site) report assessments. If sufficient measured real IRI data for a road is available, the use of RD models [27] to predict pavement performance over its life cycle is recommended.
 - For bridge response to flooding, two failure modes were considered as potentially critical (Deck-pier connection collapse and bridge collapse due to scour) and incorporated in the risk model. The procedures used to that end were simplified due to the amount of available data and several remarks can be given:
 - Being bridge a special infrastructure within a road system, it is therefore recommended to apply the risk analysis methodology presented separately to each bridge; performing a specific technical visit and collaborative failure mode identification to each of the large bridges present in a road system, in order to give the adequate robustness to the risk analysis process.
 - Apart from evaluating the deck-pier connection stability against hydrodynamic forces, single piers stability and whole-bridge-system stability should be also analyzed. In addition, debris forces should be incorporated in the stability assessment due to being a major cause of bridge failure.

- The use of ULS functions and Montecarlo simulation to assess bridge failure probability could be substituted for more accurate 2D CFD's simulations incorporating exact bridge configuration or in-lab scaled experiments.
 - Bridge scour evaluation is performed following the guidelines proposed by the FHWA [46] and simplified by only considering contraction scour and bridge piers scour. It is recommended to also incorporate long term scour processes and abutment scour in the analysis. As previously commented, the hydraulic loads for bridge scour should be based on detailed topography and hydraulic models where the exact bridge configuration and geometry could be included.
- Regarding the consequence assessment
 - The direct economic assessment has been performed by the use of global depth-damage curves for transportation infrastructure and project-specific maximum value damages for the road. In further works on this topic, other depth-damage curves from literature could be included by means of a sensitivity analysis to capture the surrounding uncertainty regarding this topic.
 - The indirect economic assessment has taken into account indirect cost associated to traffic disruption during road closure and during road rehabilitation, based on average travel time costs for developing countries and incremental vehicle operational costs in deteriorated roads. However, indirect economic damage produce by village's isolation and disruption of economic activity (industry, agriculture...) due to road malfunction has not been considered and should be included in further analysis.
 - The potential loss of human life (social risk) has not been included in the risk analysis thorough this graduation work. This could be achieved by incorporating incremental likelihood of traffic accidents occurrence due to pavement deterioration after flood or by considering all of the informal population settlements that exist close to the road, due to the economic activity around the road infrastructure.
 - Regarding the risk model and risk calculations
 - The risk model presented is a basis to derive quantitative flood risk of a road. However, critical road FMs such as road embankments landslides triggered by a hydrological event has not been included. Further work in this topic is recommended to determine more globally the risk profile on the infrastructure. The following references [89]–[92] could serve as a first guidance on the topic.
 - In addition, the quantitative risk methodology presented in this graduation work could be the starting point to optimize the bridge or drainage system (culvert) dimensions, by the performance of benefit-cost analysis, using the measure economic cost and economic risk as main variable to define the most optimal dimensions of a road particular infrastructure.
 - The risk calculations are performed based on various assumptions and considerations due to the lack of case study reliable data. To capture the uncertainty present in the process it is recommended to perform sensitivity analysis, mainly in the Failure Mode nodes, where the failure probability elicitation is based on simple methods or expert judgement.

14. REFERENCES

- [1] I. Escuder-Bueno, A. Morales-Torres, J. Castillo-Rodriguez, and S. Perales, "SUFRI Methodology for pluvial and river flooding risk assessment in urban areas to inform decision-making," 2011.
- [2] K. Berdica, "An introduction to road vulnerability: what has been done, is done and should be done," *Pergamon*, vol. 117–127, 2002.
- [3] E. Dalziell, "Risk assessment methods in road network evaluation: a study of the impact of natural hazards in the Desert Road," University of Canterbury, 1998.
- [4] J. Muriel-Villegas, K. Alvarez-Uribe, C. Patiño-Rodriguez, and J. Villegas, "Analysis of transportation networks subject to natural hazards - Insights from a Colombian case," *Elsevier*, vol. 151–165, 2016.
- [5] A. Nicholson and Z.-P. Du, "Degradable transportation systems: An integrated equilibrium model," *Transp. Res. Part B Methodol.*, vol. 31, no. 3, pp. 209–223, 1997.
- [6] A. Chen, H. Yang, H. K. Lo, and W. H. Tang, "Capacity reliability of a road network: an assessment methodology and numerical results," *Transp. Res. Part B Methodol.*, vol. 36, no. 3, pp. 225–252, 2002.
- [7] CAPRA, "Metodología de Modelación Probabilista de Riesgos Naturales," 2017.
- [8] S. Kaplan and B. J. Garrick, "On The Quantitative Definition of Risk," *Risk Anal.*, vol. 1, no. 1, pp. 11–27, 1981.
- [9] B. Gouldby and P. Samuels, "Language of Risks: Project Definitions," *FLOODsite*, 2009.
- [10] E. Dalziell. and A. Nicholson, "Risk and impact of natural hazards on a road network," *J. Transp. Eng.*, vol. 127, 2001.
- [11] J. T. Castillo-Rodriguez, I. Escuder-Bueno, L. Altarejos-Garcia, and A. Serrano-Lombillo, "The value of integrating information from multiple hazards for flood risk analysis and management," *J. Nat. Hazards Earth Syst. Sci.*, vol. DOI: 10.51, 2014.
- [12] S. N. Jonkman, R. E. Jorissen, T. Schweckendieck, and J. P. van den Bos, "Flood Defences - Lecture Notes CIE5314," 2017.
- [13] United Nations Educational Scientific and Cultural Organization (UNESCO), "World Water Assessment Programme (WWAP)," 2009.
- [14] I. Escuder-Bueno, A. Serrano-Lombillo, A. Morales-Torres, and J. Fluixá-Sanmartín, "Evaluación de la seguridad hidrológica de presas mediante modelos de riesgo simplificados," in *Risk Analysis, Dam Safety, Dam Security and Critical Infrastructure Management*, I. Escuder-Bueno, Ed. Taylor and Francis, 2012, pp. 335–342.
- [15] J. Barredo, "Normalised flood losses in Europe," *Nat. Hazards Earth Syst. Sci.*, vol. 9, no. 1, pp. 10–97, 2009.
- [16] J. Castillo-Rodriguez, "Integrated Flood Risk Management: Towards a Risk-Informed Decision Making Incorporating Natural and Human-Induced Hazards," Polytechnic University of Valencia, 2017.
- [17] Working Group F of the Common Implementation Strategy for the Water Framework Directive, "A Working Group Floods (CIS) resource document 'Flood Risk Management, Economics and Decision Making Support' Version:," 2012.
- [18] U.K Health and Safety Executive (HSE), "Reducing risks, protecting people, HSE's decision-making process," *HMSO, London*, 2001.
- [19] S. N. Jonkman, R. Jongejan, and B. Maaskant, "The Use of Individual and Societal Risk Criteria Within the Dutch Flood Safety Policy-Nationwide Estimates of Societal Risk and Policy Applications," *Risk Anal.*, 2011.
- [20] R. Slomp, H. Knoeff, A. Bizzarri, M. Bottema, and W. de Vries, "Probabilistic Flood Defence Assessment Tools," *E3S Web Conf.*, 2016.
- [21] U. S. A. C. of Engineers., *Safety of dams – Policy and procedures. Engineering and design*. Washington,

- DC, 2014.
- [22] SPANCOLD, "Technical guide n° 8: Risk analysis applied to dam safety management," 2012.
- [23] I. Escuder-Bueno, J. T. Castillo-Rodriguez, S. Zechner, C. Jöbstl, S. Perales-Momparler, and G. Petaccia, "A quantitative flood risk analysis methodology for urban areas with integration of social research data," *Nat. Hazards Earth Syst. Sci.*, vol. 12, pp. 2843–2863, 2012.
- [24] W. Graham, "A Procedure for Estimating Loss of Life Caused by Dam Failure," 1999.
- [25] Bell and Cassir, "Reliability of transport networks," *Res. Stud. Press*, 2000.
- [26] M. U. Khan, M. Mesbah, L. Ferreira, and D. J. Williams, "Assessment of flood risk to performance of highway pavements," *Proc. Inst. Civ. Eng. - Transp.*, vol. 170, no. 6, pp. 363–372, 2017.
- [27] M. Khan, L. Ferreira, D. Williams, and M. Mesbah, "Developing a new road deterioration model incorporating flooding," *Proc. ICE - Transp.*, vol. 167, pp. 322–333, 2014.
- [28] D. Yuan and S. Nazarian, "Variation in Moduli of Base and Subgrade with Moisture," 2008.
- [29] K. Helali, W. Bekheet, and R. Nicholson, "Importance of a Pavement Management System in Assessing Damage from Natural Disasters: A Case Study to Assess the Damage from Hurricanes Katrina and Rita in Jefferson Parish, Louisiana," 2008.
- [30] Z. Zhang, Z. Wu, M. Martinez, and K. Gaspard, "Pavement Structures Damage Caused by Hurricane Katrina Flooding," *J. Geotech. Geoenvironmental Eng. - J GEOTECH GEOENVIRON ENG*, vol. 134, 2008.
- [31] K. Gaspard, M. Martinez, Z. Zhang, and Z. Wu, "Impact of Hurricane Katrina on Roadways in the New Orleans Area," 2006.
- [32] Z. Li and S. Madanu, "Highway Project Level Life-Cycle Benefit/Cost Analysis under Certainty, Risk, and Uncertainty: Methodology with Case Study," *J. Transp. Eng.*, 2009.
- [33] M. S. Creagh, "Risk assessment for unbound granular material performance in rural Queensland pavements using semi-quantitative fault tree analysis," 2006.
- [34] M. Sultana, G. Chai, S. Chowdhury, and T. Martin, "Deterioration of flood affected Queensland roads – An investigative study," *Int. J. Pavement Res. Technol.*, vol. 9, no. 6, pp. 424–435, 2016.
- [35] J. B. Odoki, E. E. Stannard, and H. R. Kerali, "Improvements Incorporated in the new HDM- 4 Version 2," in *Proceedings from the International Conference on Advances in Engineering and Technology*, 2006.
- [36] J. P. Aguiar-Moya, J. A. Prozzi, and A. de Fortier Smit, "Mechanistic-Empirical IRI Model Accounting for Potential Bias," *J. Transp. Eng.*, 2011.
- [37] M. Khan, M. Mesbah, L. Ferreira, and D. Williams, "Estimating Pavement's Flood Resilience," *Transp. Eng. J. ASCE, Part B Pavements*, vol. 143, 2017.
- [38] D. M. Sheppard and J. Marin, "Wave loading on bridge decks," *Florida Dep. Transp. Tallahassee, FL, Tech. Rep. No. FDOT BD545-58, UF*, vol. 56675, p. 177, 2009.
- [39] O. K *et al.*, "Hydrodynamic and Debris Damage Failure of Bridge Decks and Piers in Steady Flow.," Delft Technical University of Technology, 2018.
- [40] MTPC, "Rapport de Degats après le passage des cyclones Hanna et I," 2008.
- [41] N. Nader *et al.*, "Numerical Simulation of Hydrodynamic Forces on Bridge Decks," Delft University of Technology, 2018.
- [42] K. Kerenyi, T. Sofu, and J. Guo, "Hydrodynamic forces on inundated bridge decks," 2009.
- [43] A. Standards, "AS5100 - Bridge design Part 1: Scope and general principles." 2004.
- [44] S. Malavasi and A. Guadagnini, "Hydrodynamic Loading on River Bridges," *J. Hydraul. Eng. - J Hydraul ENG-ASCE*, vol. 129, 2003.
- [45] M. A. Jempson, C. J. Apelt, and A. C. Parola, *Debris forces on highway bridges*, no. 445. Transportation

Research Board, 2000.

- [46] L. A. Arneson, L. W. Zevenbergen, and P. E. Clopper, "Evaluating Scour at Bridges," 2012.
- [47] K. Berdica, "TraVIS for Roads - Examples of Road Transport Vulnerability Studies," Royal Institute of Technology Stockholm Sweden Dept. of Infrastructure, 2002.
- [48] H. Wakabayashi and Y. Iida, "Upper and lower bounds of terminal reliability in road networks: an efficient method with Boolean algebra," *J. Nat. Disaster Sci.*, vol. 14, no. 1, pp. 29–44, 1993.
- [49] W. H. K. Lam, "Special issue: Network reliability and transport modelling," *J. Adv. Transp.*, vol. 33, no. 2, pp. 121–123, 2010.
- [50] A. Chen, H. Yang, H. K. Lo, and W. H. Tang, "Capacity reliability of a road network: an assessment methodology and numerical results," *Transp. Res. Part B Methodol.*, vol. 36, no. 3, pp. 225–252, 2002.
- [51] M. G. H. Bell, "A game theory approach to measuring the performance reliability of transport networks," *Transp. Res. Part B Methodol.*, vol. 34, no. 6, pp. 533–545, 2000.
- [52] Y. Iida, "Basic concepts and future directions of road network reliability analysis," *J. Adv. Transp.*, vol. 33, no. 2, pp. 125–134, 1999.
- [53] Taylor and D'Este, "Transport network vulnerability: a method for diagnosis of critical locations in transport infrastructure systems," *Crit. Infrastruct. – Reliab. vulnerability*, pp. 9–30, 2007.
- [54] E. Jenelius and L.-G. Mattsson, "Road network vulnerability analysis of area-covering disruptions: a grid-based approach with case study," *Transp. Res. Part A Policy Pract.*, vol. 46, no. n5, pp. 746–760, 2012.
- [55] G. M. D'Este and M. A. P. Taylor, "Network vulnerability: an approach to reliability analysis at the level of national strategies transport networks," *Netw. Reliab. Transp.*, 2003.
- [56] R. Kondo, Y. Shiomi, and N. Uno, "Network Evaluation Based on Connectivity Reliability and Accessibility," in *Network Reliability in Practice*, 2012, pp. 131–149.
- [57] C. J. Colbourn, "Combinatorial aspects of network reliability," *Ann. Oper. Res.*, vol. 33, no. 1, pp. 1–15, Jan. 1991.
- [58] Y.-S. Qian, M. Wang, H.-X. Kang, J.-W. Zeng, and Y.-F. Liu, "Study on the Road Network Connectivity Reliability of Valley City Based on Complex Network," *Math. Probl. Eng.*, 2012.
- [59] Da-rong, Li-bing, Ling, and Jun, "Review on road network reliability and trends in the information model," *Proc. 25th Chinese Control Decis. Conf.*, pp. 4885–4891, 2013.
- [60] F. Kurauchi, N. Uno, A. Sumalee, and Y. Seto, "Network Evaluation Based on Connectivity Vulnerability," in *Transportation and Traffic Theory 2009: Golden Jubilee: Papers selected for presentation at ISTTT18, a peer reviewed series since 1959*, W. H. K. Lam, S. C. Wong, and H. K. Lo, Eds. Boston, MA: Springer US, 2009, pp. 637–649.
- [61] E. Jenelius, T. Petersen, and L.-G. Mattsson, "Importance and exposure in road network vulnerability analysis," *Transp. Res. Part A Policy Pract.*, vol. 40, no. 7, pp. 537–560, 2006.
- [62] K. Berdica and L.-G. Mattsson, "Vulnerability: a model-based case study of the road network in Stockholm," *Crit. infrastructure– Reliab. vulnerability*, pp. 9–30, 2007.
- [63] J. Sullivan, L. Aultman-Hall, and D. Novak, "A review of current practice in network disruption analysis and an assessment of the ability to account for isolating links in transportation networks," *Transp. Lett.*, vol. 1, no. 4, pp. 271–280, 2009.
- [64] V. L. Knoop, M. Snelder, H. J. van Zuylen, and S. P. Hoogendoorn, "Link-level vulnerability indicators for real-world networks," *Transp. Res. Part A Policy Pract.*, vol. 46, no. 5, pp. 843–854, 2012.
- [65] M. Taylor and Susilawati, "Remoteness and accessibility in the vulnerability analysis of regional road networks," *Transp. Res. Part A Policy Pract.*, vol. 46, no. 5, pp. 761–771, 2012.
- [66] M. A. P. Taylor, S. V. C. Sekhar, and G. M. D'Este, "Application of Accessibility Based Methods for Vulnerability Analysis of Strategic Road Networks," *Networks Spat. Econ.*, vol. 6, no. 3, pp. 267–291,

- Sep. 2006.
- [67] D. M. Scott, D. C. Novak, L. Aultman-Hall, and F. Guo, "Network Robustness Index: A new method for identifying critical links and evaluating the performance of transportation networks," *J. Transp. Geogr.*, vol. 14, no. 3, pp. 215–227, 2006.
- [68] L. Olesen, R. Löwe, and K. A. Nielsen, "Flood Damage Assessment Literature review and recommended procedure," *Coop. Res. Cent. Water Sensitive Cities, Melbourne, Aust.*, 2017.
- [69] J. Huizinga, H. de Moel, and W. Szewczyk, "Global flood depth-damage functions," 2017.
- [70] USDOT, "Guidance on Value of Time," Washington DC, 2014.
- [71] NZ Transport Agency, "Economic evaluation manual," 2017.
- [72] MTPTC, "Pour un développement durable des infrastructures routières, Document de formulation de Stratégie," 2001.
- [73] M. W. Sayers, "On the calculation of International Roughness Index from longitudinal road profile," *Transp. Res. Rec.*, 1995.
- [74] S. K. Mitra and J. D. M. Saphores, "The value of transportation accessibility in a least developed country city - The case of Rajshahi City, Bangladesh," *Transp. Res. Part A Policy Pract.*, 2016.
- [75] D. P. van Vuuren *et al.*, "The representative concentration pathways: an overview," *Clim. Change*, vol. 109, no. 1, p. 5, Aug. 2011.
- [76] iPresas, "iPresas Calc Version 1.0.2 - Manual de Usuario." Valencia, 2017.
- [77] V. T. Chow, D. Maidment, and L. Mays, *Applied Hydrology*. New York: Mc Graw Hill, 1988.
- [78] USDA-NRCS, "Estimation of Direct Runoff from Storm Rainfall," *Natl. Eng. Handb.*, 2004.
- [79] M. Pregolato, A. Ford, S. M. Wilkinson, and R. J. Dawson, "The impact of flooding on road transport: A depth-disruption function," *Transp. Res. Part D Transp. Environ.*, 2017.
- [80] BRGM, "Atlas des Menaces Naturelles en Country Z," 2016.
- [81] T. Welle and J. Birkmann, "The World Risk Index – An Approach to Assess Risk and Vulnerability on a Global Scale," *J. Extrem. Events*, vol. 02, no. 01, p. 1550003, 2015.
- [82] IADB, "Country Z, Historical and Future Climate Change," 2015.
- [83] F. Illorme, V. W. Griffis, and D. Watkins, "Regional Rainfall Frequency and Ungauged Basin Analysis for Flood Risk Assessment in Country Z," *Am. Soc. Civ. Eng.*, 2014.
- [84] T. Mitchell Aide and H. Ricardo Grau, "Globalization, migration, and latin american ecosystems," *Science*. 2004.
- [85] S. Mora, "Extent and Socio-Economic Significance of Slope-Instability on the Island of Hispaniola (Country Z and Dominican Republic)," in *Energy and Mineral Potential of the Central American-Caribbean Region*, R. L. Miller, G. Escalante, J. A. Reinemund, and M. J. Bergin, Eds. Berlin, Heidelberg: Springer Berlin Heidelberg, 1995, pp. 403–410.
- [86] J. E. O'Connor and J. E. Costa, "Large Floods in the United States: Where They Happen and Why," *U.S. Geol. Surv. Circ.*, 2003.
- [87] V. Moron, R. Frelat, P. Karly Jean-Jeune, and C. Gaucherel, "Interannual and intra-annual variability of rainfall in Country Z," 2015.
- [88] R. K. Srivastav, A. Schar dong, and S. P. Simonovic, "Equidistance Quantile Matching Method for Updating IDF Curves under Climate Change," *Water Resour. Manag.*, vol. 28, no. 9, pp. 2539–2562, Jul. 2014.
- [89] J. Corominas *et al.*, "Recommendations for the quantitative analysis of landslide risk," *Bull. Eng. Geol. Environ.*, 2014.
- [90] F. C. Dai, C. F. Lee, and Y. Y. Ngai, "Landslide risk assessment and management: An overview," *Eng.*

Geol., 2002.

- [91] S. Lari, P. Frattini, and G. B. Crosta, "A probabilistic approach for landslide hazard analysis," *Eng. Geol.*, 2014.
- [92] R. Bell and T. Glade, "Quantitative risk analysis for landslides – Examples from Bildudalur, NW-Iceland," *Nat. Hazards Earth Syst. Sci.*, 2004.

PART V. APPENDICES

Appendix 1. Failure Modes Identification

A1.1. FMs on Road pavement.

Failure Mode A1	
Name	Large scale river flood and structural pavement deterioration
Description	
<p>In hydrological scenario, a river level increase by a flood until exceeding the road level. The water depth on the pavement causes scour, that develops until finally producing the removal of the pavement layer, leaving it totally or partially impassable, isolating local populations in cases of flood emergency.</p>	
Graphical Scheme	
<p>The diagram illustrates the failure mode in four stages: 1. Water level increases; 2. Water level exceeds road level; 3. Flow causes erosion and pavement deterioration; 4. Vehicles cannot circulate on the road.</p>	
More likely factors	Less likely factors
<ul style="list-style-type: none"> ▪ Most of the route is unpaved, which favors deterioration for a river flooding event. ▪ The route runs parallel to the river channel in several sections with small difference between the river and the road level, without flood defense works to protect against river flooding. ▪ There are blockages in some longitudinal drainage sections that increases the water level and duration on the road after a flood or storm event. ▪ Climate change is expected to increase rainfall intensity and flood levels for a certain return period. ▪ Isolation of populations during emergencies in case of impassable route. ▪ Deforestation problems of the watershed, which generates erosion, debris occurrence, higher flood peaks and lower concentration times. 	<ul style="list-style-type: none"> ▪ The design of a new route could avoid some of the zones that run parallel and close to the river channel (less flood-prone potential). ▪ In several points, bridges section seems to be enough to allow river flows and to avoid the flood by increasing river levels at the river-road intersections.

Figure 14-1: Failure Mode A1. Description and “less likely” and “more likely” occurrence factors.

Failure Mode A2	
Name	Road pavement deterioration due to run-off on steep stretches
Description	
<p>In the hydrological scenario, after high intensity rainfalls and in steep road stretches, turbulences and flow velocities generated by direct runoff can cause significant pavement deterioration.</p>	
Graphical Scheme	
<p>1. Hurricanes produce high intensity storms that fall over the road</p> <p>2. Steep road slope produces high runoff velocities</p> <p>3. Erosion slowly develops</p>	
More likely factors	Less likely factors
<ul style="list-style-type: none"> ▪ Most of the route is unpaved and not asphalted, facilitating deterioration in case of flooding. ▪ Longitudinal drainage in in bad condition and blocked by: sediments, rubbish or constructions towards particular properties entrances. ▪ Climate change will increase the rainfall intensity during cyclone episodes. ▪ In the report assessed by MTPTC, such failures are reported between PK 15-18. 	<ul style="list-style-type: none"> ▪ New ongoing rehabilitation tasks include rehabilitation and construction of longitudinal drainage works. ▪ The sections where the slope is steep are not numerous and are easily detectible along the path. ▪ The consequences are partial and localized and are not critical because they do not seriously prevent road traffic or cause potential loss of life.

Figure 14-2: Failure Mode A2. Description and “less likely” and “more likely” occurrence factors.

Failure Mode A3	
Name	Road settlement due to foundation wash-out of fine particles
Description	
<p>In hydrological scenario, if water flows through layers of natural granular terrain, fine aggregates can be washed out. This transport could decrease ground mass and favor rigid asphalted layer settlement due to the appearance of voids replacing sand, silts or other particles of small size, which facilitates the road deterioration by the river stream.</p>	
Graphical Scheme	
More likely factors	Less likely factors
<ul style="list-style-type: none"> ▪ A malfunction of the longitudinal drainage is observed. ▪ There is a lack of geotechnical studies to clarify the uncertainty surrounding the presence of cohesive soils under the pavement. ▪ There are road sections close to the riverbed that are flooded with annual recurrence. ▪ Climate change is expected to increase the rainfall intensity and flood reaching levels. ▪ The presence of trucks and high-load road traffic can accelerate the deterioration of the road pavement. 	<ul style="list-style-type: none"> ▪ Road traffic is not intense and small settlements would not seriously damage vehicle circulation (mostly motorbikes or 4x4) in the infrastructure. ▪ The design of a new route could avoid some of the zones that run parallel and close to the river channel (less flood-prone potential).

Figure 14-3: Failure Mode A3. Description and “less likely” and “more likely” occurrence factors.

Failure Mode A4	
Name	Liquefaction under road foundation
Description	
<p>In seismic scenario, vibration for a (normally) saturated non-cohesive material (usually sands or silts) induces loss of shear strength, breaking its structure by reducing its inter-granular pressure. The soil starts to behave like a fluid and there is a failure of the infrastructure built on it, causing large settlements, the deterioration of the less flexible paved material and making the road impassible.</p>	
Graphical Scheme	
More likely factors	Less likely factors
<ul style="list-style-type: none"> ▪ The northern part of the route (near Port de Paix) is close to the northern tectonic fault, being more susceptible to earthquakes. ▪ During the rainy season, the presence of water saturates the soils and potentially increases the risk of liquefaction for an earthquake event. ▪ Route with presence of embankments with non-cohesive soils. ▪ Isolation of populations during emergencies in case of impassable route. ▪ Insufficient geotechnical studies generate uncertainty for soil characterization. 	<ul style="list-style-type: none"> ▪ There is no historical record of such failures along the X route.

Figure 14-4: Failure Mode A4. Description and “less likely” and “more likely” occurrence factors.

Failure Mode A5	
Name	Road settlement due to dilution of calcareous terrain
Description	
<p>In a hydrological or normal management scenario, if the road is located on a calcareous terrain, and water flows inside one of the land layers, the terrain can dilute due to the water action on the limestone. These cavities can cause the road to sink in part of its route.</p>	
Graphical Scheme	
More likely factors	Less likely factors
<ul style="list-style-type: none"> ▪ Insufficient geotechnical studies generate uncertainty in soil characterization. ▪ Deforestation in the basin decreases rainfall interception and increases water infiltration in the soil. ▪ Shortage and poor design of longitudinal drainage works on the road. ▪ High presence of calcareous soil in the country. ▪ Climate change, which is expected to increase rainfall intensity and flood levels. 	<ul style="list-style-type: none"> ▪ This area is not as problematic for karstification as other areas in the country. ▪ This is a localized failure mode that can only cause partial damage without causing potential loss of life and/or the complete loss of function of the road. ▪ The design of a new route could avoid some of the zones that run parallel and close to the river channel (less flood-prone potential).

Figure 14-5: Failure Mode A5. Description and “less likely” and “more likely” occurrence factors.

A1.2. FMs on Drainage system.

Failure Mode B1	
Name	Clogging of longitudinal drainage by debris
Description	
<p>In the hydrological or normal management scenario, longitudinal drainage works can be blocked by debris or by sediments deposited by the local population, increasing the flood risk in the area and the duration of water levels on the route once the flood is produced.</p>	
Graphical Scheme	
<p>1. Floods and storms produces regular floods on the road</p> <p>2. Erosion induces debris flows</p> <p>3. Locals block drainage works for constructions towards their properties</p>	
More likely factors	Less likely factors
<ul style="list-style-type: none"> ▪ There are areas where the population has blocked drainage works by depositing garbage or building constructions towards their properties. ▪ Deforestation increases the risk of soil erosion and sediment volume after runoff. ▪ Climate change: The change in land uses by desertification increases soil erosion and sediments after rain. ▪ Buildings with low quality materials and poor resistance to flooding are constructed close to the road and the longitudinal drainage works. 	<ul style="list-style-type: none"> ▪ In some sections, rehabilitated longitudinal drainage works have been constructed for irrigation use, which can motivate the population not to block the drainage.

Figure 14-6: Failure Mode B1. Description and “less likely” and “more likely” occurrence factors.

Failure Mode B2	
Name	Clogging of transversal drainage by debris
Description	
<p>In hydrological scenario, river flow can drag and carry debris such as trees, plants and solid material from the watersheds that can obstruct the drainage works (culverts). This obstruction increases the upstream level, causing overflow and flooding the road section at that point.</p>	
Graphical Scheme	
More likely factors	Less likely factors
<ul style="list-style-type: none"> ▪ Agriculture or plantations in the river bed area and near the drainage works. ▪ Deforestation increases the risk of soil erosion and therefore, the debris volume after runoff. ▪ Climate change: The change in land use will increase soil erosion and debris after rain. ▪ Poor sizing of drainage works, which do not have sufficient capacity to allow sediments to pass during a flood. ▪ Poor maintenance and revision of drainage works increases risk if sediments are not removed between successive events. 	<ul style="list-style-type: none"> ▪ River flows are seasonal and during the dry season, when the level is low, it is easy to do maintenance tasks and remove sediments deposited during a flood. ▪ The design of the new route could avoid the areas that run parallel and near the river channel (flood potential). ▪ This is a localized failure mode that can only cause partial damage without causing potential loss of life and/or the complete loss of function of the road.

Figure 14-7: Failure Mode B2. Description and “less likely” and “more likely” occurrence factors.

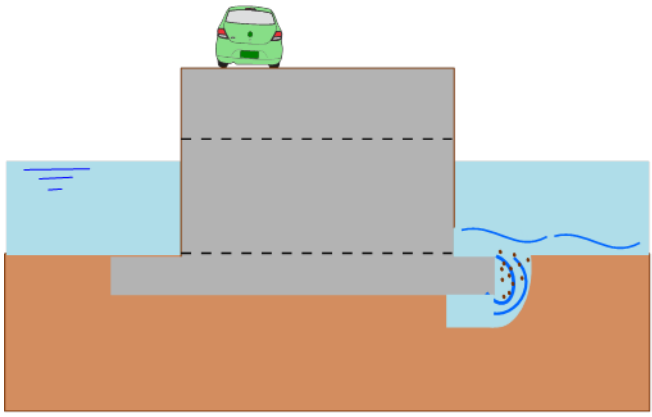
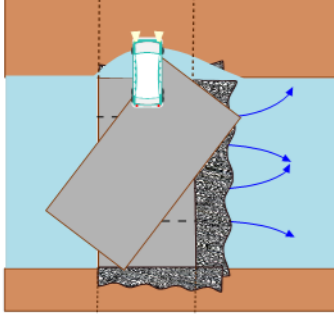
Failure Mode B3	
Name	Culvert failure due to erosion at foundation level
Description	
<p>In the hydrological scenario, the water flow velocity and the generated turbulence at the culvert exit can damage the foundation footing if this is not properly protected, producing an erosion in it, which If it progresses, it can lead to settlement and destabilization of the infrastructure by loss of support.</p>	
Graphical Scheme	
<p>Cross section</p> 	<p>Upper view</p> 
<p>1. Contraction due to culvert increases flow speed and turbulence.</p>	<p>2. Turbulences generate erosion at culvert footing</p>
	<p>3. Erosion can develop up to the abutments, destabilizing the structure.</p>
	<p>4. The river channel changes and the culvert fails.</p>
More likely factors	Less likely factors
<ul style="list-style-type: none"> ▪ Culverts foundations are shallow and with no protection against erosion. ▪ The extraction of aggregates in the river channel area can increase flow velocity and the erosion risk of the culverts. ▪ If a culvert fails during a flood, population can be isolated, increasing its vulnerability to the emergence. ▪ The climate change and the watersheds deforestation will increase in the peak flow, higher flow velocity and greater erosive potential of the flood. ▪ Insufficient maintenance difficult the identification of potential erosion at the foundation footing. 	<ul style="list-style-type: none"> ▪ In some culverts there are gabions protections against erosion. ▪ River flows are seasonal and during the dry season, when the level is low, it is easy to do maintenance tasks and remove sediments deposited during a flood. ▪ A design of the new route could avoid the areas that run parallel and near the river channel (flood potential). ▪ This is a localized failure mode that can only cause partial damage without causing potential loss of life and/or the complete loss of function of the road.

Figure 14-8: Failure Mode B3. Description and “less likely” and “more likely” occurrence factors.

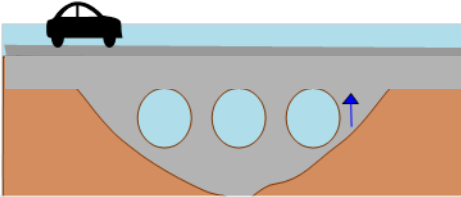
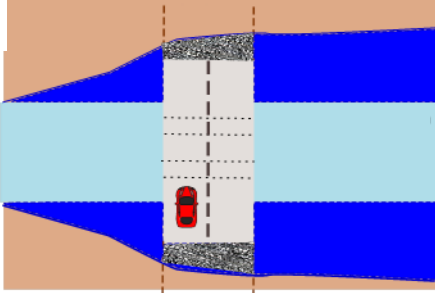
Failure Mode B4	
Name	Clogging of transversal drainage due to insufficient capacity
Description	
<p>During a hydrological event, the river flood may be of sufficient magnitude to collapse the culvert capacity along the X road. The water accumulates upstream of the culvert until it causes the overflow on the pavement and the river banks. Hindering traffic circulation on the infrastructure. The turbulence and the flow velocity generate erosion in the construction until, in the worst case, the culver collapse and fails.</p>	
Graphical Scheme	
<div style="display: flex; justify-content: space-around; align-items: flex-start;"> <div style="text-align: center;"> <p>1. Works with insufficient capacity and overtopping</p>  </div> <div style="text-align: center;">  </div> </div>	
<p>3. River level increases due to flood.</p>	<p>2. Water generates scour until works collapse</p>
More likely factors	Less likely factors
<ul style="list-style-type: none"> ▪ Several culverts have been poorly designed, and their design capacity is lower than the recommended one. Therefore, they have collapsed during past flood events (year 2008). ▪ In many cases, culverts are the only alternative to circulate. If they fail, the populations are isolated in case of an emergency. ▪ The foundations are usually shallow. Erosion generated can quickly induce the infrastructure collapse. ▪ The change of land-use by drought and deforestation increases soil erosion and sediments after rain. ▪ Climate change will increase rainfall intensity, the flood level and the debris flow towards the drainage works, facilitating clogging processes. 	<ul style="list-style-type: none"> ▪ A design of the new route could avoid the areas that run parallel and near the river channel (flood potential). ▪ This is a localized failure mode that can only cause partial damage without causing potential loss of life and/or the complete loss of function of the road.

Figure 14-9: Failure Mode B4. Description and “less likely” and “more likely” occurrence factors.

A1.3. FMs on bridges.

Failure Mode C1	
Name	Erosion in piers/abutment foundation and bridge collapse
Description	
<p>In the hydrological scenario, if the flow velocity is sufficiently high, the natural granular terrain surrounding the foundation can be eroded producing a scour hole. The scour can lead to the settlement of the entire infrastructure and loss of support. The loss of support ends up causing instabilities and final collapse, if the river level ends up below the lower part of the piers foundation.</p>	
Graphical Scheme	
More likely factors	Less likely factors
<ul style="list-style-type: none"> ▪ Extraction of aggregates in the channel area can increase the flow velocity and the risk of erosion. ▪ Climate change, which is expected to increase the rainfall intensity and floods level for a certain return period. ▪ Isolation of population in case of bridge failure during a flood event. ▪ Presence of non-cohesive and easily eroded materials in the river bed and in the piers foundation. ▪ There are no alternative routes in case of bridge failure. 	<ul style="list-style-type: none"> ▪ In dry season most piers are visible and scour problems can be detected and corrected. ▪ After the field visit it was observed that most of the large bridges are generally in good condition and there are no visible signs of scour problems. ▪ The failure is gradual and localized and does not have serious consequences of loss of life or complete loss of function of the infrastructure.

Figure 14-10: Failure Mode C1. Description and “less likely” and “more likely” occurrence factors.

Failure Mode C2	
Name	Deck-pier connection failure and bridge collapse
Description	
<p>In hydrological scenario, if river flood reaches a sufficient magnitude it can overtop the bridge deck causing a hydrodynamic force on the deck-pier connection. If the destabilizing force is large enough it can exceed the friction force between deck and pier producing the failure of the connection.</p>	
Graphical Scheme	
<p>The diagram illustrates the failure mechanism of a bridge pier-deck connection during a flood. It shows a cross-section of a bridge pier and deck. The water level is shown rising to the deck level. Three numbered annotations describe the process: 1. Flow velocity and water level increases until deck level when flood arrives. 2. Hydrodynamic drag force on deck-pier connection is greater than friction force. 3. Bridge collapse and local populations are isolated during an emergency.</p>	
More likely factors	Less likely factors
<ul style="list-style-type: none"> ▪ The extraction of aggregates in the river channel area can increase flow velocity and, thus, the hydrodynamic force on the deck-pier connection. ▪ Climate change is expected to increase the rainfall intensity and the flood level for a certain return period. ▪ Isolation of the population in case of bridge failure during a flood event. ▪ There are not always alternative routes in case of bridge failure. ▪ Narrow river channels have higher levels and flow velocities and are more likely to suffer from this type of failure. 	<ul style="list-style-type: none"> ▪ In several bridges, the riverbed is sufficiently wide, and it seems unlikely that the river can suffer such large elevations to cause overtopping of bridge deck.

Figure 14-11: Failure Mode C2. Description and “less likely” and “more likely” occurrence factors.

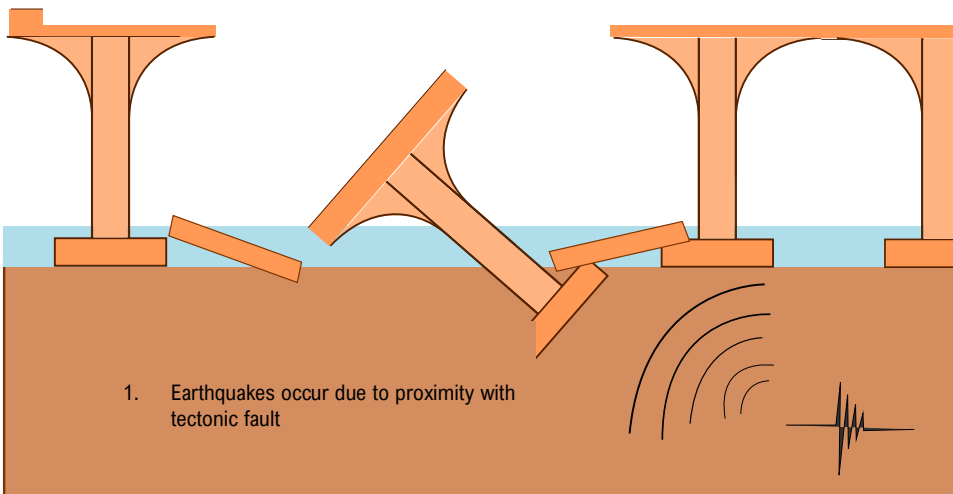
Failure Mode C3	
Name	Bridge collapse due to a seismic event
Description	
<p>In the seismic scenario, induced vibrations generate accelerations and forces near the bridge foundation. Dynamic forces intensities destabilize the supports or trigger liquefaction causing the total or partial collapse of the whole infrastructure. The collapse obstruct circulation through the infrastructure, isolating populations that have been damaged after the earthquake.</p>	
Graphical Scheme	
<div style="display: flex; justify-content: space-around; align-items: flex-start;"> <div style="text-align: center;"> <p>2. Vibrations and dynamic forces induce bridge collapse</p>  </div> <div style="text-align: center;"> <p>3. Collapse produces isolation of local population during an emergency</p> </div> </div> <div style="text-align: center; margin-top: 20px;"> <p>1. Earthquakes occur due to proximity with tectonic fault</p>  </div>	
More likely factors	Less likely factors
<ul style="list-style-type: none"> ▪ There is a lack of geodynamic characterization to determine liquefaction potential. ▪ Seismic scenarios have not been considered in the bridge design. ▪ The seismic risk in the study area is poorly characterized. ▪ Isolation of the population in case of failure during a seismic event. 	<ul style="list-style-type: none"> ▪ Large seismic events have not occurred in the past in the study area.

Figure 14-12: Failure Mode C3. Description and “less likely” and “more likely” occurrence factors.

A1.4. FMs on Road embankments

Failure Mode D1	
Name	Embankment landslide under the road
Description	
<p>In hydrological scenario, after heavy precipitation on the embankment or after a rapid descent of the water level, the water infiltrates in the subsoil through pores and fissures, producing soil saturation, reducing the effective stress and reducing soil resistance, triggering landslides under the route, making it temporarily impassable for vehicle circulation.</p>	
Graphical Scheme	
More likely factors	Less likely factors
<ul style="list-style-type: none"> ▪ Climate change is expected to increase the rainfall intensity and the flood level for a certain return period. ▪ In several areas there are road embankments in river banks without protection nor vegetation. ▪ Poor geotechnical studies prior to the embankment construction. ▪ Steep slopes are observed for some road embankments. ▪ The road embankments in river banks are subject to abrupt changes in the water level after a flood. 	<ul style="list-style-type: none"> ▪ Except for some point, the large part of the X is not subject to hilly terrain and does not have large and steep embankments. ▪ A design of the new route could avoid the areas that run parallel and near the river channel (flood potential).

Figure 14-13: Failure Mode D1. Description and “less likely” and “more likely” occurrence factors.

Failure Mode D2	
Name	Embankment landslide over the road
Description	
<p>In hydrological scenario or normal management, after heavy precipitation, the water infiltrates through pores and fissures, producing saturation, reducing the effective tension and reducing shear resistance, triggering a landslide on the route making vehicle circulation temporarily impassable. This failure may also occur without the need for prior precipitation, as long as the slopes are not stable or after earthquake.</p>	
Graphical Scheme	
More likely factors	Less likely factors
<ul style="list-style-type: none"> ▪ Climate change is expected to increase the rainfall intensity and the flood level for a certain return period. ▪ Non-stabilized steep slopes are observed for some road embankments. ▪ Poor geotechnical studies prior to the embankment construction. ▪ Building constructions with low-quality materials and close to the road embankments that increases the vulnerability in case of landslide. 	<ul style="list-style-type: none"> ▪ Except for some point, the large part of the X is not subject to hilly terrain and does not have large and steep embankments.

Figure 14-14: Failure Mode D2. Description and “less likely” and “more likely” occurrence factors.

Failure Mode D3	
Name	Rock fall over the road
Description	
<p>In normal management and/or seismic scenario, a rock detachment and its subsequent fall to the path could produce road damage making the road temporarily impassable or damaging some of the circulating vehicles.</p>	
Graphical Scheme	
<div style="text-align: center;"> <p>1. Erosion in steep slopes produces rock detachments.</p> <p>2. No protection on the slopes against rock falls.</p> <p>3. Rocks produce road damage and hinder traffic circulation.</p> </div>	
More likely factors	Less likely factors
<ul style="list-style-type: none"> ▪ In several sections, there are not protection for the embankments nor is there any protection net against rock-falls. ▪ Lack of geotechnical studies to characterize the lithology and to determine the vulnerability to this failure mode. ▪ The erosion on the road embankments increases the likelihood of landslides occurrence and rocks fall on it. 	<ul style="list-style-type: none"> ▪ Except for some point, the large part of the X is not subject to hilly terrain and does not have large and steep embankments. ▪ This phenomenon is more common in other parts of the country roads. ▪ If it occurs, its consequences would generate only partial damage in the infrastructure.

Figure 14-15: Failure Mode D3. Description and “less likely” and “more likely” occurrence factors.

Failure Mode D4	
Name	Embankment failure due to river erosion
Description	
<p>In hydrological scenario, the flow velocity can induce the erosion of the road embankments situated in the river banks. Erosion is more intense in the external stretch of the curved river channel areas. This erosion at the slope footing can trigger the landslide at that point, which can affect the normal vehicle circulation on the road. In the case of rapid lowering of water levels after a flood, the embankment saturation may increase this failure mode risk.</p>	
Graphical Scheme	
<p>3. Erosion is bigger in exterior part of river banks curves/meanders.</p> <p>4. Landslide can hinder traffic circulation.</p> <p>2. Erosion induce slope instabilities and can trigger landslide events.</p> <p>1. Flood increases scour at slope footing.</p>	
-More likely factors	Less likely factors
<ul style="list-style-type: none"> ▪ Climate change is expected to increase the rainfall intensity and the flood level for a certain return period. ▪ Insufficient protection against erosion in the river banks. ▪ The extraction of aggregates in the riverbed can increase flow velocities and thus aggravate erosion in the river banks. ▪ Embankment sections in the river meanders that favor the erosion of the river channel. 	<ul style="list-style-type: none"> ▪ The design of the new planned route avoids largely the areas that run parallel and near the runway (potentially floodable). ▪ The failure is gradual and localized and does not have serious consequences of loss of life or complete loss of function of the infrastructure.

Figure 14-16: Failure Mode D4. Description and “less likely” and “more likely” occurrence factors.

Failure Mode D5	
Name	River bank protection failure due to river action
Description	
<p>In hydrological scenario, the flow velocity can induce erosion of river banks, which in some parts are protected by gabions. If the speed and the water level are sufficient, the protection can collapse due to scour holes in the footings or human actions such as removing the gabions to obtain large rocks. The protection failure leaves unprotected the embankment slope, triggering scour and ends up failing by landslide (see Failure Mode D4).</p>	
Graphical Scheme	
More likely factors	Less likely factors
<ul style="list-style-type: none"> Climate change is expected to increase the rainfall intensity and the flood level for a certain return period Locals damage the gabion protection nets due to economic activity regarding large rocks commerce. Curved sections induce an extra force on the river banks. There are areas with narrow channels that increases flow velocity and therefore the erosive potential of the flow. 	<ul style="list-style-type: none"> River flows are seasonal and during the dry season, when the level is low, it is easy to do maintenance tasks. The failure is gradual and localized and does not have serious consequences of loss of life or complete loss of function of the infrastructure.

Figure 14-17: Failure Mode D5. Description and “less likely” and “more likely” occurrence factors.

A1.5. FMs on Road Risk Management system.

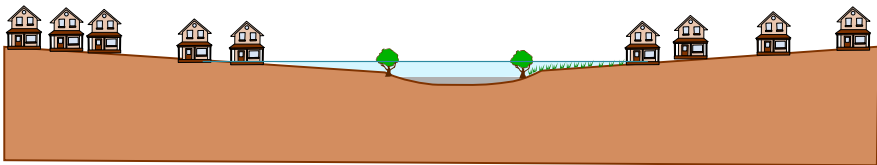
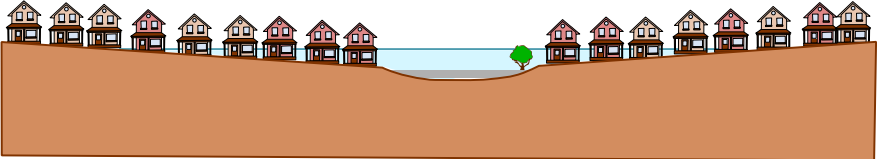
Failure Mode E1	
Name	Informal population settlements
Description	
<p>There is a significant development of informal settlements in flooded areas around the X road due to the economic activity around the road infrastructure. In the hydrological scenario, the river flooding of these populated areas produce greater damage due to a population increase and economic damage due to these settlements.</p>	
Graphical Scheme	
<div style="display: flex; flex-direction: column; align-items: center;"> <div style="display: flex; justify-content: space-between; width: 80%;"> <div style="width: 45%;"> <p>1. Informal settlements close to flood prone areas</p>  </div> <div style="width: 45%; text-align: right;"> <p>2. For a same flood-event, consequences increase due to an increase in the affected population</p> </div> </div> <div style="display: flex; justify-content: center; margin: 10px 0;">  </div> <div style="display: flex; justify-content: space-between; width: 80%;"> <div style="width: 45%;">  </div> <div style="width: 45%;"></div> </div> </div>	
More likely factors	Less likely factors
<ul style="list-style-type: none"> ▪ Sediment deposition processes and waste disposal in drainage works have reduced the draining capacity of the infrastructure. ▪ Development of informal settlements in the areas close to the road due to increasing economic activity. ▪ The resettlement of homes already located in flooded areas is a complex issue. ▪ Informal settlements are usually formed by low-quality materials and less resistant housing. 	<ul style="list-style-type: none"> ▪ The government is making efforts to integrate existing information and to improve risk management tasks. ▪ Water level meters already implanted in some X bridges, that could be incorporated to a future emergency plan to alert population in case of flood event.

Figure 14-18: Failure Mode E1. Description and “less likely” and “more likely” occurrence factors.

Failure Mode E2	
Name	Not leaving properties in case of flooding
Description	
<p>In hydrologic scenario, there is a river flood on the X. Due to the lack of awareness and training in flood risk, citizens are unaware of the protocols of action and warning systems, so they have not left their homes when flood arrives. For this reason, flooding causes greater human losses.</p>	
Graphical Scheme	
More likely factors	Less likely factors
<ul style="list-style-type: none"> ▪ Poor awareness of most of the urban population, who do not want to leave their home for fear of losing their belongings. ▪ Low educational level in the affected areas. ▪ Plans, campaigns and regulations have difficulty for reaching all residents, especially residents in informal settlements. ▪ Citizen insecurity can hinder the tasks of warning and evacuation. 	<ul style="list-style-type: none"> ▪ After the damage caused by Hurricanes I and Hanna in 2008, an awareness campaign may have a greater effect on the local population.

Figure 14-19: Failure Mode E2. Description and “less likely” and “more likely” occurrence factors.

Failure Mode E3	
Name	Failure in the alert system
Description	
<p>In a flooding event, it may occur that there are no warning procedures, or they do not work properly, so vehicles would continue to travel the road as well as people to continue in their homes, being affected when flood arrives.</p>	
Graphical Scheme	
<p>1. Malfunction of early warning systems, warnings and/or evacuation.</p> <p>2. Flood event on the road</p> <p>3. Potential drag of people and/or vehicles</p>	
More likely factors	Less likely factors
<ul style="list-style-type: none"> Currently, the alert system is underdeveloped within the government risk management system. Informal settlements are usually made up of houses with low quality materials and poor resistance to floods. 	

Figure 14-20: Failure Mode E3. Description and “less likely” and “more likely” occurrence factors.

A1.6. Considerations for Failure Mode Classification

- Considering that the main function protection of the analyzed X highway is NOT to protect against natural threats, whether they are floods, landslides or earthquakes, no failure mode has been considered of grade A.
- The A1 failure mode is classified as grade B, as it conforms the main problematic in the study area, where the route runs parallel to the river stream in several sections with little difference in level between the stream and the road pavement, without channeling or protection against flooding of the river. There have been historical failures of this type on the road, generating visible damages that still remain in the infrastructure and are prone to occur in the future due to climate change and deforestation of the watersheds. There is also enough information available to its characterization in a quantitative risk analysis.
- The A2 failure mode is considered as grade C, despite the fact that there is visible damage within the eroded margins of the road axis and that have been detected during the technical site visit, the consequences of this type of failure is partial and localized and will not cause traffic related problems or cause potential casualties.
- The A3 failure mode is considered as grade D as the occurrence of small settlements on the foundation does not imply a serious prejudice to the transit of vehicles on the infrastructure and its low incidence is not in this case of interest for inclusion in a model of risk quantitative.
- The A4 failure mode is considered as grade D. There is not historical evidence of failures of this type in infrastructure and there are not studies that determine high susceptibility of seismic phenomena occurrence in the area nor geotechnical studies that indicate the presence of cohesive soils under the road structure. Its low probability of occurrence in this case is not of interest for inclusion in a quantitative risk model.
- The A5 failure mode is considered as grade D because the area under study it is not considered problematic with respect to karstification as other areas in the country. A failure of this type will be very localized and will not affect to a great road extension and its low incidence is not, in this particular case, of interest for inclusion in a quantitative risk model.
- Every failure mode related to drainage system of the road (B1, B2, B3 and B4) are considered grade C. The reasons are similar, despite the failures of this type have been identified and are expected to occur in the future due to the effect of climate change on river floods, deforestation or extraction of aggregates on the river stream or by poor design and maintenance of works, it's localized failures only cause partial damage, which in any case would mean a potential loss of life or the complete loss of function of the road. In any case, recommendations should be included to take account of these modes of failure in the design and maintenance, and thus, reducing their probability of occurrence.
- The C1 failure mode is considered as grade B. After the field visit, it has been observed that the most of the large bridges are in good condition and the presence of this problem has not been observed in the majority of their piers. However, the predictable effect of climate change on floods along with the extraction of aggregates on the river stream may increase susceptibility to occurrence of this MF in the future. The increased occurrence susceptibility and large (direct and indirect) consequences that a failure of this type could potentially entail is a sufficient reason for its introduction in the quantitative risk model.
- The C2 failure mode is considered as grade B because, although after the field visit it has been observed that most of the major bridges are in good condition, the future climate change impact may reduce the hydraulic capacity in the channel, leading to water level elevations that could cause a collapse by hydrodynamic thrust. The increased occurrence susceptibility and large (direct and

indirect) consequences that a failure of this type could potentially entail is a sufficient reason for its introduction in the quantitative risk model.

- The C3 failure mode is considered of grade E. There is no historical evidence of failures of this type in infrastructure and there are no known studies that determine a high seismic phenomena occurrence susceptibility in the area under study. The uncertainty present in this failure mode does not discard his introduction in the quantitative risk model, but for this purpose it is necessary to gather more information about a failure of this type.
- The failure modes, D1 and D2 are of grade E. Landslides have occurred before in some sections of the current design and their occurrence in the future is foreseeable given the existence of high (and unprotected) slopes in the road section or the effect of the climate, that will increase precipitation and saturation of the slopes. However, to correctly assess landslide hazards it is necessary to gather more information regarding past landslide event (frequency and magnitude) and geo-technical information of the region under study. The uncertainty present in this failure mode does not discard his introduction in the quantitative risk model, but for this purpose it is necessary to gather more information related to this failure mode.
- The D3 Failure mode is considered of grade D regarding that the X is not subject to a steep orography and does not run between large (rocky) slopes. This phenomenon is more common in other parts of the country and in case of occurrence; its consequences would generate partial and located in infrastructure damage. Its low incidence is not of interest for its inclusion in a quantitative risk model.
- The failure modes D4 and D5 are also grade C. Both have occurred in the past as is documented in the technical visit (Appendix) and their occurrence in the future is predictable, however, they should not cause large consequences for transport infrastructure, being located failures that are simply prevented through correct maintenance during dry season when river levels/discharges are low.
- The failure modes E1, E2, and E3 are also considered as Grade E, considering that there exist a proven development of informal settlements in areas close to the X highway and that warning system are underdeveloped, which may entail a potential increase of consequences in case of natural disaster occurrence. The uncertainty present in this failure mode does not discard his introduction in the quantitative risk model, but for this purpose it is necessary to gather more information related to this failure mode.

Appendix 2. Data adjustment and Frequency extreme values analysis of maximum daily rainfall (Historical and Climate Change Scenarios)

A2.1. Historical Rainfall Vs CanESM2 Simulated data: Regression Adjustment

Climate change predictions presented in this report are based on the Canadian Earth System model (CanESM2) GCM model, which provides daily rainfall simulations for the historical scenarios, and future emission scenarios RCP 2.6, RCP 4.5 and RCP 8.5 at a global level. Data from model simulations must be subsequently validated with historical record data to obtain valid predictions for the study area. To do this, simulated daily rainfall data are downloaded for the area of interest and the same historical period of the available records.

The values of the downloaded simulated data do not coincide with those observed in the same period for the different meteorological stations. It is therefore necessary to make an adjustment by a polynomial regression, comparing the annual maximum daily rainfall data observed in the stations with the annual maximum rainfall data simulated in the model, for the same historical period. The adjustment for A and B stations of interest is shown below.

Meteorological station A

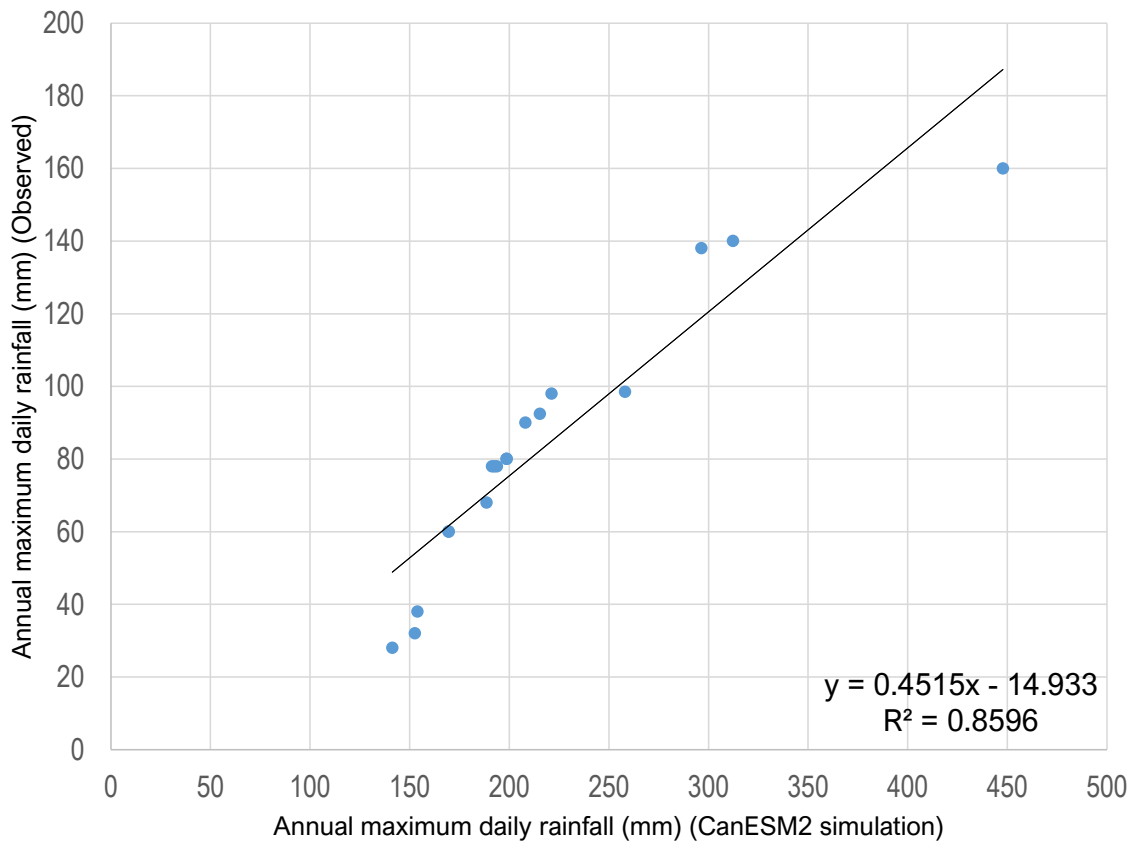


Figure 14-21: Data adjustment (CanESM2 model simulation vs Historical observed data) A station.

Meteorological station B

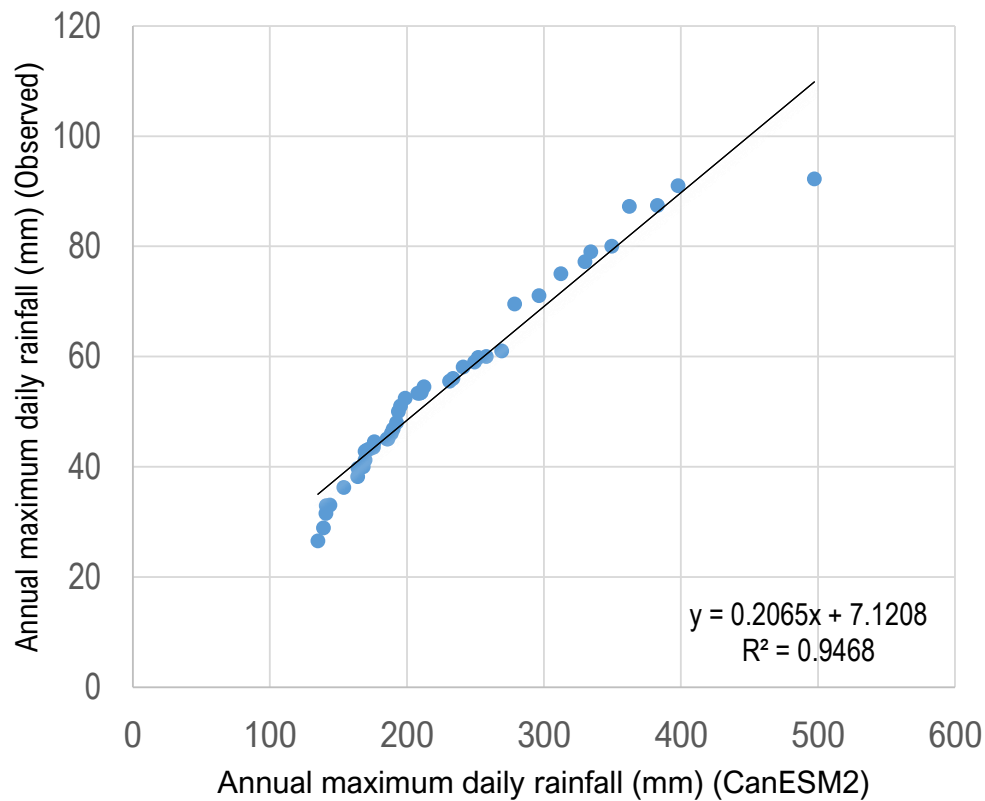


Figure 14-22: Data adjustment (CanESM2 model simulation vs Historical observed data) B station.

A2.2. Frequency extreme values analysis of maximum daily rainfall (Historical and Climate Change Scenarios)

From the historical/simulated annual maximum daily rainfall (in mm), an analysis of maximum frequencies distribution is performed, to assess which is the probability distribution that best fits the maximum daily rainfall value for different return periods for each of the stations considered in the study (A and B) and for each of the climate scenarios (Current Climate and Future Climate-trend scenarios).

During statistical analysis, an adjustment with different probability distributions (Normal, Pearson III, log-normal, log-Pearson III, Gumbel) has been tested. Finally, it has been observed that the best fit for all stations is the Gumbel distribution

Meteorological station A

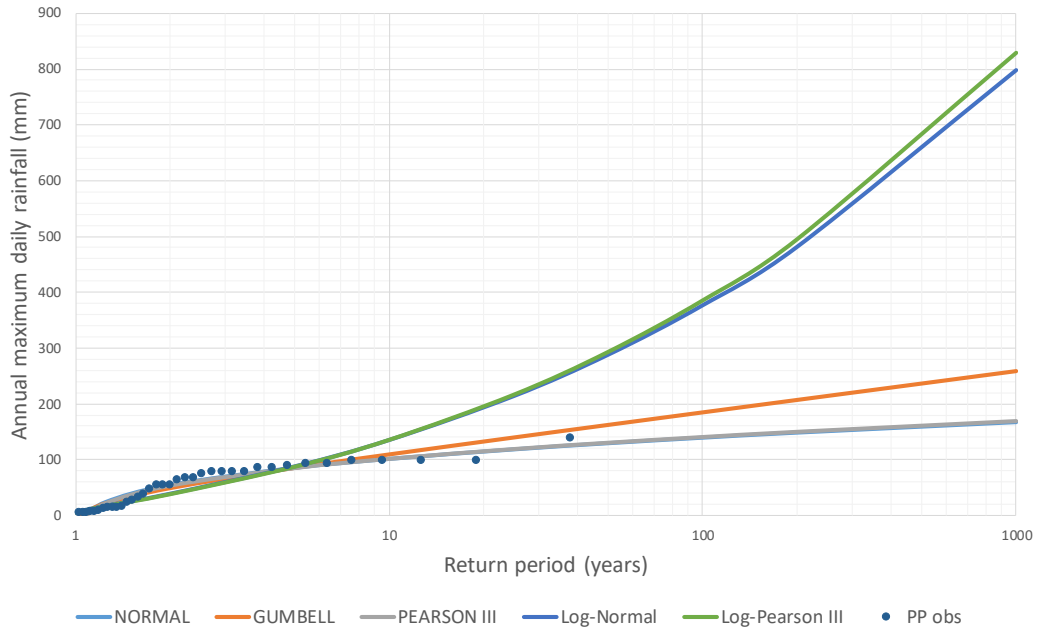


Figure 14-23: Frequency extreme value analysis for annual maximum daily rainfall. Current climate scenario. Station A.

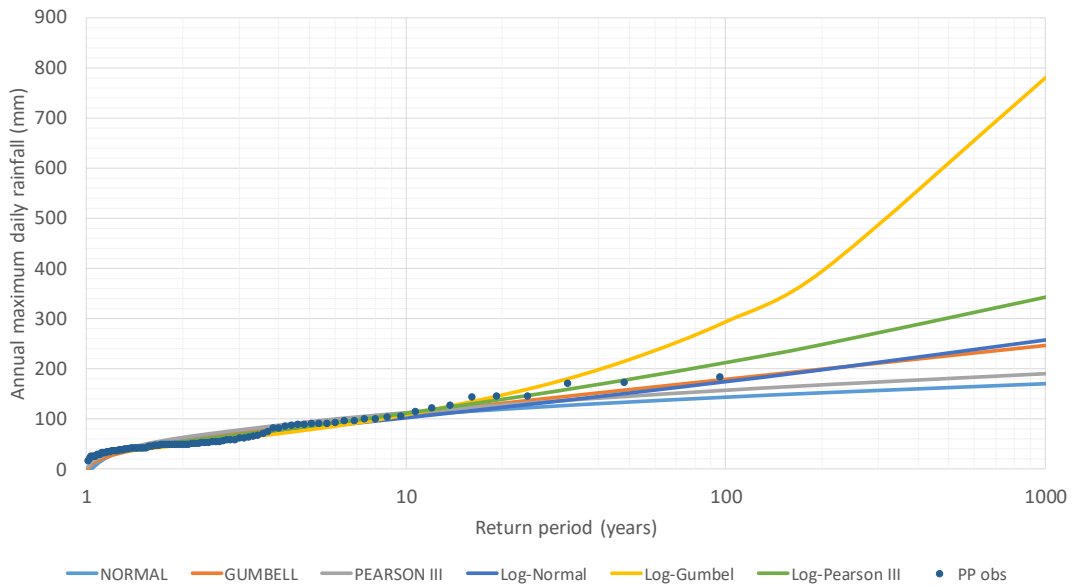


Figure 14-24: Frequency extreme value analysis for annual maximum daily rainfall. Future climate scenario RCP2.6. Station B.

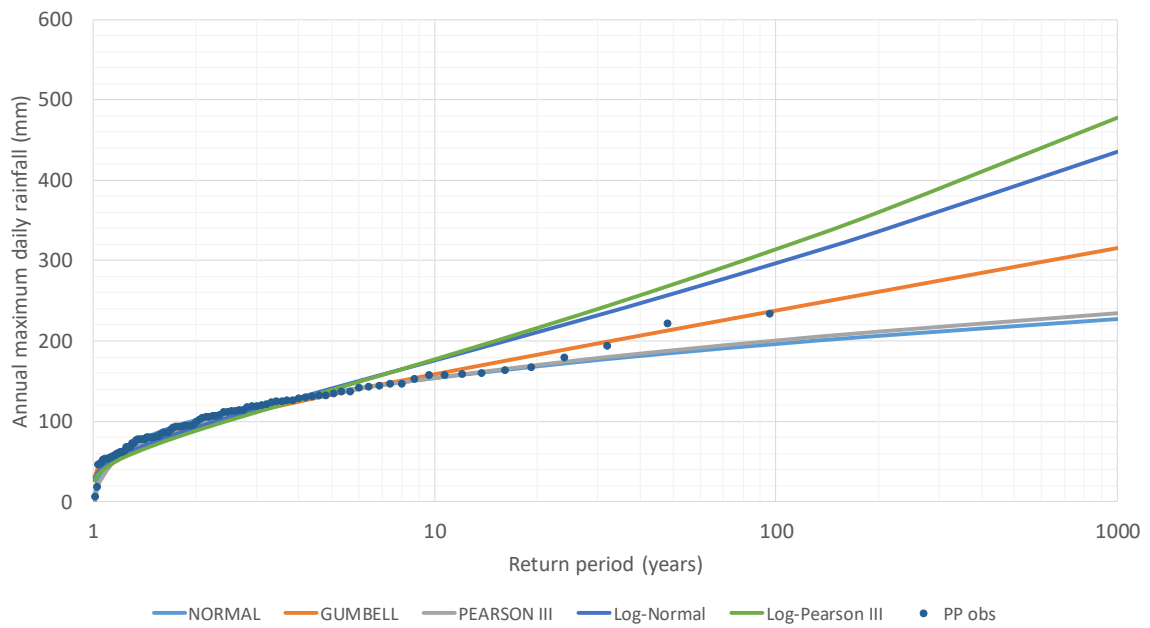


Figure 14-25: Frequency extreme value analysis for annual maximum daily rainfall. Future climate scenario RCP4.5. A Station.

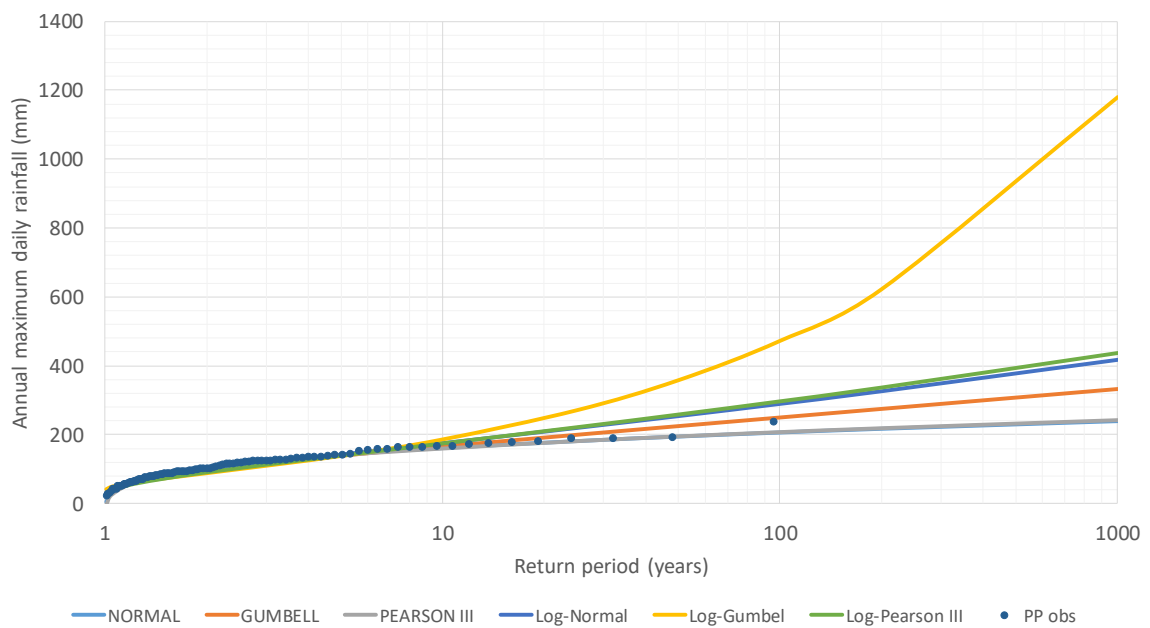


Figure 14-26: Frequency extreme value analysis for annual maximum daily rainfall. Future climate scenario RCP8.5. A Station.

B meteorological station

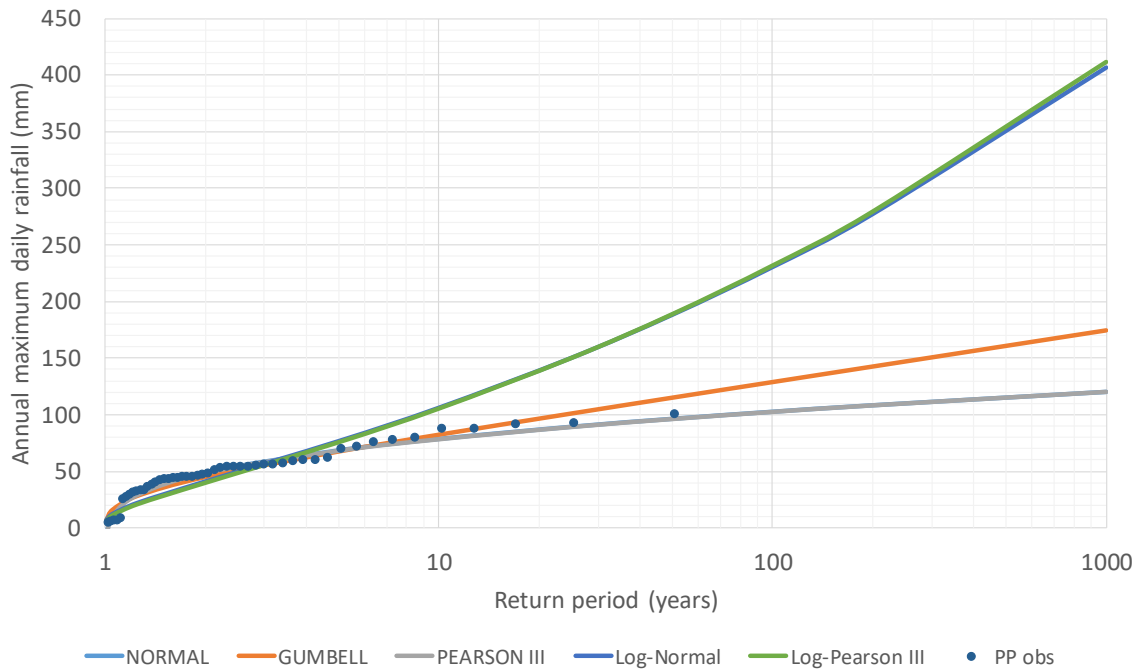


Figure 14-27: Frequency extreme value analysis for annual maximum daily rainfall. Current climate scenario. B Station.

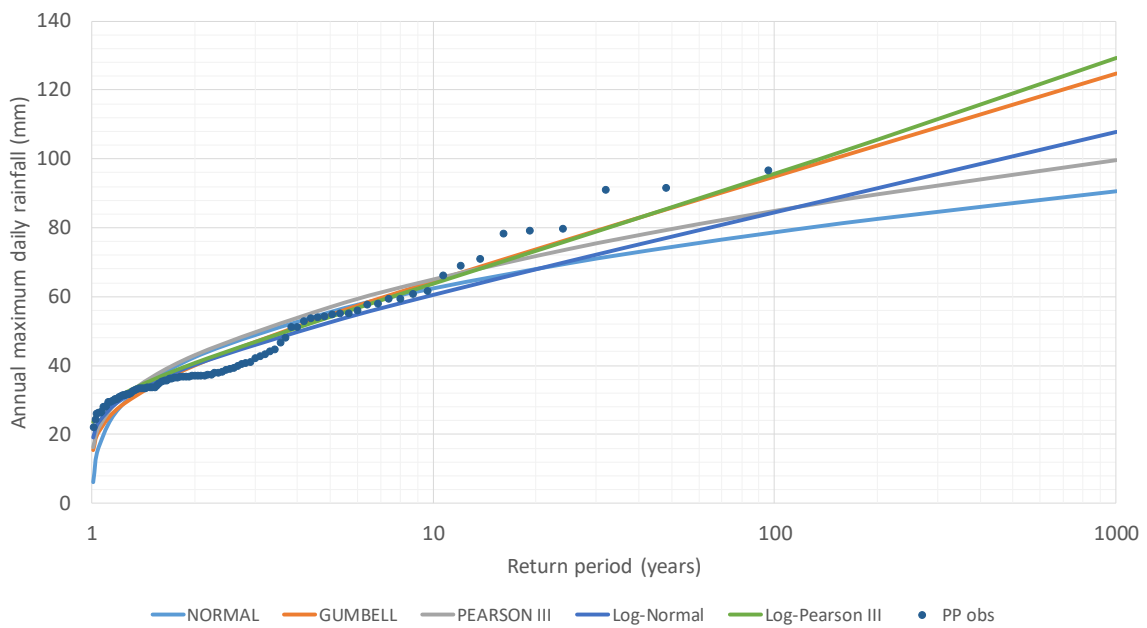


Figure 14-28: Frequency extreme value analysis for annual maximum daily rainfall. Future climate scenario RCP2.6. B Station.

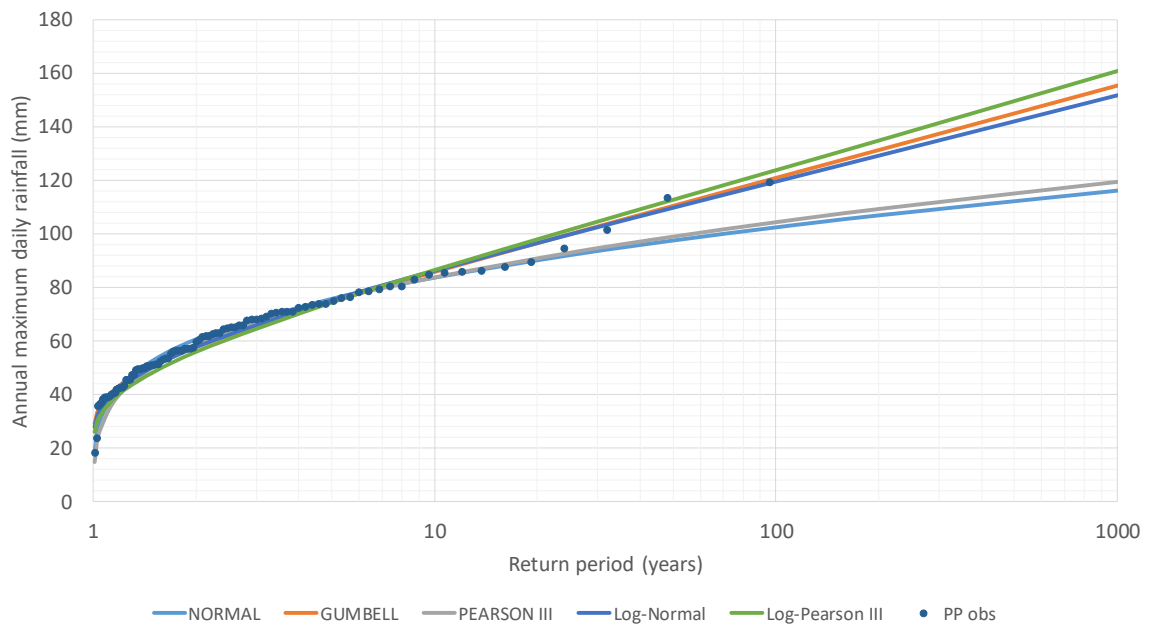


Figure 14-29: Frequency extreme value analysis for annual maximum daily rainfall. Future climate scenario RCP4.5. B Station.

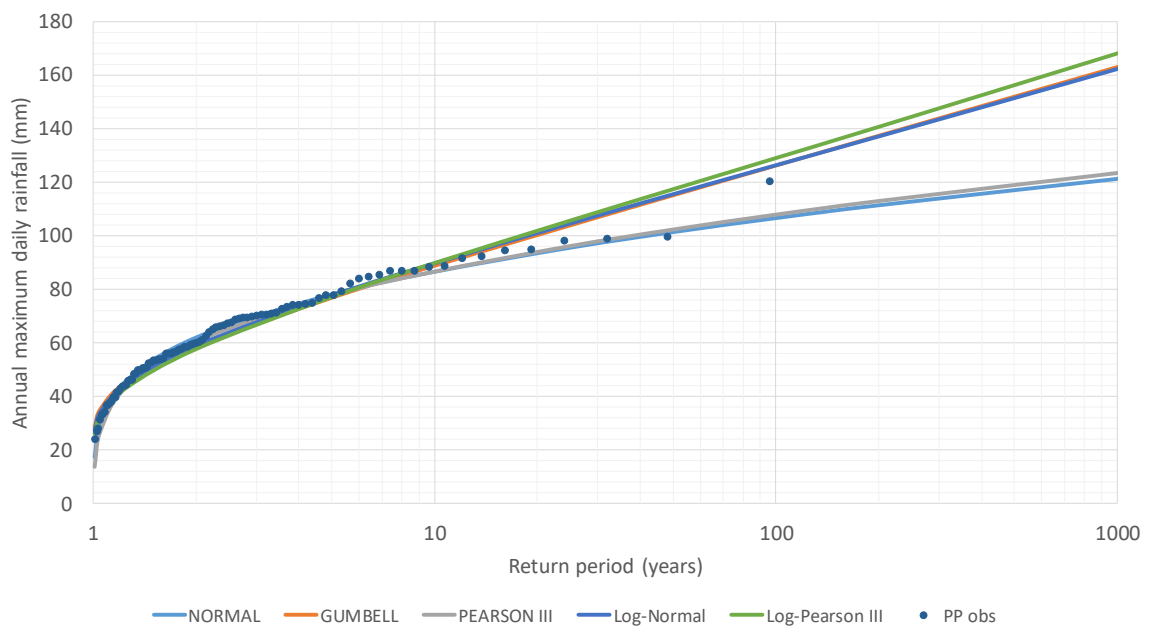


Figure 14-30: Frequency extreme value analysis for annual maximum daily rainfall. Future climate scenario RCP8.5. B Station.

Appendix 3. Hydrologic modeling results

A4.1. Watershed BS1: Hydrological results.

Hydrological modeling results obtained with HEC-HMS software for the intersection between the X road and the BS1 watershed are shown in the following figures. Results are shown for seven return periods (2, 5, 10, 25, 50, 100 and 500 years) and two climatic scenarios (Current climate and Future climate-trend scenario).

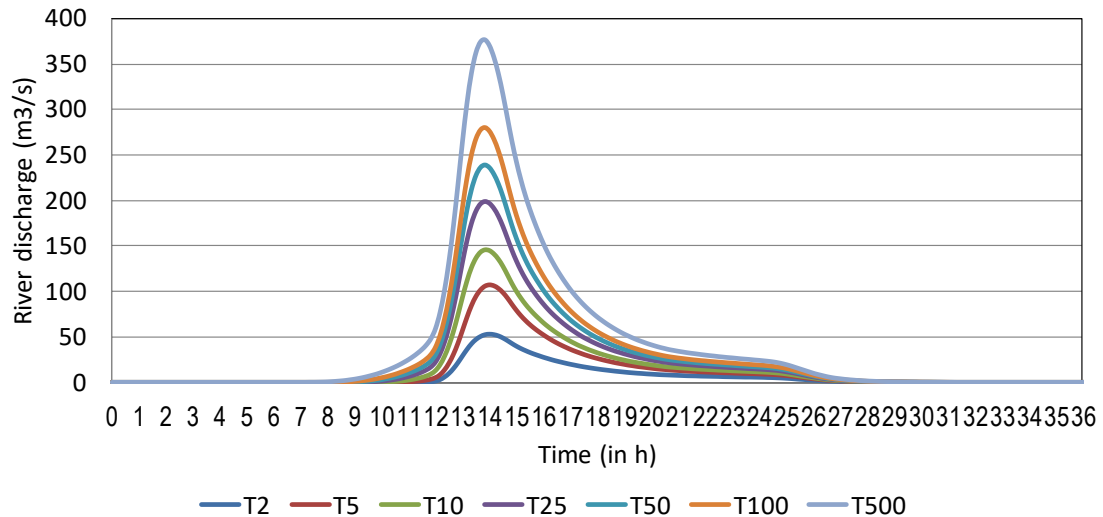


Figure 14-31: Current climate. Flood hydrograph from 24 h Design storm SCS type III. BS1 Watershed.

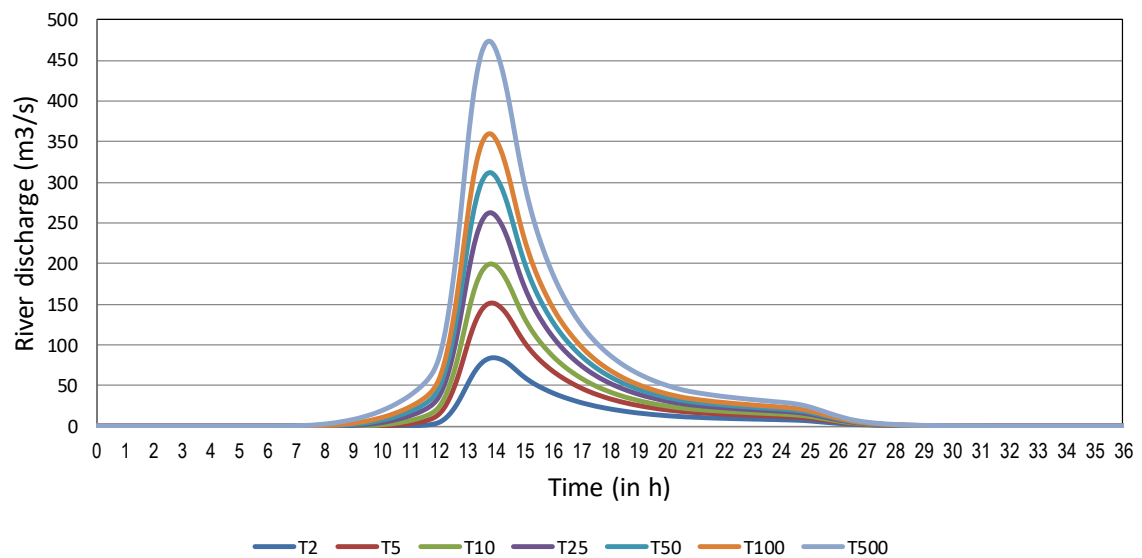


Figure 14-32: Future climate. Flood hydrograph from 24 h Design storm SCS type III). BS1 Watershed.

In addition, to visualize the effect of climate change in river peak flows in the intersection areas, the following figure presents a comparison between the flood peak flow (current scenario vs future climate scenario) for the whole range of return periods analyzed.

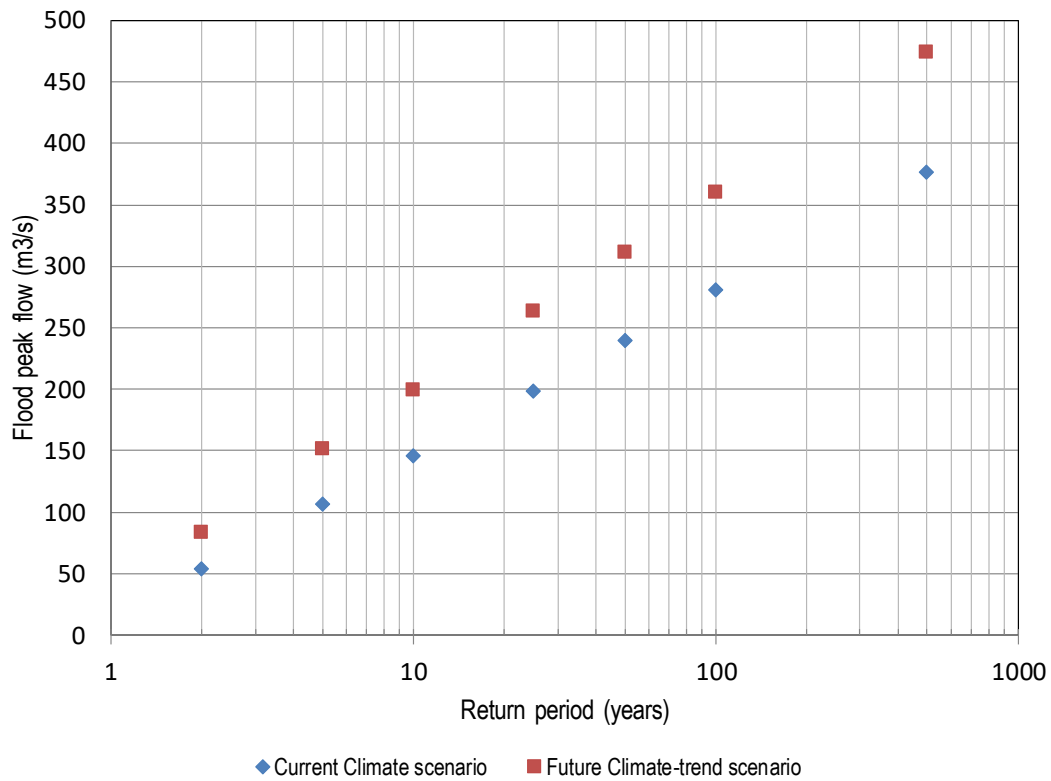


Figure 14-33: Flood peak flow (current scenario vs future climate scenario). X-BS1 intersection.

A4.2. Watershed BS2: Hydrological results.

Hydrological modeling results obtained with HEC-HMS software for the intersection between the X road and the BS2 watershed are shown in the following figures. Results are shown for seven return periods (2, 5, 10, 25, 50, 100 and 500 years) and two climatic scenarios (Current climate and Future climate-trend scenario).

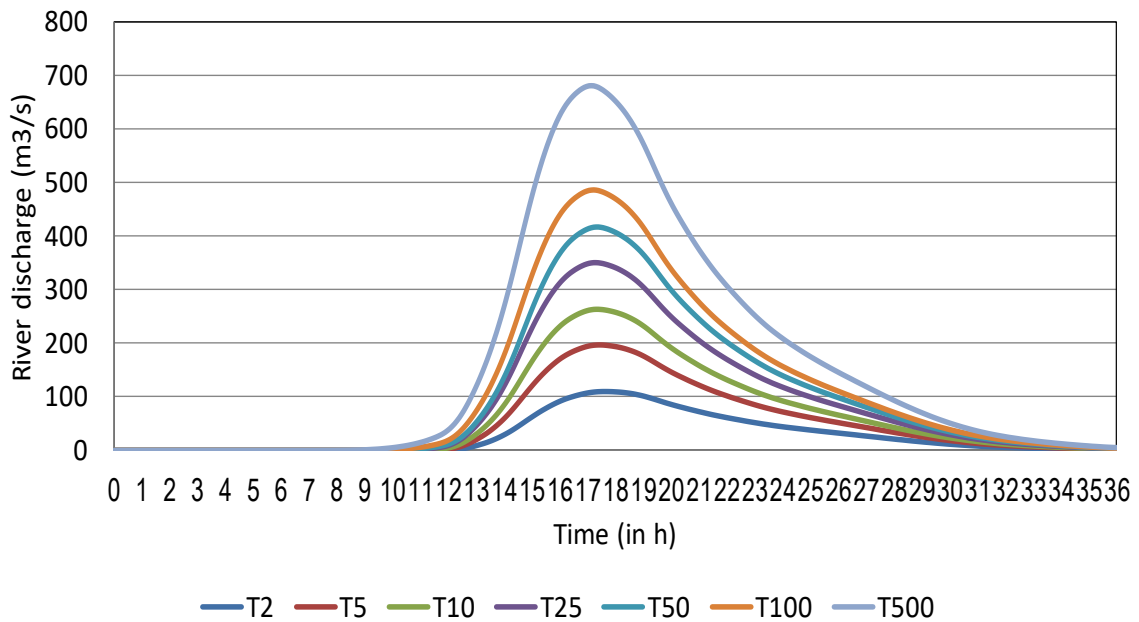


Figure 14-34: Current climate. Flood hydrograph from 24 h Design storm SCS type III). BS2 Watershed.

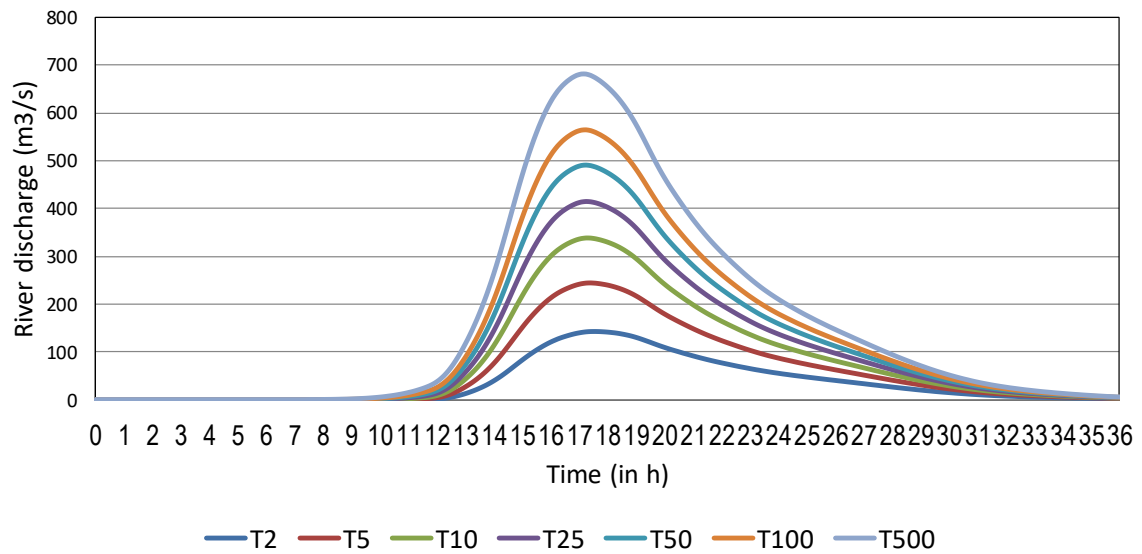


Figure 14-35: Future climate. Flood hydrograph from 24 h Design storm (SCS type III). BS2 Watershed.

In addition, to visualize the effect of climate change in river peak flows in the intersection areas, the following figure presents a comparison between the flood peak flow (current scenario vs future climate scenario) for the whole range of return periods analyzed.

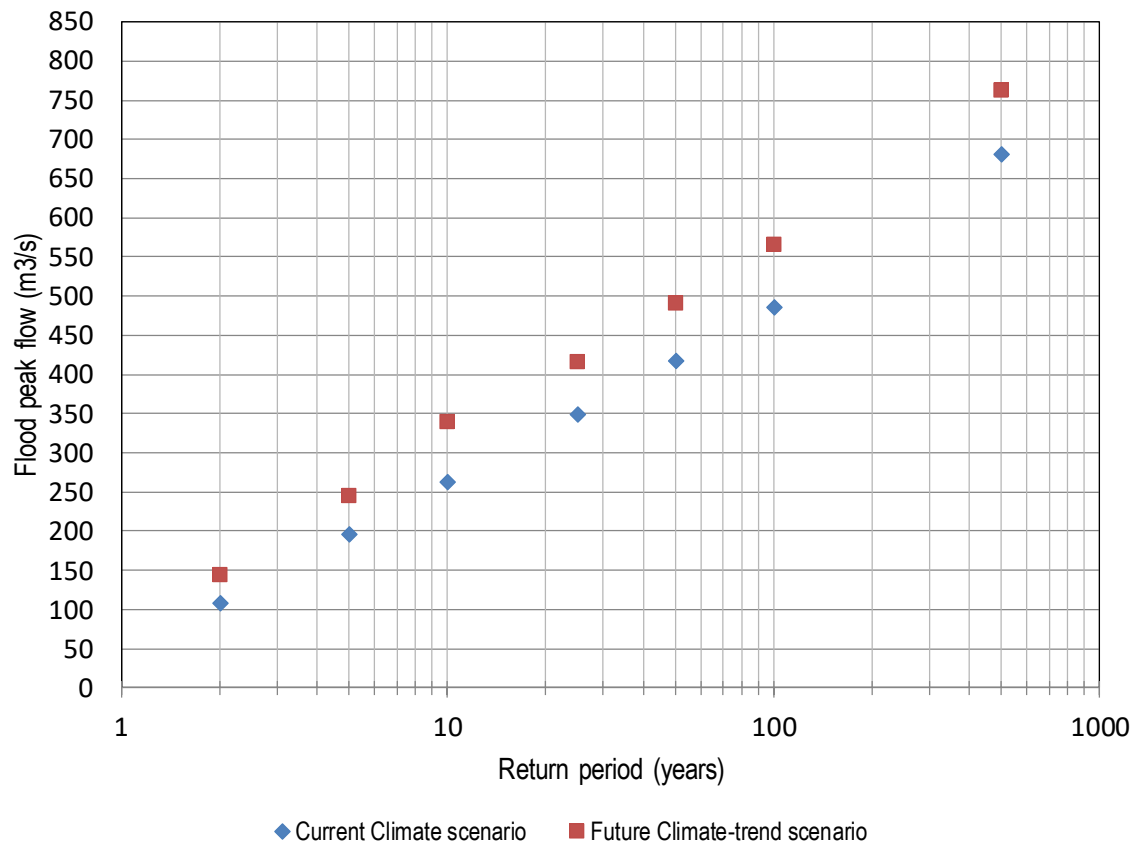


Figure 14-36: Flood peak flow (current scenario vs future climate scenario). X-BS2 intersection.

A4.3. Watershed BS3: Hydrological results.

Hydrological modeling results obtained with HEC-HMS software for the intersection between the X road and the BS3 watershed are shown in the following figures. Results are shown for seven return periods (2, 5, 10, 25, 50, 100 and 500 years), two climatic scenarios (Current climate and Future climate-trend scenario) and an optimal future scenario where a watershed reforestation (change of land-use coverage) is implemented.

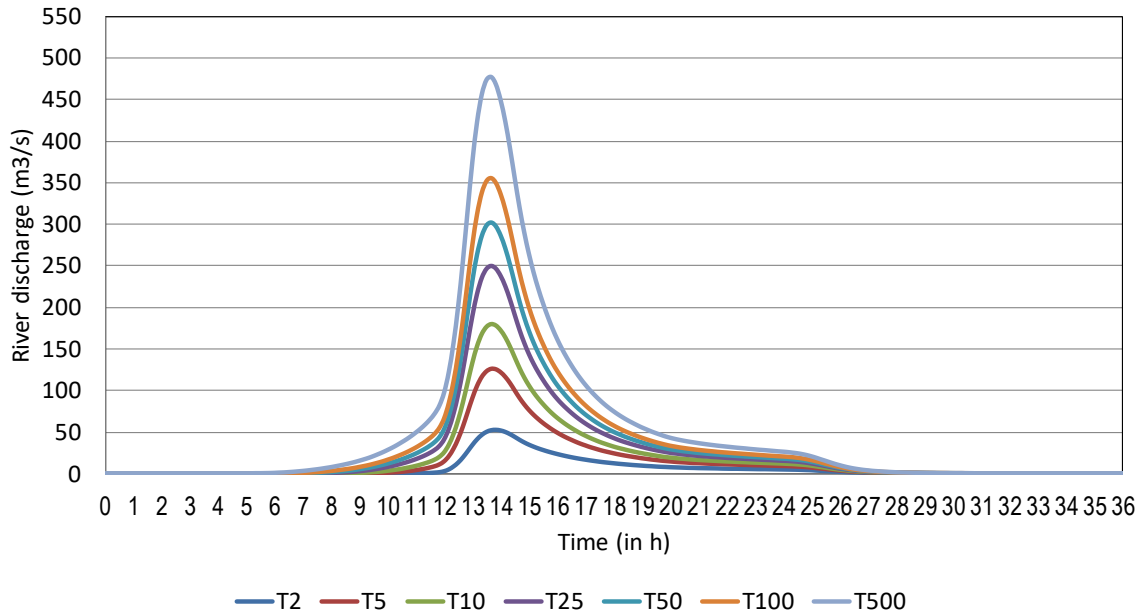


Figure 14-37: Current climate. Flood hydrograph from 24 h Design storm SCS type III. BS3 Watershed.

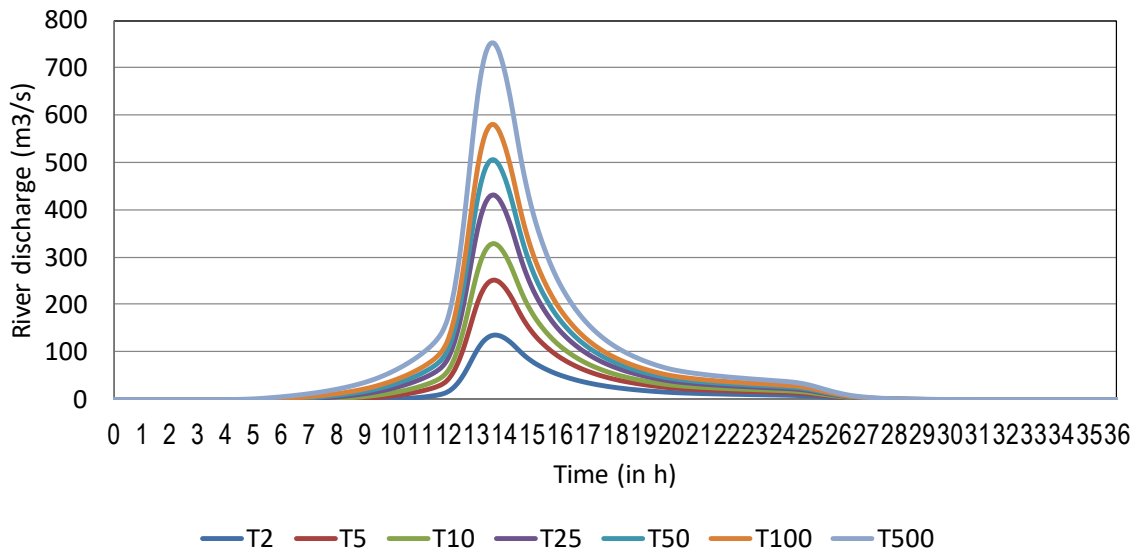


Figure 14-38: Future climate. Flood hydrograph from 24 h Design storm SCS type III. BS3 Watershed.

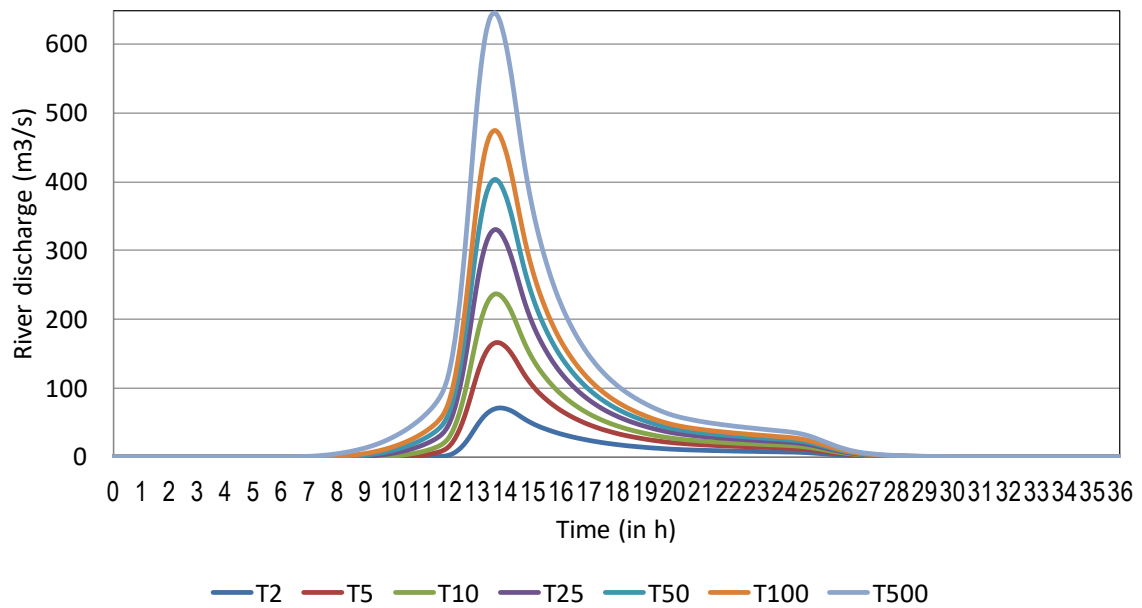


Figure 14-39: Future climate & Watershed reforestation. Flood hydrograph from 24 h Design storm SCS type III). BS3 Watershed.

In addition, to visualize the effect of climate change and water reforestation (optimal scenario) in river peak flows in the intersection areas, the following figures presents a comparison between the flood peak flow (current scenario vs future climate scenario vs optimal future scenario) for the whole range of return periods analyzed.

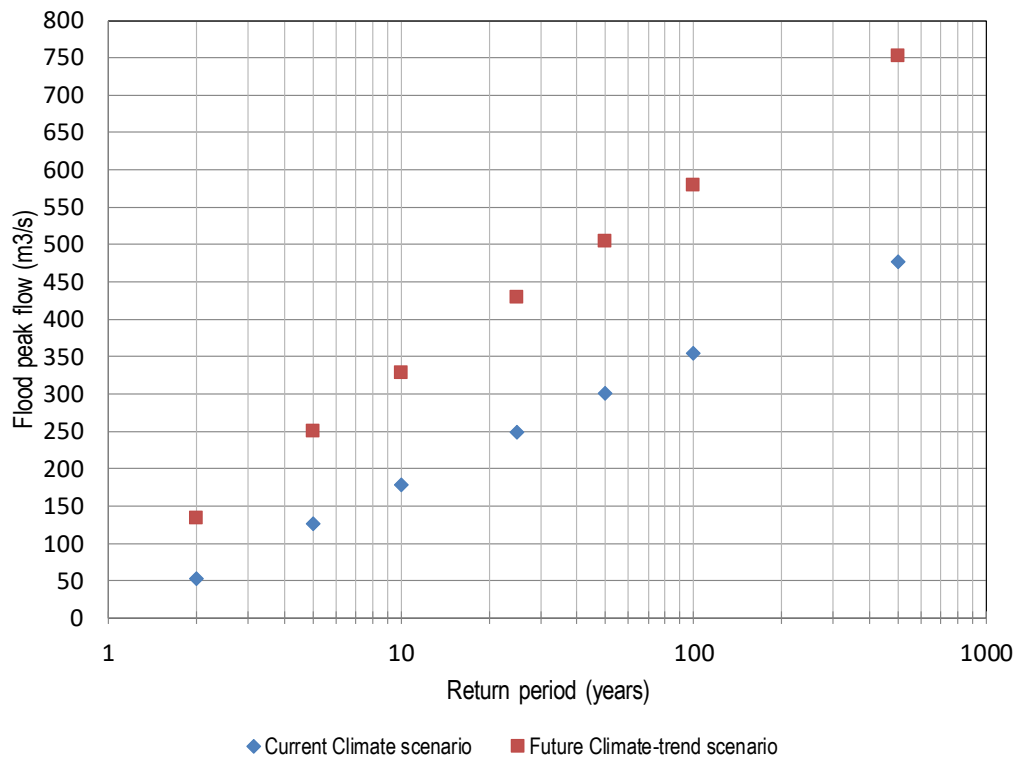


Figure 14-40: Flood peak flow (current scenario vs future climate scenario). X-BS3 intersection.

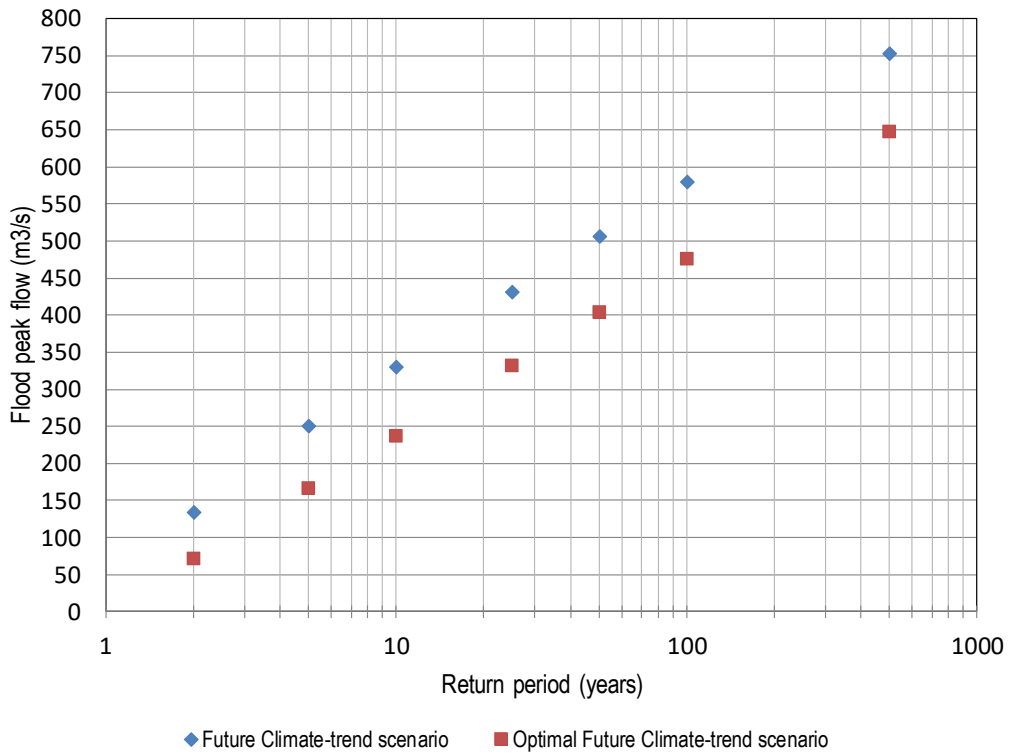


Figure 14-41: Flood peak flow (future climate scenario vs optimal future climate scenario). X-BS3 intersection.

A4.4. Watershed BS4: Hydrological results.

Hydrological modeling results obtained with HEC-HMS software for the intersection between the X road and the BS4 watershed are shown in the following figures. Results are shown for seven return periods (2, 5, 10, 25, 50, 100 and 500 years), two climatic scenarios (Current climate and Future climate-trend scenario) and an optimal future scenario where a watershed reforestation (change of land-use coverage) is implemented.

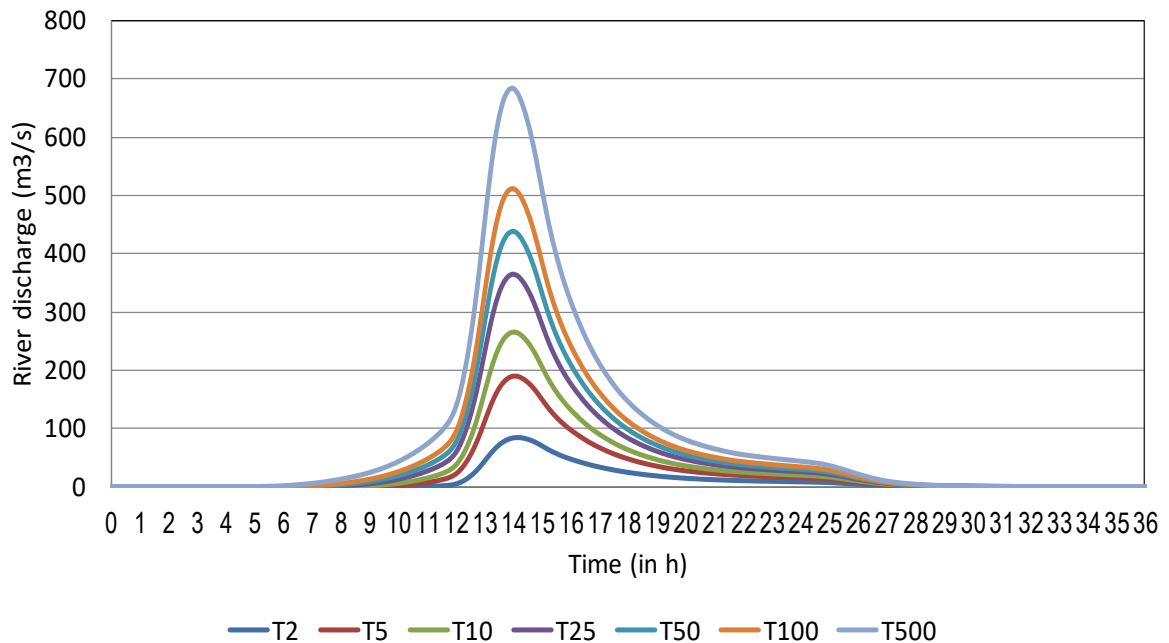


Figure 14-42: Current climate. Flood hydrograph from 24 h Design storm SCS type III. BS4 Watershed.

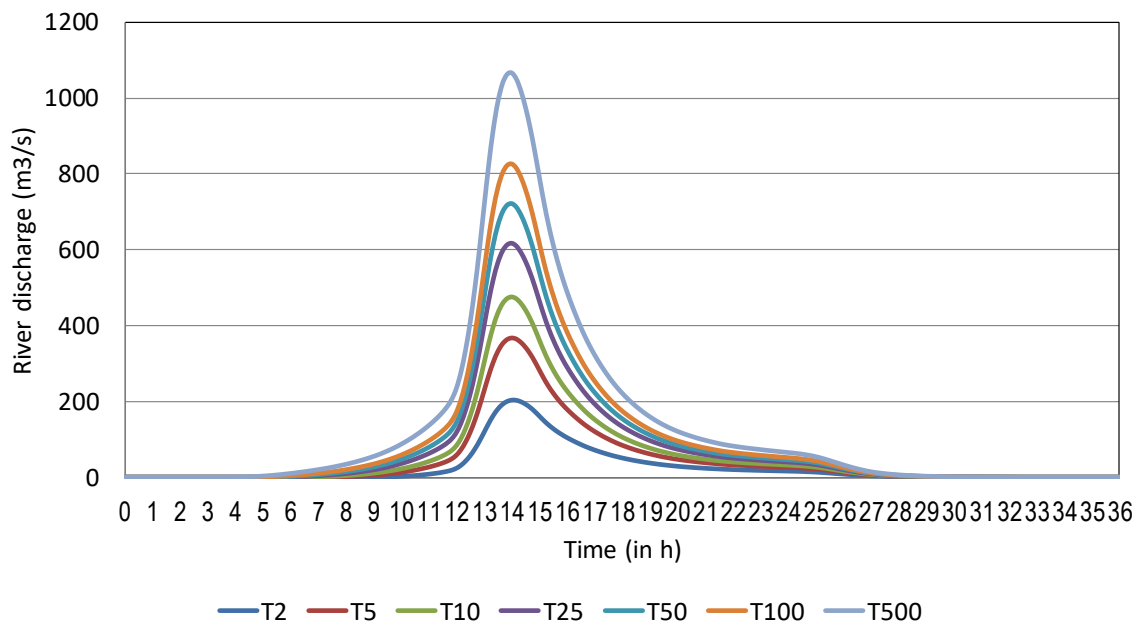


Figure 14-43: Future climate. Flood hydrograph from 24 h Design storm SCS type III). BS4 Watershed.

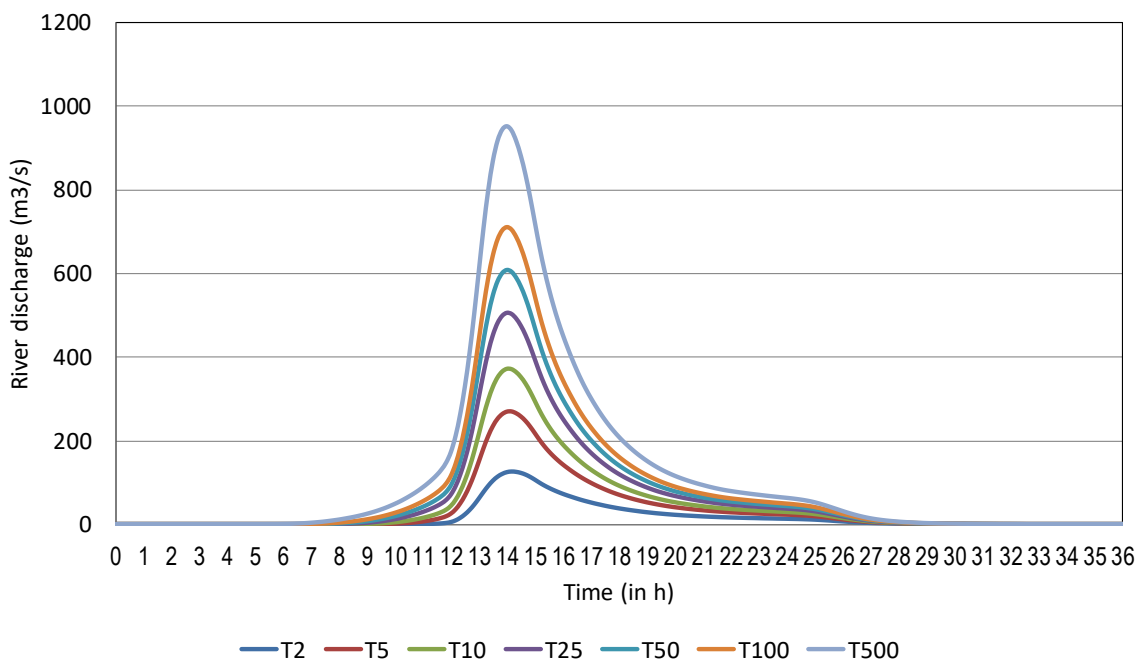


Figure 14-44: Future climate & Watershed reforestation. Flood hydrograph from 24 h Design storm SCS type III). BS4 Watershed.

In addition, to visualize the effect of climate change and water reforestation (optimal scenario) in river peak flows in the intersection areas, the following figures presents a comparison between the flood peak flow (current scenario vs future climate scenario vs optimal future scenario) for the whole range of return periods analyzed.

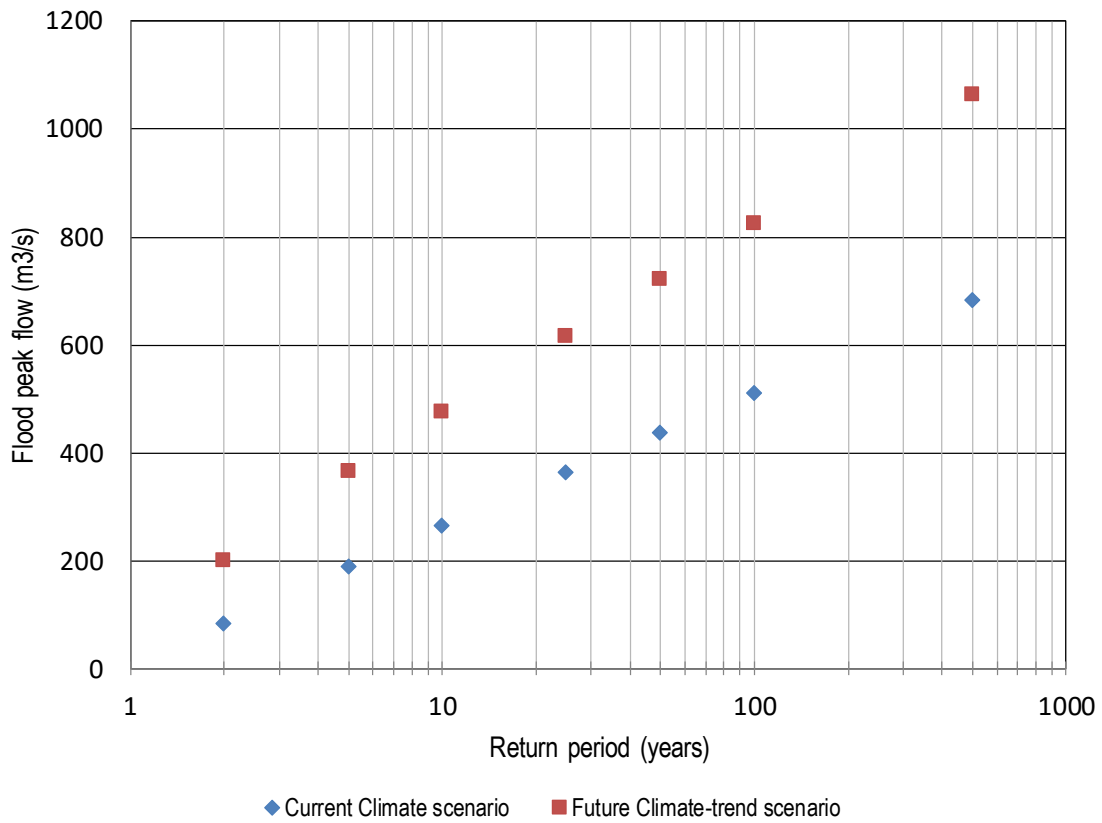


Figure 14-45: Flood peak flow (current scenario vs future climate scenario). X-BS4 intersection.

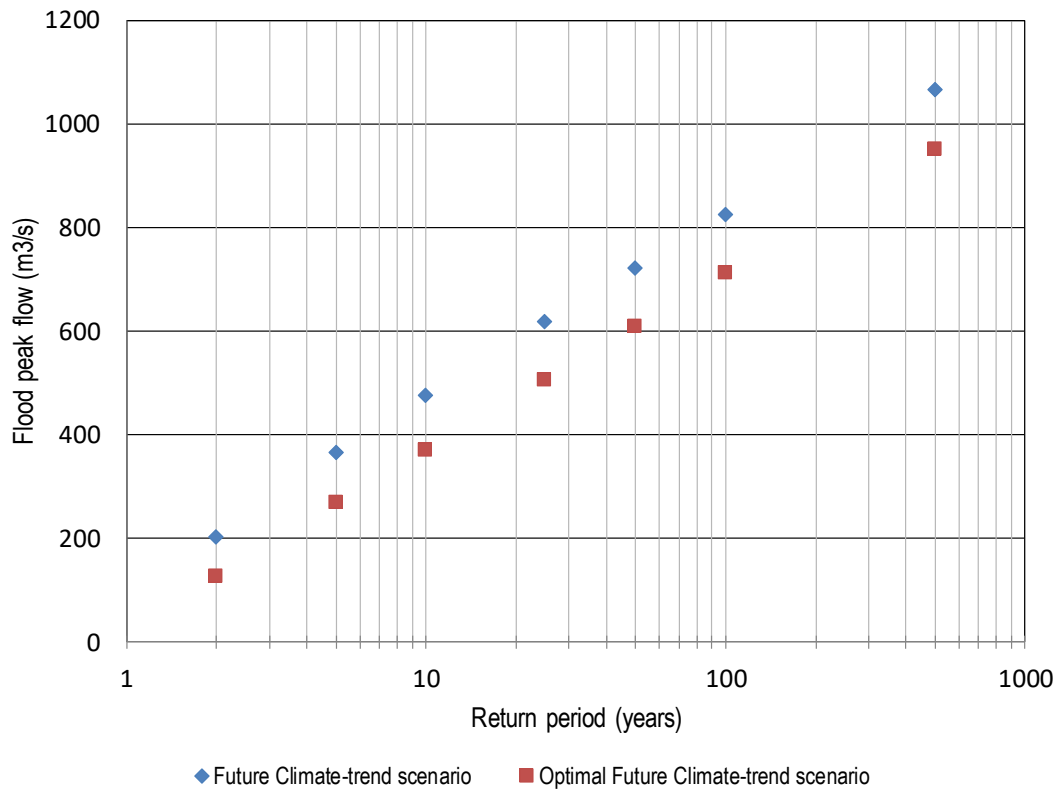


Figure 14-46: Flood peak flow (future climate scenario vs optimal future climate scenario). X-BS4 intersection.

A4.5. Watershed BS5: Hydrological results.

Hydrological modeling results obtained with HEC-HMS software for the intersection between the X road and the BS2 watershed are shown in the following figures. Results are shown for seven return periods (2, 5, 10, 25, 50, 100 and 500 years) and two climatic scenarios (Current climate and Future climate-trend scenario).

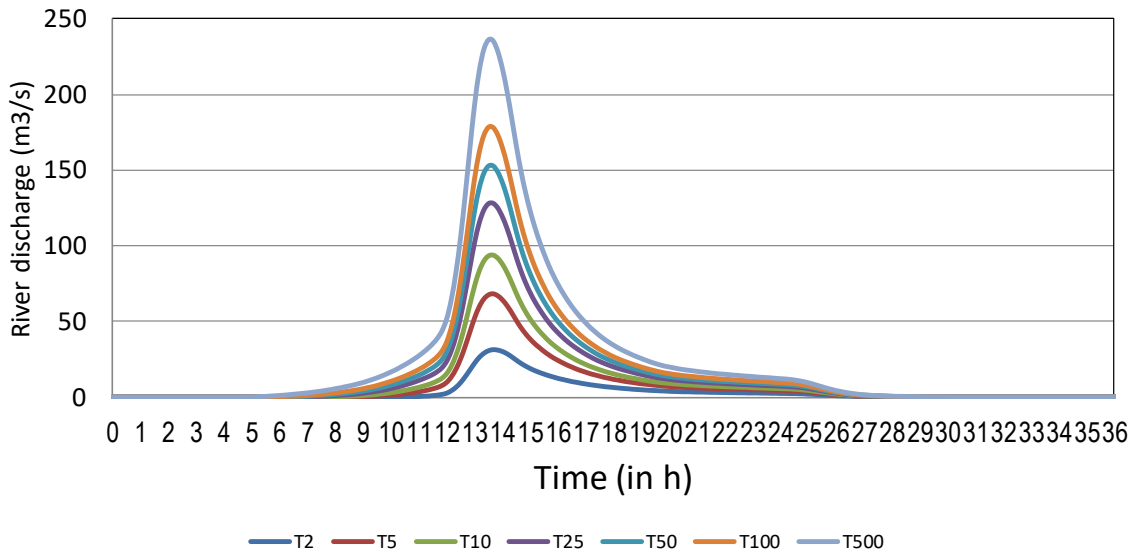


Figure 14-47: Current climate. Flood hydrograph from 24 h Design storm SCS type III. BS5 Watershed.

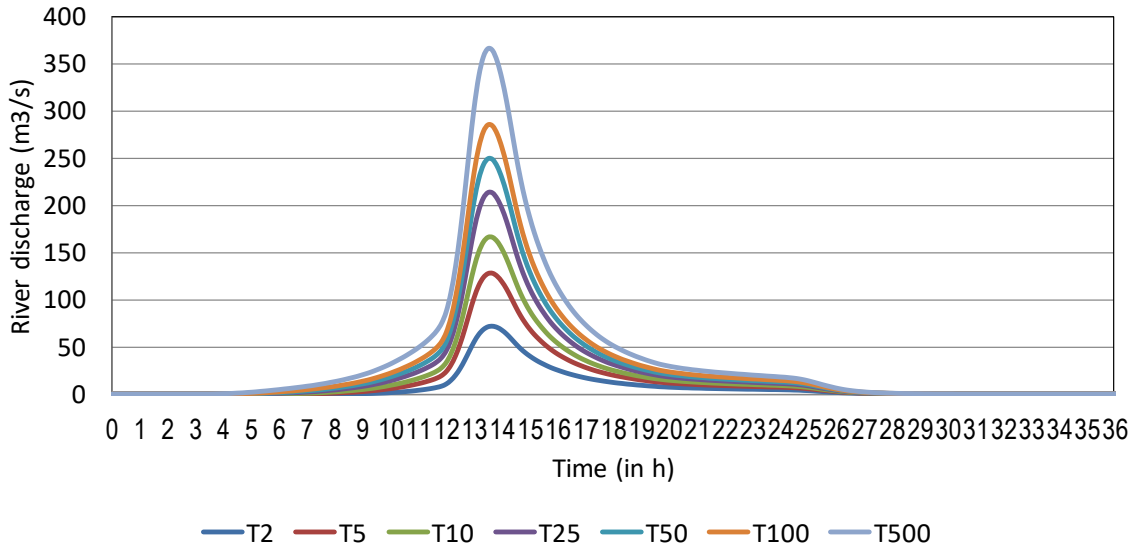


Figure 14-48: Future climate. Flood hydrograph from 24 h Design storm SCS type III). BS5 Watershed.

In addition, to visualize the effect of climate change in river peak flows in the intersection areas, the following figure presents a comparison between the flood peak flow (current scenario vs future climate scenario) for the whole range of return periods analyzed.

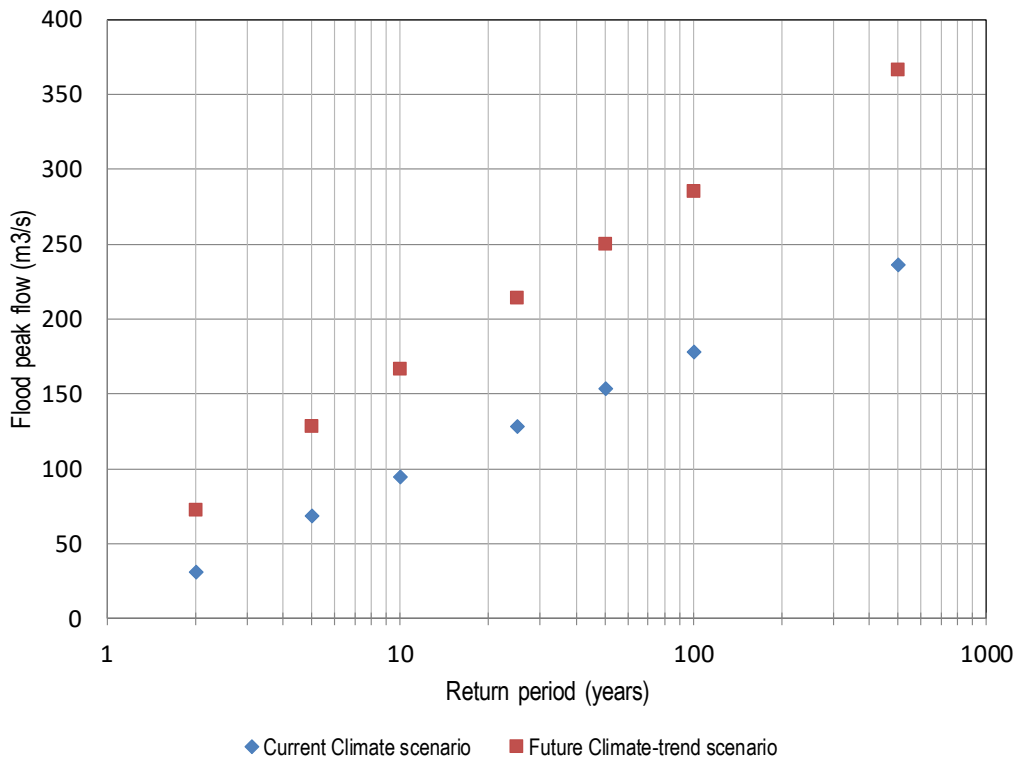


Figure 14-49: Flood peak flow (current scenario vs future climate scenario). X-BS5 intersection.

A4.6. Watershed BS6: Hydrological results.

Hydrological modeling results obtained with HEC-HMS software for the intersection between the X road and the BS2 watershed are shown in the following figures. Results are shown for seven return periods (2, 5, 10, 25, 50, 100 and 500 years) and two climatic scenarios (Current climate and Future climate-trend scenario).

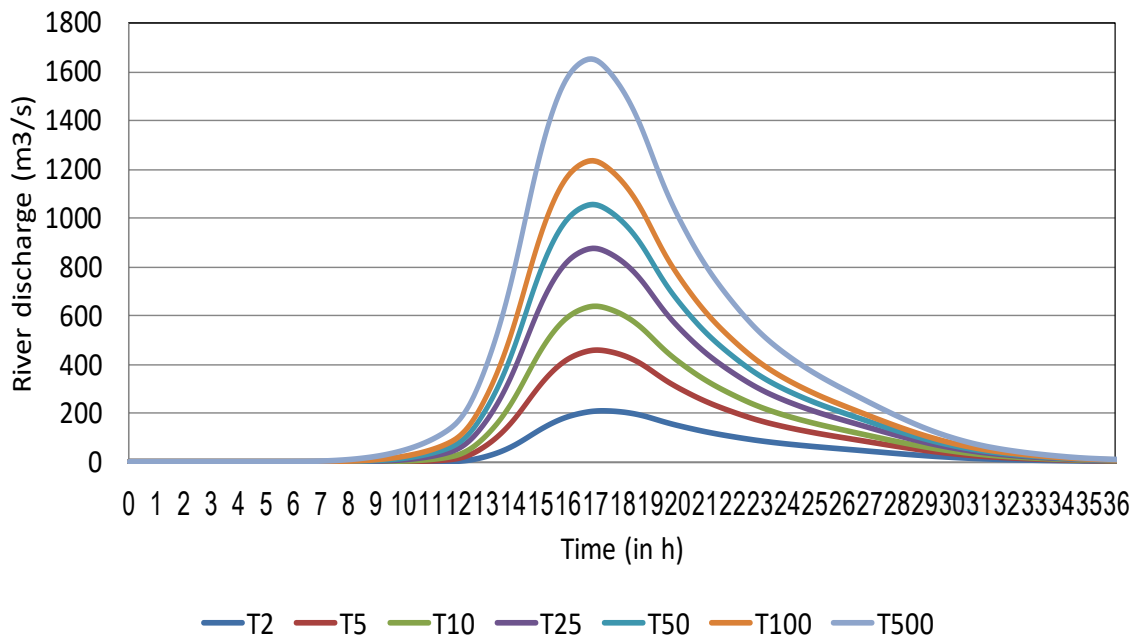


Figure 14-50: Current climate. Flood hydrograph from 24 h Design storm SCS type III. BS6 Watershed.

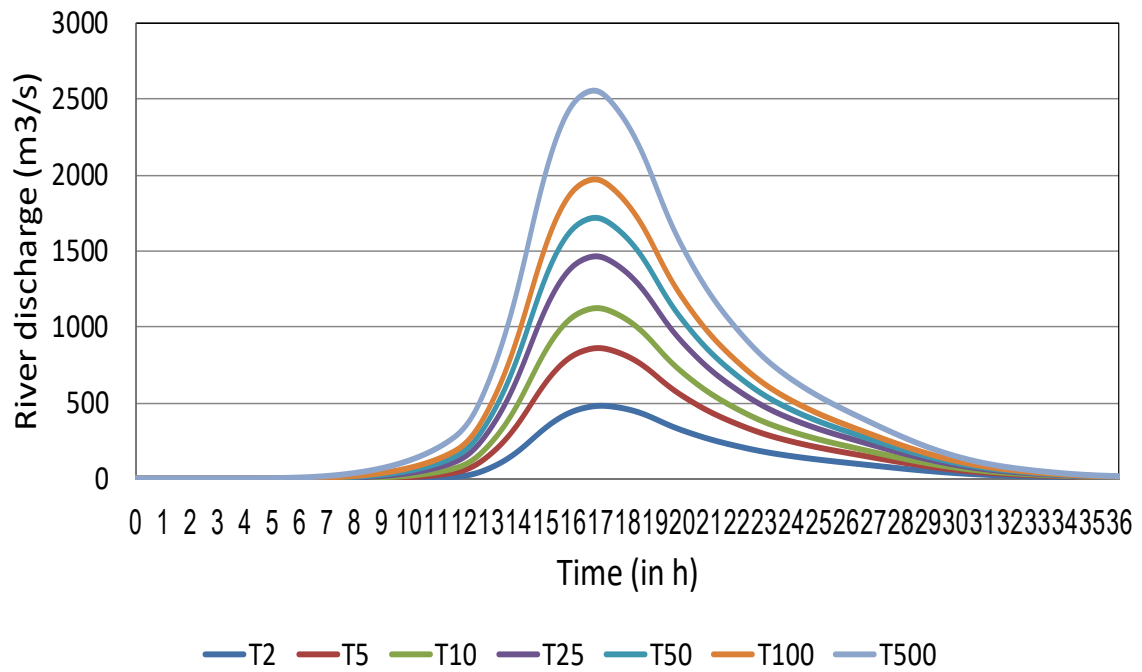


Figure 14-51: Future climate. Flood hydrograph from 24 h Design storm SCS type III). BS6 Watershed.

In addition, to visualize the effect of climate change in river peak flows in the intersection areas, the following figure presents a comparison between the flood peak flow (current scenario vs future climate scenario) for the whole range of return periods analyzed.

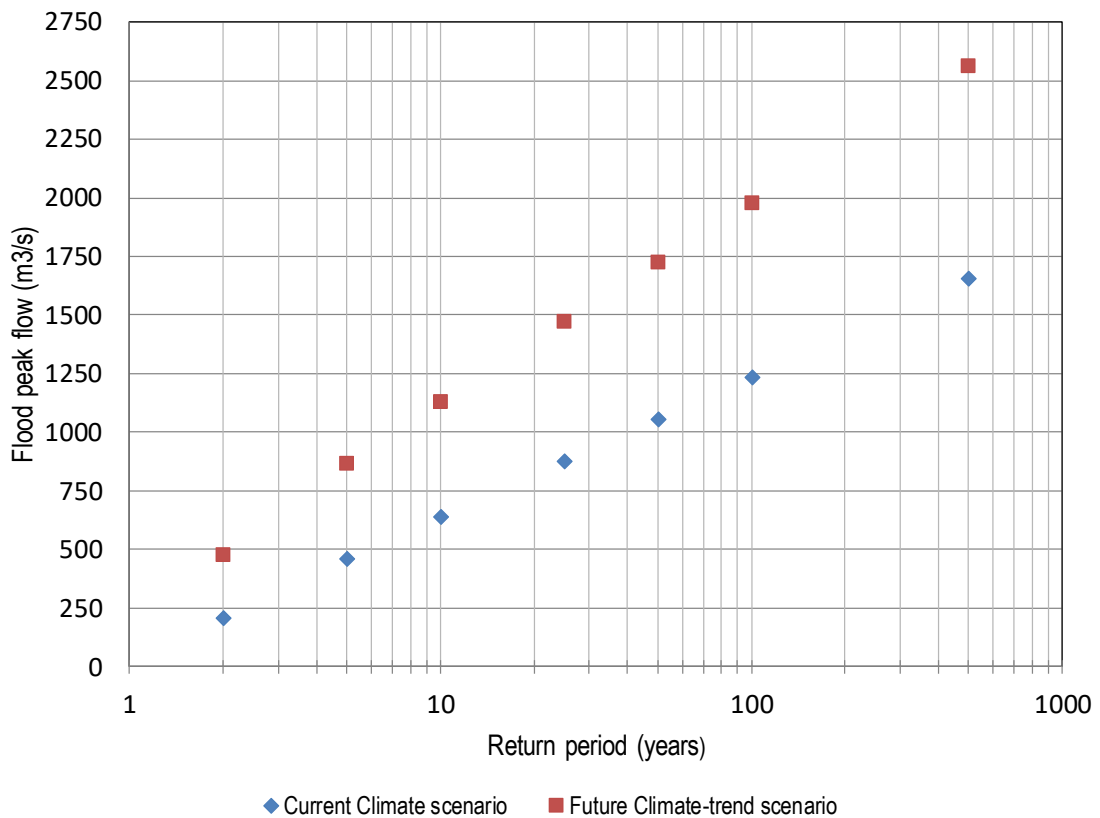


Figure 14-52: Flood peak flow (current scenario vs future climate scenario). X-BS6 intersection.

A4.7. Expressions used for concentration time calculation

- California

$$T_c = 0.87075 * \left(\frac{L^3}{H}\right)^{0.385}$$

- Kirpich

$$T_c = 0.02 * \frac{L^{0.77}}{S^{0.385}}$$

- SCS

$$T_c = \frac{L^{0.8} * \left(\frac{1000}{CN} - 10 + 1\right)^{0.7}}{1140 * (i * 100)^{0.5}}$$

- Temez

$$T_c = 0.3 * \left(\frac{L}{i^{0.25}}\right)^{0.76}$$

- Williams

$$T_c = \frac{L}{1.5 * D} \sqrt[5]{\frac{M^2}{F}}$$

- Rivero

$$T_c = 16 * \frac{L}{(1.05 - 0.2p) * (100 * S)^{0.04}}$$

- Pilgrim

$$T_c = 0.76 * A^{0.38}$$

- Valencia y Zuluaga

$$T_c = 1.7694 * A^{0.325} * L^{-0.096} * S_o^{-0.290}$$

Where T_c is the time of concentration (hours), L is the longest river channel length (km), H is the difference in level between the watershed and the output level (m), S is the average slope (m/m), S_0 is the slope in percentage, A is the area of the basin (km²), NC is the curve number, p is the ratio of the area covered by vegetation and the area of the basin, i is the pending average of the basin.

Appendix 4. Case study considerations for consequences estimation

A9.1. Direct consequences

The expression to calculate the direct reconstruction cost for a specific road section is:

$$R_{\text{cost}} = A_{\text{flood,road}} * LOD_{\text{road}} * D_{\text{max,value}} \quad (14.1)$$

Where R_{cost} is the total direct reconstruction cost in €, A_{road} is the flooded area of the road section considered, LOD_{road} the level of damage of the road section in % and D_{max} the maximum damage value for the road section in €/m².

Maximum Damage Value ($D_{\text{max,value}}$)

The maximum damage value (D_{max}), normally expressed in €/m², is specific for each project location and construction material conditions. In the case of this graduation project, the maximum flood-induced damage-cost for the road (in €/m²) will be obtained by analyzing the information from the damage assessment report prepared by [40].

The report [40] evaluates and quantifies the damage caused by hurricanes H and I in the year 2008 to the road X ROAD (Country Z). The document presents an analysis for 6 road sections and a complete damage evaluation that is presented in Table 14-1 . The unit prices for each of the road materials are also presented in [40], and shown in Table 14-2.

	Damage (%)	Asphalt (m ³)	Sub-layer (m ³)	Foundation (m ³)	Rip Rap (m ³)	Masonry (m ³)
T1 (PK 0+000 - 0+760)	100%	1660	1620	3210	300	0
T2 (PK 0+760 - 2+800)	100%	3100	4670	5570	0	1000
T3 (PK 2+800 - 8+800)	20%	7000	2600	10000	0	0
T4 (PK 8+800 - 12+900)	80%	11960	6870	13000	0	0
T5 (PK 12+900- 17+800)	60%	10870	12720	4700	0	0
T6 (PK 17+800 - 23+000)	30%	9180	1520	0	508	0
Total		50000	30000	36480	808	1000

Table 14-1: Damage quantification for X ROAD road after hurricanes I and H (2008). Source: [40]

	Unit	Unitary price (\$ 2008)
Asphalt	m ³	13
Sub-layer	m ³	16
Foundation	m ³	17
Rip-Rap	m ²	30
Masonry	m ³	80
Culvert	ml	3000

Table 14-2: Unitary prices for road construction materials. Source [40]

Combining the above tables, expected reconstruction cost in case of total damage (100% LOD) for each road section due to flooding can be calculated by means of the following expression:

$$R_{\text{cost,totaldamage}} = R_{\text{cost,event}} * \frac{1}{LOD_{\text{event}}} \quad (14.2)$$

Where, $R_{\text{cost,total,dam}}$ is the total reconstruction cost in case of 100% LOD, $R_{\text{cost,event}}$ is the reconstruction cost registered for a specific event and $\text{LOD}_{\text{event}}$ is the level of damage for the specific flood event.

for each scenario the following considerations are made for the direct economic consequences estimation:

Damage – Depth Curve	Maximum Damage Value
Unpaved road	30 \$/m ²
Paved road	50 \$/m ²

Table 14-3: Considerations for direct economic consequences calculation.

A9.2. Indirect consequences

The basis to derive indirect consequences due to road failure is Eq.(3.16)

$$C_{ind} = C_1 + C_2 = T_{clos} * F_{veh} * C_{time} * T_{work} + T_{rehab} * (CVO_{rehab} - CVO_{norm}) \quad (14.3)$$

Denoting the indirect consequences by C_{ind} , T_{clos} as the total time of road closure; F_{veh} is the average daily vehicle volume (veh/day), C_{time} is the cost of time for an average worker (\$/hour), T_{work} is the average time for a workday (in h); T_{rehab} as the total time of road rehabilitation, CVO_{rehab} as cost of vehicle exploitation during rehabilitation works and CVO_{norm} as cost of vehicle exploitation during normal road use before flood.

Cost of time (C_{time})

As explained in the Intended approach chapter 3 of this report, the estimate of the average cost of time per person/worker (in \$/ h) has been carried out on the basis of two studies: "Value of time in Least Developed Countries" [74] and "Economic Evaluation Manual" [71]

In order to extrapolate the values to the project area, comparing the GDP (Gross Domestic Product) per capita of the countries economies, the ratios are calculated between the countries where the cost of time data are available and the country of study (Country Z). Finally, a cost time value of 0.50 average \$/ hour is considered.

Country	GDP (per cápita)	Ratio	Cost of time	Cost of time (C_{time}) (Country Z)
New Zealand	36000 \$	0.02	23.25 \$/h	0.45 \$/h
Bangladesh	444 \$	1.5	0.40 \$/h	0.60 \$/h
Country Z	681 \$	1	-	0.50 \$/h

Table 14-4: Updated cost of time after GDP comparison between countries with available data. Ratios between Country Z and countries of study (New Zealand and Bangladesh)

Road closure time during flood (T_{clos})

The closure time of the road during a flood event is normally calculated based on past flood-damage assessments. In the case of absence of reliable information, values could be estimated based on the life-cycle duration of hurricanes. In the case of the project area, hurricanes caused road damage in the year 2008 and had a duration of 10 days and a duration of 14 days (National Center of hurricanes, 2008) respectively. Damage after hurricanes in 2008 [40] may be associated with 100-year return period floods [40]. The estimates for the rest of return periods are estimated by extrapolation.

Flood return period	T_{clos} (days)
2	1
5	2
10	3
25	5
50	7
100	14
500	21

Table 14-5: Road closure time vs flood event frequency. Estimates based on hurricanes duration in the study area.

Average daily traffic volume (F_{veh}) and Workday duration (T_{work})

The average daily flow of vehicles (veh/day) is normally obtained from field measurements. In the case of this project, field data is not available and the values proposed by the Ministry of transport and communications of the Government of Country Z have been considered. The report indicates that the country traffic levels are modest: less than 3000 vehicles per day on the national main road and less than 500 vehicles per day in most of the main road network. For the X ROAD, in 2001, the estimated traffic volume is 350 veh/day. Considering a 25% population increase in the country between the year 2001 (8.700.000 inhabitants) and 2018 (10.980.000 inhabitants), the current daily traffic volume is estimate on 500 veh/day.

After the rehabilitation works, the driving conditions of the X ROAD Highway are expected to significantly improve, and therefore the traffic volume on the road is expected to increase. Comparing the traffic volume in the RN1 (main paved roa) with future projections for the X ROAD, a 2000 veh/day traffic volume is estimated.

Scenario	F_{veh} (veh/day)
Current road conditions	500
Rehabilitated road conditions	2000

Table 14-6: Daily traffic volume for X ROAD road as a function of road condition.

The cost time does not vary between scenarios or flood return period and is considered to be constant value of 0.50 \$/ hour. The workday (T_{work}) duration is established in 8 hours.

Road reconstruction time (T_{reconst})

Road reconstruction time depends on the entities responsible for road maintenance management. Based on the available information, for current infrastructure management practices, road reconstruction after flood will begin late. For example, after 2008 floods, rehabilitation works did not start up to the year 2018, which implicates 10 years (520 weeks) with the pavement in a deteriorated condition. In an optimal design scenario, the reconstruction tasks should start immediately after the disaster occurrence, which entails a maximum of 1 year (52 weeks) of reconstruction in case of total damage to infrastructure.

Scenario	Reconstruction time (weeks)
Current management	520
Optimal management	52

Table 14-7: Reparation road time (in weeks) as a function of management practices.

Cost of vehicle operation (CVO) vs road deterioration condition (IRI)

The cost of vehicles exploitation (VEC) depends on the road condition. There are three factors that imply an increase of vehicles operational costs in case of pavement deterioration: lower productivity of vehicles due to a lower speed, the increased consumption of fuel due to movement resistance and higher costs of maintenance due to greater damage of the vehicles components (tires, shock absorbers...).

The road condition is evaluated according to the international roughness index (IRI), proposed by World Bank experts (UMTRI, 1998), and that represents driving comfort by simulating the movement of the accumulated vehicle suspension through a specific road profile length of the x and is expressed in (m/km)

In (MTPTC, 2001), values that allow comparing the costs of exploitation of vehicles (in \$/ km) depending on the category of the vehicle and the road conditions in the case of Country Z are shown:

Operational cost (\$/km)		Paved road			Unpaved road		
		Good condition	Moderate condition	Deteriorated	Good condition	Moderate condition	Deteriorated
Vehicle type	Traffic distribution	IRI=2	IRI=5	IRI=11	IRI=4	IRI=12	IRI=20
Particular vehicle	39%	0.21	0.24	0.33	0.21	0.36	0.52
Tap-Tap/minibus	24%	0.23	0.27	0.37	0.26	0.39	0.58
Bus	3%	0.44	0.47	0.56	0.47	0.62	0.91
Truck 2 axes	14%	0.37	0.42	0.51	0.42	0.55	0.69
Truck 3 axes	15%	0.62	0.70	0.84	0.75	0.97	1.20
Trailer	5%	0.87	0.98	1.17	1.03	1.30	1.62
Average value (\$/km)		0.34	0.38	0.49	0.38	0.54	0.72
Avg value in \$ (25 km road)		8.5	9.5	12.25	9.5	13.5	18

Table 14-8: Cost of vehicles exploitation (\$/ km) depending on the pavement condition and vehicle type for Country Z.

Source: (MTPTC, 2001)

Whereas the road under study is 25 km long, Figure 14-53 shows the average per trip cost (in \$ current 2018) and vehicle on the X ROAD Highway (paved and non-paved) type:

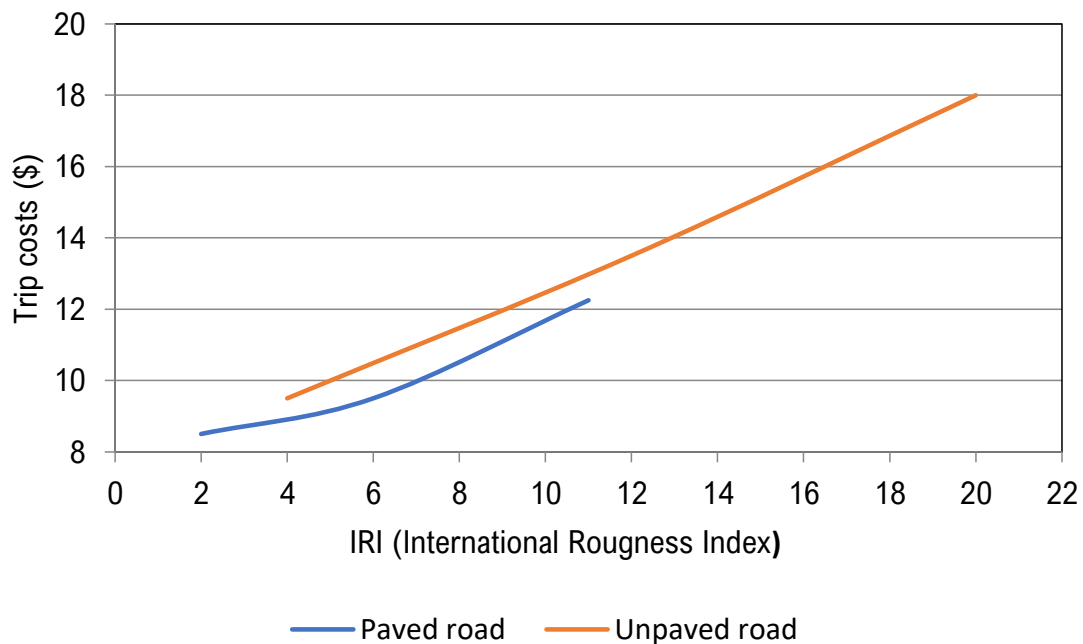


Figure 14-53: Average cost per trip and vehicle on the X ROAD (length 25km) depending on road pavement deterioration.

The next step is to relate the final road surface condition with the flood return period which causes the same damage. The following considerations are made:

- To define the current scenario pavement is considered to be in an intermediate state between moderate and bad condition and unpaved road (IRI=16).
- For future design scenario, were rehabilitation is already performed, the road condition is considered equal to a good condition and paved road (IRI=2).
- The 500 return period years flood causes a variation in pavement condition towards a bad condition. For unpaved road, this is a final condition defined by IRI = 20 and an IRI = 12 for paved road.
- The values for the rest of return periods are estimated by extrapolation.
- For climate change scenarios, it is estimated that the floods will be more severe and therefore that degradation will be slightly higher for the same return period. The difference between the IRI after a flood in the case of current and future scenario is equal to 1 unit.

Table 14-9: IRI values estimated for X ROAD road after flood as a function of flood return period, climate scenario and road type. shows IRI value after flood in the X ROAD road as a function of the return period, climate scenario and road type.

Flood return period	IRI after flood Unpaved road No CC	IRI after flood Unpaved road CC	IRI after flood Paved road No CC	IRI after flood Paved road CC
2	16	16	2	2
5	16.5	17.5	3	4
10	17	18	4	5
25	17.5	18.5	5	6
50	18	19	7	8
100	18.5	19.5	8	9
500	19	20	10	11

Table 14-9: IRI values estimated for X ROAD road after flood as a function of flood return period, climate scenario and road type.

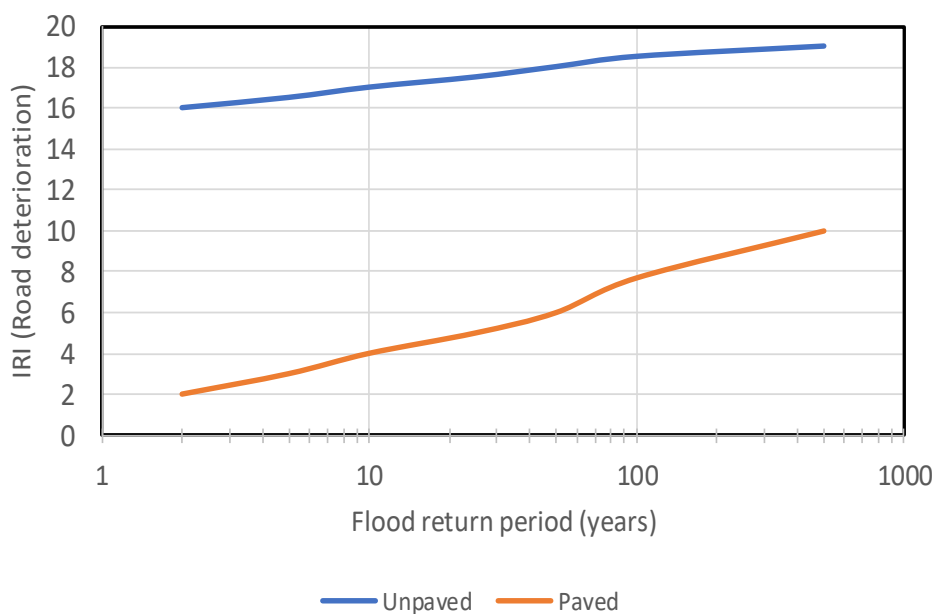


Figure 14-54: IRI values estimated for X ROAD road after flood as a function of flood return period and road type

Appendix 5. Input data for the risk model

A15.1. T Flood Node

The objective of this node is to introduce the range of load events and its probability, that is, to discretize the range of flood probabilities in different intervals to perform risk calculations through the event tree.

In this case, the return periods considered range from 1 to 500 years. This range is discretized by iPresas software in 100 equidistant intervals in a logarithmic scale, to define different branches of the event tree and their corresponding probability.

The process to estimate these probabilities and representative values is shown in Figure 14-55. For the sake of simplicity, this figure is represented using only 11 intervals (100 are considered for X road). A last interval is used to include flood events with return periods higher than 500 years. For each interval, the occurrence probability is estimated and a representative value of the return period is assigned.

Numerical data of complete hydrographs (incoming flows to the river-road intersections as a function of time, and for different return periods) are used to define hydraulic analysis at the road infrastructure system. They are not introduced in this node, but are used to perform hydraulic calculations. Outcomes are later incorporated in the *Flood analysis* node.

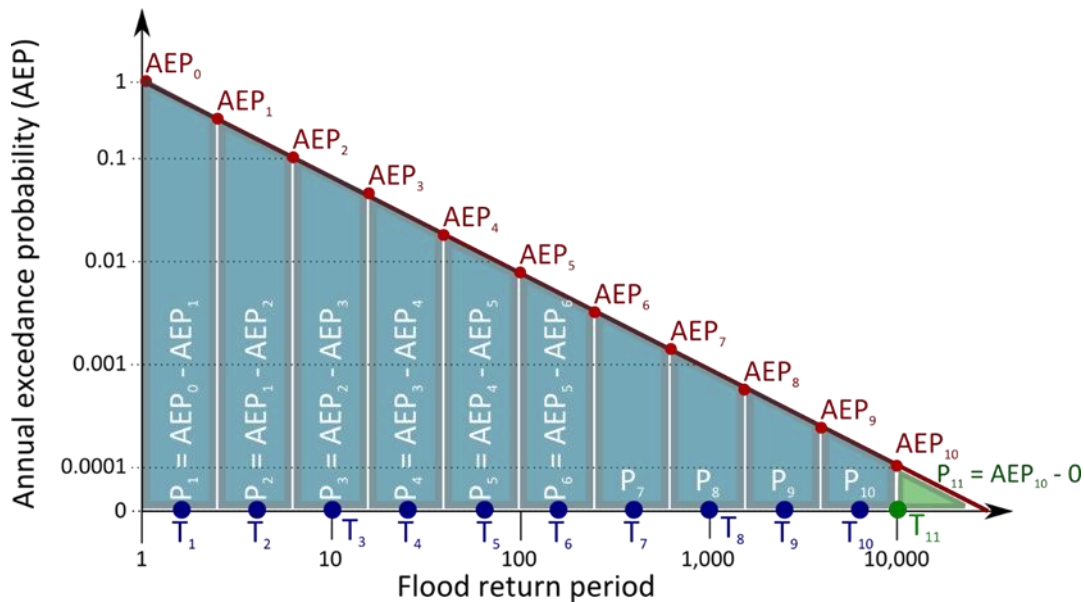


Figure 14-55: Relation between the range of return periods considered in the analysis with the annual exceedance probability.

A15.2. Section Node

The Section node allows the introduction of the critical section that will be analyzed at each step of the risk model.

For every calculation scenarios (current ,trend-based, future design, future trend-based design and optimal future trend-based design) all sections are assigned a probability of occurrence equal to 1, as all sections are present on the road during a flood event and are susceptible to be damaged during the same (See Table 14-10).

The risk model, as shown in Chapter 8.1, treats separately each critical section and finally combines the direct damages for material loss of each analyzed section to study the total risk to the infrastructure.

Section	Probability (All scenarios)
BS1	100 %
BS34	100 %
BS5	100 %
BS6	100 %
Bridge BS6	100 %

Table 14-10: Inputs for the risk model. Section node.

A15.3. Flood analysis Node

This node introduces the relation between the return periods of the storm events for the considered section, (giving rise to floods in the road) and the resulting hydraulic parameters: peak flow, average flow depth on the road and flooded area of the road. Therefore, each precipitation event (associated with a return period) it is also associated to a peak discharge hydrograph which defines the flood event on the analyzed road stretch. This maximum value, together with the average flow depth on the road (in m) and flooded area (in m²) is used in subsequent nodes to relate each event considered to the potential consequences of flooding.

From available rainfall data the design storms for different return periods (from 2 to 500 years) have been obtained. These storms have been introduced in a hydrological HEC-HMS model and flow hydrographs have been obtained for each of 6 basins identified as critical. For example, the following table shows these results for S6 basin and current climate scenario.

The hydrologic results are introduced in a hydraulic model developed with the HEC-RAS model and which has allowed to estimate the flood characteristics for every flood event analyzed (and for every climate scenario).

From the hydraulic model, the relationship between return periods and the flood parameters of the road has been introduced for each of the scenarios. Results entered for each calculation scenario and each watershed are shown in the following table.

Section	Return Period	Peak discharge (m ³ /s)			Average depth over road (m)			Flooded area (m ²)		
		Current, Current design	Climate-trend, Future design	Optimal future design	Current, Current design	Climate-trend, Future design	Optimal future design	Current, Current design	Climate-trend, Future design	Optimal future design
BS1	500	377	474	474	0.41	0.49	0.49	19920	20610	20610
	100	280	360	360	0.17	0.2	0.2	13970	16240	16240
	50	239	311	311	0.16	0.18	0.18	11180	15380	15380
	25	199	263	263	0.1	0.16	0.16	8450	13160	13160
	10	146	200	200	0.1	0.14	0.14	6660	9750	9750
	5	107	151	151	0	0.11	0.11	0	6820	6820
	2	54	84	84	0	0	0	0	0	0
BS3-BS4	500	1162	1819	1598	1.21	1.40	1.35	33549	39230	37781
	100	898	1407	1187	1.08	1.29	1.22	29873	35976	34071
	50	741	1209	1012	1.01	1.23	1.16	27883	34263	32081
	25	614	1049	837	0.93	1.16	1.07	25523	32264	29730
	10	446	807	608	0.79	1.05	0.94	21497	28953	25763
	5	323	616	434	0.64	0.93	0.79	17207	25569	21626
	2	138	337	198	0.28	0.67	0.46	6863	17995	12019
BS5	500	236	367	367	0.83	1.09	1.09	1962	2648	2648
	100	178	285	285	0.3	0.36	0.36	805.1	1085	1085
	50	153	250	250	0.24	0.29	0.29	695.7	867	867
	25	128	214	214	0.16	0.16	0.16	530.6	535	535
	10	94	166	166	0	0.15	0.15	172.5	221	221

Section	Return Period	Peak discharge (m ³ /s)			Average depth over road (m)			Flooded area (m ²)		
		Current, Current design	Climate-trend, Future design	Optimal future design	Current, Current design	Climate-trend, Future design	Optimal future design	Current, Current design	Climate-trend, Future design	Optimal future design
BS6	5	68	128	128	0	0	0	0	118	118
	2	31	72	72	0	0	0	0	0	0
	500	1656	2560	2560	0	0	0	0	0	0
	100	1236	1974	1974	0	0	0	0	0	0
	50	1056	1722	1722	0	0	0	0	0	0
	25	877	1469	1469	0	0	0	0	0	0
	10	640	1129	1129	0	0	0	0	0	0
	5	459	864	864	0	0	0	0	0	0
	2	208	477	477	0	0	0	0	0	0

Table 14-11: Input for flood analysis road.

A15.4. Pavement Failure Node

The Pavement Failure Mode node allows the introduction of the failure probability of the road pavement under river flooding.

As explained during Chapter 3.3.4 of the present report, the probability of road failure due to pavement flooding is given by the frequency (i.e. return period) from which water depths are expected to occur on the road axis. Once there is more than 0.3 cm of water depth on top of the infrastructure, the road stretch under analysis will be considered closed for vehicle traffic [79] and failure probability will be 1.

From the previous Flood analysis node, the flow depth on the road stretch (h_{flood}) is obtained for each return period and scenario.

Finally, shows the conditional failure probability for the road pavement as function of the road water depth, that were introduced in the quantitative risk model:

Water depth on road	Failure probability
0	0 %
>0.3 m	100 %

Table 14-12: Pavement Failure Node

A15.5. Piers Erosion FM Node

This node allows introducing the failure probability of the bridge due to scour at foundation level as a function of the peak flow (flow depth and Froude number) at bridge location during the flood event.

The general procedure and mathematical expressions used for scour evaluation are shown in Chapter 2.3.2 of the present report and are based on the guidelines found in [46], which gathers the current state-of-art regarding this specific topic.

The total scour at bridge foundation has been obtained by the sum of contraction scour at bridge location and localized piers scour.

Table 14-13 displays the values estimated for the variables that are relevant for contraction scour evaluation at bridge location:

- Values for average material size (D_{50}) and associated fall speed are estimated based on an average size for granular material type sand/gravel.
- The width of the constrained section is estimated by considering five piers of 1 m width.

- The longitudinal of the river slope in the section has been estimated using tools GIS and the DEM of 1.5 m resolution for the study area

Variables for the calculation of contraction scour		
Average material size (D_{50})	2	mm
Upstream section width (W_1)	140	m
Constrained section width (W_2)	135	m
River slope (S_1)	0.001	m/m
Fall velocity (T)	0.1	m/s

Table 14-13: Estimated values for the variables used in bridge scour evaluation.

Once the hydraulic modelling results for each calculation scenario are obtained, the next step is to estimate the total scour by contraction for the full range of flood events. Hydraulic parameters obtained by modelling that are relevant for this calculation are: the flood flow peak (m^3/s), the maximum flow depth (in m) in the in the constrained section without scour, the ratio between shear speed and particles fall speed (m/s).

T	Peak flow (m^3/s)	Max. Flow depth at bridge location (m)	Ratio V^*/T	Clearwater scour (m)	Live-bed scour (m)
2	208	2.83	1.67	0.00	0.00
5	459	3.73	1.91	0.00	0.00
10	640	4.2	2.03	0.00	0.00
25	877	4.73	2.15	0.76	0.31
50	1056	5.05	2.23	1.39	0.64
100	1236	5.31	2.28	2.06	0.90
500	1656	5.77	2.38	3.70	1.37

Table 14-14: Calculation of contraction scour. Current climate scenario.

T	Peak flow (m^3/s)	Max. Flow depth at bridge location (m)	Ratio V^*/T	Clearwater scour (m)	Live-bed scour (m)
2	477	3.78	1.93	0.00	0.00
5	864	4.7	2.15	0.72	0.28
10	1,129.00	5.17	2.25	1.65	0.76
25	1,469.00	5.58	2.34	2.97	1.18
50	1,722.00	5.82	2.39	3.98	1.42
100	1,974.00	6.03	2.43	4.98	1.64
500	2,560.00	6.4	2.51	7.36	2.01

Table 14-15: Calculation of contraction scour. Future climate scenario

As stated during the Literature review, for simple bridge substructure configurations and river flows in alluvial channels of sand, the equation recommended for the study of maximum scour at bridge piers foundation is the HEC-18 (Eq. (2-19 in Chapter 2.3.2).

For the case study (bridge BS6), piers are considered of rounded form, plane-bed riverbed condition, a 15° angle of flow attack; a 1 m piers width and a 7 m length ($L = 7$). Therefore: $K_1 = 1$, $K_2 = 2$ and $K_3 = 1.1$.

Based on the hydraulic modelling results, the flow depth (in m) (y_1) and the Froude number (Fr) are obtained for the full range of flood event return periods and calculation scenarios (current and future climate). Applying the HEC-18 equation, the max scour depth at bridge piers (in m) is estimated. The following tables display the results for each climate scenario.

T	Flow peak (m ³ /s)	Flow depth (m)	Flow speed (m/s)	Froude number (-)	Piers erosion HEC18 (m)
2	208	2.83	0.84	0.16	0.92
5	459	3.73	1.36	0.23	1.17
10	640	4.2	1.53	0.24	1.25
25	877	4.73	1.83	0.27	1.37
50	1056	5.05	2.10	0.30	1.47
100	1236	5.31	2.31	0.32	1.54
500	1656	5.77	2.34	0.31	1.57

Table 14-16: Bridge piers localized scour. Current climate scenario. Rounded pier ($a=1$ m / $L=7$ m), angle of flow attack =15°, plane riverbed.

T	Flow peak (m ³ /s)	Flow depth (m)	Flow speed (m/s)	Froude number (-)	Piers erosion HEC18 (m)
2	477	3.78	1.36	0.22	1.17
5	864	4.70	1.83	0.27	1.37
10	1129	5.17	2.15	0.30	1.49
25	1469	5.58	2.30	0.31	1.55
50	1722	5.82	2.37	0.31	1.58
100	1974	6.03	2.40	0.31	1.59
500	2560	6.40	2.48	0.31	1.63

Table 14-17: Bridge piers localized scour. Future climate scenario. Rounded pier ($a=1$ m / $L=7$ m), angle of flow attack =15°, plane riverbed.

Table 14-18 shows the total scour is estimated by the sum of the contraction scour and piers scour at bridge location.

T	Current climate scenario / Total Scour			Future climate scenario / Total Scour		
	Contraction	Localized	Total	Contraction	Localized	Total
2	0.00	0.92	0.92	0.00	1.17	1.17
5	0.00	1.17	1.17	0.28	1.37	1.66
10	0.00	1.25	1.25	0.76	1.49	2.25
25	0.31	1.37	1.69	1.18	1.55	2.73
50	0.64	1.47	2.11	1.42	1.58	3.00
100	0.90	1.54	2.44	1.64	1.59	3.23
500	1.37	1.57	2.94	2.01	1.63	3.64

Table 14-18: Total scour. Current and future climate scenarios. Rounded pier ($a=1$ m / $L=7$ m), angle of flow attack =15°, plane riverbed.

The last step is to evaluate the results regarding the bridge's foundation configuration. For the case of study, a simple spread footing foundation with the following geometric characteristics is considered in the analysis:

Piers foundation geometric dimensions			
hbase,udg	Depth until foundation's top level	0.5	m
hembed	Embed depth	3.0	m
hfn	Foundation depth	2.5	m
Wcim	Foundation width	6	m
Lcim	Foundation length	2	m

Table 14-19: Estimation of foundation's geometric dimension.

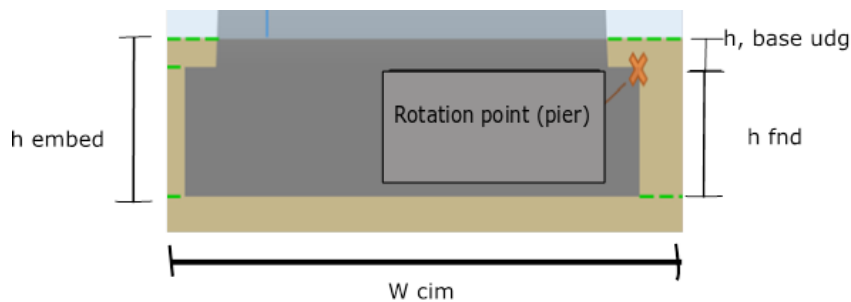


Figure 14-56: Geometric dimensions of a simple spread footing foundation.

The bridge stability evaluation against scour is based on the following principle: **If the total scour is greater than total foundation depth, the probability of failure of the bridge will be high (90-100%). If the scour depth is below the foundation depth, probability of failure will be equal to zero.**

Scour at bridge foundation (3 m of foundation depth)	Failure probability due to bridge destabilization
0	0 %
3	90 %
>3.25	100 %

Table 14-20: Relation between scour and likelihood of bridge failure for destabilization. Foundation depth equal to 3 m (simple spread footing foundation)

Finally, Table 14-21 shows the failure probability due to scour induced destabilization for both climate scenarios and full-range of flood event return periods that were introduced in the quantitative risk model:

T	Current climate scenario		Future climate scenario	
	Total scour	Pf	Total scour	Pf
2	0.92	0 %	1.17	0 %
5	1.17	0 %	1.66	0 %
10	1.25	0 %	2.25	0 %
25	1.69	0 %	2.73	0 %
50	2.11	0 %	3.00	90 %
100	2.44	0 %	3.23	95 %
500	2.94	85 %	3.64	100 %

Table 14-21: Failure probability by bridge destabilization due to scour for both climatic scenarios and seven flood return periods. BS6 bridge

A15.6. Deck connection FM Node

This node allows introducing the failure probability of the deck – pier connection of the BS6 bridge as a function of the peak flow at bridge location during the flood event.

The system (bridge deck connection) response to hydrodynamic forces is evaluated using Ultimate Limit State functions, representing the stabilizing and destabilizing forces, which are shown in Chapter 3.3.4 of the present report.

The hydrodynamic coefficients values (CD, CM, CL), vary with flow conditions, configuration and bridge geometry. There are published several results of laboratory experiments and numerical simulations as well as recommendations for selecting design values suitable for the hydrodynamic coefficients. For more detail see [45] [42].

The results found in the literature have been analyzed to define a range of potential values that can be used in the analysis of stability of the deck-pier connection against hydrodynamic forces. Minimum, medium and maximum estimates for the coefficients are used on the basis of the bridge proximity ratio (constant and equal to 3.5 for the bridge under study) and two hydraulic parameters (Froude number, inundation ratio and proximity ratio), previously calculated by hydraulic modeling for each flood return period.

Froude numbers expected in the bridge location are similar for the all return periods studied, with values close to 0.3. Inundation ratios range from 0.12 to 0.67, and therefore specified values for an inundation ratio equal to 0.5 for all floods, with the exception of the 500 years return period flood and climate-trend scenario, where the reference inundation ratio for hydrodynamic coeff calculation is taken equal to 1.

Table 14-22 and Table 14-23, show the values chosen for the three coefficients range, for each climate scenario and flood return period considered in the analysis.

T	Fr	h_{inund}	CD-	CD+	CL-	CL+	CM-	CM+
2	0.21	0	-	-	-	-	-	-
5	0.3	0	-	-	-	-	-	-
10	0.28	0	-	-	-	-	-	-
25	0.32	0	-	-	-	-	-	-
50	0.36	0	-	-	-	-	-	-
100	0.39	0	-	-	-	-	-	-
500	0.38	0.25	0.6	1.4	-6.0	0.5	-1.1	2.0

Table 14-22: Ranges for hydrodynamic coefficients values. Current climate scenario.

T	Fr	h_{inund}	CD-	CD+	CL-	CL+	CM-	CM+
2	0.28	0	-	-	-	-	-	-
5	0.32	0	-	-	-	-	-	-
10	0.36	0	-	-	-	-	-	-
25	0.37	0.12	0.6	1.4	-6.0	0.5	-1.1	2.0
50	0.38	0.28	0.6	1.4	-6.0	0.5	-1.1	2.0
100	0.37	0.42	0.6	1.4	-6.0	0.5	-1.1	2.0
500	0.39	0.67	1.2	2.3	-7.0	0.0	-1.6	1.5

Table 14-23: Ranges for hydrodynamic coefficients values. Trend-based scenario.

Also, on the submerged deck there are other acting forces such as: the gravitational force (weight and main restoring force), the buoyant force and the friction force of the deck-pier connection.

The expressions to calculate the above acting forces are found in Chapter 3.3.4 and mainly depend on bridge geometry and flow characteristics. For the friction force, the friction coefficient (μ) between the elastomeric

material and steel plate is determined by the manufacturer. The range can vary between 0.20 and 0.33 (Bearings, 2018) (Trelleborg Engineered Products., 2018). In this case, a friction coefficient of $\mu = 0.2$ (less favorable scenario) is assumed.

Once the forces acting on the deck are calculated, the ULS functions (see chapter 3.3.4) that define the bridge stability are evaluated.

The bridge stability evaluation against hydrodynamic forces is based on the following principle: **if any of the three ULS functions is less than 0, which implies that the destabilizing forces are greater than the resistant forces, then the pier-deck connection fails causing bridge deck collapse.**

Based on the values for the hydrodynamic coefficients (Table 14-22 and Table 14-23), values for the hydraulic parameters (Froude number and inundation ratio) obtained after modelling and bridge geometry (Table 14-24) the three functions ULS already presented are evaluated.

Bridge geometry for Deck-Pier connection stability assessment			
L_{deck}	Deck length (for one pier)	25	m
W_{road}	Road width	5	m
W_{deck}	Total deck width	5.5	m
$W_{deck, sides}$	Deck sides width	0.5	m
h_{girder}	Girder height	1.5	m
W_{girder}	Girder width	0.5	m
$N_{girders}$	Girder numbers	3	m
$D_{girders}$	Distance between girders	1.5	m
$D_{gird, deck}$	Distance to deck edge from girders	0.5	m
h_{rail}	Rail height	0.5	m
h_{road}	Road-layer height	0.5	m
s_f	Total deck height (with rail)	2	m
s_m	Total deck height (no rail)	1.5	m
h_b	Depth from riverbed to the deck	5.4	m
Pr	Proximity ratio	3.6	m
μ	Friction coefficient	0.2	-
$P_{concrete}$	Concrete specific weight	2400	kg/m ³
P_{water}	Water specific weight	1100	kg/m ³
g	Gravity	9.81	m/s ²

Table 14-24: Bridge geometry (typical 3-concrete girder deck).

The results are displayed in the form of sensitivity analysis, since the values of the hydrodynamic coefficients vary depending on the consulted study, presenting a range of potential values for each limit function, each return period of flooding and each climate scenario.

Stability deck-pier connection for Current climate conditions

In Figure 14-57 Figure 14-58 and Figure 14-59 show the results of evaluating the deck-pier stability against hydrodynamic forces from flood events associated with various return periods and current climate scenario conditions, for vertical, horizontal and rotation ULS directions respectively.

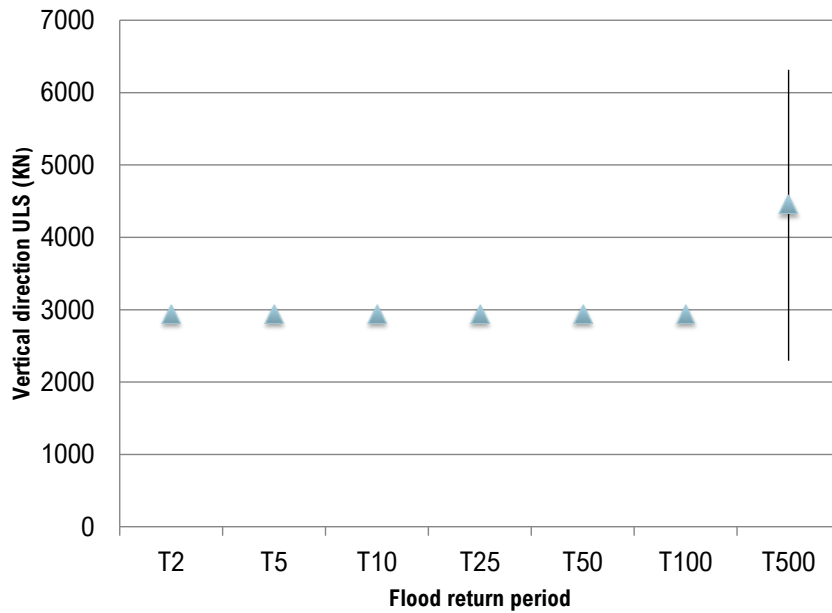


Figure 14-57: Vertical ULS stability (Zvert, d). Seven return periods. Current climate scenario. Sensitivity analysis based on hydrodynamic coefficients.

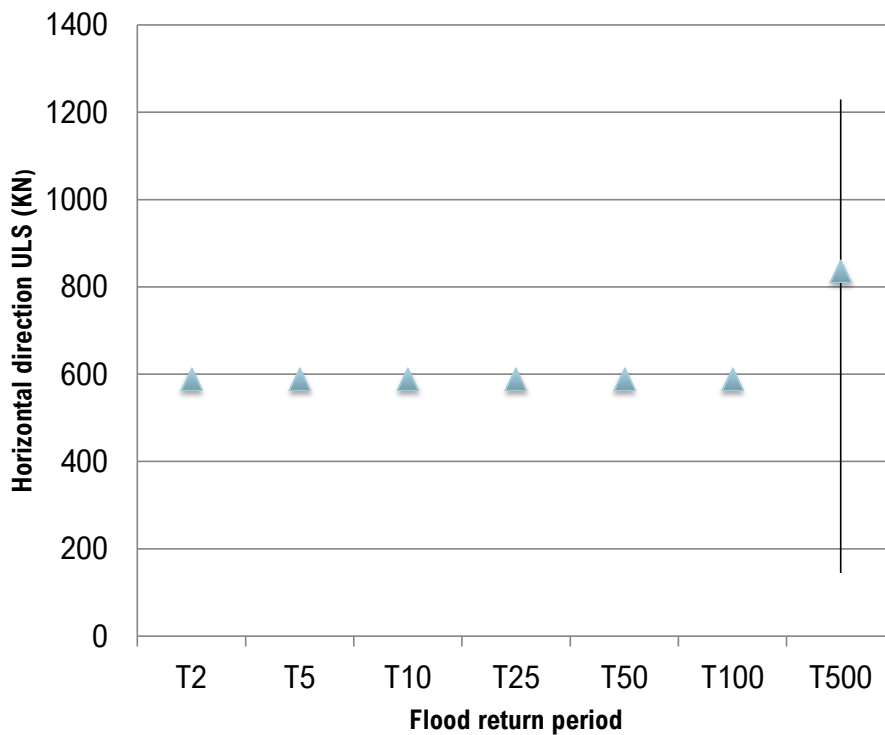


Figure 14-58: Horizontal ULS stability (Zvert, d). Seven return periods. Current climate scenario. Sensitivity analysis based on hydrodynamic coefficients.

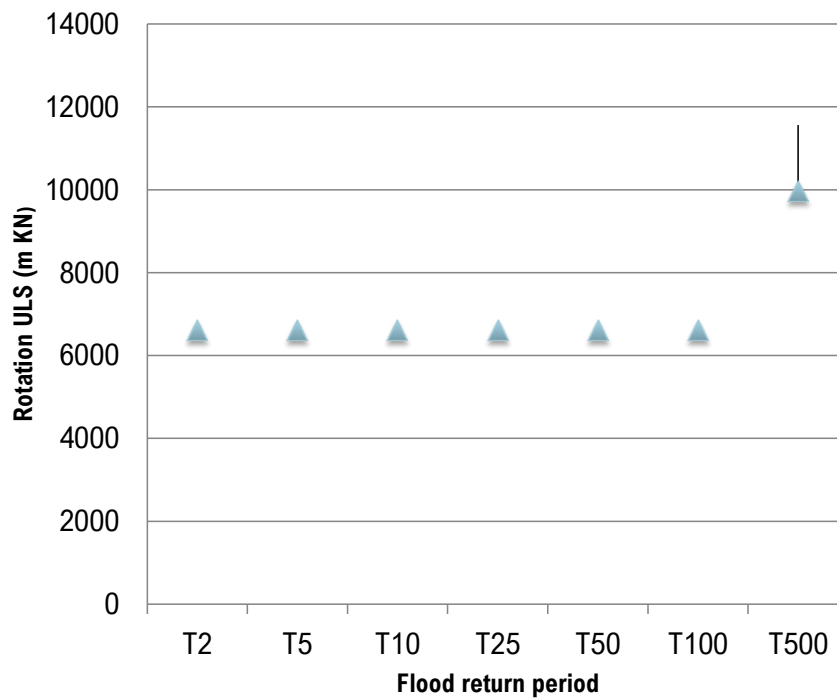


Figure 14-59: Rotation ULS stability (Zvert, d). Seven return periods. Current climate scenario. Sensitivity analysis based on hydrodynamic coefficients.

Stability deck-pier connection for Future climate-trend conditions

In Figure 14-60 Figure 14-61 Figure 14-62 show the results of evaluating the deck-pier stability against hydrodynamic forces from flood events associated with various return periods and current climate scenario conditions, for vertical, horizontal and rotation ULS directions respectively.

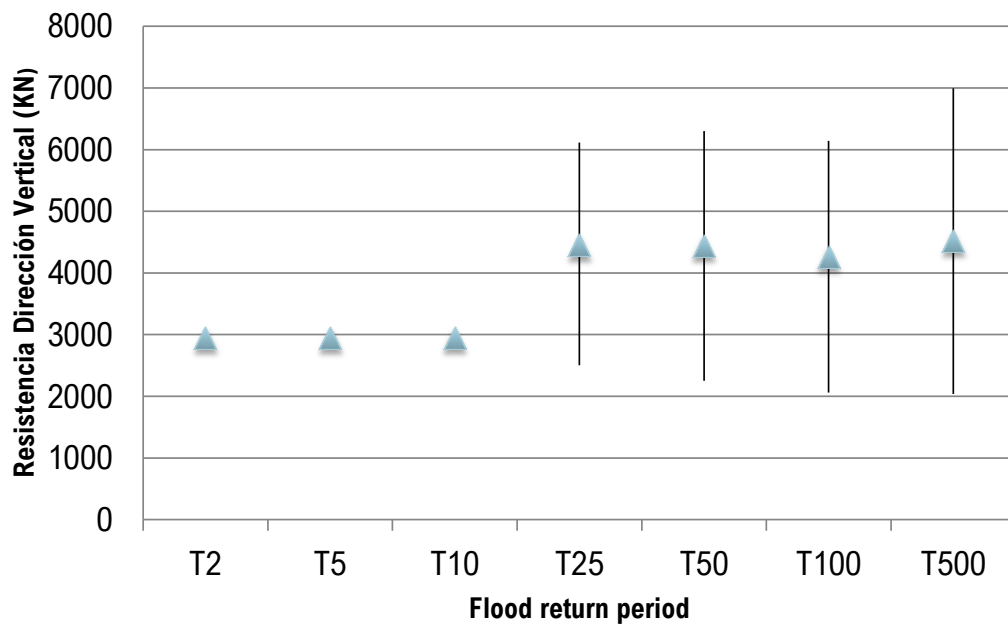


Figure 14-60: Vertical ULS stability (Zvert, d). Seven return periods. Climate trend scenario. Sensitivity analysis based on hydrodynamic coefficients.

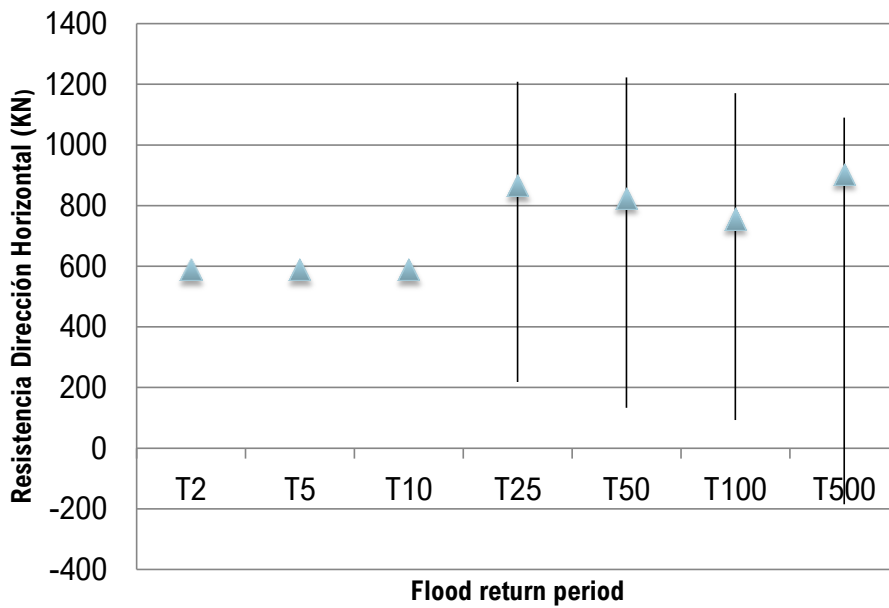


Figure 14-61: Horizontal ULS stability (Zvert, d). Seven return periods. Climate trend scenario. Sensitivity analysis based on hydrodynamic coefficients.

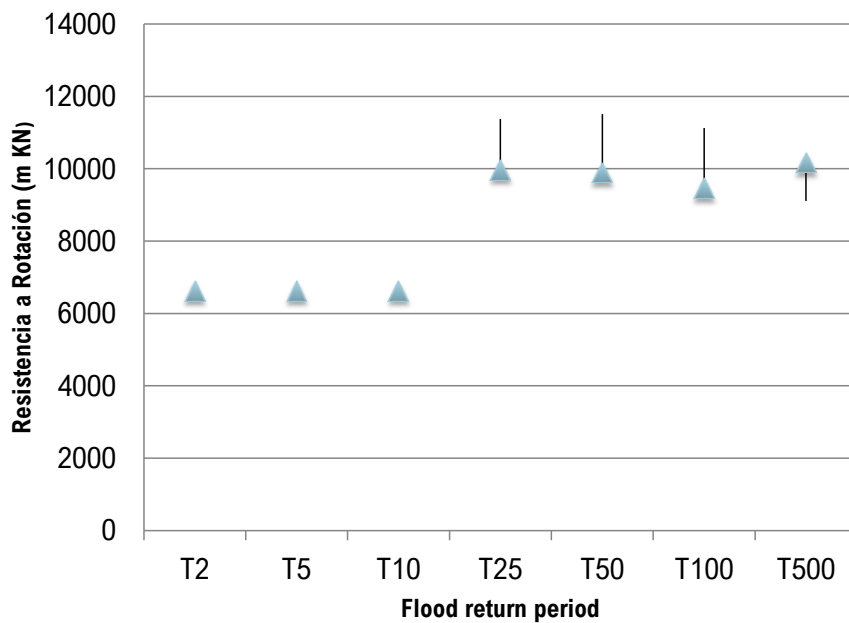


Figure 14-62: Rotation ULS stability (Zvert, d). Seven return periods. Climate trend scenario. Sensitivity analysis based on hydrodynamic coefficients.

The previous results show that the most vulnerable stability direction is the horizontal direction. i.e. the drag force cannot be countered by the friction force of the deck-pier connection.

On the other hand, using most of the values proposed in the literature, the deck-pier connection would not fail in none of the analyzed flood scenarios. However, if the less conservative values are used, deck-pier connection may fail for 500 years of return period flood on climate-trend scenario.

Considering that any value for hydrodynamic coefficients can occur with the same probability within the range established in Table 14-22 and Table 14-23 (what would equal to a Montecarlo simulation where the

hydrodynamic coefficients follow a uniform distribution between the proposed range values), the failure probability of the deck-pier connection is calculated using the ratio of values that fall below zero and values greater than zero in the Horizontal ULS function (Figure 9-10 and) Figure 9-13)

Table 14-25 shows the failure probability of the deck-pier connection for each climate scenario and the flood event return period:

T	Failure probability Current scenario	Failure probability Climate scenario
T2	0%	0%
T5	0%	0%
T10	0%	0%
T25	0%	0%
T50	0%	0%
T100	0%	0%
T500	0%	14%

Table 14-25: Failure probability of the deck-pier connection for both climate scenarios and seven flood return periods. Bridge BS6

A15.7. Direct Damage Node

This node incorporates the results concerning the direct economic damage caused by the flood on the transportation infrastructure. Input data include the potential economic losses for each considered Flood event-, in this case, identified by the average flow depth on the road and flooded area of the examined road section for hydrograph peak.

The methodology used to estimate the flood direct consequences is described in Chapter 3.3.4 and is based on the combination of flood hydraulic characteristics and the estimated values for the pavement reconstruction and the depth-damage curves proposed by [69].

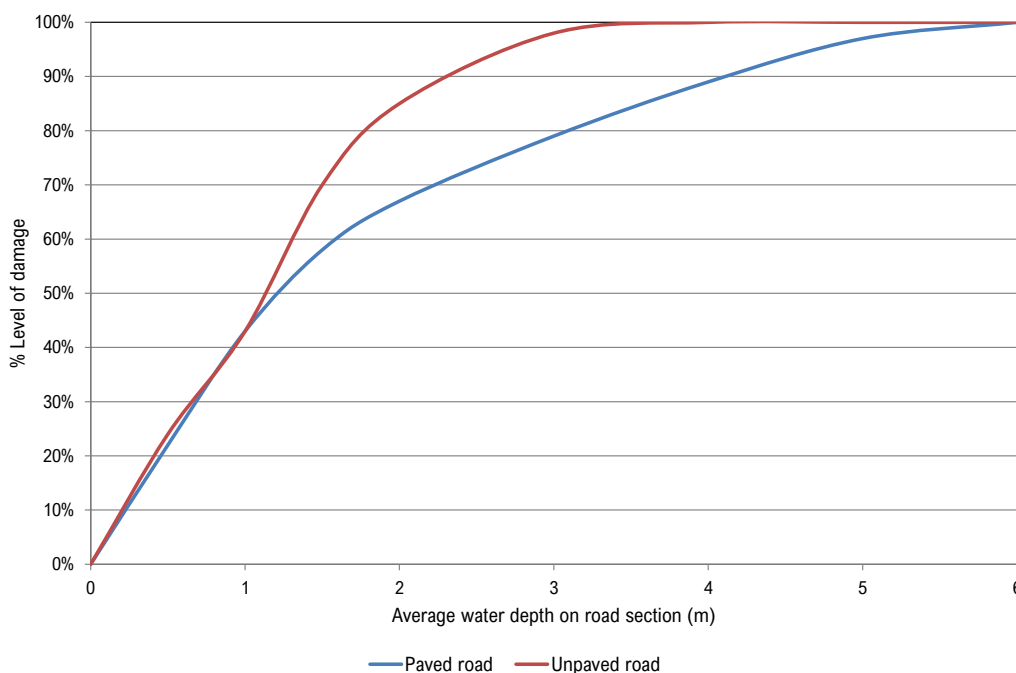


Figure 14-63: Water depth – Damage curves. Paved and unpaved roads. Source: [69]

The maximum damage value (30 \$/ m²) is obtained from 2008 reconstruction costs assessment carried out after the passage of hurricanes I and H, which is based on the current X condition. For design scenarios, future and optimal future, where rehabilitation works are implemented, the maximum damage value is estimated to be slightly higher and is considered equal to 50 \$/ m².

Therefore, for each scenario the following considerations are made for the direct economic consequences estimation.

Scenario	Damage – Depth Curve	Maximum Damage Value
Current	Unpaved road	30 \$/m ²
Future climate-trend	Unpaved road	30 \$/m ²
Current design	Paved road	50 \$/m ²
Future design	Paved road	50 \$/m ²
Optimal Future design	Paved road	50 \$/m ²

Table 14-26: Considerations for direct economic consequences calculation.

From inputs introduced in the Flood Analysis Node presented in Chapter 6.3.3 (average road flow depth and road flooded area) for each analyzed section, from the damage-depth curves and maximum damage value estimate, the direct economic consequences for each section and stage of calculation considered are finally obtained using the following expression:

$$C_{dir} = A_{afecc} * LOD * V_{max}$$

Where C_{dir} is direct damage consequences in (\$), A_{afecc} is the road flooded area (in m²), LOD is the infrastructure's level of damage (in %), V_{max} is the Maximum damage value (in \$/m²).

Table 14-27 shows the results of direct economic consequences entered into the corresponding node of risk model for each of the flood events and analyzed sections.

Section	Return Period	Level of damage (%)					Direct consequences (\$)				
		Current	Current design	Future climate-trend	Future design	Optimal Future design	Current	Current design	Future climate-trend	Future design	Optimal Future design
BS1	2	0%	0%	0%	0%	0%	-	-	-	-	-
	5	0%	0%	4%	5%	5%	-	-	8,163	15,670	15,670
	10	3%	4%	6%	6%	6%	6,698	13,854	17,216	28,819	28,819
	25	3%	4%	7%	7%	7%	8,499	17,578	28,175	44,728	44,728
	50	7%	7%	8%	8%	8%	23,936	37,998	38,649	59,130	59,130
	100	8%	7%	10%	9%	9%	32,513	50,590	46,799	69,720	69,720
	500	22%	18%	26%	22%	22%	130,788	180,774	162,417	224,426	224,426
BS3-BS4	2	16%	12%	55%	30%	20%	29,686	41,904	191,939	267,256	122,731
	5	16%	28%	63%	40%	35%	175,826	244,454	365,240	513,735	375,296
	10	23%	35%	68%	45%	41%	266,442	373,057	457,453	644,641	522,461
	25	30%	40%	71%	48%	45%	364,583	512,810	551,926	777,804	672,220
	50	35%	43%	73%	50%	48%	426,757	601,140	613,244	863,569	773,393
	100	39%	46%	75%	52%	50%	482,865	680,565	667,441	938,872	853,515
	500	63%	50%	84%	55%	54%	592,982	835,264	772,636	1,083,674	1,018,099
BS5	2	0%	0%	0%	0%	0%	-	-	-	-	-
	5	0%	0%	0%	0%	0%	-	-	-	-	-
	10	0%	0%	7%	6%	6%	-	-	431	701	701
	25	7%	7%	7%	7%	7%	1,136	1,803	1,145	1,817	1,817
	50	12%	10%	15%	13%	13%	2,511	3,615	3,904	5,492	5,492

Section	Return Period	Level of damage (%)					Direct consequences (\$)				
		Current	Current design	Future climate-trend	Future design	Optimal Future design	Current	Current design	Future climate-trend	Future design	Optimal Future design
BS6	100	16%	13%	19%	16%	16%	3,767	5,283	6,207	8,610	8,610
	500	43%	36%	54%	46%	46%	25,409	35,632	43,127	60,786	60,786
	2	0%	0%	0%	0%	0%	-	-	-	-	-
	5	0%	0%	0%	0%	0%	-	-	-	-	-
	10	0%	0%	0%	0%	0%	-	-	-	-	-
	25	0%	0%	0%	0%	0%	-	-	-	-	-
	50	0%	0%	0%	0%	0%	-	-	-	-	-
	100	0%	0%	0%	0%	0%	-	-	-	-	-
	500	0%	0%	0%	0%	0%	-	-	-	-	-

Table 14-27: Inputs for the direct consequence node.

A15.8. Indirect Damage Node

The risk model also includes the flood indirect consequences due to the economic disruption caused during the time in which the road is closed to traffic and the time in which the road increases the cost of vehicle exploitation during reconstruction by the pavement deterioration.

Based on the methodology and values shown in Chapter 3.3.4 (closure time during a hurricane, cost of time, average daily traffic volume and estimated travel time) the indirect economic cost during road closure time for each return period and calculation scenario is calculated using the following expression:

$$C_{closure} = C_1 = T_{closure} * F_{veh} * C_{time} * T_{workday}$$

Flood return period	Current scenario	Future climate-trend	Current design	Future design	Optimal design
2	2000	2000	8000	8000	8000
5	4000	4000	16000	16000	16000
10	6000	6000	24000	24000	24000
25	10000	10000	40000	40000	40000
50	14000	14000	56000	56000	56000
100	28000	28000	112000	112000	112000
500	42000	42000	168000	168000	168000

Table 14-28: Indirect economic damage (in \$) during the road closure. Calculation scenarios and flood return periods.

In addition, the indirect economic cost during road rehabilitation time due to cost of vehicle exploitation (VEC) variations induced by road deterioration after a flood event is calculated. Estimates are based on methodology and values shown in Chapter 3.3.4, and are calculated based on the following expression:

$$C_{ind, rehab} = C_2 = T_{rehab} * F_{veh} * (VEC_{rep} - VEC_{base})$$

Table 14-29 shows the weekly indirect economic costs by variation of the cost vehicles exploitation variations during the road rehabilitation. Table 14-30 shows total indirect economic costs by variation of the cost vehicles exploitation variations during the road rehabilitation considering the reconstruction times shown in Chapter 3.3.5.

Flood return period	Current scenario	Future climate-trend	Current design	Future design	Optimal design
2	-	-	-	-	-
5	984	2,953	5,845	11,690	11,690
10	1,969	3,938	11,690	17,535	17,535
25	2,953	4,922	17,535	23,380	23,380
50	3,938	5,906	29,225	35,070	35,070
100	4,922	6,891	35,070	40,915	40,915
500	5,906	7,875	46,760	52,605	52,605

Table 14-29: Weekly indirect economic damage (in \$) during the road rehabilitation. Calculation scenarios and flood return periods.

Flood return period	Current scenario	Future climate-trend	Current design	Future design	Optimal design
2	-	-	-	-	-
5	511,875	1,535,625	3,039,400	6,078,800	607,880
10	1,023,750	2,047,500	6,078,800	9,118,200	911,820
25	1,535,625	2,559,375	9,118,200	12,157,600	1,215,760
50	2,047,500	3,071,250	15,197,000	18,236,400	1,823,640
100	2,559,375	3,583,125	18,236,400	21,275,800	2,127,580
500	3,071,250	4,095,000	24,315,200	27,354,600	2,735,460

Table 14-30: Total indirect economic damage (in \$) during the road rehabilitation. Calculation scenarios and flood return periods.

The comparison of the values found in Table 14-29 (indirect costs during road closure) and Table 14-30 (indirect costs due to increase in the VEC during rehabilitation), shows that the latter are far superior to the first, which increases the importance of road rehabilitation management roll for the reduction of the economic consequences after a flood event.

Appendix 6. Risk results: FD Curves for each scenario

A16.1. Current scenario

To calculate the risk in the current road situation, the results obtained through hydraulic modeling described in Appendix 5 are used. In addition, the flood economic consequences, both direct and indirect, were estimated.

In the present work, the flood data and likelihood of occurrence is combined with the consequences data obtaining results of annual economic risk (with units of \$ per year). The data used for each of the risk model nodes in the current scenario as well as the procedures used to obtain them are shown in the previous chapters of this document.

The results obtained by combining in the risk model the floods and their probability with the flood consequences for the current scenario are shown in Table 14-31. These results show that the flood economic risk on the road is significant. The latter is consistent with the relatively frequent floods that have occurred in this area. Within these economic consequences the direct damage to the transport infrastructure is included, but also the indirect consequences of the flooding by traffic disruption and incremental increase of circulation costs through a deteriorated road.

Current scenario	
Direct economic flood risk (\$/year)	187,757
Indirect economic flood risk (\$/year)	640,905
Total economic flood risk (\$/year)	828,662

Table 14-31: Annual risk results for current scenario.

Figure 14-64 represents the FD curve for current risk scenario:

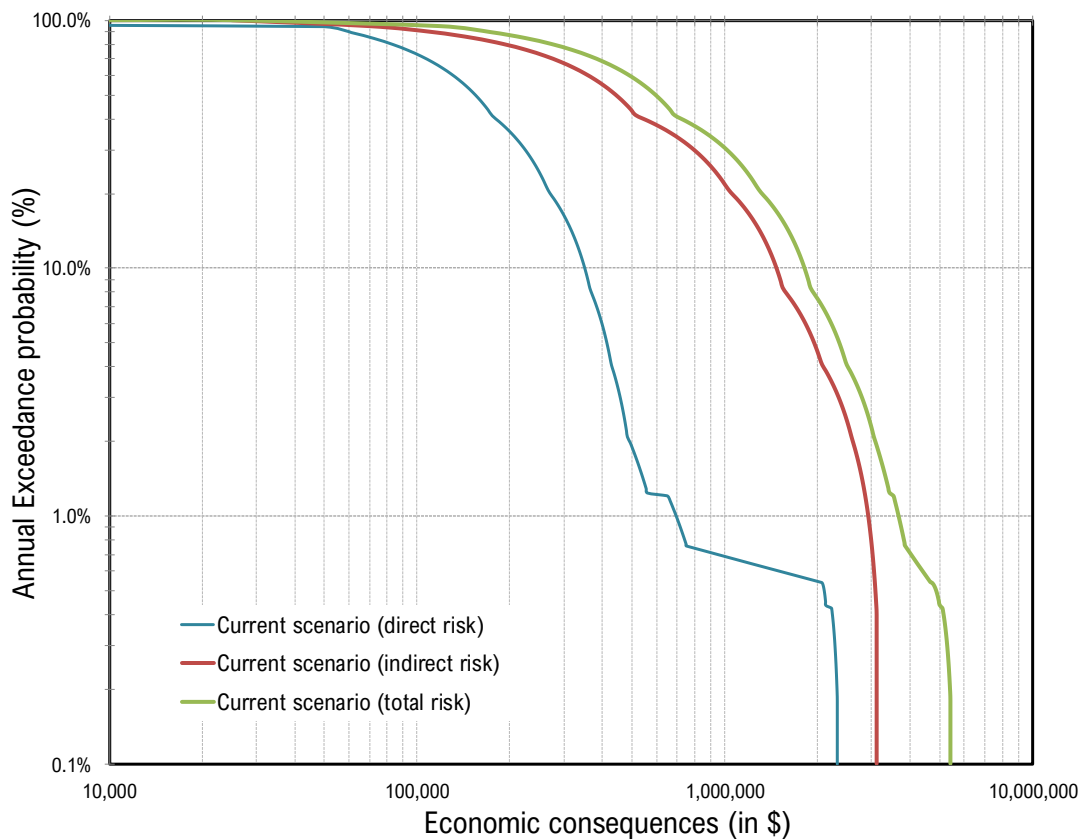


Figure 14-64: FD curve for current scenario.

Most of the economic risk is concentrated in the indirect economic consequences (due to costs associated with the road closure during the flood and, above all, by the incremental vehicle circulation costs on a deteriorated road). This is due to the current time until the reconstruction tasks are carried out (10 years), which multiplies the indirect economic losses associated with the circulation costs (higher fuel consumption, Mechanical components, cost of travel time...). For the current scenario, the average indirect economic risk equals approximately 650k \$/year.

However, direct economic risks (direct destruction and reconstruction costs) should not be ignored. In the current scenario, the average direct economic risk (by pavement flooding and risk collapse) is almost 200k \$/year, being able to exceed 350k \$/year (probability of 10%) and 600 000 \$/year (probability of 1%).

A16.2.Future Climate-trend scenario

This scenario analyses the risk variation by the end of the Century (Horizon 2050-2100) if the current route is maintained, the projected rehabilitation works are not carried out and the analyzed climate change trends are included in the model. To include this type of scenarios is important to assess road risk not only in the current situation, but also to evaluate how risk will change in the future. To carry out these calculations, the following scenarios have been considered:

- Effect of climate change on the rainfall intensity for the 2050-2100 horizon, following the recommendations and methodology summarized in the chapter 7 of this report, and which provides higher value flood peaks for the river-road intersection zones.
- Variation in the land use coverage in the upstream basins assuming that the current deforestation process continues to develop.

The risk model architecture defined in the Figure 9-3: (section 9.1) and the results of hydraulic modeling and the flood consequences calculation, which are summarized in the present report in the Appendix 7, were used in the calculations.

The risk results obtained for the future trend scenario are shown in Table 14-32.

	Current scenario	Future Climate scenario
Direct economic flood risk (\$/year)	187,757	297,075
Indirect economic flood risk (\$/year)	640,905	1,354,166
Total economic flood risk (\$/year)	828,662	1,651,242

Table 14-32: Annual risk results for future climate scenario.

Climate change will significantly increase the economic risk on the X road (multiplying by 2 the current risk scenario), both on direct and indirect damages, as the flood consequences will increase for the full flood range, from more likely floods (lower return period) to less likely floods higher return period)

Figure 14-65 represents the FD curve for future climate-trend risk scenario:

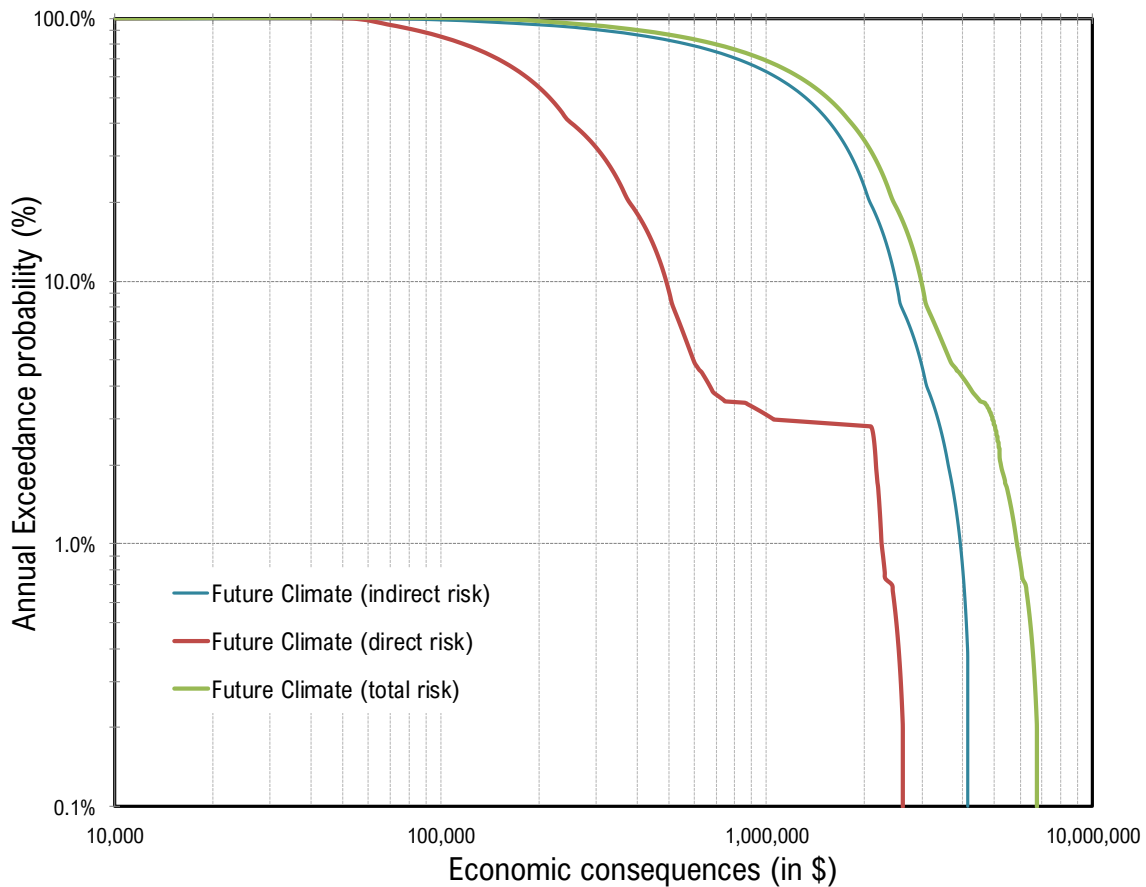


Figure 14-65: FD curve for future climate trend scenario.

As is the case for the current scenario, most of the economic risk is caused by the indirect economic consequences, due to the identical reasons to those discussed above for the current scenario. For the future climate trend scenario, the average indirect economic risk equals approximately 1.3m \$/year.

The average direct economic risk (pavement flooding and bridge collapse) is almost 300k \$/year, being capable to exceed the 400k \$/year (probability of 10%) and the 2M \$/year (probability of 1%).

A16.3. Current climate design scenario

After flood risk analysis for the current road situation (See chapter 9.1), flood risk variation due to projected rehabilitation works for the X road is evaluated. The risk model architecture defined in the Figure 9-3: (section 9.1) and the results of hydraulic modeling and the flood consequences calculation, which are summarized in the present report in the Appendix 7, were used in the calculations.

To carry out the risk calculations, the following scenarios have been considered:

- Structural effect of the pavement rehabilitation by means of: the incorporation of a new damage-depth curve that reflects the greater pavement resistance to the flood with respect to the current unpaved situation; Increase of the maximum structural damage value of a paved road with respect to the current unpaved situation; Variation of the initial road IRI (before flood) and final values after flood for the full range of flood return periods.
- Increase of traffic volume on the road due to the rehabilitation works on the X.

The risk results obtained for the current design scenario are shown in the Table 14-33.

	Current scenario	Current design scenario
Direct economic flood risk (\$/year)	187,757	360,582
Indirect economic flood risk (\$/year)	640,905	4,013,640
Total economic flood risk (\$/year)	828,662	4,374,445

Table 14-33: Annual risk results for current climate design scenario.

Figure 14-66 represents the FD curve for current climate design risk scenario:

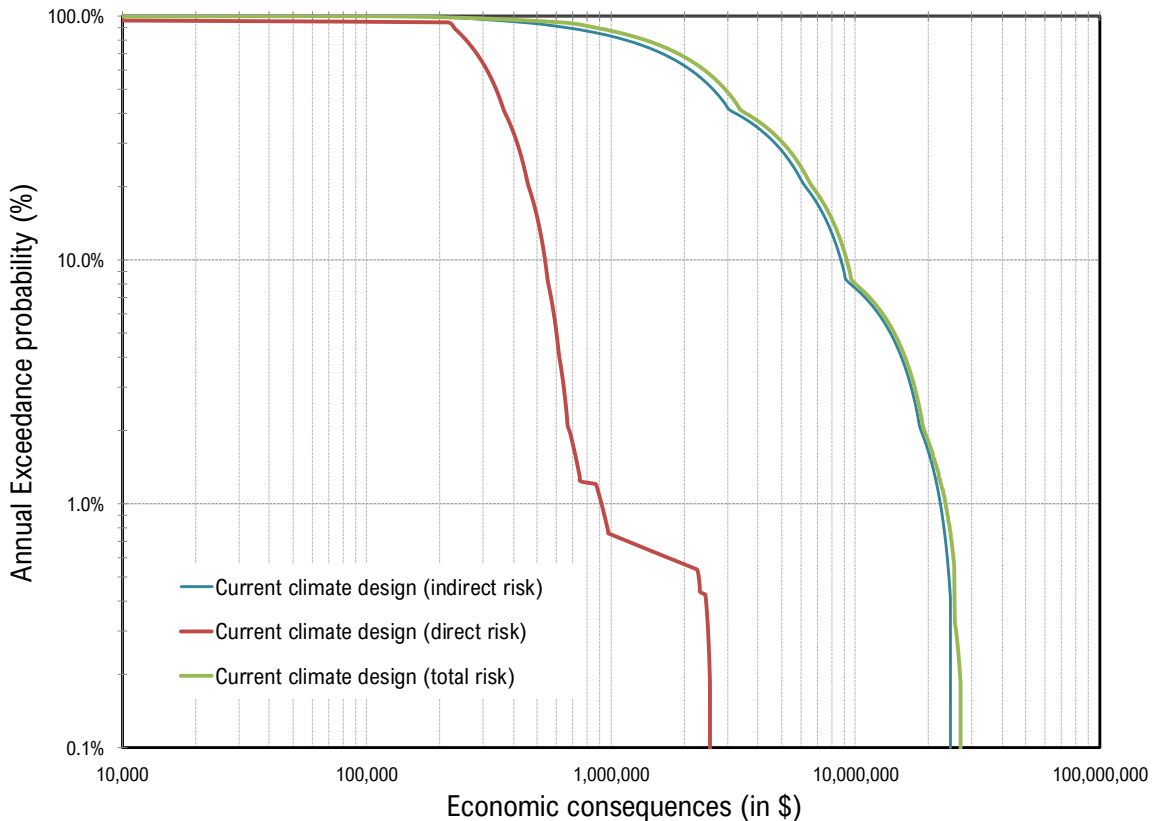


Figure 14-66: FD curve for current climate design scenario.

Rehabilitation works will significantly increase the economic risk on the X road as the flooding consequences for the full range of flood events will increased. This can be considered as a “price” to pay for the benefits derived of improving a road and that are not included in the flood risk analysis (i.e. economic development of connected population centers).

In design scenario, the structural value is greater due to the better quality of the construction materials (maximum damage value is \$50/m² for the design scenario and \$30/m² for the current scenario). Thus, the average direct economic risk will increase up to twice its value from the current scenario. On the other hand, the expected deterioration in the road after a flood is more significant in case of a paved road than on a road that is in bad condition, therefore, the incremental costs due to vehicle circulation when driving a road during repair tasks will be more significant in the design scenario than in the current base case. This is reflected in the results, as the average indirect economic risk will increase more than five times its value compared to the current scenario both on indirect and total damage.

As in current and future climate scenarios, most economic risk is due to indirect economic consequences. In the case of the design scenario this is even more significant, which is explained by the greater importance of

paved road deterioration with regard to the incremental costs of vehicles circulation costs until repair tasks are completed. For the current design scenario, the average indirect economic risk equals approximately 4m \$/year.

The average direct economic risk (by pavement flooding and bridge collapse) is almost 400k \$/year, being capable to exceed the 500k \$/year (with a probability of 10%) and 1M \$/year (with a probability of 1%).

A16.4.Future Climate-trend design

Once the flood risk has been analyzed in the current design scenario, this scenario analyses the risk variation by the end of the Century (Horizon 2050-2100) if the current route is maintained, the projected rehabilitation works are carried out and the Climate change trends estimated in this report are included. The calculation of future scenarios is necessary to assess the effect on flood risk of the projected works and the climatic change in these rehabilitation works.

To carry out these calculations, the following scenarios have been considered:

- Structural effect of the pavement rehabilitation by means of: the incorporation of a new damage-depth curve that reflects the greater pavement resistance to the flood with respect to the current unpaved situation; Increase of the maximum structural damage value of a paved road with respect to the current unpaved situation; Variation of the initial road IRI (before flood) and final values after flood for the full range of flood return periods.
- Increase of traffic volume on the road due to the rehabilitation works on the X.
- Effect of climate change on the rainfall intensity for the 2050-2100 horizon, following the recommendations and methodology summarized in the chapter 7 of this report, and which provides higher value flood peaks for the river-road intersection zones.
- Variation in the land use coverage in the upstream basins assuming that the current deforestation process continues to develop.

To analyze the risk results obtained in the future climate trend design scenario, they will be compared with the risk values previously obtained for climate-trend base scenario and current climate design scenario. In this way, the effect of climate change in the new projected design (future design scenario vs current design scenario); and the effect on flood risk of rehabilitation works for the future climate scenario (future climate scenario vs. future climate design scenario), are analyzed separately. These evaluations allow to study which of the two factors is more determinant regarding the risk variation in the road infrastructure.

The risk results obtained for the trendy design scenario are shown in Table 14-34.

	Current climate scenario	Future Climate scenario	Current climate design scenario	Future Climate design scenario
Direct economic flood risk (\$/year)	187,757	297,075	360,582	553,191
Indirect economic flood risk (\$/year)	640,905	1,354,166	4,013,640	6,119,282
Total economic flood risk (\$/year)	828,662	1,651,242	4,374,445	6,672,473

Table 14-34: Annual risk results for future climate design scenario.

Figure 14-67 represents the FD curve for Future Climate Design risk scenario:

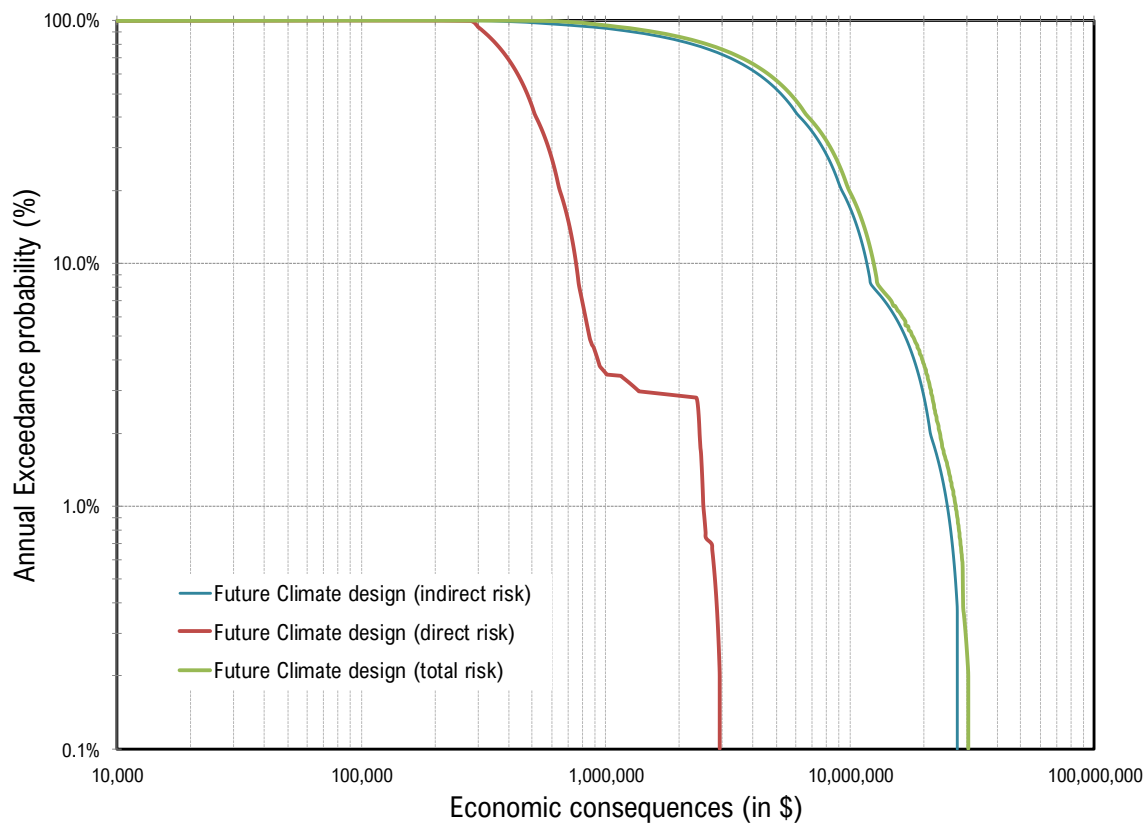


Figure 14-67: FD curve for future climate design scenario.

Projected rehabilitation works increase the flood risk in infrastructure in a future climate scenario (as with the current climate scenario). In design scenario, the structural value is higher due to the better quality of the construction materials. Thus, the average direct economic risk will increase up to 2 times its value (from 300k \$/year to 600k \$ year) compared to the future climate base scenario. On the other hand, the expected deterioration after a flood is more significant in case of a paved road (design) than in a road that is in bad condition (base), therefore, the incremental costs due to the vehicle exploitation when circulating on the road during repair tasks will be more perceptible in the design scenario than in the base case. This is reflected in the results, as the average indirect economic risk will increase 5 times its value (from 1.3m \$/year to 6m \$/year) compared to the future climate base scenario for both indirect and total damages.

Climate change will also significantly increase the direct economic risk in the new design of the X road (up to 2 times), for the full range of floods events, (for the same return period, the expected peak flows at the river-road intersection are greater and with them, road damages increase in the future climate design scenario). However, the increase in indirect economic risk, although significant (from 4m \$/year to 6m of \$ per year) is not as important as that caused by the isolated effect of the rehabilitation works. Although the CC effect in the future floods events will increase pavement deterioration, the fact of moving from an unpaved road to a paved road implies a flood-induced indirect damage during the closure and repair tasks) that it is even more significant than that caused only by the effect of the CC in the study area.

A16.5. Optimal Future Climate-trend design

Once the flood risk has been analyzed for the future climate design scenario, this scenario analyses the risk variation by the end of the Century (Horizon 2050-2100) if the current route is maintained, the projected rehabilitation works are carried out and, in addition, a better management of the reconstruction works and watersheds is implemented. The calculation of future scenarios is necessary to assess the effect on flood risk and climatic change in the projected works.

To carry out these calculations, the following scenarios have been considered:

- Structural effect of the pavement rehabilitation by means of: the incorporation of a new depth-damage curve that reflects the greater pavement resistance to the flood with respect to the current unpaved situation; Increase of the maximum structural damage value of a paved road with respect to the current unpaved situation; Variation of the initial road IRI (before flood) and final values after flood for the full range of flood return periods.
- Increase of traffic volume on the road due to the rehabilitation works on the X.
- Effect of climate change on the rainfall intensity for the 2050-2100 horizon, following the recommendations and methodology summarized in the chapter 7 of this report, and which provides higher value flood peaks for the river-road intersection zones.
- Variation in the land use coverage in the upstream basins assuming that a reforestation plan in the most problematic watersheds (BS3-BS4) is implemented to counteract the current deforestation process.
- The better road rehabilitation management practices reduce reconstruction from 10 to 1 years after the flood event.

To analyze the risk results obtained in the Optimal Future Climate-trend Design scenario, they will be compared with the risk values previously obtained for climate-trend base scenario. These evaluations allow to study which is the effect of the implemented risk-reduction measures.

The risk results obtained for the trendy design scenario are shown in Table 14-35

	Future Climate design scenario	Optimal Future Climate design scenario
Direct economic flood risk (\$/year)	566,986	553,191
Indirect economic flood risk (\$/year)	6,119,282	631,198
Total economic flood risk (\$/year)	6,672,473	1,198,184

Table 14-35: Annual risk results for optimal future climate design scenario.

It is observed that road management improvement measures are important to reduce risk in the new road design for a future climate scenario. In the Optimal Future Climate-trend design scenario, the expected flood peak flows at the most problematic watershed-road intersection (BS3-BS4) are lower than those estimated in the Future Climate design scenario, decreasing direct pavement damage. Thus, the average direct economic risk decreases to 0.9 times its value (from 570 000 \$/year to 550 000 \$/year) compared to the Future Climate design scenario. The most significant risk reduction, however, lies in reducing the indirect economic damage caused by the floods. Due to the rapid execution of the reconstruction tasks compared to the Future Climate design scenario, the incremental consequences due to vehicle circulation will be less important in the Optimal design scenario. This is reflected in the results, as the average indirect economic risk will decrease up to 6 times its value (from 6.5 M \$/year to 1.1 M \$/year) compared to the Future Climate design scenario on both indirect and total damages.

Figure 14-68 represents the FD curve for Optimal Future Climate Design risk scenario:

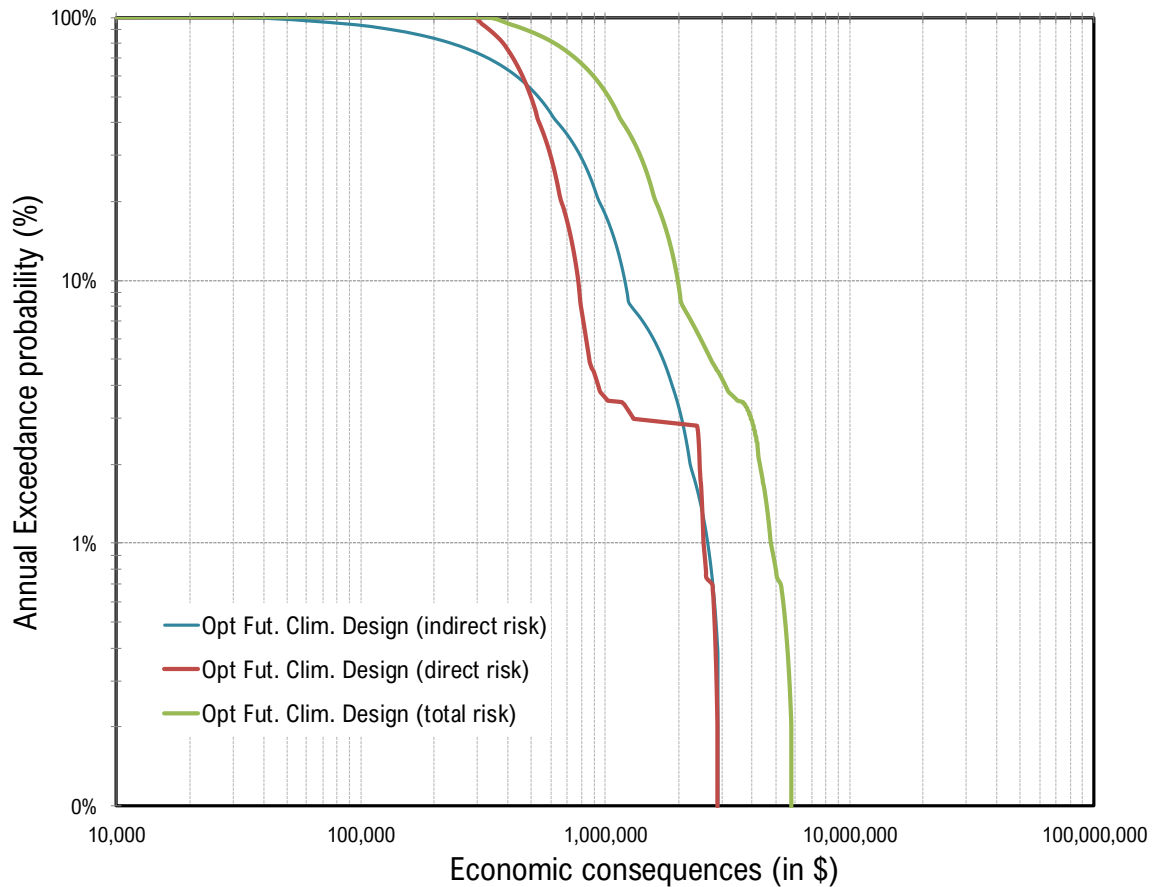


Figure 14-68: FD curve for optimal future climate design scenario.

Most of the economic risk are attributable to the indirect economic consequences. In the case of the Optimal Future Climate design scenario the indirect consequences reach the minimum expected value compared to all the analyzed scenarios, which is explained by the lower influence of the incremental costs by vehicles circulation during rehabilitation thanks to better management of maintenance and reconstruction tasks after a flood. The average indirect economic risk equals approximately 1 M \$/year.

The average direct economic risk (pavement flooding and bridge collapse) is approximately 550 k \$/year, being able to exceed 800 k \$/year (with a probability of 10%) and 3 M \$/year (with a probability of 1%).